ISSN 0004-2749
versão impressa

Arquivos Brasileiros de Oftalmologia

PUBLICAÇÃO OFICIAL DO CONSELHO BRASILEIRO DE OFTALMOLOGIA
MAIO/JUNHO 2016
79 03

Comparison of two diffractive multifocal lenses

Corneal crosslinking with dextran-free isotonic riboflavin

Visual acuity after accelerated crosslinking

Foldable intraocular lens in eyes without capsular support

Urrets-Zavalia syndrome

INDEXADA NAS BASES DE DADOS
MEDLINE | EMBASE | ISI | SciELO

PUBLICAÇÃO OFICIAL DO CONSELHO BRASILEIRO DE OFTALMOLOGIA

CODEN - AQBOAP

Arquivos Brasileiros de Oftalmologia

OFFICIAL PUBLICATION OF THE BRAZILIAN COUNCIL OF OPHTHALMOLOGY (CBO)

Continuous publication since 1938

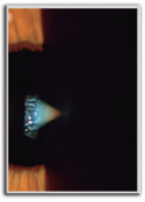

ISSN 0004-2749
(Printed version)
ISSN 1678-2925
(Electronic version)

Frequency of publication: Bimonthly

Arq Bras Oftalmol. São Paulo, v. 79, issue 3, pages 137-208, May/Jun. 2016

ABO – ARQUIVOS BRASILEIROS DE OFTALMOLOGIA • **BIMONTHLY PUBLICATION OF THE BRAZILIAN COUNCIL OF OPHTHALMOLOGY (CBO)**
Editorial Office: R. Casa do Ator, 1.117 - 2nd Floor - São Paulo - SP - Brazil - 04546-004
Phone: +55 (11) 3266-4000 - Fax: +55 (11) 3171-0953 - E-mail: abo@cbo.com.br - www.scielo.br/abo

Subscriptions - Brasil:

CBO Members: Free Distribuiton

Non-members: Annual Subscription: R$ 630.00
Single issue: R$ 95.00

Foreign: Annual Subscription: US$ 200.00
Single issue: US$ 40.00

Chief-editor: Wallace Chamon

Commercial Manager: Cristiano Caixeta Umbelino

Executive Secretary: Claudete N. Moral
Claudia Moral

Technical Editorship: Edna Terezinha Rother
Maria Elisa Rangel Braga

Cover: Ipsis

Publisher: Ipsis Gráfica e Editora S.A.
Divulgation: Brazilian Council of Ophthalmology
Circulation: 7.500 copies

Cover: Slit-lamp photograph of the prism effect on a patient implanted with a diffractive multifocal IOL. Photographer: Wallace Chamon (UNIFESP, São Paulo, SP, Brazil).

PUBLICAÇÃO OFICIAL DO CONSELHO BRASILEIRO DE OFTALMOLOGIA

Arquivos Brasileiros de Oftalmologia

OFFICIAL PUBLICATION OF THE BRAZILIAN COUNCIL OF OPHTHALMOLOGY (CBO)

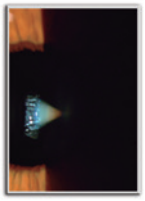

ISSN 0004-2749
(Printed version)
ISSN 1678-2925
(Electronic version)

• ABO
Arquivos Brasileiros de Oftalmologia
www.abonet.com.br

Free Medical Journals
www.freemedicaljournals.com

SciELO
Scientific Electronic Library Online
www.scielo.org

• Copernicus
www.copernicusmarketing.com

periodicos
www.periodicos.capes.gov.br

SCIRUS
for scientific information only
www.scirus.com

THOMSON REUTERS
• ISI Web of Knowledge (SM)

National Library of Medicine NLM
• MEDLINE

SCOPUS

PERIÓDICA

BVS biblioteca virtual em saúde
• LILACS
Literatura Latino-americana em Ciências da Saúde

EMBASE.com

latindex

CBO Board of Directors - 2015-2017

Homero Gusmão de Almeida (President)

José Augusto Alves Ottaiano (Vice-President)

João Marcelo de Almeida Gusmão Lyra (First Secretary)

Keila Monteiro de Carvalho (General Secretary)

Cristiano Caixeta Umbelino (Treasurer)

Societies Affiliated to the Brazilian Council of Ophthalmology and Their Presidents

Associação Brasileira de Catarata e Cirurgia Refrativa	Carlos Gabriel de Figueiredo
Centro Brasileiro de Estrabismo	Marta Halfeld Ferrari Alves Lacordia
Sociedade Brasileira de Administração em Oftalmologia	Ronald Cavalcanti
Sociedade Brasileira de Cirurgia Plástica Ocular	Murilo Alves Rodrigues
Sociedade Brasileira de Ecografia em Oftalmologia	Norma Allemann
Sociedade Brasileira de Glaucoma	Marcelo Palis Ventura
Sociedade Brasileira de Laser e Cirurgia em Oftalmologia	Fabiano Cade Jorge
Sociedade Brasileira de Lentes de Contato, Córnea e Refratometria	Cléber Godinho
Sociedade Brasileira de Oftalmologia Pediátrica	Márcia Beatriz Tartarella
Sociedade Brasileira de Oncologia em Oftalmologia	Eduardo Ferrari Marback
Sociedade Brasileira de Retina e Vítreo	André Vieira Gomes
Sociedade Brasileira de Trauma Ocular	Pedro Carlos Carricondo
Sociedade Brasileira de Uveítes	Fernanda Belga Ottoni Porto
Sociedade Brasileira de Visão Subnormal	Evandro Lopes de Araújo

Support:

CNPq Conselho Nacional de Desenvolvimento Científico e Tecnológico
CAPES
Ministério da Educação
Ministério da Ciência e Tecnologia
BRASIL UM PAÍS DE TODOS GOVERNO FEDERAL

PUBLICAÇÃO OFICIAL DO CONSELHO BRASILEIRO DE OFTALMOLOGIA

ARQUIVOS BRASILEIROS DE
Oftalmologia

OFFICIAL PUBLICATION OF THE BRAZILIAN COUNCIL OF OPHTHALMOLOGY (CBO)

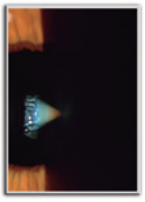

ISSN 0004-2749
(Printed version)
ISSN 1678-2925
(Electronic version)

Frequency of publication: Bimonthly

Arq Bras Oftalmol. São Paulo, v. 79, issue 3, pages 137-208, May/Jun. 2016

Contents

Editorial

Original Articles

Case Reports

Review Articles

The fever of pain: ocular chronic pain, light at the end of the tunnel

A febre da dor: dor ocular crônica, uma luz no fim do tunel

Eduardo Melani Rocha[1], Jayter Silva de Paula[1]

"Dogma says: believe the data that fit your model of the world and ignore the rest.
The world says, ignore the dogma and extend your model to fit the world."
Amit Goswami, "Quantum creativity: think quantum, be creative"

One of the most depressing situations in the outpatient clinic occurs when an individual describes a long-term incurable pain condition along with a never-ending list of unhelpful exams and treatments. Worse, when our complementary exams confirm the previous clinical impressions: no signs of inflammation, and no clues about a trigger or a possible cause.

The classic presentation of inflammation has four elements: redness, swelling, heat and, the pain, reasonable consequence of the previous three. In "the most densely innervated organ of the body", the cornea[1,2], pain, is frequently observed without the other elements of inflammation. The explanation is: neuropathic pain. Although it has a multidimensional clinical expression and is present in other conditions, such as absolute glaucoma; chronic corneal pain is receiving more awareness, and the reasons are commented below.

In 2010, Perry Rosenthal et al., started clarifying and discussing clinical support for patients under chronic corneal pain. Since their initial work, readers can find reports on what they have defined as "pain without stain", and labeled as corneal neuropathic pain or keratoadinia[3,4]. This authors supplied their working hypothesis on the potential triggers, possible pathways and why keratoadinia has been confused with dry eye disease. Both diseases are often seen in a comprehensive ophthalmic clinic, present with discordant signs and symptoms and in general there is no much to offer, except chronic medication to modestly relief for the discomfort[5]. Moreover, they have shown that several diseases beyond herpetic and diabetic neuropathic syndromes can affect the eye leading to both dry eye and neuropathic corneal pain[6,7].

In the daily practice, practitioners face differential diagnoses between keratoadinia and malingering, somatic syndromes or hysteria, which are out of the scope and expertise of ophthalmologists. In a typical scenario, a patient would have consulted more than two ophthalmologists in a recent period and presents with diagnosis and treatment of other unrelated syndromes, such as chronic fatigue, irritated bowel syndrome, and fibromyalgia[8]. Some of those medications present confusing anti-cholinergic effects that may hamper the correct diagnosis.

Those patients are more frequently 40 to 50 years-old women, living in deprived areas, but keratoadinia can be found in males and younger individuals from more affluent areas[9]. The condition itself can impact learning and carrier progression, as well as social and daily life activities. It is also challenging to conduct those cases, due to the lack of credibility on medical resources created by previous unsuccessful evaluations and treatments with confounding side effects.

Are there good news at the front? The answer is yes! Several papers and presentations in recent years are clarifying the details of so called "cornea pain without stain". Great contributions are coming from neurophysiology and molecular biology, revealing the players (membrane receptors in the cornea and neural routes) of pain induced by minor interventions and drugs, associated or not with chronic diseases[10-12].

Recent advances have facilitated the *in vivo* observation of corneal nerves, using different Optic Coherence Tomography strategies for confocal microscopy. It is not surprising that changes in the format and density of corneal nerves observed in various conditions associated with ocular pain and/or dry eye are now established as markers of this unique complex disease: the neuropathic corneal pain[3]. The decreased total number of nerves and the presence of trunks, branches, shorter length, and higher tortuosity were correlated with lower tactile sensation[13-16]. Moreover, it is now proven that corneas lacking healthy nerves have more inflammatory cells and are prompt to new vessels[17].

Were you skeptic about sympathetic ophthalmia? Believe now: clinical and histologic observations revealed that unilateral corneal damage induces bilateral changes to corneas and also to both trigeminal ganglion[13,14,17,18]. So why not uveitis? Let me explain: those peripheral nerves seen in the cornea are dendrites of cell bodies located in the trigeminal ganglion in the brain and they cross-talk with the opposite side.

Submitted for publication: May 15, 2016
Accepted for publication: May 17, 2016

[1] Departamento de Oftalmologia, Otorrinolaringologia, Cirurgia de Cabeça e Pescoço. Faculdade de Medicina de Ribeirão Preto (FMRP), Universidade de São Paulo (USP), Ribeirão Preto, SP, Brazil.

Funding: No specific financial support was available for this study.

Disclosure of potential conflicts of interest: None of the authors have any potential conflict of interest to disclose.

Corresponding author: Eduardo Melani Rocha. Departamento de Oftalmologia, Otorrinolaringologia e Cirurgia de Cabeça e Pescoço - Faculdade de Medicina de Ribeirão Preto, US. Av. Bandeirantes, 3.900 - Ribeirão Preto, SP - 14049-900 - Brazil - E-mail: emrocha@fmrp.usp.br

http://dx.doi.org/10.5935/0004-2749.20160042

The link among inflammatory response, cornea innervation, pain and involvement of the opposite side (the contralateral untouched eye in a trauma, for example) was not clear until the effects of cornea wound in the central nervous system was investigated (more specifically the route of the trigeminal nerve and its ganglion). The findings were striking. An elegant study conducted by Dr. Paolo Rama and his group revealed that an alkali burn lead to inflammation in both trigeminal ganglions of the injured mice[18]. They confirmed previous similar findings observed with herpes infection, a well-known disease that interplays the cornea and the trigeminal nerves[19]. Ironically, it was reported more than 80 years ago, that vitamin deficiency is not directly challenging for the cornea structure and tears secretion, but it would be associated with damages to the trigeminal ganglion[20].

In summary, in the central nervous system, higher-order neurons structures can be inflamed and altered after an ocular surface damage. The nerve inflammation can perpetuate and appear as a painful but apparently not injured eye. The cornea nerves and the trigeminal ganglion once injured become highly sensitized but are still not visible at gross examination. This disjoined process occurs in different conditions and in a dissimilar way in different individuals, depending on demographic and genetic backgrounds[21,22]. Putting together, these findings open avenues for the clarification of the chronic neuropathic cornea pain mechanisms, and start showing us a light at the end of the tunnel for better treatment and hence restoring patients' confidence. To reach the light on neuropathic pain related to the ocular surface, eyes should be investigated as the windows to the brain.

REFERENCES

1. Marfurt CF, Cox J, Deek S, Dvorscak L. Anatomy of the human corneal innervation. Exp Eye Res. 2010;90(4):478-92.
2. Bonini S, Rama P, Olzi D, Lambiase A. Neurotrophic keratitis. Eye (Lond). 2003;17(8):989-95.
3. Rosenthal P, Baran I, Jacobs DS. Corneal pain without stain: is it real? Ocul Surf. 2009; 7(1):28-40.
4. Rosenthal P, Borsook D. Ocular neuropathic pain. Br J Ophthalmol. 2016;100(1):128-34.
5. Nichols KK, Nichols JJ, Mitchell GL. The lack of association between signs and symptoms in patients with dry eye disease. Cornea. 2004;23(8):762-70.
6. Rosenthal P, Borsook D. The corneal pain system. Part I: the missing piece of the dry eye puzzle. Ocul Surf. 2012;10(1):2-14.
7. Dworkin RH. An overview of neuropathic pain: syndromes, symptoms, signs, and several mechanisms. Clin J Pain. 2002;18(6):343-9.
8. Aggarwal VR, McBeth J, Zakrzewska JM, Lunt M, Macfarlane GJ. The epidemiology of chronic syndromes that are frequently unexplained: do they have common associated factors? Int J Epidemiol. 2006;35(2):468-76. Comment in: Int J Epidemiol. 2006; 35(2):477-8.
9. Aggarwal VR, Macfarlane TV, Macfarlane GJ. Why is pain more common amongst people living in areas of low socio-economic status? A population-based cross-sectional study. Br Dent J. 2003;194(7):383-7; discussion 380.
10. Belmonte C, Acosta MC, Gallar J. Neural basis of sensation in intact and injured corneas. Exp Eye Res. 2004;78(3):513-25.
11. Acosta MC, Luna C, Quirce S, Belmonte C, Gallar J. Corneal sensory nerve activity in an experimental model of UV keratitis. Invest Ophthalmol Vis Sci. 2014;55(6):3403-12.
12. Pan Z, Wang Z, Yang H, Zhang F, Reinach PS. TRPV1 activation is required for hypertonicity-stimulated inflammatory cytokine release in human corneal epithelial cells. Invest Ophthalmol Vis Sci. 2011;52(1):485-93.
13. Hamrah P, Cruzat A, Dastjerdi MH, Pruss H, Zheng L, Shahatit BM, et al. Unilateral herpes zoster ophthalmicus results in bilateral corneal nerve alteration: an in vivo confocal microscopy study. Ophthalmology. 2013;120(1):40-7.
14. Cruzat A, Witkin D, Baniasadi N, Zheng L, Ciolino JB, Jurkunas UV, et al. Inflammation and the nervous system: the connection in the cornea in patients with infectious keratitis. Invest Ophthalmol Vis Sci. 2011;52(8):5136-43.
15. Hamrah P, Sahin A, Dastjerdi MH, Shahatit BM, Bayhan HA, Dana R, et al. Cellular changes of the corneal epithelium and stroma in herpes simplex keratitis: an in vivo confocal microscopy study. Ophthalmology. 2012;119(9):1791-7.
16. Dastjerdi MH, Dana R. Corneal nerve alterations in dry eye-associated ocular surface disease. Int Ophthalmol Clin. 2009;49(1):11-20.
17. Ferrari G, Hajrasouliha AR, Sadrai Z, Ueno H, Chauhan SK, Dana R. Nerves and neovessels inhibit each other in the cornea. Invest Ophthalmol Vis Sci. 2013;54(1):813-20.
18. Ferrari G, Bignami F, Giacomini C, Capitolo E, Comi G, Chaabane L, Rama P. Ocular surface injury induces inflammation in the brain: in vivo and ex vivo evidence of a corneal-trigeminal axis. Invest Ophthalmol Vis Sci. 2014;55(10):6289-300.
19. Verjans GM, Hintzen RQ, van Dun JM, Poot A, Milikan JC, Laman JD, et al. Selective retention of herpes simplex virus-specific T cells in latently infected human trigeminal ganglia. Proc Natl Acad Sci U S A. 2007;104(9):3496-501.
20. Mellanby E. Xerophthalmia, trigeminal nerve degeneration and vitamin A deficiency. J Pathol Bacteriol. 1934;38(3):391-407.
21. Galor A, Covington D, Levitt AE, McManus KT, Seiden B, Felix ER, et al. Neuropathic ocular pain due to dry eye is associated with multiple comorbid Chronic pain Syndromes. J Pain. 2016;17(3):310-8.
22. Vehof J, Sillevis Smitt-Kamminga N, Kozareva D, Nibourg SA, Hammond CJ. Clinical characteristics of dry eye patients with chronic pain syndromes. Am J Ophthalmol. 2016. [Epub ahead of print].

Effect of macular hole volume on postoperative central macular thickness

O efeito do volume de buraco macular da espessura macular central pós-operatória

Taylan Ozturk[1], Eyyup Karahan[2], Duygu Er[1], Mahmut Kaya[1], Nilufer Kocak[1], Suleyman Kaynak[1]

ABSTRACT

Purpose: To evaluate the association between macular hole volume (MHV) and postoperative central macular thickness (CMT) using spectral-domain optical coherence tomography (SD-OCT).

Methods: Thirty-three eyes of 30 patients with a large full-thickness idiopathic macular hole with or without vitreomacular traction who underwent surgical intervention were included in this cross-sectional study. Complete ophthalmological examination, including SD-OCT, was performed for all participants during the pre- and postoperative visits. MHV was preoperatively measured using SD-OCT, which captured the widest cross-sectional image of the hole. For normal distribution analysis of the data, the Kolmogorov-Smirnov test was performed, and for statistical analyses, chi-square, Student's t-test, Mann-Whitney U test, and Pearson's correlation coefficient test were performed.

Results: Mean preoperative best-corrected visual acuity (BCVA) and MHV were found to be 0.99 ± 0.36 (range, 0.3-2.0) logMAR and 0.139 ± 0.076 (range, 0.004-0.318) mm^3, respectively. Mean follow-up was 16.3 ± 14.3 (range, 3-50) months. No statistical correlations were found between MHV and postoperative BCVA (p=0.588) and between MHV and disease recurrence (p=0.544). A weak negative correlation existed between MHV and final CMT scores (p=0.04, r=-0.383).

Conclusions: Greater MHV was found to be weakly associated with lower postoperative CMT scores.

Keywords: Retinal perforations/surgery; Tomography, optical coherence; Vitrectomy; Macula lutea; Postoperative period

RESUMO

***Objetivo**: Avaliar a relação entre o volume do buraco macular (MHV) e a espessura macular central pós-operatória (CMT) por meio da tomografia de coerência óptica de domínio espectral (SD-OCT).*

***Método**: Trinta e três olhos de 30 pacientes com buracos maculares idiopáticos de espessura total grandes, com ou sem tração vitreorretiniana, que foram submetidos a intervenção cirúrgica foram incluídos neste estudo transversal. O exame oftalmológico completo, incluindo SD-OCT foi realizado nas visitas pré e pós-operatórias de todos os participantes. MHV foi medido a partir da imagem de SD-OCT pré-operatória que capturou a imagem mais larga da secção transversal do buraco. Após a análise distribuição nomral da população do estudo ter sido realizada com o teste Kolmogorov-Smirnov, os testes de qui-quadrado, t de Student, Mann-Whitney U e teste de correlação de Pearson foram utilizados para as estatísticas.*

***Resultados**: As médias pré-operatórias da melhor acuidade visual corrigida (BCVA) e MHV foram 0,99 ± 0,36 logMAR (variação de 0,3-2,0) e 0,139 ± 0,076 mm^3 (variação de 0,004-0,318). O seguimento médio foi de 16,3 ± 14,3 meses (variação de 3-50). Não foram encontradas correlações estatísticas entre MHV e BCVA pós-operatória (p=0,588), bem como MHV e recorrência da doença (p=0,544). Uma fraca correlação negativa estava presente entre MHV e pontuações finais CMT (p=0,04, r=-0,383).*

***Conclusões**: Maior MHV foi fracamente relacionado com CMT mais baixo, no pós-operatório.*

***Descritores**: Perfurações retinianas/cirurgia; Tomografia de coerência óptica; Vitrectomia; Macula lutea; Período pós-operatório*

INTRODUCTION

Major causes for developing a macular hole (MH) include anteroposterior forces applied by vitreofoveal traction and tangential traction from involutional changes in the inner retina[1-4]. Kelly and Wendell[5] reported the first successful closure of MH with pars plana vitrectomy (PPV); since then, advances in vitreoretinal surgery have contributed to successful postoperative restoration of the foveal microstructure and restoration of visual function in most patients[6-10]. Although anatomical closure of MH may be applicable to almost all patients undergoing surgical intervention, significant improvement in visual acuity can be achieved in approximately 70% of cases[8-13]. Macular atrophy may be responsible for inferior visual outcomes; therefore, the foveal microstructure has to be well identified in patients with MH prior to any surgical intervention.

Spectral-domain optical coherence tomography (SD-OCT) is a non-contact, non-invasive, laser interferometry technique, which captures high-resolution cross-sectional images in vivo and is used in diagnosing numerous macular diseases. Using SD-OCT imaging in the diagnosis of MH augments clinical staging by enabling visualization of the foveal and vitreous microstructure and the tractional association between them and calculating macular hole dimensions. Manual quantification of MH width and height can be provided using SD-OCT, which mainly identifies the presence of perifoveal cystoid edema and vitreomacular traction (VMT) and the integrity of perifoveal external retinal microstructures. The impact of preoperative OCT measurements on diagnosing or staging idiopathic MH and its predictive value for postoperative anatomical and functional outcomes have been previously investigated[14-24]. However, to the best of our knowledge, no study has elucidated the association between preoperative macular hole volume (MHV) and postoperative macular atrophy as a tool for predicting postoperative visual outcome. This study aimed to evaluate the association between MHV and postoperative central macular thickness (CMT) using SD-OCT.

Submitted for publication: January 23, 2016
Accepted for publication: February 11, 2016

[1] Department of Ophthalmology, Dokuz Eylul University School of Medicine, Izmir, Turkey.
[2] Department of Ophthalmology, Sifa University, Izmir, Turkey.

Funding: No specific financial support was available for this study.

Disclosure of potential conflicts of interest: None of the authors have any potential conflict of interest to disclose.

Corresponding author: Taylan Ozturk, MD. Albatros-9, 2040 Sokak, No: 152, Daire: 26, Mavisehir, Karsiyaka, 35540 - Izmir - Turkey - E-mail: ataylan6@yahoo.com

Approved by the following research ethics committee: Dokuz Eylul University (# 749, November 29, 2013).

Registration number of clinical trials registry: 2013/43-16.

METHODS

Thirty-three eyes of 30 patients with a diagnosis of large full-thickness idiopathic MH with or without VMT who underwent chromovitrectomy combined with internal limiting membrane (ILM) peeling and intraocular sulfur hexafluoride (SF6) tamponade in our Retina Unit between January 2010 and December 2012 were included in this study. Medical charts of the eyes were retrospectively reviewed, and all the results of complete ophthalmological examinations, including SD-OCT (Spectralis II HRA+OCT, Heidelberg Engineering Inc., Heidelberg, Germany) that were performed during pre- and postoperative visits, were recorded for each participant. Patients with systemic diseases that could affect visual acuity and patients who had a medical history of any ophthalmic surgery, except for cataract extraction, were excluded. Informed consent conforming to the Declaration of Helsinki was obtained from each study participant, and the study protocol was approved by the local ethics committee (approval number: 2013/43-16).

All eyes underwent 4-port 23-gauge PPV combined with ILM peeling and intraocular 20% SF6 tamponade. Detachment of the posterior hyaloid was induced by suction using a vitrectomy probe around the optic disc if necessary, and epiretinal membranes were removed if present. ILM peeling within a fovea-centered circular area of approximately two optic disc diameters was performed on visualizing ILM with brilliant blue dye. Twenty percent of SF6 was used as intraocular gas tamponade in all cases, and postoperative face-down positioning for 5-7 days was recommended. All subjects underwent complete ophthalmological examination, including best-corrected visual acuity (BCVA), slit-lamp biomicroscopy, ocular tonometry, dilated fundoscopy, and CMT assessment using SD-OCT that were preoperatively and postoperatively performed.

MHV was measured on the basis of preoperative SD-OCT, which captured the widest cross-sectional image of the hole. Because the outer plexiform layer (OPL) and outer nuclear layer (ONL) junctions are located just beneath the foveal contour, OPL was first marked in all preoperative macular scans for each study participant. For the purpose of this study, we pointed out the OPL level along both sides of the MH, and a border line connecting these points was drawn to estimate the possible location of the foveal contour using SD-OCT that captured the widest cross-sectional image of the hole. The space remaining under the imaginary border line of OPL was described as MHV (Figure 1). The aspect of such spaces had the shape of a conical frustum; thus, we calculated MHV for each study participant according to the formula used for calculating the volume of a truncated cone (Figure 2).

The data were stored in a computerized database and analyzed using Statistical Package for Scientific Studies for Windows v.16.0 (SPSS Inc., Chicago, IL, USA). Normal distribution analysis of the data was performed using the Kolmogorov-Smirnov test; moreover, the chi-square test, the paired t-test, Student's t-test, and the Mann-Whitney U test were performed for statistical analyses. Pearson's correlation coefficient test was also used to analyze the association among MHV, postoperative CMT, and pre- and postoperative BCVA scores. A p value of <0.05 was considered statistically significant.

RESULTS

Of the 30 patients with a mean age of 63.9 ± 11.0 (range, 15-76) years, 18 (60.0%) were females and 12 (40.0%) were males. Three participants (10.0%) had diabetes mellitus and five (16.7%) had hypertension; however, none of the subjects demonstrated signs of

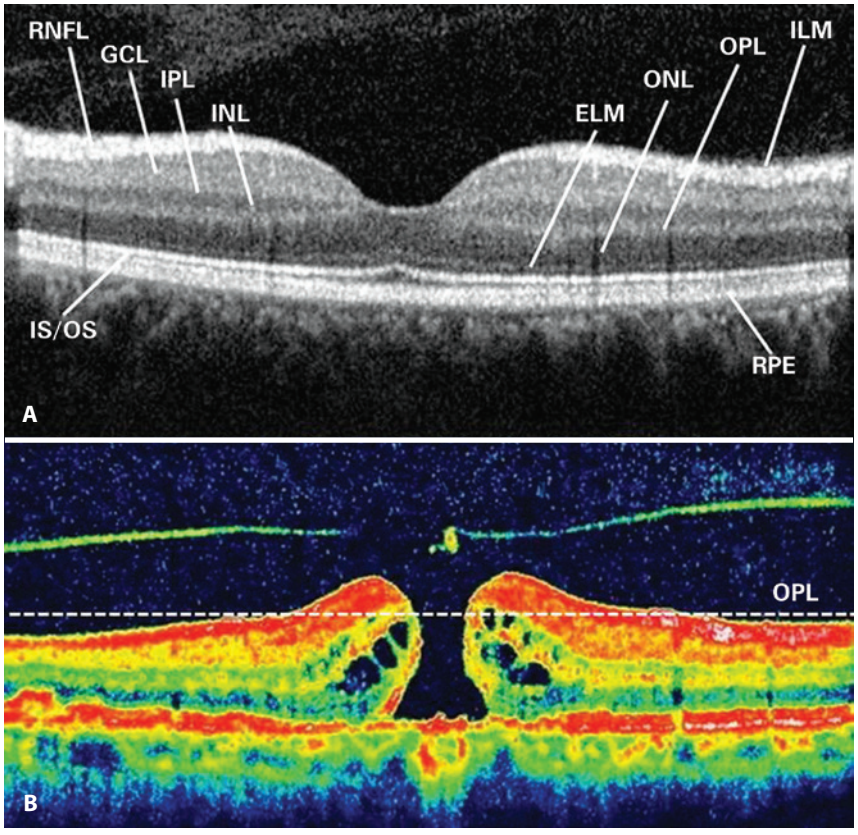

Figure 1. Retinal layers are shown in an SD-OCT image (A). An imaginary border line demonstrating the outer plexiform layer (OPL) was drawn to estimate the possible localization of the foveal contour on SD-OCT that captured the widest cross-sectional image of the hole (B).

retinopathy. Thirteen eyes (39.4%) were pseudophakic and 20 (60.6%) were phakic. Mean preoperative BCVA, intraocular pressure (IOP), and MHV were identified as 0.99 ± 0.36 (range, 0.3-2.0) logMAR, 14.7 ± 2.1 (range, 11-20) mmHg, and 0.139 ± 0.076 (range, 0.004-0.318) mm^3, respectively. Surgery was performed within 6 months of the onset of clinical symptoms; thus, MH diagnosis was established soon after. Perifoveally located intraretinal cysts relevant to a newly developed MH were found on preoperative macular SD-OCT of all participants. These scans revealed VMT in 16 eyes (48.5%) and a true retinal operculum in 10 eyes (30.3%) preoperatively. Although early anatomical success was achieved with MH surgery in all cases, MH recurred in four eyes (12.1%) after the mean follow-up of 16.3 ± 14.3 (range, 3-50) months. Demographic and ophthalmological findings are summarized in tables 1 and 2.

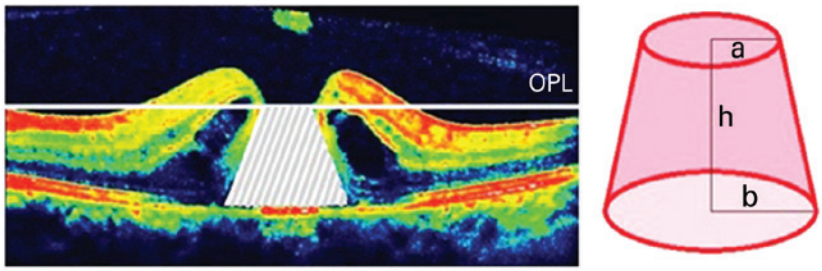

$$V = \frac{\pi}{3} h (a^2 + ab + b^2)$$

Figure 2. Calculation of the macular hole volume (MHV) according to the formula that gives the volume of a truncated cone.

Table 1. Demographic and initial ophthalmological findings

	All study eyes (n=33)	Eyes with c-MH (n=29)	Eyes with r-MH (n=4)	p value
Age (years)	63.900 ± 11.000	61.800 ± 14.400	70.200 ± 4.500	0.139
Preoperative BCVA (logMAR)	0.990 ± 0.360	0.930 ± 0.330	1.400 ± 0.350	0.013*
Preoperative IOP (mmHg)	14.700 ± 2.100	14.900 ± 2.200	13.700 ± 1.000	0.322
Macular hole volume (mm^3)	0.139 ± 0.076	0.138 ± 0.076	0.149 ± 0.075	0.777
Gender				0.643
Female	60.0%	61.5%	50.0%	
Male	40.0%	38.5%	50.0%	
Concomitant disease				
Diabetes mellitus	10.0%	11.5%	-	0.500
Hypertension	16.7%	19.2%	-	0.367
Preoperative VMT				
VMT	16 (48.5%)	16 (55.2%)	-	0.038*
A true retinal operculum	10 (30.3%)	10 (34.5%)	-	0.159
Follow-up (months)	16.3 ± 14.3	16.3 ± 14.4	15.8 ± 15.2	0.939

c-MH= closed macular hole; r-MH= recurrent macular hole; BCVA= best-corrected visual acuity; IOP= intraocular pressure; VMT= vitromacular traction; *= Statistical significance.

Table 2. Postoperative ophthalmologic findings in eyes with and without successful surgery

	All study eyes (n=33)	Eyes with c-MH (n=29)	Eyes with r-MH (n=4)	p value
Follow-up (months)	16.30 ± 14.3	16.30 ± 14.40	15.80 ± 15.2	0.939
Postoperative BCVA (logMAR)	0.64 ± 0.38	0.51 ± 0.31	1.60 ± 0.0	<0.001*
Postoperative IOP (mmHg)	14.60 ± 1.90	14.70 ± 1.90	14.00 ± 1.8	0.502
Postoperative CMT (µm)		187.60 ± 67.80		
Reestablishment of ELM	20 (60.6%)	20 (69.0%)	-	0.008*
Reestablishment of EZ	13 (39.4%)	13 (44.8%)	-	0.085
Reestablishment of COST line	8 (24.2%)	8 (27.6%)	-	0.227
Reestablishment of RPE band	28 (84.8%)	25 (86.2%)	3 (75.0%)	0.558

c-MH= closed macular hole; r-MH= recurrent macular hole; BCVA= best-corrected visual acuity; IOP= intraocular pressure; CMT= central macular thickness; ELM= external limiting membrane; EZ= ellipsoid zone; COST= cone outer segment tips; RPE= retinal pigment epithelium; *= Statistical significance.

Mean BCVA and IOP were found to be 0.64 ± 0.38 (range, 0.0-1.6) logMAR and 14.6 ± 1.9 (range, 11-20) mmHg (p<0.001 and p=0.723), respectively, at the last follow-up visit. When four eyes with recurrent disease were excluded, mean BCVA and CMT were found to be 0.51 ± 0.31 (range, 0.0-1.6) logMAR and 187.6 ± 67.8 (range, 60-247) µm, respectively, at the last follow-up in the remaining 29 eyes. Mean preoperative BCVA and MHV were 1.40 ± 0.35 logMAR and 0.149 ± 0.075 mm^3, respectively, in eyes with recurrent disease, whereas these scores were 0.93 ± 0.33 logMAR and 0.138 ± 0.076 mm^3, respectively, in successfully treated eyes (p=0.013 and p=0.777, respectively).

VMT and a true retinal operculum were not found in any eyes with resistant MH; however, such vitreomacular interface abnormalities were present in 55.2% and 34.5% of eyes with closed MH (p=0.038 and p=0.159, respectively). Changes in BCVA, CMT, and IOP are shown in figure 3. While abnormalities were preoperatively present in the foveal ellipsoid zone (EZ) of all participants, SD-OCT revealed re-establishment of EZ in 13 eyes (39.4%). There was no correlation between preoperative MHV and postoperative EZ re-establishment (p=0.713). However, better postoperative BCVA scores were observed in patients with re-established EZ (p=0.002).

Macular SD-OCT scans that were performed at the last follow-up visit also depicted the re-establishment of the external limiting membrane (ELM) in 20 eyes (60.6%), cone outer segment tip (COST) line in eight eyes (24.2%), and retinal pigment epithelium (RPE) band in 28 eyes (84.8%). Preoperative MHV was not found to be correlated with the re-establishment of ELM, COST line, or RPE band (p=0.268, p=0.283, and p=0.920, respectively). No statistical correlation was found between final BCVA and re-establishment of RPE band (p=0.411); however, reformed ELM and COST line provided a better visual prognosis in cases undergoing MH surgery (p=0.003 and p=0.005, respectively). Postoperative ocular features are summarized in table 2.

Although no statistical correlations were found between MHV and postoperative BCVA (p=0.588) and between MHV and disease recurrence (p=0.544), a negative correlation was present between MHV and CMT that was measured at the last follow-up (p=0.040). Furthermore, there was a strong correlation between pre- and postoperative BCVA scores (p<0.001). The results of Pearson's correlation coefficient test for the parameters studied are given in table 3.

DISCUSSION

Recent advances in MH surgery techniques have contributed to more successful postoperative anatomical and associated functional prognoses[6-11]. However, anatomical closure of a hole does not always correlate with a good functional result[6,17,18]. Although various preoperative SD-OCT parameters have been examined to estimate postoperative visual prognosis, studies have reported the lack of any consistent volumetric or structural feature that is closely correlated with anatomical and functional surgical successes[15-18]. In this study, there was no statistical difference in MHV measurements between eyes with and without disease recurrence; however, lower preoperative BCVA scores were found in eyes with relapsing MH. Furthermore, in our study population, preoperative SD-OCT revealed that neither VMT nor a true retinal operculum was found in any of the eyes with a recurrent hole.

Defects of foveal photoreceptors and abnormalities of external retinal microstructures that can be observed in SD-OCT images of surgically treated eyes with MH have been studied, with the goal of defining any association between such problems and the development of poorer vision. Furthermore, a significant correlation between the presence of such abnormalities and postoperative visual prognosis has been recently reported[16-20]. In this study, MHV was not found to be associated with the postoperative re-establishment of any of

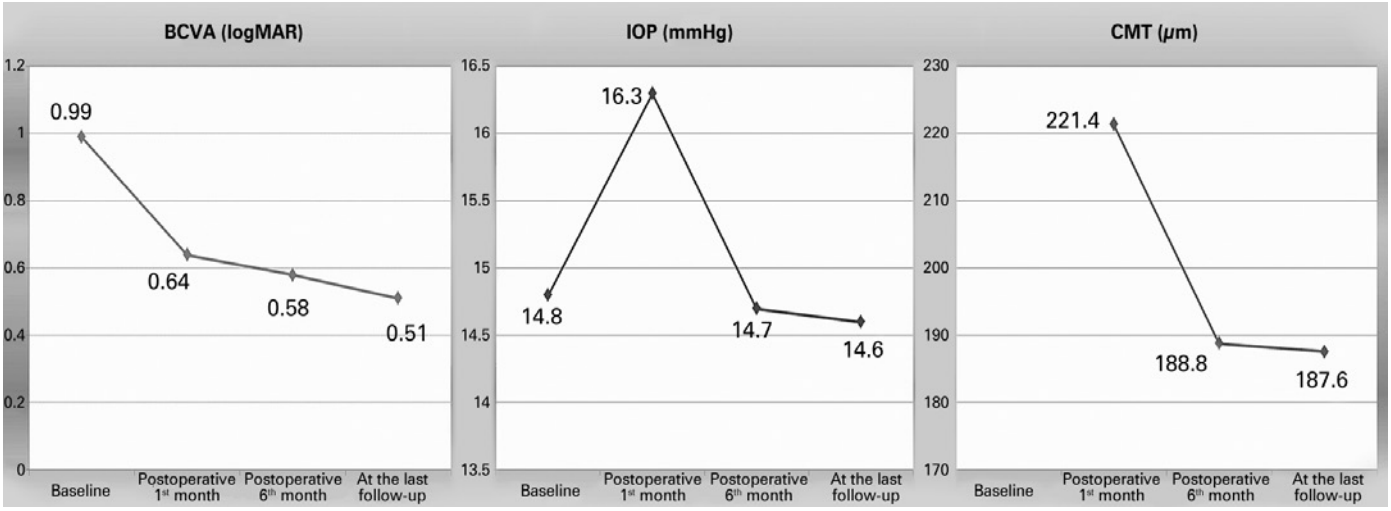

Figure 3. Changes in best-corrected visual acuity (BCVA), intraocular pressure (IOP), and central macular thickness (CMT).

Table 3. Pearson's correlation coefficient test results for studied parameters

Studied parameters		p value	r value
Macular hole volume	Preoperative BCVA (logMAR)	0.294	0.188
Macular hole volume	Final BCVA (logMAR)	0.588	0.113
Preoperative BCVA (logMAR)	Postoperative BCVA (logMAR)	<0.001*	0.660
Macular hole volume	Postoperative CMT in cases with c-MH (n=29)	0.040*	-0.383

BCVA= best-corrected visual acuity; CMT= central macular thickness; c-MH= closed macular hole; *= statistical significance.

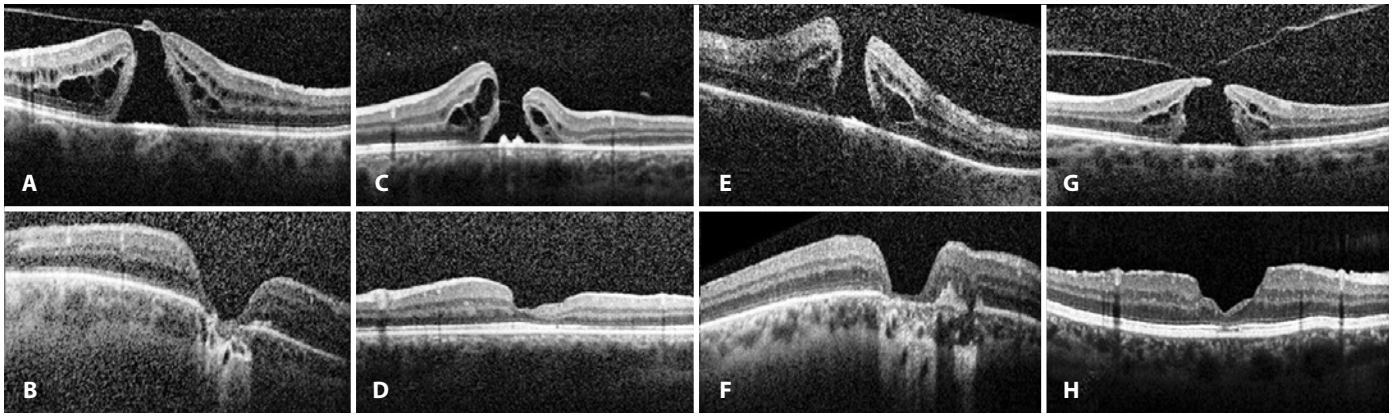

Figure 4. Preoperative (A, C, E, and G) and postoperative (B, D, F, and H) SD-OCT of patients with macular atrophy after 4-port 23-gauge PPV combined with ILM peeling and intraocular 20% SF6 tamponade.

the studied parameters of external retinal microstructure. Improved RPE band integrity on successful MH surgery was also not found to be associated with final BCVA scores; however, re-establishment of ELM, EZ, and COST line was associated with a better visual prognosis.

On the contrary, some published studies have reported a negative correlation between preoperative MH dimensions measured using OCT and postoperative visual recovery[21-26]. The MH base diameter, which was measured at the RPE level, and the minimum diameter of the hole, which represented the shortest extent of MH, appear to constitute prognostic factors for postoperative anatomical and functional outcomes. Freeman et al.[6], similarly found that MH with smaller diameters were associated with a better visual prognosis. Moreover, a hole form factor (HFF) was calculated from the base and minimum diameters to estimate the postoperative anatomical success rate. Ullrich et al.[21] reported significantly larger base diameters and greater minimum MH diameters in cases with recurrent holes. Furthermore, postoperative visual prognosis was found to be negatively correlated with both the base and minimum diameters of the hole. The authors also stated that all cases with HFF of >0.9 were surgically treated with a single intervention; however, the anatomical success rate was 67% in patients with HFF of <0.5.

Ruiz-Moreno et al.[22] reported the sensitivity of various parameters used to estimate visual prognosis after MH surgery. They demonstrated that postoperative BCVA was statistically correlated with base and minimum diameters of MH, the MH index, which is defined as the ratio of the hole height to the base diameter, and the tractional hole index, which is defined as the ratio of the maximum height to the minimum diameter of MH. Base area, base diameter, top area, top diameter, minimum diameter, MH height, and MHV were found to be significantly correlated with initial BCVA in a computer algorithm-supported study by Xu et al[23]. Moreover, they reported a significant correlation between BCVA at postoperative sixth month and MHV, base area and diameter, as well as height-to-base diameter ratio; however, after performing multivariate analyses, only base area and MHV were found to be significant predictors of six-month postoperative BCVA.

Pilli et al.[26] recommended performing ILM peeling to achieve a better visual outcome because a close correlation between inner macular volume and BCVA was observed. In our study, although no statistical correlations were found between MHV and postoperative BCVA or MHV and disease recurrence, a negative correlation was present between MHV and CMT measured at the last follow-up (p=0.04, r=-0.383). Because postoperative CMT scores were within the favorable normal range in the entire study population, except in cases with recurring MH, lower CMT scores were considered to be associated with a more severe macular atrophy (Figure 4). Visual acuity is directly related to both the extent and centricity of the macular atrophy[27,28]. However, preoperative BCVA score was the only factor consistently affecting postoperative BCVA in our study population.

The major limitation of this study was the lack of the use of real-time three-dimensional volumetric analysis of MH. Although the shape of each MH varies in its microarchitecture, we used the widest two-dimensional cross-sectional SD-OCT image of all studied holes. Nevertheless, we believe that within a close range of deviation, every MHV, regardless of the varying shape of the hole, may simply be predicted using the parameters of the formula that gives the volume of a truncated cone. The second limitation was that 20% of our study participants had concomitant diabetes mellitus, hypertension, or both. However, we deliberately selected the surgically treated cases with a newly developed idiopathic MH who did not have any other retinal abnormalities, including retinopathies and a previous history of retinal detachment. In addition, the coexistence of diabetes and/or hypertension may result in some cellular and microarchitectural changes within the retinal tissue, even in cases with no signs of retinopathy. Finally, the retrospective nature of this study and the lack of a large study population reflect other limitations.

Visual acuity may not improve as expected in some patients even when anatomical closure of the hole is attained following MH surgery. This may be related with postoperative macular atrophy, which can be diagnosed on the basis of a reduced CMT score on SD-OCT. In this study, greater MHV was associated with lower postoperative CMT scores. To the best of our knowledge, this is the first study investigating the association between preoperative MHV and macular atrophy. Long-term prospective trials with large cohorts are required to assess the correlation of macular volumetric features with postoperative anatomical and functional prognoses.

REFERENCES

1. Bainbridge J, Herbert E, Gregor Z. Macular holes: vitreoretinal relationships and surgical approaches. Eye (Lond). 2008;22(10):1301-9.
2. Steel DH, Lotery AJ. Idiopathic vitreomacular traction and macular hole: a comprehensive review of pathophysiology, diagnosis, and treatment. Eye (Lond). 2013; 27(Suppl 1):S1-S21.
3. Williamson TH, Lee E. Idiopathic macular hole: analysis of visual outcomes and the use of indocyanine green or brilliant blue for internal limiting membrane peel. Graefes Arch Clin Exp Ophthalmol. 2014;252(3):395-400.
4. Tirelli F, Sasso P, Scupola A. Idiopathic macular hole: post-operative morpho-functional assessment and prognostic factors for recovery of visual acuity. Ann 1st Super Sanita. 2013;49(3):313-6.
5. Kelly NE, Wendel RT. Vitreous surgery for idiopathic macular holes: results of a pilot study. Arch Ophthalmol. 1991;109(5):654-9.
6. Freeman WR, Azen SP, Kim JW, el-Haig W, Mishell DR 3rd, Bailey I. Vitrectomy for the treatment of full-thickness stage 3 or 4 macular holes. Results of a multicentered randomized clinical trial. The Vitrectomy for Treatment of Macular Hole Study Group. Arch Ophthalmol. 1997;115(1):11-21.Erratum in: Arch Ophthalmol. 1997;115(5):636.

7. Spiteri Cornish K, Lois N, Scott NW, Burr J, Cook J, Boachie C, et al. Vitrectomy with internal membrane peeling versus no peeling for idiopathic full-thickness macular hole. Ophthalmology. 2014;121(3):649-55.
8. Lois N, Burr J, Norrie J, Vale L, Cook J, McDonald A, Boachie C, Ternent L, McPherson G; Full-thickness Macular Hole and Internal Limiting Membrane Peeling Study (FILMS) Group. Internal limiting membrane peeling versus no peeling for idiopathic full-thickness macular hole: a pragmatic randomized controlled trial. Invest Ophthalmol Vis Sci. 2011;52(3):1586-92.
9. Morizane Y, Shiraga F, Kimura S, Hosokawa M, Shiode Y, Kawata T, et al. Autologous transplantation of the internal limiting membrane for refractory macular holes. Am J Ophthalmol. 2014;157(4):861-9.
10. Mahalingam P, Sambhav K. Surgical outcomes of inverted internal limiting membrane flap technique for large macular hole. Indian J Ophthalmol. 2013;61(10):601-3.
11. Xirou T, Theodossiadis PG, Apostolopoulos M, Kabanarou SA, Feretis E, Ladas ID, et al. Macular hole surgery with short-acting gas and short-duration face-down positioning. Clin Ophthalmol. 2012;6:1107-12.
12. Margherio RR, Margherio AR, Williams GA, Chow DR, Banach MJ. Effect of perifoveal tissue dissection in the management of acute idiopathic full-thickness macular holes. Arch Ophthalmol. 2000;118(4):495-8.
13. Lai MM, Williams GA. Anatomical and visual outcomes of idiopathic macular hole surgery with internal limiting membrane removal using low-concentration indocyanine green. Retina. 2007;27(4):477-82.
14. Altaweel M, Ip M. Macular hole: improved understanding of pathogenesis, staging, and management based on optical coherence tomography. Semin Ophthalmol. 2003;18(2):58-66.
15. Villate N, Lee JE, Venkatraman A, Smiddy WE. Photoreceptor layer features in eyes with closed macular holes: optical coherence tomography findings and correlation with visual outcomes. Am J Ophthalmol. 2005;139(2):280-9.
16. Bonnabel A, Bron AM, Isaico R, Dugas B, Nicot F, Creuzot-Garcher C. Long-term anatomical and functional outcomes of idiopathic macular hole surgery. The yield of spectral-domain OCT combined with microperimetry. Graefes Arch Clin Exp Ophthalmol. 2013;251(11):2505-11.
17. Chen WC, Wang Y, Li XX. Morphologic and functional evaluation before and after successful macular hole surgery using spectral-domain optical coherence tomography combined with microperimetry. Retina. 2012;32(9):1733-42.
18. Matsumiya W, Kusuhara S, Shimoyama T, Honda S, Tsukahara Y, Negi A. Predictive value of preoperative optical coherence tomography for visual outcome following macular hole surgery: effects of imaging alignment. Jpn J Ophthalmol. 2013; 57(3):308-15.
19. Oh J, Smiddy WE, Flynn HW Jr, Gregori G, Lujan B. Photoreceptor inner/outer segment defect imaging by spectral domain OCT and visual prognosis after macular hole surgery. Invest Ophthalmol Vis Sci. 2010;51(3):1651-8.
20. Kao TY, Yang CM, Yeh PT, Huang JY, Yang CH. The value of combining autofluorescence and optical coherence tomography in predicting the visual prognosis of sealed macular holes. Am J Ophthalmol. 2013;156(1):149-56.
21. Ullrich S, Haritoglou C, Gass C, Schaumberger M, Ulbig MW, Kampik A. Macular hole size as a prognostic factor in macular hole surgery. Br J Ophthalmol. 2002;86(4): 390-3.
22. Ruiz-Moreno JM, Staicu C, Pinero DP, Montero J, Lugo F, Amat P. Optical coherence tomography predictive factors for macular hole surgery outcome. Br J Ophthalmol. 2008;92(5):640-4.
23. Xu D, Yuan A, Kaiser PK, Srivastava SK, Singh RP, Sears JE, et al. A novel segmentation algorithm for volumetric analysis of macular hole boundaries identified with optical coherence tomography. Invest Ophthalmol Vis Sci. 2013;54(1):163-9.
24. Duker JS, Kaiser PK, Binder S, de Smet MD, Gaudric A, Reichel E, et al. The International Vitreomacular Traction Study Group classification of vitreomacular adhesion, traction, and macular hole. Ophthalmology. 2013;120(12):2611-9.
25. Haritoglou C, Neubauer AS, Reiniger IW, Priglinger SG, Gass CA, Kampik A. Long-term functional outcome of macular hole surgery correlated to optical coherence tomography measurements. Clin Exp Ophthalmol. 2007;35(3):208-13. Comment in: Clin Experiment Ophthalmol. 2007;35(3):203.
26. Pilli S, Zawadzki RJ, Werner JS, Park SS. Visual outcome correlates with inner macular volume in eyes with surgically closed macular hole. Retina. 2012;32(10):2085-95.
27. Brader HS, Ying GS, Martin ER, Maguire MG;Complications of age-related macular degeneration prevention trial (CAPT) research group. Characteristics of incident geographic atrophy in the complications of age-related macular degeneration prevention trial. Ophthalmology. 2013;120(9):1871-9.
28. Holz FG, Strauss EC, Schmitz-Valckenberg S, van Lookeren Campagne M. Geographic atrophy: clinical features and potential therapeutic approaches. Ophthalmology. 2014;121(5):1079-91.

Choroidal changes in pre-eclampsia during pregnancy and the postpartum period: comparison with healthy pregnancy

Alterações da coroide na pré-eclâmpsia durante a gravidez e período pós-parto: comparação com a gravidez saudável

Necati Duru[1], Döndü Melek Ulusoy[1], Ayşe Özköse[1], Mustafa Ataş[1], Arzu Seyhan Karatepe[1], Fatma Ataş[2], Hasan Basri Arifoğlu[1], Uğur Yilmaz[3]

ABSTRACT

Purpose: To investigate subfoveal choroidal thickness (SFCT) in patients with pre-eclampsia using enhanced depth imaging optical coherence tomography (EDI-OCT).

Methods: A sample of 73 pregnant women was studied over 28 weeks of gestation. The sample was divided into two groups: one comprising pre-eclamptic pregnant women (n=32), and the other comprising healthy pregnant women (n=41). The SFCT was determined for all patients using EDI-OCT during pregnancy and at the third month of the postpartum period.

Results: The SFCTs in pre-eclamptic pregnant women were 351.97 ± 22.44 and 332.28 ± 20.32 µm during the pregnancy and postpartum periods (p<0.001), respectively, whereas these values in healthy pregnant women were 389.73 ± 49.64 and 329.78 ± 22.36 µm (p<0.001), respectively. During pregnancy SFCT in pre-eclamptic pregnant women was significantly thinner than that in healthy pregnant women (p<0.001). However, there was no statistically significant difference during the postpartum period (p=0.623).

Conclusions: The results suggest that SFCT is significantly decreased in pre-eclamptic pregnant women than in healthy pregnant women, despite no statistically significant difference in SFCT existing between the groups during the postpartum period.

Keywords: Choroid; Choroid diseases/diagnosis; Tomography, Optical coherence; Pre-eclampsia; Fovea centralis; Axial length; eye; Pregnancy

RESUMO

Objetivo: *Investigar espessura subfoveal coroidal (SFCT) em pacientes com pré-eclâmpsia usando imagens de tomografia de coerência óptica de profundidade otimizada (EDI-OCT).*

Método: *Uma amostra de 73 mulheres grávidas foi estudado ao longo de 28 semanas de gestação. A amostra foi dividida em dois grupos: um com mulheres grávidas com pré-eclâmpsia (n=32), o outro com as mulheres grávidas saudáveis (n=41). SFCT foi determinada em todos os pacientes utilizando EDI-OCT durante a gravidez e no terceiro mês do período pós-parto.*

Resultados: *Os SFCTs em gestantes com pré-eclâmpsia foram 351,97 ± 22,44 µm e 332,28 ± 20,32 µm durante o período de gravidez e pós-parto (p<0,001), respectivamente. Estes valores em mulheres grávidas saudáveis foram 389,73 ± 49,64 µm e 329,78 ± 22,36 µm (p<0,001), respectivamente. Durante a gravidez o SFCT foi significantemente mais fino em mulheres com pré-eclâmpsia quando comparado com as mulheres saudáveis (p<0,001). No entanto, não houve diferença estatisticamente significante no período pós-parto (p=0,623).*

Conclusões: *Os resultados sugerem que SFCT é significativamente mais fino em gestantes com pré-eclâmpsia do que nas mulheres grávidas saudáveis, apesar de não haver diferença estatisticamente significativa na SFCT entre os grupos durante o período pós-parto.*

Descritores: *Coroide; Doenças da coroide/diagnóstico; Tomografia de coerência óptica; Pré-eclâmpsia; Fovea centralis; Comprimento axial do olho; Gravidez*

INTRODUCTION

Pre-eclampsia is a disorder characterized by widespread vasospasm and pathologic lesions in multiple organ systems, including the uteroplacental vascular bed. Observed in 5%-10% of all pregnancies, pre-eclampsia is a major cause of both maternal and fetal mortality and morbidity. It is typically seen after week 20 of gestation and frequently in first pregnancies[1]. In the pathophysiology of pre-eclampsia, although endothelial cell damage and impaired endothelial cell function play an important role, the cause of vascular endothelial cell dysfunction remains unknown[2]. Numerous organs, including the liver, eye, kidney, and those of the central nervous system, can be affected by pre-eclampsia due to increased systemic blood pressure and vascular endothelial damage[3]. Visual loss was reported in 30%-100% of patients with pre-eclampsia and associated with disorders of the choroidal and retinal circulation[4,5]. The presentation of the disorder involves lesions caused by ischemia in the retina pigment epithelium (RPE) and the choroid, as well as cotton wool spots, retinal hemorrhage and edema, papilledema, serous retinal detachment, and Elschnig spots[6].

As such, assessment of the choroid is crucial in ophthalmologic practice for the management of pre-eclampsia, which primarily affects the vascular system. Although indocyanine green angiography and B-scan ultrasonography are usually performed in the clinical assessment of the choroid, neither permits accurate cross-sectional imaging. Consequently, the recently developed optical coherence tomography (OCT) has proven valuable for observing changes in the retina and RPE. Furthermore, a new modality in choroidal imaging with OCT called enhanced depth imaging (EDI) has recently been increasingly used, enabling the acquisition of detailed images of tissues behind the RPE.

This study aimed to investigate subfoveal choroidal thickness (SFCT) in patients with pre-eclampsia during pregnancy and the postpartum period compared with that in healthy pregnant women using EDI-OCT.

Submitted for publication: October 25, 2015
Accepted for publication: February 10, 2016

[1] Department of Ophthalmology, Kayseri Education and Research Hospital, Kayseri, Turkey.
[2] Department of Obstetrics and Gynecology, Kayseri Education and Research Hospital, Kayseri, Turkey.
[3] Department of Ophthalmology, Niğde State Hospital, Niğde, Turkey.

Funding: No specific financial support was available for this study.

Disclosure of potential conflicts of interest: None of the authors have any potential conflict of interest to disclose.

Corresponding author: Necati Duru. Kayseri Education and Research Hospital. Department of Ophthalmology. Kayseri - Turkey - E-mail: necatiduru@gmail.com

METHODS

Study population and design

This cross-sectional study was conducted in the Ophthalmology and Gynecology Departments at Kayseri Education and Research Hospital in Kayseri, Turkey. The study adhered to the tenets of the Declaration of Helsinki and was approved by the local ethics committee. All participants received oral and written information about the study, and each participant provided written, informed consent.

A sample of 73 pregnant women was examined over a period of 28 weeks during gestation. Gestational age was based on the precise date of the woman's last period and ultrasound measurement of the crown-rump length during the first trimester. Pre-eclampsia was defined as hypertension (blood pressure of ≥140/90 on at least two occasions >4 h apart after 20 weeks of gestation) and new onset of proteinuria (≥2 + on dipstick reading, ≥0.3 g/d by 24-h urine collection, or ≥30 mg/mmol by protein-to-creatinine ratio). The study involved two groups: one of pre-eclamptic pregnant women (n=32) and another of healthy pregnant women (n=41). In cases in which both eyes of the patient were eligible for inclusion, only the right eye was included.

Examination protocol and study measurements

Each participant received a comprehensive ophthalmologic examination involving best-corrected visual acuity (BCVA), slit lamp biomicroscopy, dilated stereoscopic fundus examination, intraocular pressure (IOP) measured using Goldmann applanation tonometry, as well as axial length (AL) and OCT measurements. All examinations were performed by an experienced clinician (MU). AL was measured using IOL Master 500 (Carl Zeiss Meditec Inc, Jena, Germany). To assess SFCT, OCT (version 5.6.3.0; Spectralis OCT Heidelberg Engineering, Dossenheim, Germany) was used. All measurements were repeated at the third month of the postpartum period. Moreover, to avoid diurnal fluctuation, all examinations were performed between 10 a.m. and 12 a.m.

Exclusion criteria

Ocular exclusion criteria for this study included more than two diopters of cylindrical and/or spherical refractive error, a BCVA of less than 20/20, IOP readings >21 mmHg, glaucoma, uveitis, retinal disease, ocular trauma, dense media opacities, or a history of previous intraocular surgery, laser therapy, or significant ocular disease. Participants reporting a history of any medical or obstetrical problems (except pre-eclampsia) were excluded from the study.

EDI-OCT measurement

The method used for obtaining EDI-OCT images was previously reported[7,8]. SFCT was measured from the outer portion of the hyperreflective line corresponding to the RPE to the inner surface of the sclera. Images were acquired by an experienced clinician (MU) and assessed by an experienced clinician (MA), the later was blinded to group identity. A representative EDI-OCT choroidal image in a pregnant woman is seen in figure 1.

Statistical analysis

All statistical tests were performed using the Statistical Package for the Social Sciences v.20. Measurements of ocular parameters from the right eyes were used for analyses. For each continuous variable, normality was checked using the Kolmogorov-Smirnov test. Variables between pre-eclamptic pregnant and healthy pregnant women were compared using an independent Student's *t* test, and a paired *t* test was used to compare variables between the pregnancy and postpartum periods in each group. Probability (p) values of <0.05 were considered statistically significant.

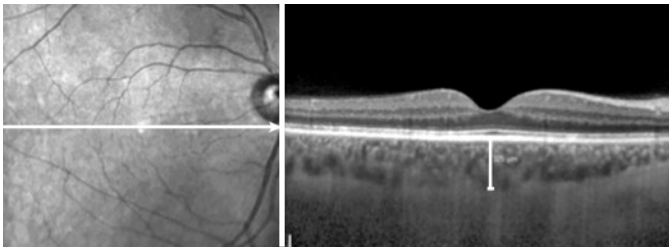

Figure 1. Measurement of subfoveal choroidal thickness performed in a pre-eclamptic pregnant women.

RESULTS

Table 1 summarizes the demographical and clinical features of the participants. No statistically significant differences were detected in terms of gestational week, age, AL, or IOP between groups (p=0.836, p=0.106, p=0.726, and p=0.936, respectively).

SFCT measurements and p values are shown in table 2. SFCT in pre-eclamptic pregnant women was 351.97 ± 22.44 µm (range, 309-403) and 332.28 ± 20.32 µm (range, 301-381) during the pregnancy and postpartum periods, respectively. In healthy pregnant women, these values were 389.73 ± 49.64 µm (range, 320-473) and 329.78 ± 22.36 µm (range, 299-399), respectively. A significant decrease in SFCT during the postpartum period compared with that during the pregnancy period was found in both groups (p<0.001), but the decrease in choroidal thickness (CT) was more prominent in healthy pregnant women. SFCT in pre-eclamptic pregnant women during pregnancy was significantly thinner than that in healthy pregnant women (p<0.001). However, there was no statistically significant difference in SFCT between the two groups during the postpartum period (p=0.623).

DISCUSSION

Although described as hypertension and proteinuria emerging during the second half of pregnancy, pre-eclampsia is a systemic, complex syndrome involving all body systems, not merely reflected by proteinuria and hypertension. Although its etiology is not entirely known, it is thought to consist of common endothelial damage, increased systemic vascular resistance, and generalized vasospasm caused by inadequate trophoblastic invasion and placentation[9,10].

Traditional methods used for assessing ocular findings in pre-eclampsia have, until recently, included indocyanine green angiography, ocular fluorophotometry and angiography, and Doppler ultrasonography[11-16]. Low image resolution, low validity ratio in measurements, and differences between observers are disadvantages of these methods. For these reasons, objective, reliable, quantitative, and highly sensitive imaging methods are required for the diagnosis and follow-up of ophthalmic disease in pregnant women. Appropriate imaging technologies were recently developed, one of which is OCT with a high-resolution tomographic section of the optic nerve head, retinal nerve fiber layer, and retina by using 800-840 nm wavelength light in a non-contact, non-invasive manner. More recently, EDI-OCT was developed for users to observe the morphology, thickness, and anatomy of the choroid.

A structurally and functionally normal choroid is critical to retinal functions. Oxygen and glucose are provided to the RPE and outer layers of the retina by choroidal circulation. The choroid also protects the thermal stability of the ocular tissues and removes ocular waste[17]. The structure and thickness of the choroid can be affected by several factors, different ocular pathologies, and systemic diseases[18-22]. Ocular pathologies such as choroidal neovascular membrane, uveal effusion syndrome, central serous chorioretinopa-

Table 1. Demographical and clinical features of healthy and pre-eclamptic pregnant women included in the study

Variables	Healthy pregnant women (control group)	Pre-eclamptic pregnant women (study group)	p*
Number of eyes/patients	41/41	32/32	
Age (year)			0.106
Average ± SD	27.54 ± 5.25	29.59 ± 5.43	
Range	18-38	18-43	
Gestational week			0.836
Average ± SD	31.98 ± 3.82	31.81 ± 2.89	
Range	28-39	28-37	
Axial length (mm)			0.726
Average ± SD	23.04 ± 0.77	23.11 ± 0.90	
Range	21.13-24.16	21.34-24.67	
Intraocular pressure (mmHg)			0.936
Average ± SD	13.37 ± 2.79	13.31 ± 2.87	
Range	9-19	9-21	

SD= standard deviation; *= independent Student's *t* test.

Table 2. The choroidal thicknesses in healthy and pre-eclamptic pregnant women at pre- and postpartum time points

	Prepartum (3rd trimester)	Postpartum (3rd month)	p†
Healthy pregnant women (SFCT) (µm) N=41 eyes			
Average ± SD	389.73 ± 49.64	329.78 ± 22.36	<0.001
Range	320-473	299-399	
Pre-eclamptic pregnant women (SFCT) (µm) N=32 eyes			
Average ± SD	351.97 ± 22.44	332.28 ± 20.32	<0.001
Range	309-403	301-381	
p*	<0.001	0.623	

SFCT= subfoveal choroidal thickness; SD= standard deviation; †= paired *t* test; *= independent Student's *t* test.

thy, Vogt-Koyanagi-Harada disease, angioid streaks, and polypoidal choroidal vasculopathy, as well as systemic diseases, including diabetes mellitus, can also affect the choroid[18-22]. Other studies have reported decreased CT in correlation with increased refractive errors, AL[23-25], or age[26]. Several studies have shown the effect of pregnancy on CT. Takahashi et al. compared CT in 30 healthy and 30 pregnant women and found no statistically significant difference between the groups[27]. Kara et al. found SFCT to be significantly increased in pregnant women than in healthy women in their study of 100 pregnant and 100 healthy non-pregnant women. They attributed this result to physiological hemodynamic changes occurring in pregnancy, such as increased cardiac output, arterial compliance, and decreased total vascular resistance[28]. Meanwhile, Sayin et al. found CT to be decreased in pre-eclamptic pregnant women than in healthy pregnant women[29]. Garg et al. assessed CT during the postpartum period in their study of 15 pre-eclamptic pregnant, 15 healthy pregnant, and 19 healthy non-pregnant women. They found that CT was significantly higher in pre-eclamptic women than in the other groups; a result that they attributed to increased vascular endothelial growth[30]. Nevertheless, until now, no study has compared CT in pre-eclamptic pregnant women between the pregnancy and postpartum periods. As such, to the best of our knowledge, the present study is the first to assess SFCT in pre-eclamptic pregnant women during and after pregnancy.

In this study, SFCT was found to be significantly thicker in healthy pregnant women than in pre-eclamptic pregnant women. CT decreased by a statistically significant margin, and both groups had similar values by the third month of the postpartum period. As such, it is possible that choroidal thinning in the pre-eclamptic group was caused by vascular vasospasm. Vascular vasospasm narrows choroidal vascular structures, resulting in decreased choroidal blood supply and, in turn, possible choroidal thinning.

In summary, vasoconstriction and the activation of thrombosis occurring with pre-eclampsia impair choroidal microcirculation by causing endothelial cell dysfunction. As a result, increased permeability and/or impairment of the normal blood-retina barrier may occur. Changes in choroidal structure should, therefore, be remembered in the differential diagnosis of visual loss in pre-eclamptic pregnant women. Future prospective studies with more patients are required, nevertheless, to establish the chorioretinal effects of pre-eclampsia.

REFERENCES

1. Perloff D. Hypertension and pregnancy-related hypertension. Cardiol Clin. 1998; 6(1):79-101.
2. Ober RR. Pregnancy-induced hypertension (preeclampsia-eclampsia). In: Ryan SJ, editor. Retina. St Louis, MO: CV Mosby; 1994. p.1393-403. Vol. 2.
3. Magee LA, Helewa M, Moutquin JM, von Dadelszen P; Hypertension Guideline Committee; Strategic Training Initiative in Research in the Reproductive Health Sciences (STIRRHS) Scholars. Diagnosis, evaluation, and management of the hypertensive disorders of pregnancy. J Obstet Gynaecol Can. 2008;30(3Suppl):S1-48.
4. Sheth BP, Mieler WF. Ocular complications of pregnancy. Curr Opin Ophthalmol. 2001;12(6):455-63.
5. Wagner HP. Arterioles of the retina in toxaemia of pregnancy. JAMA. 1933;101:1380-4.
6. Errera MH, Kohly RP, Cruz L. Pregnancy-associated retinal diseases and their management. Surv Ophthalmol. 2013;58:127-42.
7. Spaide RF, Koizumi H, Pozonni MC. Enhanced depth imaging spectral-domain optical coherence tomography. Am J Ophthalmol. 2008;146(4):496-500.
8. Margolis R, Spaide RF. A pilot study of enhanced depth imaging optical coherence tomography of the choroid in normal eyes. Am J Ophthalmol. 2009;147(5):811-5.
9. Dieti J. The pathogenesis of pre-eclampsia: new aspects. J Perinat Med. 2000;28(6): 464-71.
10. Redman CW, Sargent IL. Pre-eclampsia, the placenta and the maternal systemic inflammatory responseea review. Placenta. 2003;24(Suppl A):21-7.
11. Valluri S, Adelberg DA, Curtis RS, Olk RJ. Diagnostic indocyanine gren angiography in preeclampsia. Am J Ophthalmol. 1996;122(5):672-7.
12. Chaine G, Attali P, Gaudric A, Colin MC, Quentel G, Coscas G. Ocular fluorophotometric and angiographic findings in toxaemia of pregnancy. Arch Ophthalmol. 1986; 104(11):1632-5.
13. Fastenberg DM, Fetkenhour CL, Choromokos E, Schoch DE. Choroidal vascular changes in toxaemia of pregnancy. Am J Ophthalmol. 1980;89(3):362-8.

14. Mabie WC, Ober RR. Fluorescein angiography in toxaemia of pregnancy. Br J Ophthalmol. 1980;64(9):666-71.
15. Jaffe G, Schatz H. Ocular manifestations of preeclampsia. Am J Ophthalmol. 1987; 103(3 Pt 1):309-15.
16. Belfort MA, Saade GR. Retinal vasospasm associated with visual disturbance in preeclampsia: colour flow Doppler findings. Am J Obstet Gynecol. 1993;169(3):523-5.
17. Nickla DL, Wallman J. The multifunctional choroid. Prog Retin Eye Res. 2010;29(2): 144-68.
18. Maruko I, Iida T, Sugano Y, Ojima A, Sekiryu T. Subfoveal choroidal thickness in fellow eyes of patients with central serous chorioretinopathy. Retina. 2011;31(8):1603-8.
19. Imamura Y, Fujiwara T, Margolis R, Spaide RF. Enhanced depth imaging optical coherence tomography of the choroid in central serous chorioretinopathy. Retina. 2009;29(10):1469-73.
20. Manjunath V, Goren J, Fujimoto JG, Duker JS. Analysis of choroidal thickness in age-related macular degeneration using spectral-domain optical coherence tomography. Am J Ophthalmol. 2011;152(4):663-8.
21. Kim SW, Oh J, Kwon SS, Yoo J, Huh K. Comparison of choroidal thickness among patients with healthy eyes, early age-related maculopathy, neovascular age-related macular degeneration, central serous chorioretinopathy, and polypoidal choroidal vasculopathy. Retina. 2011;31(9):1904-11.
22. Harada T, Machida S, Fujiwara T, Nishida Y, Kurosaka D. Choroidal findings in idiopathic uveal effusion syndrome. Clin Ophthalmol. 2011;5:1599-601.
23. Maruko I, Iida T, Sugano Y, Oyamada H, Sekiryu T, Fujiwara T, et al. Subfoveal choroidal thickness after treatment of Vogt-Koyanagi-Harada disease. Retina. 2011;31(3):510-7.
24. Esmaeelpour M, Považay B, Hermann B, Hofer B, Kajic V, Hale SL, et al. Mapping choroidal and retinal thickness variation in type 2 diabetes using three-dimensional 1060-nm optical coherence tomography. Invest Ophthalmol Vis Sci. 2011;52(8):5311-6.
25. Nishida Y, Fujiwara T, Imamura Y, Lima LH, Kurosaka D, Spaide RF. Choroidal thickness and visual acuity in highly myopic eyes. Retina. 2012;32(7):1229-36.
26. Ikuno Y, Kawaguchi K, Nouchi T, Yasuno Y. Choroidal thickness in healthy Japanese subjects. Invest Ophthalmol Vis Sci. 2010;51(4):2173-6.
27. Takahashi J, Kado M, Mizumoto K, Igarashi S, Kojo T. Choroidal thickness in pregnant women measured by enhanced depth imaging optical coherence tomography. Jpn J Ophthalmol. 2013;57(5):435-9.
28. Kara N, Sayin N, Pirhan D, Vural AD, Araz-Ersan HB, Tekirdag AI, et al. Evaluation of subfoveal choroidal thickness in pregnant women using enhanced depth imaging optical coherence tomography. Curr Eye Res. 2014;39(6):642-7.
29. Sayin N, Kara N, Pirhan D, Vural A, Araz Ersan HB, Tekirdag AI, et al. Subfoveal choroidal thickness in preeclampsia: comparison with normal pregnant and nonpregnant women. Semin Ophthalmol. 2014;29(1):11-7.
30. Garg A, Wapner RJ, Ananth CV, Dale E, Tsang SH, Lee W, et al. Choroidal and retinal thickening in severe preeclampsia. Invest Ophthalmol Vis Sci. 2014;55(9):5723-9.

Six-month outcomes of corneal crosslinking with dextran-free isotonic riboflavin solution

Resultados após seis meses de crosslinking *de córnea com solução isotônica de riboflavina sem dextrano*

Refik Oltulu[1], Gunhal Satirtav[1], Meryem Donbaloglu[1], Mehmet Kemal Gunduz[1], Hurkan Kerimoglu[1], Mehmet Okka[1], Ahmet Ozkagnici[1], Adnan Karaibrahimoglu[2]

ABSTRACT

Purpose: To analyze the short-term clinical and topographic outcomes in patients with keratoconus after corneal collagen cross-linking treatment (CXL) with dextran-free isotonic riboflavin solution.

Methods: In this retrospective case series, 26 eyes from 26 patients with keratoconus were studied. The best corrected visual acuity (BCVA) and refractive and topographic findings were analyzed at a 6-month follow-up.

Results: The mean BCVA (Snellen lines) values before and 1, 3, and 6 months after CXL were 0.51 ± 0.2, 0.48 ± 0.2, 0.57 ± 0.2, and 0.64 ± 0.2, respectively, and the difference between the preoperative and 6-month values was statistically significant (p=0.006). The mean spherical equivalent refraction decreased from -5.6 ± 2.4 diopters (D) preoperatively to -5.0 ± 2.1 D, and mean simulated keratometry decreased from 48.5 ± 2.5 D to 47.8 ± 2.6 D at 6 months. (p=0.145 and p=0.001, respectively). In addition, the maximum keratometry decreased progressively and significantly from the preoperative value during follow-up (p=0.003). The central and minimal corneal thicknesses, including those of the epithelium, also decreased from 442.8 ± 25.6 µm and 430.5 ± 23.9 µm preoperatively to 420.7 ± 31.8 µm and 409.3 ± 28.7 µm at the most recent follow-up (p<0.001), respectively. No intraoperative or postoperative complications were observed.

Conclusions: CXL with dextran-free isotonic riboflavin solution appears to be a safe treatment alternative for keratoconus and yields sustained short-term improvements in visual acuity, keratometric readings, and corneal thickness. However, long-term results are needed to confirm these outcomes.

Keywords: Cornea; Collagen; Cross-linking reagents; Riboflavin/therapeutic use; Ultraviolet rays; Dextrans; Visual acuity

RESUMO

Objetivo: *Analisar os resultados clínicos e topográficos curto prazo após* crosslinking *(CXL) de córnea com solução isotônica de riboflavina sem dextrano, em pacientes com ceratocone.*

Método: *Estudamos 26 olhos de 26 pacientes com ceratocone, nesta série retrospectiva de casos. Melhor acuidade visual corrigida (BCVA), refração e achados topográficos foram analisados aos 6 meses de acompanhamento.*

Resultados: *BCVA pré-operatória (linhas de Snellen) foi de 0,51 ± 0,2. BCVA após CXL foram de 0,48 ± 0,2, 0,57 ± 0,2 e 0,64 ± 0,2 no 1º, 3º e 6º meses, respectivamente. A diferença entre a BCVA pré-operatória e mais recente foi estatisticamente significativa (p=0,006). O equivalente esférico médio diminuiu de -5,6 ± 2,4 dioptrias (D) no pré-operatório para -5.0 ± 2.1 D e a média da ceratometria simulada diminuiu de 48,5 ± 2,5 D para 47, 8± 2,6 D aos 6 meses. (p=0,145 e p=0,001, respectivamente). A ceratometria máxima diminuiu progressivamente durante o acompanhamento com as mudanças sendo significativamente diferentes do valor pré-operatório (p=0,003). As espessuras corneanas central e mínima, diminuiram de 442,8 ± 25,6 µm e 430,5 ± 23,9 µm para 420,7 ± 31,8 µm e 409,3 ± 28,7 µm, respectivamente, na visita mais recente (p<0,001). Não foram observadas complicações intraoperatórias e pós-operatórias.*

Conclusões: *CXL com solução de riboflavina isotônica sem dextrano parece ser uma opção segura de tratamento para o ceratocone com melhora mantida na acuidade visual, ceratometria e espessura corneana, no curto prazo. Resultados a longo prazo são necessários para confirmar estes resultados.*

Descritores: *Córnea; Colágeno; Reagentes para ligações cruzadas; Riboflavina/uso terapêutico; Raios ultravioleta; Dextranos; Acuidade visual*

INTRODUCTION

Keratoconus is a bilateral, asymmetric, non-inflammatory, and slowly progressive corneal disease with an approximate incidence of 1 in 2000 individuals. This condition is characterized by corneal thinning and protrusion, progressive myopia, and irregular astigmatism[1] and has conventionally been treated using modalities, such as rigid contact lenses, intrastromal corneal ring segment implantation, and keratoplasty. However, current treatment objectives include not only improved visual acuity but also the prevention of disease progression[2]. Accordingly, corneal cross-linking (CXL) is a relatively new treatment method designed to increase the mechanical and biochemical strength of the stromal tissue via exposure of the ectatic cornea to riboflavin and ultraviolet-A (UVA) light[3]. This procedure is the only currently available semisurgical therapeutic approach for patients with progressing keratoconus and has been shown to delay or even stop the progression of corneal ectasia, thus reducing the need for keratoplasty[4].

A minimum safety limit is defined as 400 µm for corneal preoperative thickness to avoid damage of ultraviolet A (UV-A) irradiation to endothelium, lens, and deeper structures[5,6].

Different CXL techniques for thin corneas have been developed, including transepithelial CXL[7] and CXL with customized pachymetric-guided epithelial debridement preserving the epithelium in thinner corneal regions[8]. Alternatively, the induction of iatrogenic corneal swelling via the administration of hypo-osmolar riboflavin solutions before CXL application has been proposed as an alternative method for corneas thinner than 400 µm[9]. However, the duration of thickening induced by hypo-osmolar solutions is controversial, given that some reports indicate a failure of this effect to persist throughout the procedure, thus rendering deeper structures vulnerable to possible

Submitted for publication: July 21, 2015
Accepted for publication: February 10, 2016

[1] Department of Ophthalmology, Meran Faculty of Medicine, Konya, Turkey.
[2] Biostatistics Unit, Department of Medical Education and Informatics, Meran Faculty of Medicine, Konya, Turkey.

Funding: No specific financial support was available for this study.

Disclosure of potential conflicts of interest: None of the authors have any potential conflicts of interest to disclose.

Corresponding author: Refik Oltulu. Department of Ophthalmology. Meram Faculty of Medicine. Necmettin Erbakan University, Meram, Konya - 42080 - Turkey - E-mail: refikoltulu@gmail.com

Approved by the following research ethics committee: Meram Faculty of Medicine, Necmettin Erbakan University (#4532, June 30th 2014).

side effects from ultraviolet light exposure towards the end of the procedure[10]. Notably, a recently introduced iso-osmolar riboflavin solution that contains hydroxymethylcellulose instead of dextran is considered a possible alternative to hypo-osmolar solutions in cases with thin corneas.

In the present study, changes in visual acuity and refractive and topographic outcomes were analyzed after CXL treatment performed with this newly introduced dextran-free, isotonic riboflavin solution.

METHODS

Twenty-six eyes of 26 patients (12 males, 14 females; mean age: 25.1 ± 4.6 years, range: 18-33 years) with progressive keratoconus who underwent CXL between September 2012 and October 2013 at Necmettin Erbakan University Meram Faculty of Medicine were included in this study. The local ethics committee approved this study, which adhered to the tenets of Declarations of Helsinki, and informed consent was obtained from all patients. The inclusion criteria were keratoconus with documented progression in the past 12 months, defined as an increase in maximum keratometry (Kmax) of 1.00 diopter (D) or more in the previous 12 months; corneal thickness of at least 400 µm at the thinnest point; age of at least 18 years; and patient-reported deterioration of visual acuity (excluding other possible non-corneal reasons for deterioration). The exclusion criteria were corneal opacity, previous ocular surgery, previous herpetic keratitis, active ocular infection, autoimmune disease, chemical injury, delayed epithelial healing, and lactation at the time of the study.

The CXL procedure was performed under sterile conditions in a surgical room according to the following description. After administering 0.5% propacaine drops (Alcaine; Alcon Pharmaceuticals, Fribourg, Switzerland) as a topical anesthestic, the corneal epithelium was removed by mechanical debridement over the central 8.0 mm. A dextran-free isotonic riboflavin solution [>0.1% riboflavin with 1.1% hydroxypropylmethylcellulose (MedioCROSS M; Kiel, Germany)] was applied to the cornea every 3 min for 30 min. After 30 min, UVA (370 nm, 3 mW/cm^2 intensity) was applied to the cornea (CCL-VARİO; Peschke Meditrade GmbH, Huenenberg, Switzerland) for 30 min. Application of the riboflavin solution continued every 3 min during irradiation. Ultrasound pachymetry (OcuScan RxP; Alcon Laboratories, Inc., Fort Worth, TX, USA) was performed on the de-epithelialized cornea at approximately the thinnest point, which had been determined preoperatively from a corneal pachymetry map obtained via corneal topography. Three repeated measurements were taken by the same surgeon (RO) after de-epithelization, at 15, 30, and 45 min into the procedure, and at the end of the procedure. For each, the average of 10 measurements was taken, and the mean value obtained from the 3 measurements was used for the evaluation. Topical anesthetics were added as needed during the procedure. Postoperatively, a bandage contact lens (PureVision (balafilcon A); Bausch & Lomb, Rochester, NY, USA) was placed, and levofloxacin and dexamethasone eyedrops were administered 4 times daily until epithelization was complete.

At baseline and each of the postoperative follow-up examinations (1, 3, 6 months), all patients underwent ophthalmological evaluations to measure the best corrected visual acuity (BCVA), refraction (spherical equivalent, diopters; D) and corneal topography (Pentacam; Oculus GmbH, Wetzlar, Germany). The preoperative and postoperative K-readings of Kmax and mean simulated keratometry (Sim K) were assessed from topography data.

All variables were found to be normally distributed according to the Kolmogorov-Smirnov test. The statistical power analysis yielded a power of approximately 35%. The Friedman two-way analysis of variance test was used to compare preoperative and postoperative data. Following a Bonferroni correction, a p value of <0.0083 was considered statistically significant in comparison tests.

RESULTS

The mean baseline BCVA was 0.51 ± 0.2 (Snellen lines), and the corresponding readings after CXL were 0.48 ± 0.2, 0.57 ± 0.2, and 0.64 ± 0.2 at the 1-, 3-, and 6-month follow-ups, respectively. A significant difference was observed between the baseline and 6-month postoperative BCVA values (p=0.006; Figure 1). The preoperative mean spherical equivalent (SEQ) refraction was -5.6 ± 2.4 D; although this parameter decreased to -5.0 ± 2.1 D at the last follow-up (SEQ change=0.59 D), this change was not statistically significant (p=0.145; Figure 2). In other words, an inverse relationship was observed between the SEQ and BCVA values.

Compared with the baseline, the mean Sim K increased slightly during the first postoperative month (p=0.407), followed by a decrease at the 3-month follow-up (p=0.361) and subsequent plateau from 48.5 ± 2.5 D to 47.8 ± 2.6 D at the 6-month follow-up (p=0.001). The mean Kmax exhibited a progressive decrease over 6 months, and this change represented a significant difference from the baseline value (p=0.003; Figure 3).

Before surgery, the central corneal thickness (CCT) and minimal corneal thickness (MCT), including the epithelium, were 442.8 ± 25.6 µm and 430.5 ± 23.9 µm, respectively. These values decreased to 417.6 ± 31.9 µm and 407.2 ± 31.1 µm, respectively, at 3 months but subsequently increased to 420.7 ± 31.8 µm and 409.3 ± 28.7 µm, respectively at 6 months. Notably, the differences between the preoperative and postoperative CCT and MCT values were statistically significant at every time point during follow-up (p<0.001; Figure 4). At baseline, the mean preoperative MCT, including the

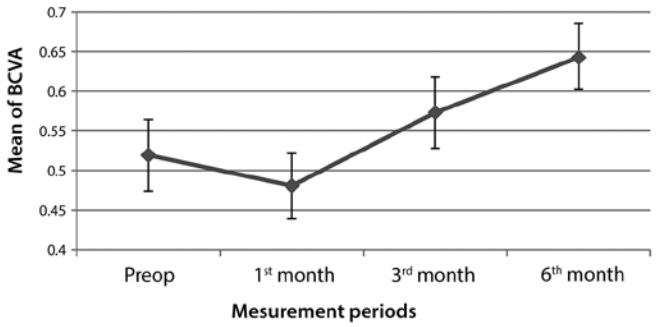

BCVA= best corrected visual acuity.

Figure 1. Graph representing changes in best corrected visual acuity over time.

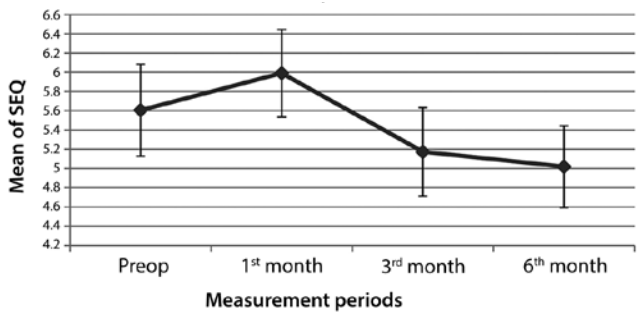

SEQ= mean spherical equivalent.

Figure 2. Graph representing changes in spherical equivalent refractive values of the eyes over time.

epithelium, measured 430.5 ± 23.9 µm; this was reduced to 396.8 ± 21.3 µm after removal of the epithelium. After the application of dextran-free isotonic riboflavin solution, the MCT exhibited a steady increase at the 15-, 30-, 45-, and 60-min time points during the procedure (422.3 ± 19.1 µm, 450.4 ± 14.9 µm, 459.1 ± 15.7 µm, and 464.9 ± 15.5 µm, respectively).

No eye exhibited a sterile or infectious infiltrate in the corneal stroma after surgery, and no complications were observed after the application of dextran-free isotonic riboflavin solution. All corneas demonstrated normal progression with respect to the epithelial healing process. At the final follow-up examination (6 months after CXL), all corneas were transparent, with no detectable stromal scarring.

DISCUSSION

Riboflavin-induced ultraviolet-light CXL has received a significant amount of attention in recent years. Previous studies have demonstrated the safety and efficacy of CXL for preventing the progression of keratoconus[10-12]. In this procedure, riboflavin serves as a photosensitizer for crosslink induction and protects the underlying tissues from the deleterious effects of UVA irradiation; in addition, it prevents corneal dehydration during the operative procedure[13]. In cases with particularly thin corneas, a 0.1% hypo-osmolar riboflavin solution can also be applied to artificially swell the cornea to a thickness of at least 400 µm before CXL, thus reducing the risk of UVA-induced endothelial cytotoxicity[9].

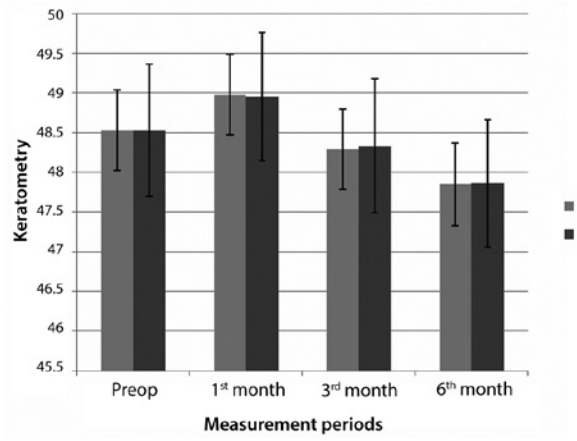

Sim K= average simulated keratometry; Kmax= maximal keratometry.

Figure 3. Bar graph demonstrating the Kmax and Sim K values (measures of keratoconus) before surgery and at 1, 3, and 6 months after corneal crosslinking.

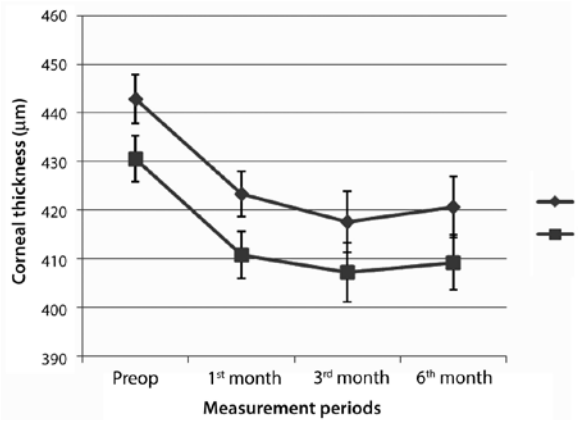

CCT= central corneal thickness; MCT= minimal corneal thickness.

Figure 4. Changes in the central corneal thickness and minimum corneal thickness measurements over time in patients with keratoconus.

According to an earlier protocol described by Hafezi et al., UVA treatment was administered after inducing iatrogenic corneal swelling with hypo-osmolar riboflavin solution to a minimum corneal thickness of 400 µm, a procedure that was found to efficiently increase the stromal thickness by 25% after 30 min[9]. In this procedure, the application of iso-osmolar riboflavin solution continued during UVA irradiation. This led to concerns regarding the durability of corneal thickness throughout the procedure such as those raised by Kaya et al., who suggested that the iatrogenic swelling induced by a hypo-osmolar riboflavin solution might be short-acting and thus would not persist throughout UVA application, following an observed decrease in the corneal thickness upon the installation of the iso-osmolar riboflavin solution[10].

Previous studies and the standard CXL procedure have generally used an iso-osmolar riboflavin 0.1% solution containing 20% dextran (402.7 mOsmol/L), which exerts a temporary dehydrating effect and consequent corneal thinning. In contrast, we performed the CXL procedure with a dextran-free isotonic riboflavin solution and observed that the corneal thickness increased throughout the procedure, in agreement with the results of a previous study[14]. However, the safety CXL in the presence of an artificially swollen cornea remains controversial because the lower concentration of collagen fibers in the hydrated stroma is expected to weaken the crosslinking effect of UVA, as demonstrated in experiments with collagen gels[15].

The current study aimed to analyze the variables related to short-term outcomes in a group of patients with keratoconus who were treated via corneal CXL with a dextran-free isotonic riboflavin solution. After an initial worsening of all keratoconus indices and BCVA, likely due to epithelial debridement, continuous improvements were observed in most keratometric and topographic indices for up to 6 months after surgery. In previous studies, BCVA has been reported to improve by 2 Snellen lines at 36 months and 1.05 Snellen lines at 12 months after CXL[12,16]. In another study, Goldich et al. observed a significant improvement in the BCVA (0.21 ± 0.1 to 0.14 ± 0.1; p=0.002)[17]. Our results demonstrated a significant improvement of 1.03 Snellen lines in the BCVA at 6 months.

A previous study conducted by Wittig-Silva et al. failed to exhibit changes in the SEQ or the spherical or cylindrical component of subjective refraction[18]. However, other studies have reported changes in SEQ ranging from +0.40 D to +2.13 D[12,19,20]. Similarly, Caporossi et al. observed a decrease in the SEQ value of 2.21 D at 3 months after CXL[21], and Wollensak et al. reported a significant improvement of 1.14 D in the average SEQ at 6 months postoperatively[11]. In our study, we observed a mean improvement in the SEQ of 0.6 D at the 6-month follow-up; in addition, this was the lowest SEQ observed in this study. However, the change in this parameter failed to reach statistical significance, possibly as a result of the limited number of patients in our study.

With respect to corneal curvature, we observed significant reductions in the mean Kmax and Sim K values of 1.26 and 0.73 D, respectively, at 6 months postoperatively. Caporossi et al. reported similar results, with a postoperative average reduction in the mean keratometry measurement of 1.96 D[21]. Similarly, Wollensak et al. reported a reduction in the mean keratometry reading of 2.01 D[11].

Similar to previous studies, the corneal thickness decreased from the preoperative to the final time point, indicating corneal compaction[20,22,23]. In our study, statistically significant differences between the pre- and postoperative measurements were detected when the corneal thicknesses at the apex of the keratoconus (MCT) and pupil center (CCT) were measured. Notably, the CCT initially decreased significantly from the baseline up to the 3-month time point but exhibited

significant improvement at the 6-month follow-up. The MCT values similarly decreased from the baseline, although the 6-month value remained significantly below the preoperative value.

To the best of our knowledge, the outcomes of CXL treatment with a dextran-free isotonic riboflavin solution have not been reported previously. This study demonstrated improvements in outcomes related to keratometry and visual acuity in patients undergoing CXL with a dextran-free isotonic riboflavin solution, similar to the improvements observed in patients from previous studies who were treated with dextran-containing solutions. Furthermore, we reported that the use of a dextran-free iso-osmolar riboflavin solution during CXL induced a steady increase in corneal thickness throughout the procedure. This finding might be beneficial with respect to an increased indication for CXL in patients with thin corneas, as it removes the concern of unpredictable intraoperative thinning below the safety margin reported in our other study[14]. We note that the improvements in visual acuity and keratometry readings were found to occur progressively throughout the postoperative follow-up period, suggesting that a longer follow-up is needed to determine the total functional and anatomic effects of CXL and to obtain stable functional and keratometric values. The small number of subjects in the study group, lack of a control group comprising patients treated with a standard dextran-containing riboflavin solution, and the short follow-up period were limitations of our present study.

In conclusion, this study has demonstrated the safety of CXL with a dextran-free isotonic riboflavin solution for the treatment keratoconus. This procedure was found to yield good visual results and to reduce disease progression, as well as iso-osmolar solutions containing dextran.

REFERENCES

1. Rabinowitz YS. Keratoconus. Surv Ophthalmol. 1998;42(4):297-319.
2. Jhanji V, Sharma N, Vajpayee RB. Management of keratoconus: current scenario. Br J Ophthalmol. 2011;95(8):1044-50.
3. Sedaghat M, Naderi M, Zarei-Ghanavati M. Biomechanical parameters of the cornea after collagen crosslinking measured by waveform analysis. J Cataract Refract Surg. 2010; 36(10):1728-31.
4. Raiskup-Wolf F, Hoyer A, Spoerl E, Pillunat LE. Collagen cross-linking with riboflavin and ultraviolet-A light in keratoconus: long-term results. J Cataract Refract Surg. 2008; 34(5):796-801.
5. Wollensak G, Spoerl E, Wilsch M, Seiler T. Endothelial cell damage after riboflavin-ultraviolet-A treatment in the rabbit. J Cataract Refract Surg. 2003;29(9):1786-90.
6. Wollensak G, Spoerl E, Wilsch M, Seiler T. Keratocyte apoptosis after corneal collagen cross-linking using riboflavin/UVA treatment. Cornea. 2004;23(1):43-9.
7. Çerman E, Toker E, Ozarslan Ozcan D. Transepithelial versus epithelium-off crosslinking in adults with progressive keratoconus. J Cataract Refract Surg. 2015;41(7):1416-25.
8. Kymionis GD, Diakonis VF, Coskunseven E, Jankov M, Yoo SH, Pallikaris IG. Customized pachymetric guided epithelial debridement for corneal collagen cross linking. BMC Ophthalmol. 2009;9:10-4.
9. Hafezi F, Mrochen M, Iseli HP, Seiler T. Collagen crosslinking with ultraviolet-A and hypoosmolar riboflavin solution in thin corneas. J Cataract Refract Surg. 2009;35(4): 621-4.
10. Kaya V, Utine CA, Yılmaz ÖF. Intraoperative corneal thickness measurements during corneal collagen cross-linking with hypoosmolar riboflavin solution in thin corneas. Cornea. 2012;31(5):486-90. Comment in: Cornea. 2012;31(12):1508-9; Cornea. 2013; 32(1):110.
11. Wollensak G, Spoerl E, Seiler T. Riboflavin/ultraviolet-a-reduced collagen crosslinking for the treatment of keratoconus. Am J Ophthalmol. 2003;135(5):620-7.
12. Hersh PS, Greenstein SA, Fry KL. Corneal collagen crosslinking for keratoconus and corneal ectasia: one-year results. J Cataract Refract Surg. 2011;37(1):149-60.
13. Caporossi A, Mazzotta C, Baiocchi S, Caporossi T. Long-term results of riboflavin ultraviolet a corneal collagen cross-linking for keratoconus in Italy: the Siena eye cross study. Am J Ophthalmol. 2010;149(4):585-93.
14. Oltulu R, Şatirtav G, Donbaloğlu M, Kerimoğlu H, Özkağnici A, Karaibrahimoğlu A. Intraoperative corneal thickness monitoring during corneal collagen cross-linking with isotonic riboflavin solution with and without dextran. Cornea. 2014;33(11):1164-7.
15. Ahearne M,Yang Y, Then KY, Liu KK. Non-destructive mechanical characterisation of UVA/riboflavin crosslinked collagen hydrogels. Br J Ophthalmol. 2008;92(2):268-71.
16. O'Brart DP, Kwong TQ, Patel P, McDonald RJ, O'Brart NA. Long-term follow-up of riboflavin/ultraviolet A (370 nm) corneal collagen cross-linking to halt the progression of keratoconus. Br J Ophthalmol. 2013;97(4):433-7.
17. Goldich Y, Marcovich AL, Barkana Y, Mandel Y, Hirsh A, Morad Y, et al. Clinical and corneal biomechanical changes after collagen cross-linking with riboflavin and UV irradiation in patients with progressive keratoconus: results after 2 years of follow-up. Cornea. 2012;31(6):609-14.
18. Wittig-Silva C, Chan E, Islam FM, Wu T, Whiting M, Snibson GR. A randomized, controlled trial of corneal collagen cross-linking in progressive keratoconus: three-year results. Ophthalmology. 2014;121(4):812-21.
19. Vinciguerra R, Romano MR, Camesasca FI, Azzolini C, Trazza S, Morenghi E, et al. Corneal cross-linking as a treatment for keratoconus: four-year morphologic and clinical outcomes with respect to patient age. Ophthalmology. 2013;120(5):908-16.
20. Vinciguerra P, Albe E, Trazza S, Rosetta P, Vinciguerra R, Seiler T, et al. Refractive, topographic, tomographic, and aberrometric analysis of keratoconic eyes undergoing corneal cross-linking. Ophthalmology. 2009;116(3):369-78.
21. Caporossi A, Baiocchi S, Mazzotta C, Traversi C, Caporossi T. Parasurgical therapy for keratoconus by riboflavin-ultraviolet type A rays induced cross-linking of corneal collagen. J Cataract Refract Surg. 2006;32(5):837-45. Comment in: J Cataract Refract Surg. 2007;33(7):1143-4; author reply 1144.
22. Greenstein SA, Shah VP, Fry KL. Corneal thickness changes after corneal collagen cross-linking for keratoconus and corneal ectasia: one-year results. J Cataract Refract Surg. 2011;37(4):691-700.
23. Vinciguerra P, Albe E, Trazza S, Seiler T, Epstein D. Intraoperative and post-operative effects of corneal collagen cross-linking on progressive keratoconus. Arch Ophthalmol. 2009;127(10):1258-65.

Factors affecting visual acuity after accelerated crosslinking in patients with progressive keratoconus

Fatores que afetam a acuidade visual após crosslinking *acelerado entre pacientes com ceratocone progressivo*

Ahmet Kirgiz[1], Kürşat Atalay[1], Kübra Şerefoğlu Çabuk[1], Havva Kaldirim[1], Muhittin Taşkapili[2]

ABSTRACT

Purpose: The present study aimed to report the outcomes of patients with progressive keratoconus who were treated via accelerated crosslinking (CXL) 6 months earlier and to determine the factors that promoted improved visual acuity after treatment.

Methods: This retrospective study included 35 eyes of 34 patients with progressive keratoconus who underwent CXL. Topographical measurements were obtained preoperatively and in the first, third, and sixth months postoperatively using a rotating Scheimpflug camera. The uncorrected visual acuity (UCVA), best-corrected visual acuity (BCVA), flat keratometry (K) value (K1), steep K value (K2), average K value (avgK), topographic cylindrical value (Cyl), apical keratoscopy front (AKf), apical keratoscopy back (AKb), symmetry index front (SIf), symmetry index back (SIb), and thinnest point of the cornea (ThkMin) were recorded.

Results: At the 6-month follow-up, the mean UCVA and BCVA values were improved, and the K values remained stable. Statistically significant decreases in AKf (p=0.04) and the thinnest point of the cornea (p=0.001) and a statistically significant increase in AKb (p=0.01) were observed. A correlation analysis revealed that the preoperative BCVA, UCVA, K1, K2, avgK, AKf, and AKb values significantly affected visual acuity at the 6-month follow-up.

Conclusions: Accelerated CXL is an effective treatment for the prevention or even reversal of keratoconus progression. The preoperative K values and apexes of the anterior and posterior cornea were found to affect visual acuity at 6 months after accelerated CXL. Both AKb steepening and AKf flattening appear to be important factors in the stabilization of keratometric values and improvement of visual outcomes.

Keywords: Cornea; Keratoconus/therapy; Riboflavin/therapeutic use; Ultraviolet rays; Cross-linking reagents; Visual acuity

RESUMO

***Objetivo**: O objetivo do estudo é relatar os resultados do sexto mês após o tratamento de* crosslinking *acelerado (CXL) em pacientes com ceratocone progressivo e determinar os fatores que afetam a melhora da acuidade após o tratamento.*

***Métodos**: Neste estudo retrospectivo, foram incluídos 35 olhos de 34 pacientes com ceratocone progressivo que se submeteram CXL. Acuidade visual não corrigida (UCVA) e melhor acuidade visual corrigida (BCVA) foram registradas. Medidas topográficas foram obtidas utilizando uma câmara Scheimpflug rotativa no pré-operatório e no 1º, 3º e 6º meses após a cirurgia. Os valores de ceratometria (K) mais plana (K1), K mais curva (K2), médio de K (avgK), astigmatismo topográfico (Cyl), ápice anterior da ceratoscopia (AKf), ápice posterior da ceratoscopia (AKb), índice anterior de simetria (SIf), índice posterior de simetria (SIb) e ponto mais fino da córnea (ThkMin) foram avaliados.*

***Resultados**: A média UCVA e BCVA melhoraram, enquanto valores de K ficaram estáveis 6º mês. Houve uma diminuição estatisticamente significativa na AKf e um aumento estatisticamente significativo na AKb (p=0,04, p=0,01, respectivamente). O ponto mais fino da córnea diminuiu significativamente (p=0,001). Na análise de correlações, além da UCVA e BCVA pré-operatórias; valores K1, K2, avgK, AKf e AKb pré-operatórios influenciaram significativamente a acuidade visual no 6º mês de acompanhamento.*

***Conclusões**: CXL acelerado é uma forma eficaz de tratamento na prevenção ou no mesmo inversão da progressão do ceratocone. A acuidade visual no 6º mês após CXL acelerado foi afetada a partir dos valores de K e dos ápice anterior e posterior da córnea. Encurvamento do AKb e aplanamento do AKf parecem ser fatores importantes na estabilização dos valores ceratométricos e na melhora da acuidade visual.*

***Descritores**: Córnea; Ceratocone/terapia; Riboflavina/uso terapêutico; Raios ultravioleta; Reagentes para ligações cruzadas; Acuidade visual*

INTRODUCTION

Keratoconus is a bilateral, asymmetric, degenerative disorder of the cornea with an unknown etiology and is characterized by progressive distortion of the anterior corneal surface and apical thinning of the stroma, leading to significant visual morbidity[1]. Currently, corneal collagen crosslinking (CXL), which induces covalent binding between individual collagen fibers to increase the stiffness and rigidity of the anterior corneal stroma, is considered the most effective treatment modality for delaying the progression of keratoconus[2-4]. CXL treatment relies on a photochemical reaction between riboflavin (vitamin B2) and ultraviolet A (UVA); specifically, riboflavin acts as a photosensitizer to induce crosslinking between collagen fibrils and as a shield to protect underlying tissues from UVA damage[5]. Accelerated CXL delivers a higher irradiation dose to the cornea and reduces the required light exposure time, thus improving patient comfort and decreasing the likelihood of complications[6].

CXL alters the corneal shape and structure and improves visual acuity, and thus the results of this treatment may be affected by structural changes[7]. In particular, CXL is known to reduce the anterior corneal keratometric values; however, elucidation of the postoperative posterior corneal changes requires further investigation[2-4]. Although previous studies have evaluated biomechanical and clinical changes in this context, the effects of these changes on visual acuity remain unclear[8]. In this study, we aimed to report the 6-month results of accelerated CXL in patients treated for progressive keratoconus and to determine the factors affecting visual acuity after treatment.

Submitted for publication: October 22, 2015
Accepted for publication: February 11, 2016

[1] Department of Opthalmology, Bagcilar Training and Research Hospital, Istanbul, Turkey.
[2] Beyoglu Eye Training and Research Hospital, Istanbul, Turkey.

Funding: No specific financial support was available for this study.

Disclosure of potential conflicts of interest: None of the authors have any potential conflicts of interest to disclose.

Corresponding author: Ahmet Kırgız. Bagcilar Training and Research Hospital, Eye Clinic. Merkez MH, Mimar Sinan CD, 6 - Istanbul - Turkey - E-mail: ahmetk1@yahoo.com

Approved by the following research ethics committee: Bagcilar Training and Research Hospital (# 213, 13 May 2015).

METHODS

This retrospective study was approved by the local ethics committee. The subjects included 35 eyes (19 right, 16 left) of 34 patients (14 female, 20 male; mean age: 24.77 ± 6.87 years) with progressive keratoconus who underwent CXL between July 2014 and January 2015 at in Bagcilar Education and Research Hospital, Istanbul, Turkey. Progressive keratoconus was defined as an increase of at least 1.00 diopter (D) in the steepest keratometry (K) measurement or the loss of at least 2 lines in the best corrected distance visual acuity within 1 year. Patients with history of corneal surgery, chemical injury, or delayed epithelial healing, those with a corneal pachymetry less than 400 µm, and women who were pregnant or lactating during the course of the study were excluded.

All patients underwent accelerated CXL according to the following procedure. Initially, a topical anesthetic agent was administered, and the central 8.0-mm epithelium was removed with a blunt spatula. Riboflavin (0.1% in 20% dextran solution) was then administered topically every 3 minutes for 30 minutes. The cornea was aligned and exposed to UVA (365 nm) for 5 minutes at an irradiance of 18 mW/cm^2 (Peschke Meditrade GmbH, Hünenberg, Switzerland). Isotonic riboflavin administration was continued every minute during UVA exposure. After treatment, the eye surface was washed with 20.0 mL of a balanced salt solution. Postoperatively, antibiotic and corticosteroid drops were administered and a soft contact lens bandage was placed. This contact lens was removed after the closure of the epithelial defect. Antibiotics and corticosteroid drops were continued 4 times daily for 1 week and 2 weeks, respectively. Patients were examined before surgery and at 1-, 3-, and 6-month intervals after corneal CXL treatment.

Visual acuity was determined using Snellen charts, and scores were converted to logMAR units for analysis. The uncorrected visual acuity (UCVA) and best corrected visual acuity (BCVA) were recorded. The following topographical measurements were obtained preoperatively and at 1, 3, and 6 months postoperatively using a rotating Scheimpflug camera (Sirius, Costruzione Strumenti Oftalmici, Italy) and recorded: flat keratometry (K) value (K1), steep K value (K2), average K value (avgK), topographic cylindrical value (topographic astigmatism) (Cyl), apical keratoscopy front (AKf), apical keratoscopy back (AKb), symmetry index front (SIf), symmetry index back (SIb), and thinnest point of the cornea (minimum corneal thickness; ThkMin). The AKf (maximum keratometric value) was defined as the steepest point of the anterior corneal surface, whereas the AKb was defined as the steepest point of the posterior corneal surface. SIf, the symmetry index of the anterior curvature, was defined as the difference of the mean anterior tangential curvatures of 2 circular zones centered on the vertical axis in the inferior and superior hemispheres. Similarly, SIb, the symmetry index of the posterior curvature, was defined as the difference of the mean posterior tangential curvatures of 2 circular zones centered on the vertical axis in the inferior and superior hemispheres.

Statistical analysis

SPSS software (version 21; IBM SPSS Statistics, Chicago, IL, USA) was used for the statistical analyses of the results. These results are presented as means ± standard deviations for continuous variables and as proportions (%) for categorical variables. Student's *t*-test for paired data was used for most analyses; however, the Pearson correlation test was used for the correlation analysis. A p value of <0.05 was considered statistically significant.

RESULTS

According to a Snellen chart evaluation of UCVA at the 6-month follow-up, UCVA remained stable in 19 (54.3%) eyes, improved by 1 line in 7 (20.0%) eyes, improved by 2 lines in 3 (8.6%) eyes, and improved by ≥3 lines in 2 (5.7%) eyes. However, UCVA decreased by 1 line in 2 (5.7%) eyes and by 2 lines in 2 (5.7%) eyes. A similar evaluation of BCVA at the 6-month follow-up, revealed a stable BCVA in 12 (34.3%) eyes, improvement by 1 line in 13 (37.1%) eyes, 2 lines in 5 (14.2%) eyes, and ≥3 lines in 2 (5.7%) eyes, and a decrease by 1 line in 3 (8.6%) eyes.

The results of the preoperative and 6-month follow-up evaluations are summarized in table 1. The mean UCVA and BCVA values improved, whereas the K values remained stable with topographic astigmatism (Figures 1 and 2). Statistically significant decreases in

Table 1. Preoperative period and 6-month follow-up data

	Preoperative period	6-month follow-up	p
UCVA (logMAR)	0.76 ± 0.28	0.68 ± 0.29	**0.020**
BCVA (logMAR)	0.43 ± 0.22	0.34 ± 0.20	**0.010**
K1 (D)	45.74 ± 2.01	45.66 ± 2.15	0.500
K2 (D)	48.94 ± 2.40	48.75 ± 2.50	0.090
Avg K (D)	47.28 ± 2.10	47.15 ± 2.20	0.240
Cyl	3.20 ± 1.42	3.10 ± 1.40	0.080
AKf (D)	55.76 ± 3.99	55.25 ± 4.26	**0.040**
AKb (D)	81.37 ± 10.09	84.71 ± 10.25	**0.010**
SIf	6.42 ± 2.87	6.00 ± 2.82	**0.001**
SIb	1.63 ± 0.70	1.67 ± 0.75	0.390
ThkMin (Mµ)	455.97 ± 31.46	422.66 ± 40.11	**0.001**

UCVA= uncorrected visual acuity; BCVA= best corrected visual acuity; K1= flat keratometry value; K2= steep keratometry value; Avg K= average keratometry value; Cyl= topographic cylindrical value; AKf= apical keratoscopy front; AKb= apical keratoscopy back; SIf= symmetry index front; SIb= symmetry index back; ThkMin= thinnest point of the cornea; D= diopters.

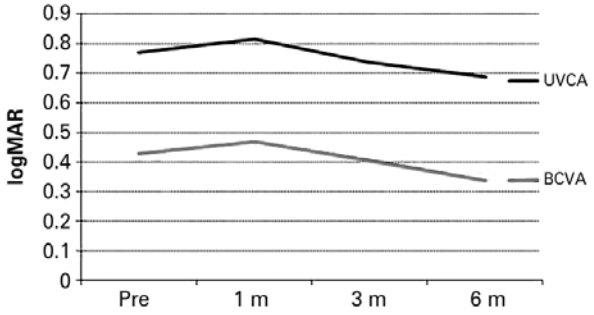

Figure 1. Alterations in the best corrected visual acuity (BCVA) and uncorrected visual acuity (UCVA) values during follow-up.

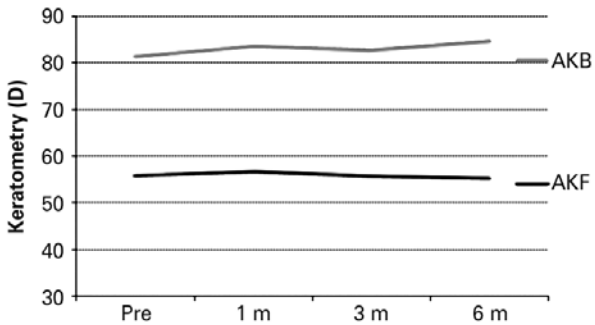

Figure 2. Alterations in the apical keratoscopy front (AKf) and apical keratoscopy back (AKb) values during follow-up.

AKf and SIf and a significant increase in AKb were observed (p=0.04, p=0.001, p=0.01, respectively). In addition, the ThkMin exhibited a statistically significant decrease after 6 months (p=0.001; Figure 3).

Table 2 summarizes the results of a correlation analysis of the parameters related to visual acuity at the 6-month follow-up. The preoperative BCVA, UCVA, K1, K2, average K, Akf, and Akb values were found to significantly affect the visual acuity at the 6-month follow-up.

DISCUSSION

In this study, we analyzed the factors affecting visual acuity at a 6-month follow- up evaluation in patients treated with accelerated CXL for progressive keratoconus and determined that the preoperative K1, K2, average K, Akf, and Akb values had significant effects on visual acuity at this follow-up time point. Notably, visual acuity improved significantly after treatment as the AKf decreased and AKb increased. Although we did not observe statistically significant differences between the pre-and post-operative K1, K2, and average K values, we found that all K values, including Akf, affected visual acuity. Notably, we observed negative correlations between K values and visual acuity; in other words, lower preoperative K values were associated with better visual acuity at the 6-month follow-up. Although the corneal thickness decreased after treatment, we did not observe a correlation between this parameter and visual acuity. Furthermore, we observed a statistically significant increase in postoperative AKb values, as well as positive correlations between visual acuity and AKb values during both the preoperative and postoperative periods.

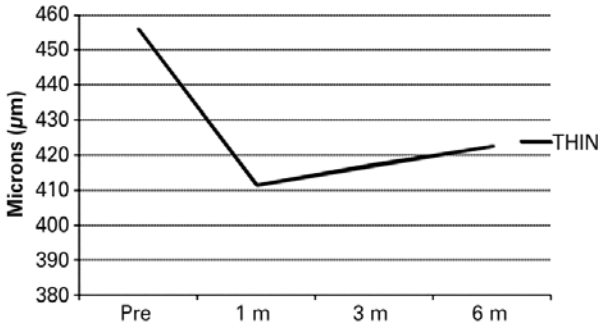

Figure 3. Alterations in the corneal thinnest point during follow-up.

Table 2. Results of the correlation analysis

	BCVA[a]		UCVA[b]	
	r	p	R	p
Age	-0.050	0.760	0.13	0.460
BCVA[a]	0.770	**0.010**	0.47	**0.004**
UCVA[a]	0.460	**0.005**	0.76	**0.010**
K1[a]	0.530	**0.001**	0.37	**0.020**
K2[a]	0.440	**0.008**	0.56	**0.010**
Avg K[a]	0.500	**0.002**	0.49	**0.003**
Cyl[a]	0.001	0.990	0.41	**0.010**
AKf[a]	0.450	**0.006**	0.23	0.170
AKb[a]	0.540	**0.001**	0.36	**0.030**
SIb[a]	0.120	0.490	0.10	0.530
SIf[a]	-0.020	0.880	0.03	0.840
ThkMin[a]	-0.190	0.260	-0.12	0.490
K1[b]	0.520	**0.001**	0.39	**0.020**
K2[b]	0.490	**0.002**	0.59	**0.010**
Avg K[b]	0.530	**0.001**	0.52	**0.001**
Cyl[b]	0.080	0.640	0.44	**0.008**
AKf[b]	0.510	**0.001**	0.39	**0.040**
AKb[b]	0.640	**0.010**	0.35	**0.040**
SIf[b]	-0.080	0.640	-0.03	0.860
SIb[b]	0.090	0.600	0.04	0.840
ThkMin[b]	-0.220	0.200	0.01	0.960

UCVA= uncorrected visual acuity; BCVA= best corrected visual acuity; K1= flat keratometry value; K2= steep keratometry value; Avg K= average keratometry value; Cyl= topographic cylindrical value; AKf= apical keratoscopy front; AKb= apical keratoscopy back; SIf= symmetry index front; SIb= symmetry index back; ThkMin= thinnest point of the cornea; r= correlation coefficient. [a]= for preoperative; [b]= for 6-month follow-up.

Corneal collagen CXL, which increases the biomechanical stability of the cornea, is the preferred treatment for the management of progressive keratoconus[9]. McAnea and O'Keefe described the visual, refractive, and topographic outcomes following CXL in pediatric patients with keratoconus and reported improvements in BCVA and stable Kmax, Kmin, and Kmean values at 1 year[10]. Sedaghat et al. also reported statistically significant improvements in BCVA and UCVA during a 1-year follow-up after CXL, along with significant decreases in the mean average keratometry values and apex corneal thickness[11]. Berger et al. further reported stabilization of the average keratometry values along with BCVA values in a 12-month follow-up after CXL; similar to our findings, these results also supported the preventive effects of CXL against keratoconus progression[12].

Accelerated CXL represents a reformation of standard CXL and is characterized by significantly reduced treatment times, patient discomfort, and complication rates. Recently, Hashemi et al. compared the 6-month results of accelerated and standard collagen CXL treatments for progressive keratoconus and determined that the mean changes in uncorrected and corrected visual acuities, as well as the mean decreases in the maximum K and mean K values, did not differ statistically significantly between the groups[13]. Elbaz et al. retrospectively studied the efficacy of accelerated CXL in 16 keratoconus-affected eyes and reported the effectiveness of this procedure for the stabilization of topographic parameters, including Ksteep, Kflat, average K, corneal astigmatism, and maximal curvature reading at the corneal apex, after 12 months of follow-up[14]. Mita et al. also evaluated the effectiveness of accelerated CXL in 39 eyes and reported significantly improved UCVA and Kmax values at 6 months after treatment[15].

The maximum keratometry value (Kmax or AKf) has been considered a key topographic indicator of CXL success, and has been reported as stable or decreased after CXL in many studies[3,15-17]. Similarly, we also observed significantly decreased AKf values after treatment. In contrast, AKb, which represents the steepest point of the posterior cornea, increased significantly after treatment. Additionally, we observed a positive correlation between the visual acuity and AKb values during both the preoperative period and the 6-month follow-up. In our opinion, this increase in AKb might be associated with reduced corneal thickness and/or flattening of the anterior cornea, and might help to stabilize K values. Notably, these increased AKb values were found to associate with increased visual acuity. To the best of our knowledge, previous studies have not investigated an association of the steepest point of the posterior cornea with visual acuity in the context of CXL, thus warranting further evaluation of this phenomenon in larger studies.

We additionally determined a significant decrease in the ThkMin at 6 months after CXL. Similarly, Derakhshan et al. and Vinciguerra et al. reported a significant decrease in the apex corneal thickness during a 1-year follow-up after CXL but did not report changes between the 6- and 12-month time points[16,18]. However, Greenstein et al. also reported corneal thinning up to 3 months after CXL, after

which this parameter returned to the baseline value after 3-6 months and remained similar to the preoperative value at the 1-year follow-up[19]. Moreover, McAnea and O'Keefe defined a significant reduction in the baseline mean thinnest corneal area at 6 months after CXL, followed by a recovery at 1 year[10]. In our study, the lowest value for the thinnest corneal point was measured at 1 month after CXL; this value increased slightly until the 6-month time point but did not reach preoperative levels. We did not determine any effects of the ThkMin on visual acuity.

Currently, the available information regarding factors affecting the outcome of accelerated CXL is limited. Notably, Toprak et al. reported that in patients with progressive keratoconus, age, baseline visual acuity, and baseline thinnest pachymetry affected the success of CXL treatment[20]. In contrast, we did not determine any effects of age or the ThkMin on visual acuity. Recently, De Angelis et al. reported a significant improvement in the 1-year postoperative BCVA, but no significant change in the 1-year postoperative Kmax, and identified a low preoperative BCVA, high refractive astigmatism, and advanced keratoconus as factors predictive of BCVA improvement[21]. In contrast, we determined that astigmatism had some significant effects on UCVA but not on BCVA, at a 6-month follow-up. In addition, we also identified a positive correlation between preoperative and postoperative visual acuity but observed that preoperative K values had a negative effect on visual acuity. In our study, eyes with better preoperative visual acuity and less severe keratoconus (lower K values) had better visual acuities at 6 months after CXL.

We note that the major limitations of this study are the small sample size and short duration of follow-up. Larger studies with longer follow-up periods will be required to define the factors affecting the outcomes of accelerated CXL.

In conclusion, accelerated CXL is an effective treatment for the prevention or even reversal of keratoconus progression. The K values and the steepest points of the anterior and posterior cornea were found to affect the visual acuity at 6 months after accelerated CXL. Posterior corneal steepening appears to be as important as anterior corneal flattening for stabilizing the keratometric values and achieving a better postoperative visual outcome.

REFERENCES

1. Jeyabalan N, Shetty R, Ghosh A, Anandula VR, Ghosh AS, Kumaramanickavel G. Genetic and genomic perspective to understand the molecular pathogenesis of keratoconus. Indian J Ophthalmol. 2013;61(8):384-8.
2. Wollensak G. Crosslinking treatment of progressive keratoconus: New Hope. Curr Opin Opthalmol. 2006;17(4):356-60.
3. Wollensak G, Spoerl E, Seiler T. Riboflavin/ultraviolet-A-induced collagen cross-linking for the treatment of keratoconus. Am J Ophthalmol. 2003;135(5):620-7.
4. Ghanem RC, Santhiago MR, Berti T. Topographic, corneal wavefront, and refractive outcomes 2 years after collagen cross-linking for progressive keratoconus. Cornea. 2014;33(1):43-8.
5. Iseli HP, Thiel MA, Hafezi F, Kampmeier J, Seiler T. Ultraviolet A/riboflavin corneal cross-linking for infectious keratitis associated with corneal melts. Cornea. 2008; 27(5):590-4.
6. Koller T, Mrochen M, Seiler T. Complication and failure rates after corneal cross-linking. J Cataract Refract Surg. 2009;35(8):1358-62.
7. Greenstein SA, Fry KL, Hersh PS. Corneal topography indices after corneal collagen crosslinking for keratoconus and corneal ectasia: One-year results. J Cataract Refract Surg. 2011;37(7):1282-90.
8. Goldich Y, Marcovich AL, Barkana Y, Mandel Y, Hirsh A, Morad Y, Avni I, et al. Clinical and corneal biomechanical changes after collagen cross-linking with riboflavin and UV irradiation in patients with progressive keratoconus: results after 2 years of follow-up. Cornea. 2012;31(6):609-14.
9. Kanellopoulos AJ. Collagen cross-linking in early keratoconus with riboflavin in a femtosecond laser-created pocket: initial clinical results. J Refract Surg. 2009;25(11):1034-7.
10. McAnena L, O'Keefe M. Corneal collagen crosslinking in children with keratoconus. J AAPOS. 2015;19(3):228-32.
11. Sedaghat M, Bagheri M, Ghavami S, Bamdad S. Changes in corneal topography and biomechanical properties after collagen cross linking forkeratoconus: 1-year results. Middle East Afr J Ophthalmol. 2015;22(2):212-9.
12. Berger Y, Ezra-Nimni O, Skaat A, Fogel M, Grinbaum A, Barequet I. Corneal collagen cross-linking novel technique for prevention of keratoconus progression: results after one-year at the Sheba Medical Center. Harefuah. 2015;154(2):118-21.
13. Hashemi H, Fotouhi A, Miraftab M, Bahrmandy H, Seyedian MA, Amanzadeh K, et al. Short-term comparison of accelerated and standard methods of corneal collagen crosslinking. J Cataract Refract Surg. 2015;41(3):533-40.
14. Elbaz U, Shen C, Lichtinger A, Zauberman NA, Goldich Y, Chan CC, et al. Accelerated (9-mW/cm^2) corneal collagen crosslinking for keratoconus-A 1-year follow-up. Cornea. 2014;33(8):769-73.
15. Mita M, Waring GO, Tomita M. High-irradiance accelerated collagen crosslinking for the treatment of keratoconus: six-month results. J Cataract Refract Surg. 2014; 40(6):1032-40.
16. Derakhshan A, Shandiz JH, Ahadi M, Daneshvar R, Esmaily H. Short-term outcomes of collagen crosslinking for early keratoconus. J Ophthalmic Vis Res. 2011;6(3):155-9.
17. Raiskup F, Theuring A, Pillunat LE, Spoerl E. Corneal collagen crosslinking with riboflavin and ultraviolet-A light in progressive keratoconus: ten-year results. J Cataract Refract Surg. 2015;41(1):41-6.
18. Vinciguerra P, Albè E, Trazza S, Rosetta P, Vinciguerra R, Seiler T, et al. Refractive, topographic, tomographic, and aberrometric analysis of keratoconic eyes undergoing corneal cross-linking. Ophthalmology. 2009;116(3):369-78.
19. Greenstein SA, Shah VP, Fry KL, Hersh PS. Corneal thickness changes after corneal collagen crosslinking for keratoconus and corneal ectasia: One-year results. J Cataract Refract Surg. 2011;37(4):691-700.
20. Toprak I, Yaylalı V, Yildirim C. Factors affecting outcomes of corneal collagen cross-linking treatment. Eye (Lond). 2014;28(1):41-6.
21. De Angelis F, Rateau J, Destrieux C, Patat F, Pisella PJ. [Predictive factors for visual outcome after corneal collagen crosslinking treatment in progressive keratoconus: One-year refractive and topographic results]. J Fr Ophtalmol. 2015;38(7):595-606. French.

Effect of intravitreal anti-VEGF on choroidal thickness in patients with diabetic macular edema using spectral domain OCT

Efeito de injeção intravítrea na espessura de coroide em pacientes com edema macular diabético utilizando OCT de domínio espectral

Vinicius F. Kniggendorf[1,2], Eduardo A. Novais[2], Sergio L. Kniggendorf[1], Camilla Xavier[2], Emily D. Cole[3], Caio V. Regatieri[2,3]

ABSTRACT

Purpose: To evaluate choroidal thickness (CT) using spectral domain optical coherence tomography (SD-OCT) imaging at baseline and 6 months after intravitreal anti-vascular endothelial growth factor (anti-VEGF) treatment in patients with diabetic macular edema (DME).

Methods: A retrospective chart review was performed to identify patients with DME who underwent intravitreal injection of anti-VEGF (bevacizumab or ranibizumab) in a pro re nata (PRN) regimen. Subfoveal choroidal thickness was compared between values obtained at baseline and at 6-month follow-up visits.

Results: Thirty-nine eyes (15 females, 24 males) from 39 patients were enrolled (mean age, 62.43 ± 8.7 years; range, 44-79 years). Twenty-three and 16 eyes were treated with ranibizumab and bevacizumab respectively. The mean number of anti-VEGF injections was 2.28 ± 1.27 (range, 1-5). Mean nasal, subfoveal, and temporal choroidal thickness (CT) measurements at baseline were 234.10 ± 8.63 µm, 246.89 ± 8.94 µm, and 238.12 ± 8.20 µm, respectively, and those at 6 months post-treatment were 210.46 ± 8.00 µm, 215.66 ± 8.29 µm, and 212.43 ± 8.14 µm, respectively. Significant differences in CT were observed between baseline and the 6-month follow-up at all measured points (p=0.0327).

Conclusions: Over a 6-month period, the use of intravitreal anti-VEGF was associated with significant thinning of the choroid in patients with DME. The clinical significance of a thinner choroid in DME is currently unknown; however, it may contribute to long-term adverse effects on choroidal and retinal function, representing an area requiring future investigation.

Keywords: Angiogenesis inhibitors; Choroid; Diabetic retinopathy; Intravitreal injections; Tomography, optical coherence

RESUMO

Objetivos: *Avaliar a espessura de coroide pré-tratamento e após 6 meses da injeção intravítrea de anti-fator de crescimento vascular endotelial (anti-VEGF) em pacientes com edema macular diabético (EMD), utilizando a tomografia de coerência óptica de domínio espectral (SD-OCT).*

Métodos: *Análise retrospectiva, com revisão de prontuários, foi realizada para identificação de pacientes submetidos a tratamento com injeções intravítreas de anti-VEGF, no regime pro re nata, para tratamento de EMD. As medidas da espessura de coroide pré-tratamento foi comparada com as medidas após acompanhamento de 6 meses.*

Resultados: *Trinta e nove olhos de 39 pacientes (15 femininos, 24 masculinos) foram incluídos, com idade média de 62,43 ± 8,7 anos (variando de 44-79 anos). Trinta e três olhos foram tratados com ranibizumab e 18 com bevacizumab. O número médio de injeções de anti-VEGF foi 2,28 ± 1,27 (variando de 1-5). A medida média pré-tratamento da espessura de coroide nasal, subfoveal e temporal foi 234,10 ± 8,63 µm, 246,89 ± 8,94 µm e 238,12± 8,20 µm, respectivamente. Após acompanhamento de 6 meses as medidas médias da espessura de coroide foram 210,46 ± 8,00 µm, 215,66 ± 8,29 µm e 212,43 ± 8,14 µm. A diferença entre as medidas médias pré e pós tratamento foi estatisticamente significante (p=0,0327) em todos os pontos medidos.*

Conclusão: *Após um período de 6 meses, o uso de injeções intravítreas de anti-VEGF foi associado com diminuição significante da espessura de coroide nos pacientes com EMD. O significado clínico de uma coroide mais fina nos pacientes com EMD é desconhecido mas pode causar eventos adversos a longo prazo para função da coroide e retina, representando uma área para futura investigações.*

Descritores: *Inibidores da angiogênese; Coroide; Injeções intravítreas; Retinopatia diabética; Tomografia de coerência óptica*

INTRODUCTION

More than 90 million people worldwide are affected by diabetic retinopathy (DR), causing significant vision loss[1,2], with macular edema and proliferative retinopathy as the leading causes of visual impairment[2,3]. Anti-vascular endothelial growth factor (anti-VEGF) drugs are widely used in the treatment of diabetic macular edema (DME); this is supported by an extensive body of literature, demonstrating substantial improvements in visual and anatomic outcomes[4-10].

The choroid is a vascularized tissue that plays a vital role in providing metabolic support to the outer retina, including the photoreceptors and prelaminar portion of the optic nerve head[11,12]. Abnormal choroidal blood volume and compromised flow may result in dysfunctioning of the photoreceptor and mortality[13]. Choroidal vasculopathy, such as obstruction of the choriocapillaris, vascular degeneration, choroidal aneurysms, and neovascularization, may be involved in the pathogenesis of DR[13-15].

Enhanced depth imaging using spectral domain optical coherence tomography (SD-OCT) enables improved visualization of the choroid and assessment of choroidal thickness[16,17]. Results of clinical studies have indicated that choroidal thickness may be related to DR severity, and the presence of DME is associated with a significant decrease in choroidal thickness[16]. In patients with neovascular age-related macular degeneration (AMD), anti-VEGF drugs have been shown to induce significant thinning in choroidal thickness, which may lead to unknown long-term consequences or complications[18].

Submitted for publication: October 27, 2015
Accepted for publication: February 15, 2016

[1] Hospital Oftalmológico de Brasília, Brasília, DF, Brazil.
[2] Department of Ophthalmology and Visual Sciences, Escola Paulista de Medicina (EPM), Universidade Federal de São Paulo (UNIFESP), São Paulo, SP, Brazil.
[3] Tufts University School of Medicine, Boston, MA, USA.

Funding: This study was supported in part by CNPq (EAN - Grant number 479648/2012-3) and CAPES foundation.

Disclosure of potential conflicts of interest: None of the authors have any potential conflict of interest to disclose.

Corresponding author: Caio Vinicius Saito Regatieri. Universidade Federal de São Paulo. Departamento de Oftalmologia. Rua Botucatu, 821 - 1ª andar - São Paulo, SP - 04023-062 - Brazil
E-mail: caiore@gmail.com

Approved by the following research ethics committee: UNIFESP (#1.093.853).

Currently, intravitreal anti-VEGF injections are the most common treatment for DME. Though anti-VEGF injections improved visual acuity, several studies demonstrated an association with decreased central retinal thickness[18,19]. However, there is currently a lack of studies investigating the effect of anti-VEGF injections on the choroid in patients with diabetes. The purpose of the present study was to evaluate the effect of intravitreal anti-VEGF injections on choroidal thickness using SD-OCT in patients treated for DME.

METHODS

This was a retrospective chart analysis conducted at the Federal University of São Paulo (UNIFESP) and Hospital Oftalmológico de Brasília, Brazil. The present study was approved by the UNIFESP Institutional Review Boards (CEP 1.093.853) and adhered to the tenets of the Declaration of Helsinki. Informed consent was obtained from all subjects after explanation of the nature of the present study.

Subjects

Exploratory chart review of data collected from patients with type 2 diabetes previously treated for DME with intravitreal anti-VEGFs between January 2012 and June 2014. Clinically significant macular edema (CSME) was assessed by clinical examination and SD-OCT imaging. The diagnosis of CSMA was defined according to the Early Treatment Diabetic Retinopathy Study (ETDRS) protocol. A pro re nata (PRN) protocol was used to treat DME in all patients. Major exclusion criteria included the following: previous anti-VEGF or intravitreous corticosteroid treatment for DME within 6 months of the first visit; vitreomacular traction syndrome; suspected or confirmed glaucoma; proliferative diabetic retinopathy; previous retinal laser therapy; previous pars plana vitrectomy; high myopia and age-related macular degeneration; and other causes of macular edema.

Choroidal thickness measurement

SD-OCT scans were performed using EDI SD-OCT (Spectralis OCT, Heidelberg Engineering, Heidelberg, Germany). The scan pattern used was a high-definition 1-line raster scanning of 30° consisting of 768 A-scans per frame, followed by an average of 100 frames[20]. Measurements were performed before and after anti-VEGF treatment. For images to be included in the present study, the signal-to-noise ratio (SNR) had to be at least 20 dB (considered best quality) and should be taken as close to the fovea as possible (thinnest macular point), with the understanding that slight differences in positioning affect the measured thicknesses[21]. Using the Spectralis linear measurement tool, two independent observers measured CT perpendicularly from the outer edge of the hyper-reflective RPE to the inner sclera at 500-mm intervals temporal and nasal to the fovea up to 1,000 mm. Measurements were performed prior to treatment and at a 6-month follow-up (Figure 1).

Statistical analysis

Data are expressed as means ± standard error of the mean. Statistical analyses were performed using a paired t-test for comparing between baseline and follow-up choroidal thickness measurements. The Pearson correlation coefficient was used to evaluate the correlation between choroidal thickness and central foveal thickness. A 95% confidence interval with a 5% level of significance was adopted; thus, P values of <0.05 were considered to be statistically significant. Analysis of variance (ANOVA) with the Bonferroni correction was used to compare groups treated with bevacizumab and ranibizumab. All statistical analyses were performed using Graph Pad Prism 5.0 software for MAC.

RESULTS

Thirty-nine eyes from 39 patients (15 female, 24 male) were included in the study analysis. The mean age was 62.43 ± 8.7 years, with a range of 44-79 years. Twenty-three eyes were treated with ranibizumab and 16 eyes were treated with bevacizumab. The average number of anti-VEGF injections administered was 2.28 ± 1.27 (range, 1-5) over the 6-month follow-up. Central retinal thickness improved in all patients after 6-month anti-VEGF treatment.

The choroid was noted to be thinnest nasally, thicker temporally, and thickest in the subfoveal region. This pattern was observed at baseline and after the 6-month follow-up, which is consistent with that reported in previous studies[22]. Figure 2 shows the mean CT at each location. Choroidal thickness was significantly thinner (p=0.0327) at all measured points following anti-VEGF treatment. Mean nasal, subfoveal, and temporal choroidal thickness measurements at baseline were 234.10 ± 8.63 µm, 246.89 ± 8.94 µm, and 238.12 ± 8.20 µm, respectively, and at the 6-month follow-up were 210.46 ± 8.00 µm, 215.66 ± 8.29 µm, and 212.43 ± 8.14 µm, respectively.

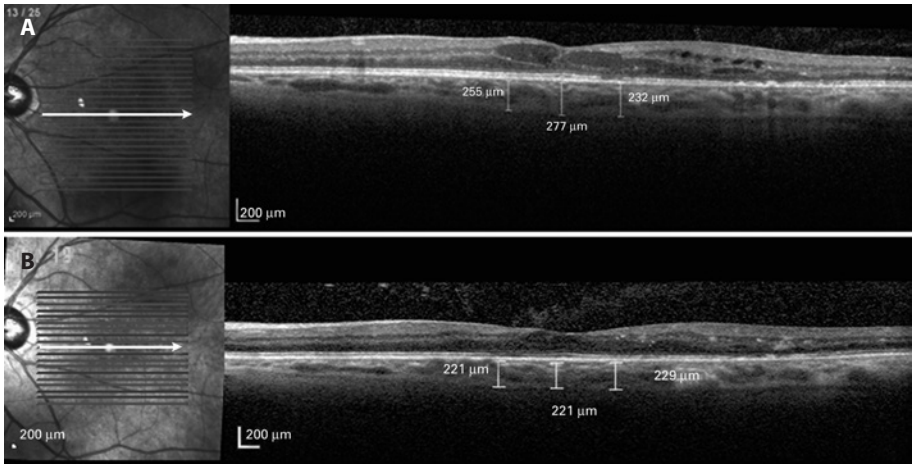

Figure 1. Spectral Domain OCT. Central choroidal thickness measurements. A) prior anti-VEGF treatment and; B) post-treatment.

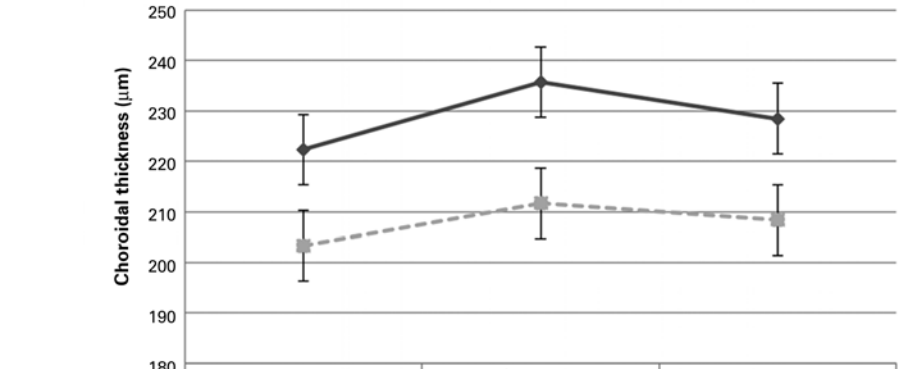

	Nasal	Subfoveal	Temporal
Baseline	222.36	235.76	228.48
Post treatment	203.34	211.7	208.4

Figure 2. Mean choroidal thickness at the fovea and at 500-µm intervals nasally and temporally at baseline and at the 6-month follow-up.

In a subgroup analysis of patients who received intravitreal bevacizumab, mean nasal, subfoveal, and temporal choroidal thickness measurements at baseline were 241.25 ± 14.40 µm, 259.50 ± 13.93 µm, and 249.87 ± 13.30 µm, respectively, with significant decreases to 212.75 ± 12.70 µm, 221.12 ± 12.26 µm, and 221.12 ± 12.06 µm, respectively, at the 6-month follow-up. In the ranibizumab group, mean nasal, subfoveal, and temporal choroidal thickness measurements at baseline were 229.13 ± 10.83 µm, 238.13 ± 11.56 µm, and 229.95 ± 10.28 µm, respectively, with significant decreases to 208.86 ± 10.53 µm, 211.87 ± 11.34 µm, and 206.40 ± 11.00 µm, respectively, at the 6-month follow-up. No significant difference ($p>0.05$) in foveal CT was observed between eyes treated with ranibizumab (211.87 ± 11.34 µm) and those treated with bevacizumab (221.12 ± 12.26 µm). Decreases in central retinal thickness were not correlated with choroidal thinning after 6-month anti-VEGF treatment.

DISCUSSION

The choroid plays an integral role in the metabolic support of the retinal pigment epithelium (RPE), optic nerve, and outer retina; normal choroidal vasculature is essential for appropriate functioning of the retina[11,12]. Compromised choroidal blood flow may result in dysfunctioning of the photoreceptor and insufficient removal of metabolites generated by RPE cells, resulting in an accumulation of waste at Bruch's membrane[13]. Previous studies have reported abnormal choroidal findings in patients with diabetes such as increased blood vessel tortuosity, focal vascular dilation and narrowing, hypercellularity, vascular loops, microaneurysms, areas of non-perfusion, and sinus-like structure formation between the choroidal lobules[14,23]. Choroidal thinning, increased thickness of the extracellular matrix, and decreased vessel diameter have been observed on SD-OCT imaging in the eyes of patients with diabetes[16,24,25].

Anti-VEGF treatment has demonstrated utility in improving visual and anatomical outcomes in DME[4-10]. The effects of anti-VEGF therapy on choroidal thickness in various diseases, including AMD and DM, have been reported in several previous studies[18,19]. Yiu *et al.* demonstrated that central choroidal thickness decreases following anti-VEGF therapy for DME after 6 months[19]. The present study also found a statistically significant decrease in choroidal thickness among patients following anti-VEGF injections.

The results of the present study indicate that intravitreal anti-VEGF therapy may influence choroidal structure in eyes with diabetic retinopathy treated for DME. This result may be attributable to the findings that both full-length antibody (bevacizumab) and Fab fragment (ranibizumab) drugs are able to penetrate into all retinal layers, reach the choroid, and accumulate in the wall of the choroidal vessel[26-28]. As VEGF functions by inducing vessel dilation and increasing ocular blood flow, which is mediated by increased nitric oxide production[29], VEGF inhibition by these drugs may cause constriction of the choroidal vessels. Choroidal thickness is already decreased in patients with diabetes, and the consequences of further thinning of the choroidal vasculature secondary to anti-VEGF administration are unknown. Altered choroidal blood flow may result in dysfunctioning of the photoreceptor and mortality, contributing to the higher anatomical and functional responses to anti-VEGF treatment in patients with thicker choroids, as demonstrated by a previous report[30].

One of the major limitations of the present study was the retrospective design. We were unable to determine which anti-VEGFs were administered, and we were unable to identify a control group. Additionally, visual acuity data were not analyzed as the major objective of the present study was to evaluate changes in choroidal thickness.

As anti-VEGF drugs are commonly used in the treatment of DME and other retinal pathologies, a full understanding of the effects of anti-VEGF drugs on the choroidal vasculature is warranted. Further prospective studies are required to completely determine the long-term effects of anti-VEGF therapy on choroidal thickness. Decreased choroidal thickness induced by anti-VEGF administration may have long-term adverse effects on choroidal and retinal functions.

REFERENCES

1. Yau JW, Rogers SL, Kawasaki R, Lamoureux EL, Kowalski JW, Bek T, et al. Global prevalence and major risk factors of diabetic retinopathy. Diabetes Care. 2012;35(3):556-64.
2. Moss SE, Klein R, Klein BE. The 14-year incidence of visual loss in a diabetic population. Ophthalmology. 1998;105(6):998-1003.
3. Klein R, Klein BE, Moss SE, Cruickshanks KJ. The Wisconsin Epidemiologic Study of diabetic retinopathy. XIV. Ten-year incidence and progression of diabetic retinopathy. Arch Ophthalmol. 1994;112(9):1217-28.
4. Boyer DS, Hopkins JJ, Sorof J, Ehrlich JS. Anti-vascular endothelial growth factor therapy for diabetic macular edema. Ther Adv Endocrinol Metab. 2013;4(6):151-69.
5. Nguyen QD, Brown DM, Marcus DM, Boyer DS, Patel S, Feiner L, et al. Ranibizumab for diabetic macular edema: results from 2 phase III randomized trials: RISE and RIDE. Ophthalmology. 2012;119(4):789-801.
6. Michaelides M, Kaines A, Hamilton RD, Fraser-Bell S, Rajendram R, Quhill F, et al. A prospective randomized trial of intravitreal bevacizumab or laser therapy in the management of diabetic macular edema (BOLT study) 12-month data: report 2. Ophthalmology. 2010; 117(6):1078-86 e2.

7. Korobelnik JF, Do DV, Schmidt-Erfurth U, Boyer DS, Holz FG, Heier JS, et al. Intravitreal aflibercept for diabetic macular edema. Ophthalmology. 2014;121(11):2247-54.
8. Mitchell P, Bandello F, Schmidt-Erfurth U, Lang GE, Massin P, Schlingemann RO, et al. The RESTORE study: ranibizumab monotherapy or combined with laser versus laser monotherapy for diabetic macular edema. Ophthalmology. 2011;118(4):615-25.
9. Massin P, Bandello F, Garweg JG, Hansen LL, Harding SP, Larsen M, et al. Safety and efficacy of ranibizumab in diabetic macular edema (RESOLVE Study): a 12-month, randomized, controlled, double-masked, multicenter phase II study. Diabetes Care. 2010;33(11):2399-405.
10. Nguyen QD, Shah SM, Khwaja AA, Channa R, Hatef E, Do DV, et al. Two-year outcomes of the ranibizumab for edema of the mAcula in diabetes (READ-2) study. Ophthalmology. 2010;117(11):2146-51.
11. McCourt EA, Cadena BC, Barnett CJ, Ciardella AP, Mandava N, Kahook MY. Measurement of subfoveal choroidal thickness using spectral domain optical coherence tomography. Ophthalmic Surg Lasers Imaging. 2010;41 Suppl:S28-33.
12. Tan CS, Cheong KX, Lim LW, Li KZ. Topographic variation of choroidal and retinal thicknesses at the macula in healthy adults. Br J Ophthalmol. 2014;98(3):339-44.
13. Cao J, McLeod S, Merges CA, Lutty GA. Choriocapillaris degeneration and related pathologic changes in human diabetic eyes. Arch Ophthalmol. 1998;116(5):589-97.
14. Hidayat AA, Fine BS. Diabetic choroidopathy. Light and electron microscopic observations of seven cases. Ophthalmology. 1985;92(4):512-22.
15. Shiragami C, Shiraga F, Matsuo T, Tsuchida Y, Ohtsuki H. Risk factors for diabetic choroidopathy in patients with diabetic retinopathy. Graefes Arch Clin Exp Ophthalmol. 2002;240(6):436-42.
16. Regatieri CV, Branchini L, Carmody J, Fujimoto JG, Duker JS. Choroidal thickness in patients with diabetic retinopathy analyzed by spectral-domain optical coherence tomography. Retina. 2012;32(3):563-8.
17. Spaide RF, Koizumi H, Pozzoni MC. Enhanced depth imaging spectral-domain optical coherence tomography. Am J Ophthalmol. 2008;146(4):496-500.
18. Branchini L, Regatieri C, Adhi M, Flores-Moreno I, Manjunath V, Fujimoto JG, et al. Effect of intravitreous anti-vascular endothelial growth factor therapy on choroidal thickness in neovascular age-related macular degeneration using spectral-domain optical coherence tomography. JAMA Ophthalmol. 2013;131(5):693-4.
19. Yiu G, Manjunath V, Chiu SJ, Farsiu S, Mahmoud TH. Effect of anti-vascular endothelial growth factor therapy on choroidal thickness in diabetic macular edema. Am J Ophthalmol. 2014;158(4):745-51 e2.
20. Branchini L, Regatieri CV, Flores-Moreno I, Baumann B, Fujimoto JG, Duker JS. Reproducibility of choroidal thickness measurements across three spectral domain optical coherence tomography systems. Ophthalmology. 2012;119(1):119-23.
21. Balasubramanian M, Bowd C, Vizzeri G, Weinreb RN, Zangwill LM. Effect of image quality on tissue thickness measurements obtained with spectral domain-optical coherence tomography. Opt Express. 2009;17(5):4019-36.
22. Manjunath V, Taha M, Fujimoto JG, Duker JS. Choroidal thickness in normal eyes measured using Cirrus HD optical coherence tomography. Am J Ophthalmol. 2010; 150(3):325-9 e1.
23. Fryczkowski AW, Sato SE, Hodes BL. Changes in the diabetic choroidal vasculature: scanning electron microscopy findings. Ann Ophthalmol. 1988;20(8):299-305.
24. Regatieri CV, Branchini L, Fujimoto JG, Duker JS. Choroidal imaging using spectral-domain optical coherence tomography. Retina. 2012;32(5):865-76.
25. Adhi M, Brewer E, Waheed NK, Duker JS. Analysis of morphological features and vascular layers of choroid in diabetic retinopathy using spectral-domain optical coherence tomography. JAMA Ophthalmol. 2013;131(10):1267-74.
26. Heiduschka P, Fietz H, Hofmeister S, Schultheiss S, Mack AF, Peters S, et al. Penetration of bevacizumab through the retina after intravitreal injection in the monkey. Invest Ophthalmol Vis Sci. 2007;48(6):2814-23.
27. Pieramici DJ, Rabena MD. Anti-VEGF therapy: comparison of current and future agents. Eye (Lond). 2008;22(10):1330-6.
28. Shahar J, Avery RL, Heilweil G, Barak A, Zemel E, Lewis GP, et al. Electrophysiologic and retinal penetration studies following intravitreal injection of bevacizumab (Avastin). Retina. 2006;26(3):262-9.
29. Fukumura D, Gohongi T, Kadambi A, Izumi Y, Ang J, Yun CO, et al. Predominant role of endothelial nitric oxide synthase in vascular endothelial growth factor-induced angiogenesis and vascular permeability. Proc Natl Acad Sci U S A. 2001;98(5):2604-9.
30. Rayess N, Rahimy E, Ying GS, Bagheri N, Ho AC, Regillo CD, et al. Baseline choroidal thickness as a predictor for response to anti-vascular endothelial growth factor therapy in diabetic macular edema. Am J Ophthalmol. 2015;159(1):85-91 e1-3.

Implantation of foldable posterior chamber intraocular lens in aphakic vitrectomized eyes without capsular support

Implantação lente intraocular dobrável de câmara posterior em olhos afácicos vitrectomizados sem apoio capsular

Gurkan Erdogan[1], Cihan Unlu[1], Betul Onal Gunay[1], Esra Kardes[1], Ahmet Ergin[1]

ABSTRACT

Purpose: To evaluate the outcomes of three different surgical techniques for foldable posterior chamber intraocular lens (PCIOL) implantation in vitrectomized eyes without capsular support.

Methods: A total of 60 patients with aphakic and vitrectomized eyes without capsular support were enrolled. All patients underwent three-piece foldable PCIOL implantation into the posterior chamber through a small corneal incision. Transscleral fixation (TSF), iris fixation (IF), and intrascleral tunnel fixation (ISF) surgical techniques were performed.

Results: Postoperative PCIOL subluxation or dislocation occurred in one case in the TSF group and two cases in the ISF group. Intraoperative PCIOL dislocation occurred in two patients in the IF group. The incidence of temporary postoperative complications, such as mild intraocular hemorrhage and cystoid macular edema, was higher in the ISF group. No statistically significant difference in PCIOL-related astigmatism was observed between groups. Visual acuity improved in all groups.

Conclusions: Postoperative outcomes were comparable between TSF, IF, and ISF for PCIOL in vitrectomized eyes without capsular support.

Keywords: Lens implantation, intraocular/methods; Iris/surgery; Suture techniques; Aphakia

RESUMO

Objetivo: *Avaliar os resultados de três diferentes técnicas cirúrgicas para implantação da lente intraocular de câmara posterior (PCIOL) dobrável em olhos vitrectomizados sem apoio capsular.*

Métodos: *Um total de 60 olhos de 60 pacientes afácicos vitrectomizados, sem apoio capsular foram inscritos. Todos os pacientes foram submetidos ao implante de PCIOL dobrável de três peças na câmara posterior, através de uma pequena incisão na córnea. Foram utilizados as técnicas cirúrgicas de fixação transescleral (TSF), fixação iriana (IF) e túnel de fixação intraescleral (ISF).*

Resultados: *Subluxação ou luxação da PCIOL ocorreu em um caso no grupo TSF e em dois casos no grupo ISF. Deslocamentos intraoperatórios da PCIOL ocorram em dois pacientes no grupo IF. Frequência de complicações pós-operatórias temporárias como hemorragia intraocular leve e edema macular cistóide foi maior no grupo ISF. Não houve diferença estatisticamente significativa do astigmatismo relacionado à PCIOL entre os grupos. A acuidade visual melhorou em todos os grupos.*

Conclusões: *Nenhuma das três técnicas cirúrgicas teve destaque em termos de resultados cirúrgicos comparativos.*

Descritores: *Implante de lente intraocular/métodos; Íris/cirurgia; Técnicas de sutura; Afacia*

INTRODUCTION

The capsule of the crystalline lens, if sufficiently present, is used as a support tissue for intraocular lens (IOL) implantation surgery performed on vitrectomized eyes. Eye trauma or iatrogenic damage during complicated cataract surgery, loss of position and zonule connections of the crystalline lens, and IOL via dislocation may cause loss of support tissue for lens capsule implantation prior to pars plana vitrectomy (PPV). During PPV, the iatrogenic removal of the lens capsule may be required depending on the etiology and severity of the vitreoretinal disease. Posterior chamber IOL implantation may be performed via posterior chamber transscleral fixation[1-7], iris fixation[8-11], intrascleral fixation[12-22], angle supported anterior chamber IOL[23,24], or iris claw IOL implantation[25,26].

Advantages of PCIOL fixation include the distant position from anterior segment structures, such as the corneal endothelium, and proximity to the focal point of the eye where the lens is naturally situated. However, the lack of the volume creation and supporting effect of the vitreous, and the fact that the surgery is generally performed under irrigation fluid, may complicate PCIOL fixation in vitrectomized eyes. In these cases, a small corneal tunnel incision may be used to create a closed and more stable surgical space. In cases with no capsular support, the implantation of a foldable IOL can be performed through a small corneal incision into the posterior chamber with suture fixation to the sclera or iris[4-11]. Alternatively, IOL implantation can be performed through a small incision to the posterior chamber with sutureless intrascleral fixation[12-22].

In the present study, we evaluated three separate groups of patients with vitrectomized aphakic eyes lacking capsular support in whom foldable IOL were implanted through a small corneal incision using either transscleral fixation, iris fixation, or intrascleral fixation. Outcomes and complications were compared between the surgical methods.

Submitted for publication: November 10, 2015
Accepted for publication: February 11, 2016

[1] Department of Ophthalmology, Umraniye Training and Research Hospital, Istanbul, Turkey.

Funding: No specific financial support was available for this study.

Disclosure of potential conflicts of interest: None of the authors have any potential conflict of interest to disclose.

Corresponding author: Betul Onal Gunay. Elmalıkent Mah. Adem Yavuz Cad. No: 1 - Umraniye, Istanbul - Turkey - E-mail: drbetulonal@yahoo.com

Approved by the following research ethics committee: Umraniye Training and Research Hospital (#2, January 13, 2014).

METHODS

We performed a retrospective observational case-controlled study of vitrectomized aphakic eyes in patients who had undergone foldable intraocular lens implantation into the posterior chamber. Patients lacking capsular support were divided into three groups according to the surgical intervention received between January 2008 and December 2014. Transscleral fixation was performed between January 2008 and June 2010 (TSF group), iris fixation between April 2010 and May 2012 (IF group), and intrascleral fixation since April 2012 (ISF group). In the ISF group, we did not include the initial eight cases of IOL implantation using folding method rather than injection during the learning period. We included consecutive cases that had undergone surgery between August 2012 and December 2014. Ethical approval for present the study was obtained from the local ethics committee. Detailed informed consent was obtained from each patient. The present study followed the tenets of the Declaration of Helsinki.

Ophthalmic examinations, including best-corrected visual acuity (BCVA) and intraocular pressure (IOP) measurements, dilated intraocular slit-lamp examination, autorefractometry, keratometry, and spectral domain optical coherence tomography (SD-OCT) (Optovue Inc., Fremont, CA) evaluation were performed during preoperative and postoperative study visits. Preoperative ocular condition, and intraoperative, and postoperative complications were evaluated. Astigmatism related to IOL was detected using "power vector analysis (PVA)" with the consideration of preoperative and final examination keratometry values. The incidence of postoperative astigmatism related to IOL and BCVA was compared between groups. Patients with a follow-up period of <3 months or with preoperative corneal opacity were excluded from the study.

Surgical methods

All surgeries were performed by one surgeon (G.E). Retrobulbar anesthesia was performed in all patients. Continuous anterior chamber or pars plana infusion was used during surgery. A three-piece IOL (Sensar AR40e; Abbott Medical Optics, USA) was inserted through a superior clear corneal incision in all techniques. In cases with a dislocated IOL, exchange was performed if a single-piece IOL was present. However, the primary IOL was used for fixation if a three-piece IOL was present.

Transscleral fixation technique

Transscleral fixation of foldable PCIOL was performed using the method described by Lewis[27]. Local conjunctival peritomies were performed on quadrants 3 and 9 followed by formation of the limbus based partial-thickness triangular flaps at 180°. A straight needle carrying 10-0 polyprolene was inserted into the posterior chamber under a scleral flap and was removed from beneath the opposite scleral tissue with the guidance of a 27-gauge needle. A 3.5-mm corneal incision was performed superiorly. The suture traversing the posterior chamber was pulled under the pupil with the assistance of a hook and removed from the main incision, cut, and then tied to the IOL haptics. The IOL was folded on the 6 o'clock and 12 o'clock axis and placed into the anterior chamber. Sutures were gently pulled to centralize the IOL. The polyprolene sutures were tied under the scleral flaps and the conjunctiva was closed using an 8-0 polyglactin suture.

Iris fixation technique

Iris fixation of foldable PCIOL was performed using the method described by Condon[8]. Pupillary constriction was provided by preoperative application of 4% topical pilocarpine. Paracentesis was applied with a 23-gauge MVR at 3, 6, and 9 o'clock. The IOL was folded into the desired shape, such that the haptics were in a mustache configuration, and placed through the corneal incision at 12 o'clock into the anterior chamber in a captured position with both haptics placed into the posterior iris extending into the 3 and 9 o'clock quadrants. In order to prevent posterior dislocation of the lens, the optic body was posteriorly supported with a spatula inserted at 6 o'clock. The optic was mildly elevated superiorly with a spatula to visualize the haptic under the iris. Using a modified McCannel-type technique, a 10-0 polyprolene suture was passed under the haptic and retrieved through the proximal paracentesis before the haptic was fixed to the peripheral iris. Similarly, the other haptic was sutured, with the optic manipulated into the posterior chamber.

Intrascleral fixation technique

Intrascleral fixation of foldable PCIOL was performed via injection using a similar method as described by Gabor and Pavlidis[12]. The conjunctiva was opened at two clock-hour in the superior and inferior quadrants prior to cauterization. Scleral tunnels of 3 mm length were formed 1.5 mm from, and parallel to, the limbus using a 25-gauge trocar blade at the 6 o'clock and 12 o'clock positions. Infusions were then instilled into the anterior chamber or pars plana. A clear incision of 3 mm was made superiorly before the creation of a side port incision at 3 o'clock using a 23 MVR blade at the cornea. The leading haptic at the edge of the cartridge was grasped using 25-gauge forceps in the inferior scleral tunnel. The optic was then opened in the anterior chamber gradually while the cartridge was withdrawn and the trailing haptic unfolded outside the anterior chamber through the corneal incision. The leading haptic was externalized from the inferior scleral tunnel. Consequently, the trailing haptic was transferred from the superior corneal incision to the 23-gauge forceps in the side port at the 3 o'clock position and later grasped by the 25-gauge forceps in the superior scleral tunnel using the handshake technique[22] and externalized. The haptics were fixed by suturing around the scleral tunnels with 8-0 polyglactin suture and the conjunctiva was closed.

Statistical analysis

NCSS (Number Cruncher Statistical System) 2007 & PASS (Power Analysis and Sample Size 2008 Statistical Software, Utah, USA) were used for statistical analyses. BCVA values were converted to logarithm of the minimum angle of resolution (logMAR) units in all patients. The Kruskal-Wallis test was used to compare three and more groups demonstrating abnormal distributions. The Mann-Whitney U test was used to compare qualitative data between groups. The Wilcoxon signed rank test was used intra-group comparisons of parameters demonstrating an abnormal distribution. P-values of <0.05 were considered statistically significant.

RESULTS

The present study included 60 patients (60 aphakic vitrectomized eyes) without sufficient capsular support. No significant difference in patient age was observed between groups (P=0.50). Table 1 summarizes the demographic characteristics of the study population. Ocular conditions prior to IOL implantation are shown in table 2.

Table 3 presents the timings of IOL implantation. BCVA changes before and after surgery are provided in table 4. Statistically significant increases in visual acuity were observed postoperatively in all groups, except for the TSF group in which there was a trend toward increased BCVA postoperatively (P=0.092). No significant differences in preoperative VA were observed between groups (P=0.123); however, postoperative values were found to differ significantly between groups (P=0.003). Postoperative VA values were highest in the IF group. No significant difference in BCVA was observed between groups (P=0.790)

Intraoperative complications were observed only in the IF group. Intraoperative IOL dislocation occurred in two patients, with one instance of recurrence observed in one of these patients. Postoperative complications are summarized in table 5. Mild temporary intraocular

hemorrhage (IOH), which resolved in 1-3 weeks, and postoperative cystoid macular edema (CME), demonstrated by optical coherence tomography, were more common among patients in the ISF group.

Table 1. Baseline characteristics and ophthalmic data

Number of eyes	60
Age, yrs (mean ± SD)	65.6 ± 12.2
Male/female	53/36
Type of IOL implantation	
Transscleral fixation	13
Iris fixation	17
Intrascleral fixation	30
Follow up, months (mean ± SD)	7.0 ± 3.7

IOL= intraocular lens; SD= standard deviation.

Table 2. Ocular conditions prior to IOL implantation

	TSF group	IF group	ISF group
IOL subluxation/dislocation	1	5	7
Crystalline lens subluxation/dislocation	5	4	3
Dislocated lens fragments during cataract surgery	4	3	5
Capsular damage during cataract surgery	3	3	3
Trauma/intraocular foreign body		1	6
Endophthalmitis		1	6

IOL= intraocular lens; TSF= transscleral fixation; IF= iris fixation; ISF= intrascleral fixation.

Table 3. Timing of IOL implantation

	Time of IOL implantation	
Groups	**During PPV, n (%)**	**After PPV, n (%)**
All groups	16 (27)	44 (73)
TSF group	3 (23)	10 (77)
IF group	4 (23)	13 (77)
ISF group	9 (30)	21 (70)

IOL= intraocular lens; PPV= pars plana vitrectomy; TSF= transscleral fixation; IF= iris fixation; ISF= intrascleral fixation.

Table 4. Preoperative and postoperative best-corrected visual acuities

	TSF group	IF group	ISF group	
Preoperative BCVA (logMAR) (mean ± SD)	1.36 ± 0.99	0.94 ± 0.71	1.33 ± 0.79	0.123
Postperative BCVA (logMAR) (mean ± SD)	0.89 ± 0.84	0.40 ± 0.30	0.84 ± 0.42	[c]0.003**
[b]P-value	0.092	0.001**	0.00**	
Change in BCVA (mean ± SD)	0.47 ± 1.00	0.55 ± 0.56	0.43 ± 0.67	0.790

SD= standard deviation; BCVA= best-corrected visual acuity; logMAR= logarithm of the minimum angle of resolution; TSF= transscleral fixation; IF= iris fixation; ISF= intrascleral fixation.
[a]= Kruskal-Wallis test; [b]= Wilcoxon signed ranks test; [c]= Mann-Whitney U test.
*= P<0.05; **= P<0.01.

CME occurred 1-3 months postoperatively and resolved within 6 months in all patients. Postoperative endophthalmitis was not observed in the present study.

No statistically significant difference between in the incidence of IOL-related astigmatism, calculated according to the PVA method, was observed between groups. However, while mean IOL-related astigmatism values were 0.91 diopter (D) in the IF group and 1.35 D in the ISF group, a value of 1.65 D was observed in the TSF group (P=0.20; Table 6).

DISCUSSION

The vitreous humor plays an important role in providing structure and volume due to its semi-solid gel-like properties. In a proportion of vitrectomized eyes, in addition to reduced amounts of vitreous humor, the eye anatomy may be altered due to surgery, trauma, inflammation, and natural events such as old age and myopia, leading to decreased scleral rigidity. The creation of a stable surgical environment in vitrectomized eyes during anterior segment surgery is typically challenging, and IOP regulation may be provided via anterior chamber or pars plana continuous fluid infusion.

In order to maintain stable and consistent vitreal volumes, low-fluctuating IOP (i.e., a balance between entering and exiting fluids) is required. As the incision is extended, it becomes more difficult to maintain stable and maintained IOP. Further, fluid regurgitation, sudden pressure drops, and risk of collapse all increase with surgical manipulations. Young *et al.*[28] attempted to overcome these challenges using a scleral tunnel incision rather than a corneal incision. Further, the use of bridle sutures in the rectus muscle reportedly have utility in preventing globe collapse intraoperatively[5].

The presence or absence of capsular support in vitrectomized eyes is important in determining the most appropriate surgical approach. While the surgical method is simple and evident in eyes with capsular support, the lack of a capsule requires the use of more complex surgical procedures. Posterior chamber implantation has many advantageous over anterior chamber implantation - the IOL is distant from the sensitive anterior chamber structures, aqueous flow

Table 5. Postoperative complications

	TSF group	IF group	ISF group
ERM			1
CME	1	1	4
Secondary glaucoma		1	
Transient intraocular pressure rise	3	1	5
Temporary IOH	1		4
Dense IOH		1	
IOL subluxation/dislocation	1		3
Retinal detachment		1	1
Temporary corneal edema			1

TSF= transscleral fixation; IF= iris fixation; ISF= intrascleral fixation; ERM= epiretinal membrane; CME= cystoid macular edema; IOH= intraocular hemorrhage; IOL= intraocular lens.

Table 6. Postoperative IOL related astigmatism

	TSF group	IF group	ISF group	[a]P-value
IOL related astigmatism (mean ± SD)	1.65 ± 1.00	0.91 ± 0.40	1.35 ± 1.67	0.200

SD= standard deviation; TSF= transscleral fixation; IF= iris fixation; ISF= intrascleral fixation; IOL= intraocular lens.
a= Kruskal-Wallis test.

paths, and cornea endothelium. Further, placement of the IOL close to the natural position of the crystalline lens has particular optical advantages.

Of the 13 patients that received ISF, CME was observed in one, IOL subluxation in one, and temporary IOH in one. Ahn *et al.*[5] performed foldable IOL transscleral fixation on 21 vitrectomized eyes. The authors observed temporary IOH in one patient and a reopened macular hole in one. Kaynak *et al.*[6] used a similar surgical technique on a series of 20 patients (of whom half were vitrectomized eyes), and reported suture erosion in two patients and CME in two patients. In studies in which transscleral fixation was applied with a large incision in vitrectomized eyes, higher complication rates of 39%-49% were reported in patients required repeat surgery[1-3]. A disadvantage of sutures in scleral fixation is the potential development of suture erosion over time[3,29]. We observed IOL subluxation in one patient in the present study. In the present study population of 13 cases, we observed a mean lens-related astigmatism of 1.65 D according to PVA measurements. There was a trend toward higher values in the TSF group than in the other groups.

In the second group, we applied the iris fixation technique in 17 patients. As the lens is stabilized parallel to the iris plane during iris fixation, IOL-related astigmatism was less in this group (0.91 D). In aphakic victrectomized eyes, the iris may be mid-dilated and iris atrophy leading to difficult iris fixation under fluid infusion may be observed. During the present study, we encountered posterior segment IOL dislocation in two cases, occurring twice in one case during the same procedure. Further, it is not always possible to maintain a round and regular pupil during iris fixation, with an associated risk of poor dilatation often during the postoperative period. We detected CME in one patient, secondary glaucoma in one, dense IOH in one, and retinal detachment in one. Complication rates were comparable in the present study to similar previous studies[9,10]. Previous studies have used iris claw lenses for iris fixation to correct aphakia in vitrectomized eyes[25,26]. While the lack of suture usage was an advantage in these studies, the requirement of a large incision and anterior chamber implantation were disadvantages[25,26].

Two major methods of suture-free intrascleral IOL implantation have been reported in previous literature. In this technique, the haptics are fixated under scleral flaps using tissue adhesive glue[20-22] or into a narrow scleral tunnel parallel to the limbus[12-19]. Fixation into the scleral tunnel has advantages, such as removing the requirement need for an additional tissue adherent or the use of scleral flaps. In the third group of the present study, we applied the intrascleral tunnel fixation technique in 30 patients. In contrast to previous studies, the haptics of the IOL were sutured with polyglactin sutures in order to achieve better early postoperative fixation in vitrectomized eyes. We detected ERM in one patient, CME in four, temporary IOH in four, IOL subluxation/dislocation in three, and retinal detachment in one. Temporary IOH and postoperative CME were also observed more frequently in this group. Temporary IOH at 1-3 weeks and CME at 6 months completely resolved during the study period. These postoperative complications have also been reported in similar previously-reported studies[13,16-19].

No significant difference in VA change was observed between groups in the present study (P=0.79) While there was no difference in preoperative VA, a statistical difference between postoperative VA values was observed between groups (P=0.003). In the IF group, patients had higher VA values. The non-uniform diagnosis of patients between groups and the reduced sample size may have influenced postoperative visual outcomes and resulted in the observed differences between groups.

In conclusion, none of the three surgical techniques were associated with superior postoperative results, with no prominence observed in terms of comparative surgical outcomes. The present study was limited by a lack of randomization and the time difference between the three groups. Further controlled studies in larger study samples may provide further information regarding the relative efficacy of these techniques.

REFERENCES

1. Johnston RL, Charteris DG, Horgan SE, Cooling RJ. Combined pars planavitrectomy and sutured posterior chamber implant. Arch Ophthalmol. 2000;118(7):905-10.
2. Bading G, Hillenkamp J, Sachs HG, Gabel VP, Framme C. Long-term safety and functional outcome of combined pars plana vitrectomy and scleral-fixated sutured posterior chamber lens implantation. Am J Ophthalmol. 2007;144(3):371-377.
3. Vote BJ, Tranos P, Bunce C, Charteris DG, Da Cruz L. Long-term outcome of combined pars plana vitrectomy and scleral fixated sutured posterior chamber intraocular lens implantation. Am J Ophthalmol. 2006;141(2):308-312.
4. Regillo CD, Tidwell J. A small-incision technique for suturing a posterior chamber intraocular lens. Ophthalmic Surg Lasers. 1996;27(6):473-5.
5. Ahn JK, Yu HG, Chung H, Wee WR, Lee JH. Transscleral fixation of a foldable intraocular lens in aphakic vitrectomized eyes. J Cataract Refract Surg. 2003;29(12):2390-6.
6. Kaynak S, Ozbek Z, Pasa E, Oner FH, Cingil G. Transscleral fixation of foldable intraocular lenses. J Cataract Refract Surg. 2004;30(4):854-7.
7. Zhang ZD, Shen LJ, Liu XQ, Chen YQ, Qu J. Injection and suturing technique for scleral fixation foldable lens in the vitrectomized eye. Retina. 2010;30(2):353-6.
8. Condon GP. Simplified small-incision peripheral iris fixation of an AcrySof intraocular lens in the absence of capsule support. J Cataract Refract Surg. 2003;29(9):1663-7.
9. Condon GP, Masket S, Kranemann C, Crandall AS, Ahmed II. Small-incision iris fixation of foldable intraocular lenses in the absence of capsule support. Ophthalmology. 2007;114(7):1311-8.
10. Kopel AC, Carvounis PE, Hamill MB, Weikert MP, Holz ER. Iris-sutured intraocular lenses for ectopia lentis in children. J Cataract Refract Surg. 2008;34(4):596-600.
11. Benevento JD, Ponce EA, Dayan AR. Injection of an intraocular lens in an eye without capsular support. J Cataract Refract Surg. 2007;33(1):15-8.
12. Gabor SG, Pavlidis MM. Sutureless intrascleral posterior chamber intraocularlens fixation. J Cataract Refract Surg. 2007;33(11):1851-4.
13. Scharioth GB, Prasad S, Georgalas I, Tataru C, Pavlidis M: Intermediate results of sutureless intrascleral posterior chamber intraocular lens fixation. J Cataract Refract Surg. 2010;36(2):254-9.
14. Prenner JL, Feiner L, Wheatley HM, Connors D. A novel approach for posterior chamber intraocular lens placement or rescue via a sutureless scleral fixation technique. Retina. 2012;32(4):853-5.
15. Totan Y, Karadag R. Trocar-assisted sutureless intrascleral posterior chamber foldable intra-ocular lens fixation. Eye. 2012;26(6):788-91.
16. Prasad S. Transconjunctival sutureless haptic fixation of posterior chamber IOL: a minimally traumatic approach for IOL rescue or secondary implantation. Retina. 2013; 33(3):657-60.
17. Ohta T, Toshida H, Murakami A. Simplified and safe method of sutureless intrascleral posterior chamber intraocular lens fixation: Y-fixation technique. J Cataract Refract Surg. 2014;40(1):2-7.
18. Yamane S, Inoue M, Arakawa A, Kadonosono K. Sutureless 27-gauge needle-guided intrascleral intraocular lens implantation with lamellar scleral dissection. Ophthalmology. 2014;121(1):61-6.
19. Liu S, Cheng S. Modified method of sutureless intrascleral posterior chamber intraocular lens fixation without capsular support. Eur J Ophthalmol. 2013;23(5):732-7.
20. Agarwal A, Kumar DA, Jacob S, Baid C, Agarwal A, Srinivasan S. Fibrin glue-assisted sutureless posterior chamber intraocular lens implantation in eyes with deficient posterior capsules. J Cataract Refract Surg. 2008;34(9):1433-8.
21. Kumar DA, Agarwal A, Prakash D, Prakash G, Jacob S, Agarwal A. Glued intrascleral fixation of posterior chamber intraocular lens in children. Am J Ophthalmol. 2012; 153(4):594-601.
22. Agarwal A, Jacob S, Kumar DA, Agarwal A, Narasimhan S, Agarwal A. Handshake technique for glued intrascleral haptic fixation of a posterior chamber intraocular lens. J Cataract Refract Surg. 2013;39(3):317-22.
23. Malinowski SM, Mieler WF, Koenig SB, Han DP, Pulido JS. Combined pars plana vitrectomy-lensectomy and open-loop anterior chamber lens implantation. Ophthalmology. 1995;102(2):211-6.
24. Kazemi S, Wirostko WJ, Sinha S, Mieler WF, Koenig SB, Sheth BP. Combined pars plana lensectomy-vitrectomy with open-loop flexible anterior chamber intraocular lens (AC IOL) implantation for subluxated lenses. Trans Am Ophthalmol Soc. 2000;98:247-253.
25. Acar N, Kapran Z, Altan T, Kucuksumer Y, Unver YB, Polat E. Secondary iris claw intraocular lens implantation for the correction of aphakia after pars plana vitrectomy. Retina. 2010;30(1):131-9.
26. Riazi M, Moghimi S, Najmi Z, Ghaffari R. Secondary Artisan-Verysise intraocular lens implantation for aphakic correction in post-traumatic vitrectomized eye. Eye. 2008; 22(11):1419-24.
27. Lewis JS. Ab externo sulcus fixation. Ophthalmic Surg. 1991;22(11):692-5.
28. Young AL, Leung GY, Cheng LL, Lam DS. A modified technique of scleral fixated intraocular lenses for aphakic correction. Eye. 2005;19(1):19-22.
29. Price MO, Price FW Jr, Werner L, Berlie C, Mamalis N. Late dislocation of scleral-sutured posterior chamber intraocular lenses. J Cataract Refract Surg. 2005;31(7):1320-6.

Bacteriological profile in conjunctival, lacrimal sac, and nasal specimens and conjunctival normalization time following external, endoscopic, and transcanalicular multidiode laser dacryocystorhinostomy

Perfil bacteriológico e tempo de normalização conjuntival de espécimes de conjuntiva, saco lacrimal e nasais após dacriocistorrinostomia externa, endoscópica e transcanalicular com laser de multi diodo

Melike Balikoglu-Yilmaz[1,2], Ayse Banu Esen[3], Tolga Yilmaz[2], Umit Taskin[4], Muhittin Taskapili[2], M. Faruk Oktay[4], Emine Sen[5], Timur Kose[6]

ABSTRACT

Purpose: To compare the conjunctival, lacrimal sac, and nasal flora cultures and conjunctival normalization time following external (EX-), endoscopic (EN-), and transcanalicular multidiode laser (TC-) dacryocystorhinostomy (DCR) and to evaluate the relationship between culture positivity and surgical success. We further performed antibiotic sensitivity analyses for lacrimal sac culture samples.

Methods: A total of 90 patients with primary acquired nasolacrimal duct obstruction were recruited and divided into EX-DCR (n=32), EN-DCR (n=28), and TC-DCR (n=30) groups. Conjunctival, nasal, and lacrimal sac cultures and antibiograms were analyzed.

Results: In all three groups, coagulase-negative *Staphylococcus* (CNS) was predominantly isolated preoperatively from the conjunctiva, nose, and lacrimal sac and postoperatively from the conjunctiva. Preoperative and postoperative conjunctival culture positivity rates were similar between all the groups (p>0.05). A statistically significant difference in the growth rate of culture in the lacrimal sac was observed between the three groups (p=0.001). CNS and *Staphylococcus aureus* cultures were predominantly sensitive to linezolid, teicoplanin, tigecycline, vancomycin, and mupirocin. Conjunctival normalization times were similar between the three groups (p>0.05). Anatomical and functional success rates were not found to be significantly correlated with preoperative conjunctival and lacrimal sac culture positivity (p>0.05).

Conclusions: Similar rates of preoperative and 1-week postoperative conjunctival culture positivity were observed in all the groups; a significantly lower bacterial growth rate was observed in postoperative conjunctival cultures. CNS was the most commonly isolated organism. Bacterial growth rates in the lacrimal sac samples were significantly higher in the EN-DCR group. Bacterial growth rates obtained preoperatively from the conjunctival and lacrimal sac culture samples were not correlated with DCR success.

Keywords: Conjunctiva; Dacryocystorhinostomy; Nasolacrimal duct; Antibiotic sensitivity tests; *Staphylococcus aureus*, Transcanalicular multidiode laser

RESUMO

Objetivo: *Comparar a flora conjuntival, do saco lacrimal e nasal com o tempo de normalização após dacriocistorrinostomia (DCR) externa (EX-), endoscópica (EN-) e transcanalicular a laser de multi diodo (TC-) para correlacionar a positividade da cultura com o sucesso cirúrgico, assim como identificar a sensibilidade aos antibióticos em amostras de saco lacrimal.*

Métodos: *Neste estudo prospectivo, 90 pacientes com obstrução do canal nasolacrimal adquirida primária foram incluídos e divididos em grupos EX-DCR (n=32), EN-DCR (n=28) e TC-DCR (n=30). Culturas e antibiogramas conjuntivais, nasais e do saco lacrimal foram analisados.*

Resultados: Staphylococcus *coagulase-negativo (CNS) foi o organismo predominante isolado no pré-operatório (conjuntiva e nariz), no transoperatório (saco lacrimal) e pós-operatório (conjuntiva), nos 3 grupos. Taxas de positividade de cultura da conjuntiva pré- e pós-operatórias nos três grupos foram semelhantes (p>0,05). A diferença nas taxas de crescimento do saco lacrimal dos três grupos foi estatisticamente significativa (p=0,001). CNS e S.* aureus *foram mais sensíveis a linezolida, teicoplanina, a tigeciclina, vancomicina e mupirocina. O tempo de normalização conjuntival foi semelhante nos três grupos (p>0,05). Não houve relação estatisticamente significativa entre as taxas de sucesso anatômicas e funcionais e a positividade da cultura conjuntival e de saco lacrimal pré-operatória (p>0,05).*

Conclusões: *Pacientes submetidos a EX-DCR, EN-DCR, e TC-DCR apresentaram positividades de cultura conjuntival semelhantes no pré-operatório e na 1ª semana pós-operatória. Houve uma redução significativa na taxa de crescimento das culturas da conjuntiva pós-operatórias. O organismo mais comumente isolado foi o CNS. A taxa de crescimento de bactérias a partir do saco lacrimal foi significativamente maior no grupo PT-DCR. O crescimento bacteriano da conjuntiva no pré-operatório e de amostras do saco lacrimal no transoperatório não se relacionaram com o sucesso da DCR.*

Descritores: *Conjuntiva; Dacriocistorinostomia; Ducto nasolacrimal; Testes de sensibilidade microbiana; Lasers semicondutores*

INTRODUCTION

Nasolacrimal duct obstruction (NLDO) is a common ophthalmic presentation and has been reported to represent 3% of clinic visits[1]. NLDO is typically treated using either external (EX-) or endoscopic (EN-) dacryocystorhinostomy (DCR) or using transcanalicular multidiode laser (TC-) to create a fistula between the lacrimal sac and nasal cavity, allowing tear flow. Each type of DCR is associated with specific advantages and disadvantages[2,3]. The traditional DCR procedure (EX-DCR) can cause cutaneous scarring, disruption of the medial canthus, and excessive intra-operative bleeding. Advantages of EN-DCR

Submitted for publication: August 10, 2015
Accepted for publication: February 10, 2016

[1] Department of Ophthalmology, Faculty of Medicine, Izmir Katip Celebi University, Izmir, Turkey.
[2] Department of Ophthalmology, Bagcilar Education and Research Hospital, Istanbul, Turkey.
[3] Department of Microbiology and Clinical Microbiology Bagcilar Education and Research Hospital, Istanbul, Turkey.
[4] Department of Otorhinolaryngology, Bagcilar Education and Research Hospital, Istanbul, Turkey.
[5] Department of Ophthalmology, Ulucanlar Eye Education and Research Hospital, Ankara, Turkey.
[6] Department of Biostatistics and Medical Informatics, Faculty of Medicine, Ege University, Izmir, Turkey.

Funding: The present study was supported by the Institutional Review Board of Bagcilar Education and Research Hospital, Istanbul, Turkey (#1852).

Disclosure of potential conflicts of interest: None of the authors have any potential conflicts of interest to disclose.

Corresponding author: Melike Balikoglu-Yilmaz. Department of Ophthalmology, Izmir Katip Celebi University. Faculty of Medicine. Izmir - Turkey - E-mail: drmelkebalkoglu@yahoo.com

Approved by the following research ethics committee: Bagcilar Education and Research Hospital (#2011/13).

and TC-DCR include the absence of a cutaneous scar and decreased operative duration. The new TC-DCR has demonstrated safe utility in elderly patients with systemic diseases[4-8].

A unique combination of stasis and moisture in NLDO may create an optimal environment for the growth of lacrimal sac flora. Numerous bacterial species have been implicated in chronic dacryocystitis[9]. Furthermore, the types of isolated pathogens may change over time[10,11]. Accurate identification of the pathogens responsible for chronic dacryocystitis is critical for the selection of appropriate antibiotic agents[12]. Therefore, to the best of our knowledge, we were the first to compare the three types of DCR with respect to culture results with a view to select an appropriate antibiotic cover following each technique. Here we aimed to compare bacterial species preoperatively isolated from the involved and contralateral conjunctival samples and from the involved and contralateral nasal and lacrimal sac samples together with those isolated from the involved side conjunctival samples after performing EX-DCR, EN-DCR and TC-DCR in patients. The present study also aimed to assess the relationship between culture results and success rates of each DCR type, identify the bacterial species most commonly responsible for dacryocystitis, and evaluate corresponding antibiograms of cultured isolates.

METHODS

This prospective, non-randomized, and comparative clinical study was conducted at the Departments of Ophthalmology and Otorhinolaryngology of Bagcilar Education and Research Hospital in Istanbul, Turkey, between February 2011 and December 2012. The present study was conducted in accordance with the ethical guidelines of the Declaration of Helsinki after obtaining approval from the Institutional Ethics Committee. All patients provided informed consent.

We included patients with symptoms of epiphora who were diagnosed with PANDO upon detection of obstruction on syringing and probing or on performing antero-posterior and lateral dacryocystography using lipiodol. Exclusion criteria were as follows: previous nasal or nasolacrimal system surgery; pre-saccal obstruction; canalolithiasis; lacrimal system tumor; previous trauma to the ocular and nasal regions; bony deformity; abnormal intranasal anatomy, including an advanced deviated nasal septum, middle turbinate (MT) hypertrophy, or concha bullosa; nasal polyps; and previous treatment with topical or systemic antibiotics a month prior to undergoing DCR.

A total of 90 patients scheduled to undergo primary DCR were included in the present study. Data regarding clinical outcomes of this study population were previously reported[13]. Patients were non-randomly assigned into the EX-DCR (n=32), EN-DCR (n=28), and TC-DCR (n=30) groups according to the type of DCR requested. Patients were provided information regarding the EX-DCR, EN-DCR, and TC-DCR methods. Surgeries were performed in a standardized manner according to previously published methods[13]. EX-DCR and TC-DCR were performed by three ophthalmic surgeons (M.B.Y., T.Y., and M.A.) who were highly experienced in EX-DCR and moderately experienced in TC-DCR. EN-DCR was performed by an experienced otolaryngologist (U.T.).

The techniques used in the present study were as follows:

EX-DCR: A 15-20-mm straight incision was created medial to the angular vein at the level of the anterior lacrimal crest. The lacrimal fossa was exposed by blunt dissection of the orbicularis muscle and opening of the periosteum prior to D-shaped osteotomy to create a bone window extending from the medial canthal tendon to the proximal nasolacrimal duct, with the posterior lacrimal crest at the posterior aspect. An H-shaped incision was then created in the lacrimal sac and nasal mucosa using a surgical blade, and opposing mucosal flaps were sutured with absorbable 6/0 vicryl. To prevent canalicular "cheese wiring," a bicanalicular silicone tube was placed and tied gently and the skin was sutured with continuous 6/0 polypropylene to provide good cosmesis.

EN-DCR: The maxillary fissure on the lateral nasal wall was initially identified before the creation of a 2 × 1.5-cm mucoperiosteal flap. The lacrimal bone was then exposed and drilled into with a diamond burr to expose at least a 1 × 1-cm area of the sac while protecting the uncinate process. A lateral nasal wall opening was created through the MT axilla. The sac medial wall bulged from the new opening upon the application of pressure over the sac. A vertical incision was then created in the sac and the medial wall was excised, followed by the insertion of a bicanalicular silicone tube from both the upper and lower puncta and tying of the free ends in the nasal cavity.

TC-DCR: We first dilated the superior and inferior puncta, followed by the insertion of a semirigid 600-µm quartz multidiode laser fiber (Multidiode S30 OFT, INTERmedic Arfran, Madrid, Spain) through the canaliculus. The fiber was then rotated in an oblique orientation such that it rested against the medial lacrimal sac wall. Laser parameters used were as follows: power, 10 W and pulse length, 400 milliseconds, adjusted as necessary with an interval between pulses of 400 milliseconds. We used a 0°, 4-mm rigid nasal endoscope as the nasal probe and a periosteal elevator to deviate the MT medially to provide good exposure for the last procedure. We were also able to provide protection from the laser probe using this technique. The red aiming beam of the laser probe was then directed at the lateral nasal wall and used to create an ostium of adequate size. The laser was then used to ablate the lacrimal bone and nasal mucosa. This osteotomy site was immediately anterior and inferior to the root of the MT. Osteotomy was widened using the laser prior to the placement of bicanalicular silicone tubes once the laser probe was withdrawn.

Postoperatively, all patients were prescribed oral antibiotics, an anti-inflammatory drug, combination antibiotic-steroid eye drops four times a day for 1 week, and a nasal corticosteroid spray twice a day after nasal irrigation with 0.9% normal saline for 1 month to eradicate fibrin clots.

For each patient, conjunctival and nasal (inferior meatus) samples were obtained preoperatively from both the involved and contralateral sides. Lacrimal sac cultures were obtained directly from the lacrimal sac during DCR. Antibiograms for cultures from the lacrimal sac were also evaluated. Patients were re-examined weekly during the first 2 postoperative months, and subsequently followed up on a monthly basis. We continued to postoperatively obtain and analyze conjunctival cultures from the involved side each week until negative culture results were obtained twice. Silicone tubes were removed at the 2-month postoperative visit. Anatomical success was defined as endoscopic endonasal ostium patency and successful nasolacrimal irrigation without reflux. Functional success was defined as resolution of epiphora. Conjunctival normalization time was defined as the time from DCR until the second negative result of conjunctival culture from the involved side.

Conjunctival, lacrimal, and nasal culture

Preoperative conjunctival and nasal and postoperative conjunctival, culture samples were inoculated onto 5% sheep's blood, chocolate, MacConkey, and Sabouraud dextrose agar media (Premed, Turkey). Lacrimal sac culture samples were also inoculated on the same media as well as on anaerobic agar and thioglycolate broth media during DCR. Both blood and chocolate agars were incubated at 37°C in a 5%-10% CO_2 atmosphere for 24-72 hours. MacConkey agar was incubated at 37°C in ambient air for 24-72 hours. Sabouraud Dextrose agar was incubated at both 25°C and 37°C for 21 days. Anaerobic agar and thioglycolate broth media were incubated at 37°C under anaerobic conditions using the GasPak Anaerobe Pouch System (BD, USA) for 48 hours. Organisms isolated from samples were examined using Gram's stain and KOH mount and identified using the Vitec 2 compact system (bioMerieux, Marcy-l'Etoile, France). Susceptibility testing of isolated species was performed using the same system.

Statistical analysis

IBM SPSS Statistics, version 20.0 software (SPSS Inc. Chicago, IL, USA) was used for all statistical analyses. Continuous variables were presented as mean ± standard deviation and categorical data were presented as numbers and percentages. The chi-square (χ^2) test or Fisher's exact test was used to compare categorical variables between the groups. Numerical variables were compared between the three groups using analysis of variance (one-way ANOVA) or the Kruskal-Wallis test. The Mann-Whitney U test or Fisher's exact test was used for pairwise comparisons of variables found to significantly differ between groups according to the Kruskal-Wallis test. The McNemar test was used to analyze culture positivity before and after DCR. All hypothesis controls were applied at a significance level of α=0.05 (p values of ≤0.05 were considered to be statistically significant).

RESULTS

The present study included 69 (77%) female and 21 (23%) male patients, with a mean age of 49.8 ± 18.9 (range, 4-86) years. EX-DCR, EN-DCR, and TC-DCR were used in 32, 28, and 30 patients, respectively. The mean follow-up time was 16.1 ± 2.5 (range, 10-20) months. Descriptive patient characteristics are presented in table 1.

Bacteria isolated from conjunctival, nasal, and lacrimal sac samples are presented in table 2. Coagulase-negative *Staphylococcus* (CNS) was the predominant organism isolated from pre- and postoperatively obtained first-week conjunctival samples (14.4% for involved eyes and 12.2% for other eyes preoperatively, and 11.1% for involved eyes postoperatively) as well as from the preoperative nasal mucosa (67.8% for both sides) and lacrimal sac samples (22.2%). *Bacteroides fragilis* was the only anaerobic bacterial strain isolated from lacrimal sac samples; that sample was from a single patient in the EX-DCR group.

EX-, EN- and TC-DCR groups had similar conjunctival culture positivity rates of 46.9%, 42.9%, and 30%, respectively, at the first preoperative week and 18.8%, 3.6%, and 13.3%, respectively, at the first postoperative week (preoperative, p=0.372; and postoperative, p=0.196; Table 3). Conjunctival culture positivity rates were significantly lower after EX- and EN-DCR (p=0.022 and p=0.001, respectively). Although there was a trend toward a lower conjunctival culture positivity rate after TC-DCR, this trend was not statistically significant (p=0.267). The conjunctival growth rate was 40.0% (36 patients) at the involved site and 23.3% (21 patients) at the contralateral site, with a statistically significant difference observed (p=0.004). In contrast, the nasal growth rate was 98.9% (89 patients) at the involved site and 97.8% (88 patients) at the contralateral side, with no statistically significant difference observed (p=1.000).

The lacrimal sac culture growth rate was significantly higher in the EN-DCR (85.7%) group than in the EX-DCR (40.6%) and TC-DCR groups (46.7%, p=0.001). Comparison between conjunctival flora and lacrimal sac flora isolated from the involved side demonstrated a significantly higher lacrimal sac growth rate (56.7%, 51 patients) than the conjunctival growth rate (40.0%, 36 patients; p=0.011). Conjunctival normalization times were similar between the three groups (1.5 ± 1.1, 1.0 ± 0.2, and 1.2 ± 0.5 weeks for EX-, EN-, and TC-DCR, respectively; p=0.166; Table 3).

Anatomical and functional success rates were not found to be associated with preoperative conjunctival and lacrimal sac culture positivity rates within the three groups and among all patients included in the present study (p>0.05 for all; Table 4).

CNS and *Staphylococcus aureus* were most sensitive to linezolid, teicoplanin, tigecycline, vancomycin, and mupirocin (antibiotic sensitivity, 100% for all) (Table 5) and most resistant to penicillin G and tetracycline (antibiotic resistance, 95.5% and 62.5%, respectively).

DISCUSSION

The microbiological properties of the lacrimal sac in PANDO patients has been a topic of interest in recent years as the spectrum of organisms constituting the lacrimal flora appears to have changed due to many factors[11,14,15]. Despite a large number of comparative studies on DCR, none have previously compared three separate methods in terms of microbiological findings. Accordingly, we believe that the present study is the first to compare clinico-bacteriological outcomes between conjunctival, nasal, and lacrimal sac samples isolated following three types of DCR (EX, EN, and TC).

The pathogens responsible for chronic dacryocystitis are typically gram-positive bacteria, including CNS, *S. aureus,* and Streptococci[16]. Staphylococci, particularly *S. aureus,* have now replaced Streptococci as the most common cause of chronic dacryocystitis following the discovery of effective antibiotics, such as penicillin and cephalosporins, to which they have demonstrated greater resistance[10,11]. Coden *et al.*[17] evaluated culture samples from purulent lacrimal sac contents in 236 patients with dacryocystitis who were undergoing DCR and reported that the most common bacteria were *S. epidermidis* (27.3%) and *S. aureus* (22.1%), with a positive culture rate of 52%. Owji *et al.*[15] studied lacrimal sac cultures from the involved side and conjunctival cultures from the involved and normal sides of patients with NLDO and chronic dacryocystitis, and they found that the most frequently isolated organisms from the lacrimal sac and conjunctiva of the involved side were *S. aureus* (47.5% and 47.5%, respectively) and *S. epidermidis* (22.5% and 20%, respectively). On the other hand, the most frequently isolated organisms from the conjunctiva of the normal side and from that of the control healthy subjects were *S. epidermidis* (60% and 60%, respectively) and *S. aureus* (47.5% and 30%, respectively)[15]. Pradeep *et al.*[18] reported that the most common isolates from lacrimal sac specimens in chronic dacryocystitis cases were CNS and *S. aureus* (71% and 14%, respectively). In the present study, the most commonly isolated organisms from the involved conjunctival side during the preoperative and first postoperative week, involved nasal side preoperatively, lacrimal sac preoperatively, and contralateral conjunctival and nasal sites preoperatively were *S. epidermidis* (14.4%, 11.1%, 67.8%, 22.2%, 12.2%, and 67.8%, respectively) and *S. aureus*

Table 1. Patient characteristics

	EX-DCR (n=32)	EN-DCR (n=28)	TC-DCR (n=30)	Total (n=90)	*p* value
Age (years)*	52.2 ± 16.5	46.8 ± 20.9	50.1 ± 19.8	49.8 ± 18.9	0.544[a]
Female: male	26:6	20:8	23:7	69:21	0.669[b]
Laterality (right: left)	17:15	14:14	15:15	46:44	0.961[b]
Follow-up time (months)*	17.0 ± 2.1	13.9 ± 2.3[d,e]	17.3 ± 1.3	16.1 ± 2.5	<0.001[c]

EX-DCR= external dacryocystorhinostomy; EN-DCR= endoscopic dacryocystorhinostomy; TC-DCR= transcanalicular dacryocystorhinostomy with multidiode laser.
*= Values are presented as mean ± standard deviation; [a]= One-way ANOVA; [b]= Chi-square (χ^2) test; [c]= Kruskal-Wallis test; [d]= p<0.001 compared with the EX-DCR group, Mann-Whitney U test; [e]= p<0.001 compared with the TC-DCR group, Mann-Whitney U test.

Table 2. Results of preoperative conjunctival, nasal, and lacrimal sac cultures as well as of postoperative conjunctival cultures

	EX-DCR (n=32)		EN-DCR (n=28)		TC-DCR (n=30)		Total (n=90)	
	I	C	I	C	I	C	I	C
Preoperative conjunctival culture								
No bacteria isolated	17 (53.1)	21 (65.6)	16 (57.1)	20 (71.4)	21 (70.0)	28 (93.3)	54 (60.0)	69 (76.7)
MSSA	1 (3.1)	2 (6.3)	1 (3.6)	3 (10.7)	3 (10.0)	1 (3.3)	5 (5.6)	6 (6.7)
MRSA	-	-	1 (3.6)	1 (3.6)	1 (3.3)	1 (3.3)	2 (2.2)	2 (2.2)
Staph. epidermidis	6 (18.8)	7 (21.9)	6 (21.4)	4 (14.3)	1 (3.3)	-	13 (14.4)	11 (12.2)
Staph. hominis	-	1 (3.1)	-	-	-	-	-	1 (1.1)
Staph. lugdunensis	1 (3.1)	-	-	-	-	-	1 (1.1)	-
Staph. haemolyticus	-	-	-	-	2 (6.7)	-	2 (2.2)	-
Staph. warneri	-	-	1 (3.6)	-	-	-	1 (1.1)	-
Strep. pluranimalium	1 (3.1)	-	-	-	-	-	1 (1.1)	-
Strep. sanguinis	1 (3.1)	-	-	-	-	-	1 (1.1)	-
Strep. pneumoniae	-	-	2 (7.1)	-	-	-	2 (2.2)	-
Haemophilus influenzae	1 (3.1)	-	-	-	-	-	1 (1.1)	-
Pseudomonas aeruginosa	1 (3.1)	-	-	-	-	-	1 (1.1)	-
Proteus mirabilis	1 (3.1)	1 (3.1)	-	-	1 (3.3)	-	2 (2.2)	1 (1.1)
Citrobacter koseri	1 (3.1)	-	-	-	1 (3.3)	-	2 (2.2)	-
Sphingomonas paucimobilis	1 (3.1)	-	-	-	-	-	1 (1.1)	-
Neisseria elongata	-	-	1 (3.6)	-	-	-	1 (1.1)	-
Preoperative nasal culture								
No bacteria isolated	-	1 (3.1)	1 (3.6)	1 (3.6)	-	-	1 (1.1)	2 (2.2)
MSSA	5 (15.6)	7 (21.9)	8 (28.6)	7 (25.0)	4 (13.3)	3 (10.0)	17 (18.9)	17 (18.9)
MRSA	-	-	-	-	3 (10.0)	3 (10.0)	3 (3.3)	3 (3.3)
Staph. epidermidis	25 (78.1)	23 (71.9)	16 (57.1)	19 (67.9)	20 (66.7)	19 (63.3)	61 (67.8)	61 (67.8)
Staph. hominis	1 (3.1)	1 (3.1)	1 (3.6)	-	-	-	2 (2.2)	1 (1.1)
Staph. haemolyticus	-	-	1 (3.6)	-	2 (6.7)	2 (6.7)	3 (3.3)	2 (2.2)
Strep. pneumoniae	-	-	1 (3.6)	1 (3.6)	-	1 (3.3)	1 (1.1)	2 (2.2)
Pseudomonas aeruginosa	-	-	-	-	1 (3.3)	1 (3.3)	1 (1.1)	1 (1.1)
Serratia marcescens	-	-	-	-	-	1 (3.3)	-	1 (1.1)
Sphingomonas paucimobilis	1 (3.1)	-	-	-	-	-	1 (1.1)	-
Lacrimal sac culture								
No bacteria isolated	19 (59.4)	-	4 (14.3)	-	16 (53.3)	-	39 (43.3)	-
Aerobic bacteria								
MSSA	1 (3.1)	-	6 (21.4)	-	4 (13.3)	-	11 (12.2)	-
MRSA	-	-	1 (3.6)	-	1 (3.1)	-	2 (2.2)	-
Staph. epidermidis	4 (12.5)	-	11 (39.3)	-	5 (16.7)	-	20 (22.2)	-
Staph. lugdunensis	1 (3.1)	-	-	-	-	-	1 (1.1)	-
Staph. haemolyticus	-	-	1 (3.6)	-	1 (3.1)	-	2 (2.2)	-
Corynebacterium jeikeium	-	-	1 (3.6)	-	-	-	1 (1.1)	-
Strep. pluranimalium	1 (3.1)	-	-	-	-	-	1 (1.1)	-
Strep. mitis	1 (3.1)	-	1 (3.6)	-	-	-	2 (2.2)	-
Strep. pneumonia	-	-	1 (3.6)	-	-	-	1 (1.1)	-
Strep. pyogenes	-	-	1 (3.6)	-	-	-	1 (1.1)	-
Haemophilus influenzae	1 (3.1)	-	-	-	-	-	1 (1.1)	-
Pseudomonas aeruginosa	1 (3.1)	-	-	-	1 (3.1)	-	2 (2.2)	-
Serratia marcescens	-	-	-	-	1 (3.1)	-	1 (1.1)	-
Citrobacter koseri	1 (3.1)	-	-	-	1 (3.1)	-	2 (2.2)	-
Sphingomonas paucimobilis	1 (3.1)	-	-	-	-	-	1 (1.1)	-
Kocuria kristinae	-	-	1 (3.6)	-	-	-	1 (1.1)	
Anaerobic bacteria								
Bacteroides fragilis	1 (3.1)	-	-	-	-	-	1 (1.1)	-
First postoperative week conjunctival culture								
No bacteria isolated	26 (81.2)	-	27 (96.4)	-	26 (86.7)	-	79 (87.8)	-
Staph. aureus	-	-	-	-	1 (3.3)	-	1 (1.1)	-
Staph. epidermidis	6 (18.8)	-	1 (3.6)	-	3 (10.0)	-	10 (11.1)	-
Second postoperative week conjunctival culture*								
No bacteria isolated	27 (87.1)	-	25 (100.0)	-	29 (96.7)	-	81 (94.1)	-
Staph. aureus	-	-	-	-	1 (3.3)	-	1 (1.2)	-
Staph. epidermidis	3 (9.7)	-	-	-	-	-	3 (3.5)	-
Staph. hominis	1 (3.2)	-	-	-	-	-	1 (1.2)	-
Third postoperative week conjunctival culture*								
No bacteria isolated	4 (66.7)	-	2 (100.0)	-	3 (100.0)	-	9 (81.8)	-
Staph. epidermidis	2 (33.3)	-	-	-	-	-	2 (18.2)	-
Fourth postoperative week conjunctival culture*								
No bacteria isolated	2 (66.7)	-	-	-	1 (100.0)	-	3 (75.0)	-
Staph. aureus	1 (33.3)	-	-	-	-	-	1 (25.0)	-

Values are presented as number (percentage). I= involved eye; C= contralateral eye; MSSA= methicillin-sensitive *Staph. aureus;* MRSA= methicillin-resistant *Staph. aureus*.
*= at the second, third, and fourth postoperative week, conjunctival culture specimens of the involved side were taken from 86, 11, and 4 patients, respectively.

Table 3. Bacterial growth rate and normalization time according to study group

	EX-DCR (n=32)	EN-DCR (n=28)	TC-DCR (n=30)	Total (n=90)	*p* value
Preoperative conjunctival site bacterial growth, n (%)					
Involved side	15 (46.9)	12 (42.9)	9 (30.0)	36 (40.0)	0.372[a,j]
Contralateral side	11 (34.4)	8 (28.6)	2 (6.7)	21 (23.3)	0.026[a,j]
p value				0.004[b,e]	
Preoperative nasal site bacterial growth, n (%)					
Involved side	32 (100.0)	27 (96.4)	30 (100.0)	89 (98.9)	0.326[a,j]
Contralateral side	31 (96.9)	27 (96.4)	30 (100.0)	88 (97.8)	0.596[a,j]
p value				1.000[b,f]	
Intraoperative lacrimal sac bacterial growth, n (%)					
Involved side	13 (40.6)	24 (85.7)	14 (46.7)	51 (56.7)	0.001[a,j]
p value	0.727[b,g]	0.002[b,g]	0.180[b,g]	0.011[b,g]	
First postoperative week conjuntival site bacterial growth, n (%)					
Involved side	6 (18.8)	1 (3.6)	4 (13.3)	11 (12.2)	0.196[a,j]
p value	0.022[b,h]	0.001[b,h]	0.267[b,h]	<0.001[b,h]	
Conjunctival normalization time (weeks, mean ± S.D.)					
Involved side	1.47 ± 1.08	1.04 ± 0.19	1.17 ± 0.46	1.23 ± 0.72	0.166[d,j]
Conjunctival flora growth					
No growth	1.29 ± 0.85	1.00 ± 0.00	1.24 ± 0.54	1.19 ± 0.59	
Growth	1.67 ± 1.29	1.08 ± 0.29	1.00 ± 0.00	1.31 ± 0.89	
p value	0.292[c,k]	0.248[c,k]	0.168[c,k]	0.659[c,k]	
Lacrimal sac flora growth					
No growth	1.26 ± 0.81	1.00 ± 0.00	1.06 ± 0.25	1.15 ± 0.59	
Growth	1.77 ± 1.36	1.04 ± 0.20	1.29 ± 0.61	1.29 ± 0.81	
p value	0.159[c,k]	0.683[c,k]	0.218[c,k]	0.264[c,k]	

EX-DCR= external dacryocystorhinostomy; EN-DCR= endoscopic dacryocystorhinostomy; TC-DCR= transcanalicular multidiode laser dacryocystorhinostomy.
[a]= Chi-square (χ^2) test; [b]= McNemar test; [c]= Mann-Whitney U test; [d]= Kruskal-Wallis test; [e]= preoperative flora growth rate in the involved conjunctival side compared with that in the contralateral conjunctival side; [f]= preoperative flora growth rate in the involved nasal side compared with that in the contralateral nasal side; [g]= aerobic flora growth rate in the lacrimal sac sample compared with preoperative flora growth rate at the involved conjunctival side; [h]= preoperative flora growth rate in the involved conjunctival side compared with the flora growth rate in the involved conjunctival side at the first postoperative week; [j]= comparison of external, endoscopic, and transcanalicular dacryocystorhinostomy; [k]= comparison of groups without and with growth based on sterilization week.

(7.8%, 1.1%, 22.2%, 14.4%, 8.9%, and 22.2%, respectively). Anatomical and functional success rates did not correlate with preoperative conjunctival and lacrimal sac bacterial growth rates.

Methicillin-resistant *S. aureus* (MRSA) has been implicated in dacryocystitis[19,20]. In a study of dacryocystitis caused by community-onset MRSA, Kotlus *et al.*[20] stated that all their patients were at a risk of developing community-onset MRSA infections due to a hospital-acquired strain of MRSA as they had been hospitalized for at least 3 months for chronic or comorbid conditions prior to presenting with dacryocystitis symptoms. They detected seven patients with acute or subacute MRSA dacryocystitis between 2001 and 2003[20]. In contrast, Pradeep *et al.*[18] found no MRSA in their series and stated that the flora of their patients was community acquired and not hospital acquired as they had been admitted to hospital on the day immediately prior to surgery. In the present study, only 2 patients (2.2 %) had dacryocystitis caused by MRSA. Similar to Kotlus *et al.*[20], we believe obtaining cultures and performing sensitivity testing to determine whether antibiotic treatment is important for reducing the risk of exposure to MRSA in patients with dacryocystitis who do not respond to conservative treatment.

Gram-negative and anaerobic organisms have been reported to be present in 20%-27% and 7%-16% of patients with dacryocystitis, respectively[11,17,21,22], and the incidence of these infections appears to be rising[10]. Gram-negative bacteria, including *Pseudomonas aeruginosa, Enterobacter*, *Citrobacter* spp., *Haemophilus influenzae*, and *Escherichia coli,* have also been reported as causative agents of dacryocystitis[10]. Coden *et al.*[17] reported *P. aeruginosa* as the most common gram-negative organism in dacryocystitis at an incidence rate of 8.7%. Brook *et al.* assessed the aerobic and anaerobic microbiology of 62 patients with dacryocystitis and reported a pure anaerobic growth rate of 32%, with *Peptostreptococcus* spp. and *Propionibacterium* spp. being the most frequently isolated species among anaerobes. These authors obtained specimens intraoperatively and used an anaerobic transport medium to transport them to the laboratory[23]. Coden *et al.*[17] found an anaerobic organism growth rate of 7.0%, with *Propionibacterium acnes* as the most commonly isolated anaerobic organism. *Proteus* spp. and *B. fragilis* have been reported as other pathogens responsible for dacryocystitis[11,17,24,25]. In our series, the only anaerobic bacteria isolated from the lacrimal sac was *B. fragilis* (3.1%), and this patient was in the EX-DCR group. The lower anaerobic growth rate in the present study may be attributable to difficulty in ensuring the growth of anaerobes despite lacrimal sac samples being inoculated preoperatively.

Owji *et al.*[15] reported that microorganism growth rates in samples from the lacrimal sac and involved and contralateral sides of the conjunctiva in a group of patients with NLDO and chronic dacryocystitis were 100%, 100%, and 97.5, respectively, while those in samples from the conjunctiva of healthy subjects was 82.5%. The same organism was isolated from the lacrimal sac and conjunctiva of the involved side in 90% of patients. They further reported that anaerobes, gram-negative bacteria, *Corynebacterium*, and *Streptococcus* spp. were isolated slightly more frequently from the involved

Table 4. Preoperative conjunctival and lacrimal sac bacterial growth according to surgical success.

		Preoperative conjunctival bacterial growth, n (%)			Lacrimal sac bacterial growth, n (%)		
		+	-	*p* value	+	-	*p* value
EX-DCR (n=32)							
Anatomical success	Successful	13 (86.7)	13 (76.5)	0.659[b]	11 (84.6)	15 (78.9)	1.000[b]
	Unsuccessful	2 (13.3)	4 (23.5)		2 (15.4)	4 (21.1)	
Functional success	Successful	13 (86.7)	13 (76.5)	0.659[b]	11 (84.6)	15 (78.9)	1.000[b]
	Unsuccessful	2 (13.3)	4 (23.5)		2 (15.4)	4 (21.1)	
EN-DCR (n=28)							
Anatomical success	Successful	8 (66.7)	13 (81.3)	0.418[b]	17 (70.8)	4 (100.0)	0.545[b]
	Unsuccessful	4 (33.3)	3 (18.8)		7 (29.2)	-	
Functional success	Successful	8 (66.7)	12 (75.0)	0.691[b]	16 (66.7)	4 (100.0)	0.295[b]
	Unsuccessful	4 (33.3)	4 (25.0)		8 (33.3)	-	
TC-DCR (n=30)							
Anatomical success	Successful	7 (77.8)	16 (76.2)	1.000[b]	10 (71.4)	13 (81.2)	0.675[b]
	Unsuccessful	2 (22.2)	5 (23.8)		4 (28.6)	3 (18.8)	
Functional success	Successful	6 (66.7)	16 (76.2)	0.666[b]	9 (64.3)	13 (81.0)	0.417[b]
	Unsuccessful	3 (33.3)	5 (23.8)		5 (35.7)	3 (20.0)	
Total (n=90)							
Anatomical success	Successful	28 (77.8)	42 (77.8)	1.000[a]	38 (74.5)	32 (82.1)	0.394[a]
	Unsuccessful	8 (22.2)	12 (22.2)		13 (25.5)	7 (17.9)	
Functional success	Successful	27 (75.0)	41 (75.9)	0.920[a]	36 (70.6)	32 (82.1)	0.210[a]
	Unsuccessful	9 (25.0)	13 (24.1)		15 (29.4)	7 (17.9)	

EX-DCR= external dacryocystorhinostomy; EN-DCR= endoscopic dacryocystorhinostomy; TC-DCR= transcanalicular multidiode laser dacryocystorhinostomy.
*= values are presented as number (percentage); [a]= Chi-square (χ^2) test; [b]= Fisher's exact test.

Table 5. Sensitive susceptibility testing results for *Staphylococcus* spp. isolated from the lacrimal sac

	Sensitive for CNS	Sensitive for *S. aureus*	Sensitive for CNS and *S. aureus*
	n (%)	n (%)	n (%)
Clindamycin	16/21 (76.2)	11/12 (91.7)	27/33 (81.8)
Erythromycin	11/20 (55.0)	12/13 (92.3)	23/33 (69.7)
Fosfomycin	6/7 (85.7)	3/3 (100.0)	9/10 (90.0)
Fucidic acid	6/9 (66.7)	5/0 (100.0)	11/14 (78.6)
Gentamicin	13/18 (72.2)	11/11 (100.0)	24/29 (82.8)
Levofloxacin	9/12 (75.0)	9/9 (100.0)	18/21 (85.7)
Linezolid	7/7 (100.0)	3/3 (100.0)	10/10 (100.0)
Moxifloxacin	3/4 (75.0)	3/3 (100.0)	6/7 (85.7)
Oxacillin	5/18 (27.8)	9/11 (81.8)	14/29 (48.3)
Penicillin G	1/13 (7.7)	0/9 (0.0)	1/22 (4.5)
Rifampicin	8/13 (61.5)	3/4 (75.0)	11/17 (64.7)
Teicoplanin	5/5 (100.0)	3/3 (100.0)	8/8 (100.0)
Tetracycline	2/12 (16.7)	4/4 (100.0)	6/16 (37.5)
Tigecycline	2/2 (100.0)	2/2 (100.0)	4/4 (100.0)
Tobramycin	12/18 (66.7)	11/11 (100.0)	23/29 (79.3)
Trimethoprim Sulfamethoxazole	12/17 (70.6)	10/10 (100.0)	22/27 (81.5)
Vancomycin	6/6 (100.0)	3/3 (100.0)	9/9 (100.0)
Mupirocin	12/12 (100.0)	6/6 (100.0)	18/18 (100.0)

CNS= coagulase-negative *Staphylococcus*.

side than the contralateral normal side of the conjunctiva; however, this difference was not statistically significant, most likely due to the small sample size.

Pradeep *et al.*[18] reported the microorganism growth rate from the lacrimal sac, conjunctival, and nasal samples as 48%, 34%, and 70%, respectively. The same authors[18] demonstrated a statistically

significant similarity between isolates from lacrimal and nasal/conjunctival samples and stated that the commensal flora of the nose and conjunctiva may have a direct role in the pathogenesis of chronic dacryocystitis. They obtained culture specimens directly from the lacrimal sac under an operating microscope and emphasized the reduced contamination during sample collection associated with this technique compared to the other methods of collection, such as applying pressure over the lacrimal sac or waiting for purulent material to exit the lacrimal sac via reflux[9]. The microorganism growth rates from lacrimal sac samples, involved and contralateral side conjunctival and nasal samples obtained preoperatively, and involved conjunctival samples obtained at first and second postoperative week were 56.7%, 40%, 23.3%, 98.9%, 97.8%, 12.2%, and 5.9%, respectively. All bacterial growth rates were similar between the three groups, except in culture samples obtained preoperatively from the lacrimal sac and the contralateral conjunctiva. The culture positivity rate from the lacrimal sac was significantly higher in the EN-DCR than in the EX-DCR and TC-DCR groups and was higher than the culture positivity rate of samples obtained preoperatively from the involved side conjunctiva for EN-DCR cases and all cases together. The similar positivity rates for lacrimal sac cultures during EN-DCR and preoperative nasal cultures indicate that lacrimal sac samples may become contaminated with nasal flora while the lacrimal sac sample is being obtained intranasally. The positivity rate of lacrimal sac culture in endoscopic DCR may have been high for this reason. After DCR, conjunctival culture positivity rates were significantly reduced in all groups except in the TC-DCR group; this result is in close agreement with previous reported results[26]. The most significant reduction in conjunctival culture positivity after DCR was observed in the EN-DCR group. Although not statistically significant, a reduction was also observed in the TC-DCR group. This reduction may be associated with the use of topical and oral antibiotics prescribed to patients during the first postoperative week and with the elimination of the infection source (lacrimal sac) via lacrimal surgery.

In a study on 40 consecutive adult NLDO patients by Owji *et al.*[15], the mean conjunctival normalization time after EX-DCR was 4.5 (range, 3-8) weeks. While the authors reported significant associations among normalization times, type of organism isolated from the lacrimal sac (particularly anaerobes and *Streptococcus*), a colony count of $\geq 10^3$, and presence of a silicone tube, they found no relationship between normalization times and the presence or duration of epiphora or the presence of previous attacks of acute dacryocystitis[15]. Furthermore, Owji *et al.*[15] stated that the delay period should be at least 4 weeks after DCR as the conjunctival flora normalized after 4 weeks in 67.5% of their patients. In another study by Eshraghi *et al.*[26] on the conjunctival flora and changes following EX-DCR, the mean normalization time was reported as 3.8 (range, 1-7) weeks in 38 patients with purulent regurgitation, 2.6 (range, 1-5) weeks in 33 patients without purulent regurgitation, and 3.3 weeks in all 71 patients. The authors reported significant associations among normalization times, pathogenic bacterial growth, higher colony counts, presence of a silicone tube, and purulent regurgitation[26]. The most common organism to grow in the conjunctival cultures in patients with and without purulent regurgitation was *S. epidermidis* (26.3% and 42.4%, respectively)[26]. Eshraghi *et al.*[26] also suggested that cataract surgery can be performed 7 weeks after DCR as conjunctival cultures were negative by this time in their series. The authors in both studies defined conjunctival normalization time as the interval between undergoing DCR and obtaining a negative culture result or as the time to achieve a colony count below that of the normal side[15,26]. The mean conjunctival normalization time was 1.47 (range, 1-5) weeks for EX-DCR, 1.04 weeks for EN-DCR (range, 1-2), and 1.17 (range, 1-3) weeks for TC-DCR in the present study. These results indicate that intraocular surgery may be scheduled after waiting for a conjunctival normalization time of approximately 5 weeks following DCR due to the risk of endophthalmitis. Furthermore, we observed no significant association between mean conjunctival normalization times and type of surgery. However, we defined conjunctival normalization time, which differs from the definitions for the same in the two above-mentioned studies[15,26].

Pinar-Sueiro *et al.* reviewed the clinical records of 697 patients who had undergone EX-DCR and found *S. aureus* to be most sensitive to gentamicin, co-trimoxazole, rifampicin, clindamycin, vancomycin, tobramycin, mupirocin, cefuroxime-axetil, chloramphenicol, tetracycline, fusidic acid, and cefalotin (100% sensitivity to all), while penicillin demonstrated the worst activity against *S. aureus* with 83.3% resistance[27]. In a study by Pradeep *et al.*[18], antibiogram results demonstrated that Staphylococci represented the majority of cultured organisms (85%), and the most effective antibiotics against it were vancomycin, amikacin, third-generation cephalosporins, and amoxyclav (100%, 89%, 83%, and 78% sensitivity, respectively). Penicillin (72% resistance) and erythromycin (75% resistance) were the least effective antibiotics. The authors[18] suggested that amoxyclav and third-generation cephalosporins should be used to treat chronic dacryocystitis, while vancomycin and amikacin should be preferred in severe cases as they can be administered parenterally. Kotlus *et al.*[20] reported that tetracycline, trimethoprim/sulfamethoxazole, and vancomycin were the most effective antibiotics against MRSA dacryocystitis. In the present study, CNS and *S. aureus,* the most commonly isolated (36.7%) microorganisms from the lacrimal sac, demonstrated the highest sensitivity to linezolid, teicoplanin, tigecycline, vancomycin, and mupirocin (antibiotic sensitivity rates of 100% for all).

The following are the strengths of the present study: prospective design; first report to compare the culture results of EX-DCR, EN-DCR, and TC-DCR; long follow-up period; assessment of the postoperative microorganism growth rate; inclusion of anaerobic cultures of lacrimal samples; and evaluation of the antibiotic susceptibility of microorganisms isolated from the lacrimal sac. The present study also had a few limitations. We were unable to evaluate fungal pathogens and patients could not be randomized, which may be seen as a limitation; however, patient preference was considered a priority in the present study.

In conclusion, PANDO patients had similar conjunctival flora preoperatively and during the first week after undergoing EX-, EN-, and TC-DCR. A decrease in the growth rate of conjunctival cultures was observed after EX- and EN-DCR, but not after TC-DCR. CNS was the predominant organism isolated from pre- and post-operative conjunctival, pre-operative nasal, and per-operative lacrimal sac samples in all groups. The most significant bacterial growth in the culture sample from the lacrimal sac was observed in the EN-DCR group. Bacterial growth in pre-operative conjunctiva and pre-operative lacrimal sac samples was not associated with the success rate of DCR. Mean conjunctival normalization times were similar between the three groups at 1.47 weeks for EX-DCR, 1.04 weeks for EN-DCR, and 1.17 weeks for TC-DCR. It is necessary to wait for approximately 5 weeks for conjunctival normalization after DCR before planning intraocular surgery due to the risk of endophthalmitis. Greater understanding of the association between lacrimal flora and lacrimal surgery outcomes may facilitate the development of new strategies in treating PANDO. Further studies on the clinico-bacteriological outcomes of different surgical techniques in larger study samples are therefore required.

REFERENCES

1. Shun-Shin GA1, Thurairajan G. External dacryocystorhinostomy--an end of an era? Br J Ophthalmol. 1997;81(9):716-7.
2. Massaro BM, Gonnering RS, Harris GJ. Endonasal laser dacryocystorhinostomy. A new approach to nasolacrimal duct obstruction. Arch Ophthalmol. 1990;108(8):1172-6.
3. Woog JJ, Metson R, Puliafito CA. Holmium:YAG endonasal laser dacryocystorhinostomy. Am J Ophthalmol. 1993;116(1):1-10.
4. Hartikainen J, Grenman R, Puukka P, Seppä H. Prospective randomized comparison of external dacryocystorhinostomy and endonasal laser dacryocystorhinostomy. Ophthalmology. 1998;105(6):1106-13.

5. Athanasiov PA, Prabhakaran VC, Mannor G, Woog JJ, Selva D. Transcanalicular approach to adult lacrimal duct obstruction: a review of instrument and methods. Ophthalmic Surg Lasers Imaging. 2009;40(2):149-59.
6. Meister EF, Otto M, Rohrwacher F, Mozet C. [Current recommendations of dacryocystorhinostomy]. Laryngorhinootologie. 2010;89(6):338-44. German.
7. Roithmann R, Burman T, Wormald PJ. Endoscopic dacryocystorhinostomy. Braz J Otorhinolaryngol. 2012;78(6):113-21.
8. Piédrola Maroto D, Franco Sánchez J, Reyes Eldblom R, Monje Vega E, Conde Jiménez M, Ortiz Rueda M. [Endonasal versus trans-canalicular endoscopic dacriocystorhinostomy using diode laser. Surgical techniques and outcomes]. Acta Otorrinolaringol Esp. 2008;59(6):283-7. Spanish.
9. Pinar-Sueiro S, Sota M, Lerchundi T, Gibelalde A, Berasategui B, Vilar B, Hernandez JL. Dacryocystitis: systematic approach to diagnosis and therapy. Curr Infect Dis Rep. 2012;14(2):137-46.
10. Briscoe D, Rubowitz A, Assia EI. Changing bacterial isolates and antibiotic sensitivities of purulent dacryocystitis. Orbit. 2005;24(2):95-8.
11. Hartikainen J, Lehtonen OP, Saari KM. Bacteriology of lacrimal duct obstruction in adults. Br J Ophthalmol. 1997;81(1):37-40.
12. Chaudhary M, Bhattarai A, Adhikari SK, Bhatta DR. Bacteriology and antimicrobial susceptibility of adult chronic dacryocystitis. Nepal J Ophthalmol. 2010;2(2):105-13.
13. Balikoglu-Yilmaz M1, Yilmaz T, Taskin U, Taskapili M, Akcay M, Oktay MF, Eren S. Prospective comparison of 3 dacryocystorhinostomy surgeries: external versus endoscopic versus transcanalicular multidiode laser. Ophthal Plast Reconstr Surg. 2014; 31(1):13-8.
14. Badhu BP, Karki BS, Khanal B, Dulal S, Das H. Microbiological patterns of chronic dacryocystitis. Ophthalmology. 2006;113(12):2377.e1-2.
15. Owji N, Khalili MR. Normalization of conjunctival flora after dacryocystorhinostomy. Ophthal Plast Reconstr Surg. 2009;25(2):136-8.
16. Bharathi MJ, Ramakrishnan R, Maneksha V, Shivakumar C, Nithya V, Mittal S. Comparative bacteriology of acute and chronic dacryocystitis. Eye (Lond). 2008;22(7):953-60.
17. Coden DJ, Hornblass A, Haas BD. Clinical bacteriology of dacryocystitis in adults. Ophthal Plast Reconstr Surg. 1993;9(2):125-31.
18. Pradeep AV, Patil SS, Koti SV, Arunkumar JS, Garag SS, Hegde JS. Clinico-bacteriological study of chronic dacryocystitis cases in northern karnataka, India. J Clin Diagn Res. 2013;7(11):2502-4.
19. Kubo M, Sakuraba T, Arai Y, Nakazawa M. Dacryocystorhinostomy for dacryocystitis caused by methicillin- resistant Staphylococcus aureus: report of four cases. Jpn J Ophthalmol. 2002;46(2):177-82.
20. Kotlus BS, Rodgers IR, Udell IJ. Dacryocystitis caused by community-onset methicillin-resistant Staphylococcus aureus. Ophthal Plast Reconstr Surg. 2005;21(5):371-5.
21. Huber-Spitzy V, Steinkogler FJ, Huber E, Arocker-Mettinger E, Schiffbänker M. Acquired dacryocystitis: microbiology and conservative therapy. Acta Ophthalmol (Copenh). 1992;70(6):745-9.
22. Seal DV, Barrett SP, McGill JI. Aetiology and treatment of acute bacterial infection of the external eye. Br J Ophthalmol. 1982;66(6):357-60.
23. Brook I, Frazier EH. Aerobic and anaerobic microbiology of dacryocystitis. Am J Ophthalmol. 1998;125(4)552-4.
24. Evans AR, Strong JD, Buck AC. Combined anaerobic and coliform infection in acute dacryocystitis. J Pediatr Ophthalmol Strabismus. 1991;28(5):292.
25. McKeag D, Kamal Z, McNab AA, Sheorey H. Combined coliform and anaerobic infection of the lacrimal sac. Clin Experiment Ophthalmol. 2002;30(1):52-4.
26. Eshraghi B, Masoomian B, Izadi A, Abedinifar Z, Falavarjani KG. Conjunctival bacterial flora in nasolacrimal duct obstruction and its changes after successful dacryocystorhinostomy surgery. Ophthal Plast Reconstr Surg. 2014;30(1):44-6.
27. Pinar-Sueiro S, Fernández-Hermida RV, Gibelalde A, Martínez-Indart L. Study on the effectiveness of antibiotic prophylaxis in external dacryocystorhinostomy: a review of 697 cases. Ophthal Plast Reconstr Surg. 2010;26(6):467-72.

Comparative study on optical performance and visual outcomes between two diffractive multifocal lenses: AMO Tecnis® ZMB00 and AcrySof® IQ ReSTOR® Multifocal IOL SN6AD1

Estudo comparativo de desempenho óptico e resultado visual entre duas lentes multifocais difrativas: Tecnis ZMB00 e AcrySof SN6AD1

Mario Augusto Pereira Dias Chaves[1,2], Wilson Takashi Hida[1], Patrick Frenzel Tzeliks[3], Michelle Rodrigues Gonçalves[2], Fernando de Bortoli Nogueira[1], Celso Takashi Nakano[4], Antonio Francisco Pimenta Motta[5], André Gustavo Rolim de Araújo[1], Milton Ruiz Alves[6]

ABSTRACT

Purpose: To compare the optical performance and visual outcomes between two diffractive multifocal lenses: AMO Tecnis® ZMB00 and AcrySof® ReSTOR® SN6AD1.

Methods: This prospective, non-randomized comparative study included the assessment of 74 eyes in 37 patients referred for cataract surgery and candidates for multifocal intraocular lens implants. Exclusion criteria included existence of any other eye disease, previous eye surgery, high axial myopia, preoperative corneal astigmatism of >1.00 cylindrical diopter (D), and intraoperative or postoperative complications. Ophthalmological evaluation included the measurement of uncorrected distance visual acuity (UDVA), corrected distance visual acuity (CDVA), distance-corrected near visual acuity (DCNVA), and distance-corrected intermediate visual acuity (DCIVA), with analysis of contrast sensitivity (CS), wavefront, and visual defocus curve.

Results: Postoperative UDVA was 0.09 and 0.08 logMAR in the SN6AD1 and ZMB00 groups, respectively (p=0.868); postoperative CDVA was 0.04 and 0.02 logMAR in the SN6AD1 and ZMB00 groups, respectively (p=0.68); DCIVA was 0.17 and 0.54 logMAR in the SN6AD1 and ZMB00 groups, respectively (p=0.000); and DCNVA was 0.04 and 0.09 logMAR in the SN6AD1 and ZMB00 groups, respectively (p=0.001). In both cases, there was an improvement in the spherical equivalent and UDVA (p<0.05). Under photopic conditions, the SN6AD1 group had better CS at low frequencies without glare (p=0.04); however, the ZMB00 group achieved better sensitivity at high frequencies with glare (p=0.003). The SN6AD1 and ZMB00 lenses exhibited similar behavior for intermediate vision, according to the defocus curve; however, the ZMB00 group showed a shorter reading distance than the SN6AD1 group. There were no significant differences regarding aberrometry between the two groups.

Conclusion: Both lenses promoted better quality of vision for both long and short distances and exhibited a similar behavior for intermediate vision. The SN6AD1 and ZMB00 groups showed better results for CS under photopic conditions at low and high spatial frequencies, respectively.

Keywords: Lenses, intraocular; Contrast sensitivity; Aberrometry; Visual acuity

RESUMO

Objetivo: *Comparar o desempenho óptico e resultado visual entre duas lentes multifocais difrativas: AMO Tecnis® ZMB00 e AcrySof® ReSTOR® SN6AD1.*

Métodos: *O estudo prospectivo, comparativo não randomizado incluiu avaliação de 74 olhos em 37 pacientes com indicação de facectomia e candidatos a implante de lente multifocal. Critérios de exclusão foram: presença de outras doenças oculares; cirurgia ocular prévia; alta miopia axial; astigmatismo cornenano maior que 1,00 D cilíndrica; complicações intraoperatórias ou pós-operatórias. A avaliação oftalmológica contou com medida da acuidade visual para longe corrigida (CDVA) e não corrigida (UDVA), intermediária (DCIVA) e curta distância (DCNVA) com melhor correção óptica para longe; teste de sensibilidade ao contraste; análise de frente de onda e curva visual de Defocus.*

Resultados: *A UDVA foi de 0,09 logMAR para o grupo SN6AD1 e 0,08 logMAR para o grupo ZMB00; com correção foi de 0,04 logMAR para SN6AD1 e 0,02 para o grupo ZMB00 (p>0,05). O grupo SN6AD1 obteve valor de 0,04 logMAR e o grupo ZMB00 de 0,09 logMAR para DCNVA (p<0,05) e DCIVA de 0,17 logMAR para SN6AD1 e 0,54 logMAR para ZMB00 (p=0,000). Houve melhora do equivalente esférico e da UDVA em ambos os grupos (p<0,05). Em condições fotópicas, o grupo SN6AD1 teve melhor sensibilidade ao contraste em baixas frequências sem ofuscamento (p<0,05), contudo grupo ZMB00 obteve melhor sensibilidade em altas frequências (p<0,05) com ofuscamento. As lentes SN6AD1 e ZMB00 obtiveram comportamento semelhantes para visão intermediária na curva de Defocus, porém, o grupo ZMB00 mostrou menor distância de leitura que o grupo SN6AD1. Não houve diferença com significância estatística relacionada à aberrometria na comparação dos dois grupos.*

Conclusão: *As duas lentes promoveram melhor qualidade de visão para longe e perto e comportamento semelhante para visão intermediária. O grupo ZMB00 exibiu melhores resultados para sensibilidade ao contraste em condições fotópicas em alta frequência espacial e SN6AD1 em baixa frequência espacial.*

Descritores: *Lentes intraoculares; Sensibilidades de contraste; Aberrometria; Acuidade visual*

INTRODUCTION

Cataract surgery is the most common surgical procedure performed worldwide and has become increasingly reliable and reproducible since the addition of phacoemulsification. Only in the United States, two million procedures are annually performed due to an increase in early diagnoses and demands of patients who wish to maintain productivity and daily activities[1].

Multifocal intraocular lenses (IOLs) were introduced in the early 1980s and offer the benefit of promoting both near and distance vision simultaneously[2,4]. However, after 30 years, adverse phenomena

Submitted for publication: March 23, 2015
Accepted for publication: January 23, 2016

[1] Cataract Sector, Hospital Oftalmológico de Brasília, Brasília, DF, Brazil.
[2] Hospital Visão, João Pessoa, PB, Brazil.
[3] Cornea Sector, Hospital Oftalmológico de Brasília, Brasília, DF, Brazil.
[4] Instituto de Olhos Santa Cruz, São Paulo, SP, Brazil.
[5] Universidade Federal de Minas Gerais, Belo Horizonte, MG, Brazil.
[6] Faculdade de Medicina, Universidade de São Paulo, São Paulo, SP, Brazil.

Funding: This study was supported by Hospital Oftalmológico de Brasília (HOB) and Centro de Estudos Oftalmológicos Renato Ambrósio (CEORA).

Disclosure of potential conflicts of interest: The authors declare no potential conflict of interest.

Corresponding author: Mario Augusto Chaves. Rua São Gonçalo, 416/1602 - João Pessoa, PB - 58038-330 - Brazil - E-mail: marioaugustochaves@gmail.com

Approved by the following research ethics committee: Hospital das Forças Armadas, Brasília, DF, (#172.922).

ClinicalTrials.govIdentifier: NCT01763411

remain challenging, requiring careful patient selection since some patients could experience less clarity, decrease in contrast, and photopic phenomena when two images are overlapped[1,5-7]. Moreover, the same optical quality cannot be expected as with a monofocal lens[3,6].

Several types of materials and technologies have been employed in designing IOLs, with refractive, diffractive, and hybrid models being the most widely used by surgeons. Moreover, asphericity was introduced as a means to compensate positive corneal spherical aberration[2,3]. The addition promoted by the lens, whether it is +2.5 diopters (D), +3.0 D, or +4.0 D, influences the best reading distance and depth of focus. These different compositions culminate in distinctly different optical aberrometric behaviors[8-10].

In this study, we compared visual parameters, optical performance, contrast sensitivity (CS), and wavefront analysis results between two different types of multifocal lenses currently available in the market: AcrySof® IQ ReSTOR® Multifocal IOL SN6AD1 (Alcon Laboratories, Inc., Irvine, CA, USA) and AMO Tecnis® ZMB00 (Abbott Medical Optics, Santa Ana, CA, USA).

The AcrySof® IQ ReSTOR® Multifocal IOL SN6AD1 is a single piece lens composed of foldable hydrophobic acrylic, aspheric, adding a negative aberration of -0.20 µm to the human eye. With a refractive-diffractive hybrid design and apodized diffractive anterior surface, it shows a better near-distance visual acuity for smaller pupils and better long-distance visual acuity for larger pupils[11,12]. It has a 3.6-mm diffractive optic zone, consisting of nine concentric rings that decrease from the center to the periphery (apodization), with a central ring of 0.856 mm and provides bifocality with a addition of 3 D, thus corresponding to 2.4 D in the lens plane[3,12].

The AMO Tecnis® ZMB00 lens is an evolution of the ZM900 IOL, which is constructed of a single piece of foldable hydrophobic acrylic material, with a diffractive posterior surface and aspheric anterior surface crafted to add a negative spherical aberration of -0.27 µm. It has 32 concentric rings, with a central ring of 1 mm and promotes an addition of 4 D, thus corresponding to 3.2 D in the lens plane, regardless of pupil size[6,11].

METHODS

This study was conducted in accordance with the ethical standards of clinical and surgical research and was approved by the ethics committee for Analysis of Research Projects (CAPPesq) of the Medical Staff of the Hospital Oftalmológico de Brasília and the Hospital das Forças Armadas, Brasília, Brazil. This prospective, non-randomized, comparative study included 74 eyes of 37 patients, selected from a list of cataract outpatients of the Hospital Oftalmológico de Brasília, who underwent cataract extraction with IOL implant between January 2011 and July 2013.

All surgeries were performed by the same surgeon (W.T.H.). The main incision was made in the steepest corneal meridian in three planes to encourage self-sealing. Continuous circular capsulorhexis and hydrodissection were performed and followed by viscoelastic soft-shell technique[10]. Phacoemulsification was followed by irrigation and aspiration of the lenticular cortex and was concluded with implantation of one of the following lenses into the capsular bag: AcrySof® IQ ReSTOR® Multifocal IOL SN6AD1 or AMO Tecnis® ZMB00.

The inclusion criteria were (1) presence of a senile bilateral cataract, (2) interest in multifocal lens implant, (3) corneal astigmatism of ≤1.00 cylindrical diopter in both eyes, (4) pupil diameter of >3.0 mm under mesopic conditions, and (5) none of the following exclusionary factors: (a) existence of any other eye pathology or neuropathy that could decrease visual acuity, (b) CS or visual field sensitivity, (c) high axial myopia, (d) preoperative or postoperative complications, (e) concerns regarding an IOL implant inside the capsular bag, or (f) IOL decentration of >0.5 mm, as measured with a slit lamp.

We considered working and reading habits when choosing the lens for implantation. Patients with habits that demanded better intermediate vision were included in the IOL implantation group that aimed to achieve an addition of +3 D (SN6AD1). The remaining patients were included in the IOL group that aimed to achieve an addition of +4 D (ZMB00).

All patients underwent a complete ophthalmological evaluation on all visits, before and after surgery. Data from the 180-day visit of all patients were used for comparative analysis. Acuity of short-distance vision (33 cm) with and without refraction correction was measured using the reading table model of the Early Treatment Diabetic Retinopathy Study chart (ETDRS; Precision Vision, Ltd., Aurora, CO, USA). The same procedure was performed to test long-distance vision (4 m), although the chart was backlit to 100% contrast. All values were calculated according to the logMAR rating scale[13].

IOL dioptric power was calculated according to the optical interferometry technique using the IOLMaster® 500 Optical Biometer (Carl Zeiss, Jena, Germany), which sought emmetropia or the first positive value calculated by the following three formulas: Hoffer-Q for axial lengths of <22 mm, Holladay between 22 and 24.50 mm, and Sanders-Retzlaff-Kraff/T for axial lengths of >24.50 mm[14].

The postoperative scheme of medication (eye drops) was similar for all patients. The evaluation included the testing of monocular CS under photopic (with and without glare) and mesopic conditions using the Optec® 6500P Vision Screener (Stereo Optical Company, Inc., Chicago, IL USA) with spatial frequencies ranging between 1.5 and 18 cycles/degree and using the Functional Acuity Contrast Test chart provided by the manufacturer, which consists of columns that grow at different rates of 0.15 log units, which are then converted into base 10 logarithmic units for statistical analysis[2,15-20].

The same assessment was analyzed across the wavefront function, and the monocular optical aberrations were gathered using an OPD-Scan III aberrometer (Nidek Co., Ltd., Gamagori, Japan). Unlike other studies, we sought to evaluate aberrometry under conditions of mesopic pupil in an attempt to detect the manifestation of wavefront function under physiological conditions without the use of pharmacological mydriasis[13]. The following variables were collected: (1) total aberration, (2) high-order spherical aberration, (3) tilt, (4) coma, and (5) Strehl ratio[8,9]. Finally, the visual monocular defocus curve was evaluated in long-distance visual acuity, corrected using the same ETDRS chart at a distance of 4 m, at intervals of 0.50 spherical diopters from -5.00 to +2.50 D[21].

Significance was tested using the Tukey, Wilcoxon, Kruskal-Wallis, ANOVA, and chi-square tests by adjusting to a level of significance of 5% ($p<0.05$) and using SPSS for Windows statistical analysis software (IBM-SPSS, Inc., Chicago, IL, USA).

RESULTS

The study involved the participation of 37 subjects, 22 women (59.5%) and 15 men (40.5%), and a total of 74 eyes. There was homogeneity in the group distribution of lenses regarding to gender, age, axial length of the eye, and chosen diopter, as shown in table 1. The average preoperative spherical equivalence (SE) of all subjects was 1.58 D, and there was no relevant statistical difference between the groups (Table 1).

Preoperative uncorrected distance visual acuity (UDVA) was better in the SN6AD1 group than in the ZMB00 group (0.62 vs. 0.50 logMAR, $p=0.058$), although this difference was not statistically significant (Table 1). There were no statistically significant differences in postoperative data of SE, UDVA, or corrected long-distance visual acuity (CDVA) between the groups (Table 1).

There was a statistically significant difference in pre- and postoperative SE and in pre- and postoperative UDVA between groups (Table 1).

Considering short-distance vision, there was a significant difference in the average short-distance visual acuity, as analyzed with correction for long-distance (DCNVA) between the SN6AD1 and

Table 1. Descriptive measures for age, implanted IOL refractive power (Diopters), axial length, preoperative spherical equivalent, preoperative and postoperative visual acuities for SN6AD1 and ZMB00 lenses

						95% Confidence interval for mean				p-value between groups	
		N	Mean	Std. dev	Std. error	Lower bound	Upper bound	Min	Max	Student's t-test	Mann-Whitney U test
Age	SN6AD1	34	62.12	5.48	0.94	60.21	64.03	51.00	72.00	0.184	0.170
	ZMB00	40	63.85	5.59	0.88	62.06	65.64	53.00	76.00		
Diopters	SN6AD1	34	22.26	3.20	0.55	21.15	23.38	17.50	31.00	0.969	0.521
	ZMB00	40	22.24	2.82	0.45	21.34	23.14	14.00	27.00		
AL	SN6AD1	34	23.16	1.00	0.17	22.81	23.51	20.60	24.75	0.197	0.533
	ZMB00	40	23.47	1.06	0.17	23.13	23.81	22.08	25.94		
preSE	SN6AD1	34	1.82	1.66	0.28	1.24	2.40	-1.00	7.00	0.262	0.929
	ZMB00	40	1.35	1.90	0.30	0.74	1.96	-4.00	4.00		
preUDVA	SN6AD1	34	0.26	0.45	0.08	0.11	0.42	0.00	1.00	0.058	0.081
	ZMB00	40	0.50	0.60	0.09	0.31	0.69	0.00	2.00		
postSE	SN6AD1	34	-0.05	0.37	0,06	-0.18	0.08	-1.00	1.00	0.640	0.525
	ZMB00	40	-0.02	0.28	0,04	-0.11	0.07	-0.50	0.75		
postUDVA	SN6AD1	34	0.09	0.09	0.02	0.06	0.13	0.00	0.40	0.601	0.677
	ZMB00	40	0.08	0.09	0.01	0.05	0.11	0.00	0.30		
postCDVA	SN6AD1	34	0.04	0.05	0.01	0.02	0.06	0.00	0.18	0.056	0.076
	ZMB00	40	0.02	0.04	0.01	0.01	0.03	0.00	0.10		
postDCNVA	SN6AD1	34	0.04	0.07	0.01	0.01	0.06	0.00	0.18	0.009	0.000
	ZMB00	40	0.09	0.09	0.01	0.06	0.11	0.00	0.30		
postDCIVA	SN6AD1	34	0.17	0.13	0.02	0.12	0.20	0.00	0.40	0.000	0.006
	ZMB00	40	0.54	0.13	0.02	0.50	0.60	0.20	0.80		

AL= axial length; preSE= preoperative spherical equivalent; preUDVA= preoperative uncorrected distance visual acuity; postSE= postoperative spherical equivalent; postUDVA= postoperative uncorrected distance visual acuity; postCDVA= postoperative corrected distance visual acuity; postDCNVA= postoperative distance-corrected near visual acuity postoperative; postDCIVA= postoperative distance-corrected intermediate visual acuity.

ZMB00 groups (0.04 vs. 0.09 logMAR, p=0.009), and in intermediate vision (0.17 vs. 0.54 logMAR, p=0.000) (Table 1 and Figure 1). Preoperative and postoperative spherical equivalent (SE) results are demonstrated in figure 2.

None of the patients required any type of short- or long-distance correction in their everyday life following surgery.

CS under photopic conditions without glare was better at a low frequency (1.5 cpd) for the SN6AD1 lens (p=0.039) and at a high frequency (18 cpd) for the ZMB00 lens (p=0.62). Under photopic conditions with glare, the ZMB00 lens performed better at high frequencies (18 cpd) with p = 0.003. Under mesopic conditions, the lenses exhibited similar behavior (p>0.05) (Figures 3, 4, and 5).

Regarding defocus curve, there was a difference in almost all of the distances assessed between lenses (converted into diopters, p<0.001). The ZMB00 lens showed peaks close to -3.0 D (33 cm) and 0.0 D, with an average visual acuity of 0.09 and 0.02 logMAR, respectively. The line corresponds to the SN6AD1 lens and showed peaks at -2.5 D (40 cm) and 0.0 D, with visual acuity of 0.06 and 0.02 logMAR, respectively. Regarding intermediate deflection vision, both occurred at -1.5 D (66 cm), with a visual acuity of 0.28 and 0.29 logMAR, respectively, but with no statistically significant difference from this point (p=0.68) to -2.5 D (40 cm) (p=0.12) (Figure 6).

Wavefront analysis demonstrated that, in absolute values, the ZMB00 lens showed better results in the decomposition of the wavefront function; however, there was no statistically significant difference between groups (p>0.05) (Table 2).

DISCUSSION

The analysis of groups distribution demonstrates homogeneity and enables comparisons between groups, indicating its suitability for comparison to other publications[7,10,21-24].

As demonstrated in other studies, the good quality of distance and near vision was attested through both types of lenses, regardless of which addition had been used. The improvement in UDVA, in addition to the excellent individual results, for both long and short distance confirmed the efficacy of the treatment and provided independence from glasses[1-3,6,12,13,17,21-23,25]. Such inference is particularly evident when considering postoperative SE.

Analysis of DCNVA highlighted advantages of the SN6AD1 lens (p<0.05). However, when converting the Jaeger table visual scale to logMAR, values that transcend the understanding of the different visual levels for short distances may appear. Given that J1 corresponds to 0.00 logMAR and at the level immediately below, J2 corresponds to 0.1 logMAR, both groups presented average DCNVA level at J1 and better than J2[11].

Considering CS under photopic conditions, the ZMB00 lens showed better results at high spatial frequencies (p<0.05). Low spatial frequencies are associated with the perception of motion (magnocellular pathway), whereas high frequencies are associated with the perception of detail (parvocellular pathway)[26]. Hida et al. compared the SN60D3 IOL to the ZM900 IOL and found similar results applicable to this study since SN6AD1 and ZMB00 lenses are the evolution of the SN60D3 and ZM900 IOLs[13]. Cillino et al. compared the visual CSs of

SN6AD1, SN6AD3, and ZMA00 lenses and found no statistical difference among the three groups. However, the study was performed using the Pelli-Robson method to evaluate CS, which has a greater chance of being influenced by the environment, unlike the automated method[11]. Afonso et al. found similar values for the SN6AD1 lens, as did de Vries et al. for average values at high frequencies (1.13 at 12 cpd and 0.65 at 18 cpd)[2,12].

The differences in Mesopic CS were not significant when comparing the two groups at any spatial frequency. This finding was consistent with those in other publications[2,12,13,22].

It must be considered that under photopic and mesopic conditions, the two groups showed averages below their corresponding monofocal IOLs peers, as described in other studies. Considering CS, ZA9003 IOL has been considered better than the ZMA00 IOL[10,22,23].

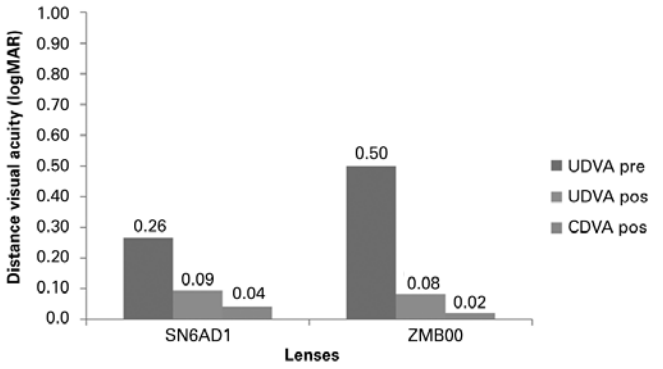

Figure 1. Preoperative long-distance visual acuity without (UDVA) correction, versus post-operative UDVA versus postoperative visual acuity for long-distance with (CDVA) correction for SN6AD1 and ZMB00 lenses.

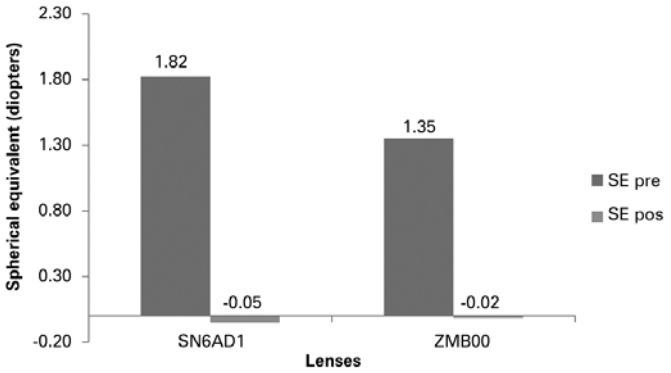

Figure 2. Preoperative and postoperative spherical equivalent (SE), for SN6AD1 and ZMB00 lenses.

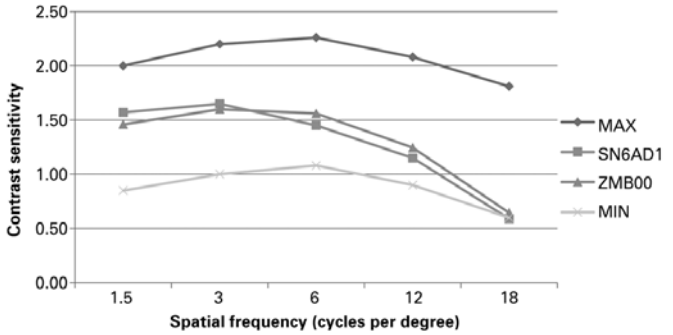

Figure 3. Comparison for the SN6AD1 and ZMB00 lenses with respect to the photopic situation without glare.

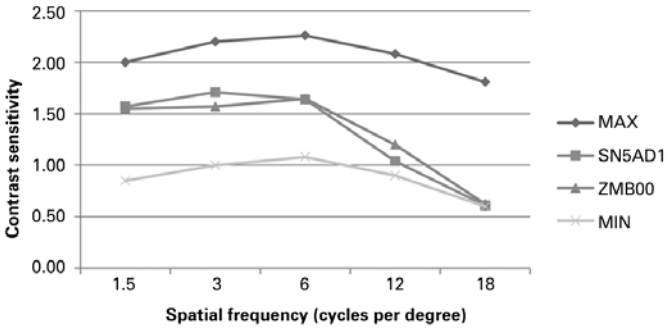

Figure 4. Comparison for the SN6AD1 lenses and the ZMB00, with respect to the photopic with glare situation.

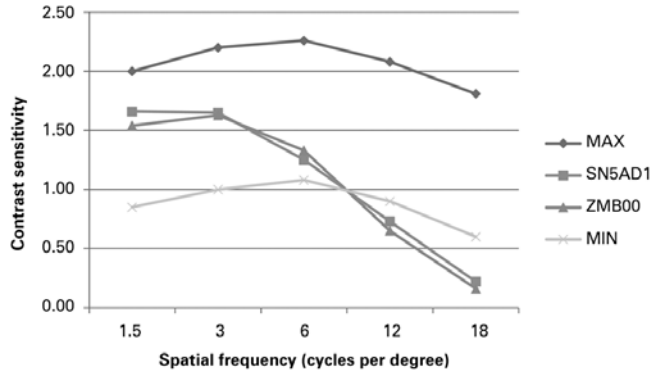

Figure 5. Comparison for the SN6AD1 lenses and the ZMB00 lenses with respect to the mesopic with glare situation.

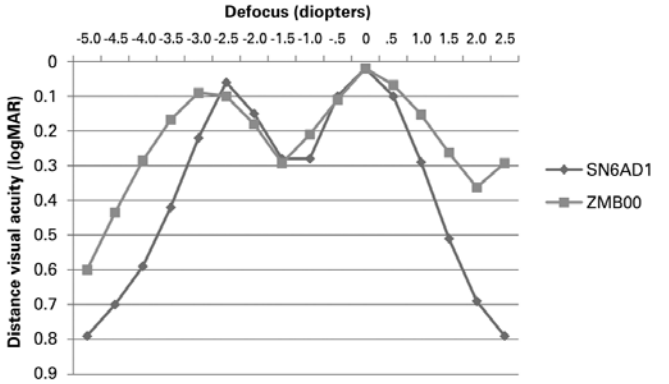

Figure 6. Defocus curve for SN6AD1 lenses and ZMB00.

Table 2. Comparison of wavefront function analysis between SN6AD1 and ZMB00

	SN6AD1	ZMB00	*p*-value	
	Mean	Mean	Student's t test	Mann-Whitney U test
Total	0.775	0.742	0.784	0.793
Tilt	0.338	0.288	0.554	0.734
HOA	0.408	0.328	0.231	0.156
Coma	0.161	0.149	0.785	0.422
Sph	0.105	0.077	0.400	0.107
Strehl ratio	0.048	0.052	0.663	0.459

HOA= high order aberrations; Sph= spherical aberration.

Nakano et al. and Vingolo et al. concluded the same by comparing SN60WF and SA60AT IOLs with SN60D3 and ZM900 IOLs[27,28]. This phenomenon could be explained through the analysis of the concept of multifocality promoted by these kind of lenses by splitting light energy into two foci and overlapping near and far images.

Afonso et al. correlated greater pupil diameters to better CS at all frequencies under photopic and mesopic conditions[20]. This idea seems plausible because a larger amount of light enters the optical system, which is proportional to the increase in pupil diameter. In our study, we did not perform analysis of any such correlation.

Considering visual defocus curve, it was clear that both groups reached two peaks of improved visual acuity corresponding to near and far distances. Considering near vision, significantly better vision was found close to 33 cm with the ZMB00 lens than with the SN6AD1 at this point, although the SN6AD1 lens demonstrated greater near vision at a 40-cm reading distance, but with no statistical significance when compared with the ZMB00 lens at this focus point. This is a different result from what was found at the near visual acuity test and may be related to pupillary function that improves the near visual acuity for refractive-diffractive hybrid design lenses.

When assessing intermediate vision of 66 cm, the two groups showed similar low performances when compared with the peak curve points of better vision. Schmickler et al. reached similar values when individually assessing the ZMB00 lens[6]. Similarly, Afonso et al., de Vries et al., and Petermeier et al. depicted the same defocus curve pattern for the SN6AD1 lens[2,12,21].

Nevertheless, analysis of the two IOL defocus patterns suggests that there should be a relative permanence of the curve near the better vision peaks, which indicates a reasonable depth of focus around these two top focal points. To be more specific, the reading distance might not be confined only to certain near distance, and it would have an amplitude of approximately 12 cm in diameter around the best near focal point. Although it seems little, it may make a difference for better adaptation of patients with more intermediate visual habits.

Regarding the results of aberrometry, both lenses were successful in decreasing corneal positive spherical aberration. However, self-criticism is necessary to evaluate the method employed. Because a multifocal lens simultaneously generates two distinct wavefronts, it may be difficult to achieve separate and accurate measurements with a particular device. Nevertheless, it is understood that the same difficulty in measurement was imposed upon both groups, making comparisons reasonable. Hida et al. compared the ZM900 and SN60D3 lenses and found similar aberrometric results, as did Nakano et al.[10,27]. Moreno et al. evaluated a system for analyzing the wavefront of a double-passage Optical Quality Analysis System (Visiometrics, S.L., Cerdanyola, BCN, Spain) that could differentiate the two wavefronts and thereby assess the optical quality more accurately for better differentiation[29].

It is important to emphasize the Strehl ratio variable. This value corresponds to the ratio between the peak of the measured point spread function (PSF) and a PSF peak in an aberration-free optical system. Values range from 0 to 1, where 1 represents an ideal optical system. The value usually decreases as the pupil increases, expanding the influence of optical aberrations that compromise quality. Larger or smaller values for similar pupil conditions correspond to better or worse visual quality[9]. Our results suggested equivalence between the two lenses. Artigas et al., compared the SN60D3 and ZM900 lenses and suggested better results for the SN60D3 lens, using an artificial eye as model[30].

In conclusion, the two lenses were effective in enabling better vision for both long and short distances, although neither exhibited excellent visual acuity on intermediate vision, despite this equivalence. Both groups had a reasonable range of focus around the two best focus points (near and far). The ZMB00 lens recorded better results in CS under photopic conditions at high frequencies, although both lenses demonstrated inferior results when compared to their monofocal peers described in past publications. The ZMB00 and SN6AD1 lenses are equivalent with regards to wavefront function, although more studies are needed to better assess aberrometry.

REFERENCES

1. Maxwell WA, Cionni RJ, Lehmann RP, Modi SS. Functional outcomes after bilateral implantation of apodized diffractive aspheric acrylic intraocular lenses with a +3.0 or +4.0 diopter addition power: Randomized multicenter clinical study. J Cataracr Refract Surg. 2009;35(12):2054-61.
2. Alfonso JF, Fernández-Vega L, Blázquez JI, Montés-Micó R. Visual function comparison of 2 aspheric multifocal intraocular lenses. J Cataract Refract Surg. 2012;38(2):242-8.
3. de Vries NE, Nuijts RM. Multifocal intraocular lenses in cataract surgery: Literature review of benefits and side effects. J Cataract Refract Surg. 2013;39(2):268-78.
4. Alfonso JF, Fernández-Vega L, Baamonde MB, Montés-Micó R. Prospective visual evaluation of apodized diffractive intraocular lenses. J Cataract Refract Surg. 2007;33(7):1235-43.
5. Woodward MA, Randleman JB, Stulting RD. Dissatisfaction after multifocal intraocular lens implantation. J Cataract Refract Surg. 2009;35(6):992-7.
6. Schmickler S, Bautista CP, Goes F, Shah S, Wolffsohn JS. Clinical evaluation of a multifocal aspheric diffractive intraocular lens. Br J Ophthalmol. 2013;97(12):1560-4.
7. Rabsilber TM, Rudalevicius P, Jasinskas V, Holzer MP, Auffarth GU. Influence of +3.00 D and +4.00 D near addition on functional outcomes of a refractive multifocal intraocular lens model. J Cataract Refract Surg. 2013;39(3):350-7.
8. Oliveira CM, Ferreira A, Franco S. Wavefront analysis and Zernike polynomial decomposition for evaluation of corneal optical quality. J Cataract Refract Surg. 2012;38(2):343-56.
9. Mello GR, Rocha KM, Santhiago MR, Smadja D, Krueger RR. Applications of wavefront technology. J Cataract Refract Surg. 2012;38(9):1671-83.
10. Hida WT, Nakano CT, Yamane IS, Motta AF, Tzeliks PF, Alencar LM, et al. Desempenho visual dos pacientes pseudofácicos com diferentes lentes intraoculares. Rev Bras Oftalmol. 2013;72(5):287-93.
11. Cillino G, Casuccio A, Pasti M, Bono V, Mencucci R, Cillino S. Working-age cataract patients: visual results, reading performance, and quality of life with three diffractive multifocal intraocular lenses. Ophthalmology. 2014;121(1):34-44.
12. de Vries NE, Webers CA, Montés-Micó R, Ferrer-Blasco T, Nuijts RM. Visual outcomes after cataract surgery with implantation of a +3.00 D or +4.00 D aspheric diffractive multifocal intraocular lens: comparative study. J Cataract Refract Surg. 2010;36(8):1316-22.
13. Hida WT, Motta AF, Kara-José Júnior N, Costa H, Tokunaga C, Cordeiro LN, et al. Estudo comparativo do desempenho visual e análise de frente de onda entre as lentes intra-oculares multifocais difrativas Tecnis® ZM900 e AcrySof® ResTor® SN60D3. Arq Bras Oftalmol. 2008;71(6):788-92.
14. Aristodemou P, Knox Cartwright NE, Sparrow JM, Johnston RL. Formula choice: Hoffer Q, Holladay 1, or SRK/T and refractive outcomes in 8108 eyes after cataract surgery with biometry by partial coherence interferometry. J Cataract Refract Surg. 2011;37(1):63-71.
15. Jindra LF, Zemon V. Contrast sensitivity testing: a more complete assessment of vision. J Cataract Refract Surg. 1989;15(2):141-8.
16. Richman J, Spaeth GL, Wirostko B. Contrast sensitivity basics and a critique of currently available tests. J Cataract Refract Surg. 2013;39(7):1100-6.
17. Bautista CP, González DC, Gómez AC. Evolution of visual performance in 70 eyes implanted with the Tecnis(®) ZMB00 multifocal intraocular lens. Clin Ophthalmol (Auckland, N.Z.); 2012;6:403-7.
18. Hong YT, Kim SW, Kim EK, Kim T-i. Contrast sensitivity measurement with 2 contrast sensitivity tests in normal eyes and eyes with cataract. J Cataract Refract Surg. 2010;36(4):547-52.

19. Pesudovs K, Hazel CA, Doran RM, Elliott DB. The usefulness of Vistech and FACT contrast sensitivity charts for cataract and refractive surgery outcomes research. Br J Ophthalmol. 2004;88(1):11-6.
20. Alfonso JF, Fernández-Vega L, Baamonde MB, Montés-Micó R. Correlation of pupil size with visual acuity and contrast sensitivity after implantation of an apodized diffractive intraocular lens. J Cataract Refract Surg. 2007;33(3):430-8.
21. Petermeier K, Messias A, Gekeler F, Szurman P. Effect of +3.00 diopter and +4.00 diopter additions in multifocal intraocular lenses on defocus profiles, patient satisfaction, and contrast sensitivity. J Cataract Refract Surg. 2011;37(4):720-6.
22. Ye PP, Li X, Yao K. Visual outcome and optical quality after bilateral implantation of aspheric diffractive multifocal, aspheric monofocal and spherical monofocal intraocular lenses: a prospective comparison. Int J Ophthalmol. 2013;6(3):300-6.
23. Yamauchi T, Tabuchi H, Takase K, Ohsugi H, Ohara Z, Kiuchi Y. Comparison of visual performance of multifocal intraocular lenses with same material monofocal intraocular lenses. PLoS One. 2013;8(6):e68236.
24. de Vries NE, Webers CA, Touwslager WR, Bauer NJ, de Brabander J, Berendschot TT, et al. Dissatisfaction after implantation of multifocal intraocular lenses. J Cataract Refract Surg. 2011;37(5):859-65.
25. Sood P, Woodward MA. Patient acceptability of the Tecnis multifocal intraocular lens. Clin Ophthalmol (Auckland, N.Z.). 2011;5:403-10.
26. Souza GS, Lacerda EM, Silveira VA, Araújo CS, Silveira LC. A visão através dos contrastes. Estudos Avançados. 2013;27(77):45-60.
27. Nakano CT, Hida WT, Kara-Jose Junior N, Motta AF, Fante D, Masson VF, et al. Comparison between OPD-scan results and contrast sensitivity of three intraocular lenses: spheric AcrySof SN60AT, aspheric AcrySof SN60WF and multifocal AcrySof Restor lens. Rev Bras Ophthalmol. 2009;68(4):216-22.
28. Vingolo EM, Grenga P, Iacobelli L, Grenga R. Visual acuity and contrast sensitivity: AcrySof ReSTOR apodized diffractive versus AcrySof SA60AT monofocal intraocular lenses. J Cataract Refract Surg. 2007;33(7):1244-7.
29. Moreno LJ, Piñero DP, Alió JL, Fimia A, Plaza AB. Double-pass system analysis of the visual outcomes and optical performance of an apodized diffractive multifocal intraocular lens. J Cataract Refract Surg. 2010;36(12):2048-55.
30. Artigas JM, Menezo JL, Peris C, Felipe A, Díaz-Llopis M. Image quality with multifocal intraocular lenses and the effect of pupil size: comparison of refractive and hybrid refractive-diffractive designs. J Cataract Refract Surg. 2007;33(12):2111-7.

Evaluation of anterior segment parameters in patients with pseudoexfoliation syndrome using Scheimpflug imaging

Avaliação de parâmetros do segmento anterior por imagem Scheimpflug em pacientes com síndrome de pseudoexfoliação

Alime Gunes[1], Musa Yigit[1], Levent Tok[1], Ozlem Tok[1]

ABSTRACT

Purpose: To evaluate anterior segment parameters in patients with pseudoexfoliation syndrome (PXS) using Scheimpflug imaging.

Methods: Forty-three PXS patients and 43 healthy control subjects were included in this cross-sectional study. All participants underwent a detailed ophthalmologic examination. Anterior segment parameters were measured using a Scheimpflug system.

Results: Considering the PXS and control groups, the mean corneal thicknesses at the apex point (536 ± 31 and 560 ± 31 µm, respectively, *p*=0.001), at the center of the pupil (534 ± 31 and 558 ± 33 µm, respectively, *p*=0.001), and at the thinnest point (528 ± 30 and 546 ± 27 µm, respectively, *p*=0.005) were significantly thinner in PXS patients. Visual acuity was significantly lower (0.52 ± 0.37 versus 0.88 ± 0.23, *p*<0.001) and axial length was significantly longer (23.9 ± 0.70 mm versus 23.2 ± 0.90 mm, *p*=0.001) in the PXS eyes than in the control eyes. There were no statistically significant differences in the mean values of keratometry, anterior chamber angle, anterior chamber depth, corneal volume, and anterior chamber volume between the PXS and control eyes.

Conclusions: The patients with PXS had thinner corneas, worse visual acuity, and longer axial length compared with those in the healthy controls.

Keywords: Anterior eye segment; Exfoliation syndrome; Corneal topography; Cornea/anatomy and histology; Visual acuity

RESUMO

Objetivo: *Avaliar os parâmetros do segmento anterior em pacientes com síndrome de pseudoexfoliação (PXS) utilizando imagens de Scheimpflug.*

Métodos: *Quarenta e três pacientes com PXS e 43 indivíduos saudáveis foram incluídos neste estudo transversal. Todos os participantes foram submetidos ao exame oftalmológico detalhado. Parâmetros do segmento anterior foram medidos por sistema de Scheimpflug.*

Resultados: *Considerando os grupos PXS e controle, respectivamente, as espessuras médias da espessura corneana no ápice (536 ± 31 µm e 560 ± 31 µm, p=0,001), no centro da pupila (534 ± 31 µm e 558 ± 33 µm, p=0,001), e no ponto mais fino (528 ± 30 µm e 546 ± 27 µm, p=0,005), foram significativamente mais finas em pacientes com PXS. A acuidade visual foi significativamente menor (0,52 ± 0,37 contra 0,88 ± 0,23, p<0,001) e comprimento axial foi significativamente maior (23,9 ± 0,70 milímetros contra 23,2 ± 0,90 milímetros, p=0,001) em olhos com PXS comparados com os olhos controle. Não houve diferenças estatisticamente significativas entre PXS e controle olhos em valores médios de ceratometria, ângulo da câmara anterior, profundidade da câmara anterior, volume da córnea e volume de câmara anterior.*

Conclusões: *Os pacientes com PXS tem córneas mais finas, pior acuidade visual, e maior comprimento axial em comparação com controles saudáveis.*

Descritores: *Segmento anterior do olho; Síndrome de exfoliação; Topografia da córnea; Córnea/anatomia & histologia; Acuidade visual*

INTRODUCTION

Pseudoexfoliation syndrome (PXS) is a common, age-related, systemic, extracellular matrix disorder characterized by the production and progressive accumulation of abnormal fibrillar extracellular material in intraocular and extraocular tissues[1]. The exfoliation material is produced by different intraocular cell types, such as lens epithelium, ciliary epithelium, iris, vascular endothelial cells, trabecular endothelium, basement membrane of the corneal epithelium, and corneal endothelium[1,2]. Tissue differentiation predisposes to several intraocular and surgical complications, including glaucoma, zonular dehiscence, phacodonesis and lens subluxation, capsular rupture or vitreous loss during cataract surgery, blood-aqueous barrier dysfunction, and corneal endothelial decompensation[3,4].

In previous studies, the deposition of exfoliation material on the corneal endothelium, decreased endothelial cell density, changes of the basal epithelium with the alterations of the subepithelial nerve plexus, decreased corneal sensation, and dry eye with the disturbances of the precorneal tear film have been reported[5-8]. However, there are conflicting studies about central corneal thickness (CCT) in patients with PXS or pseudoexfoliative glaucoma. Most studies have reported similar CCT in PXS and normal eyes[9-13], but some authors have reported a thinner[14,15] or thicker[16,17] CCT in PXS eyes than in normal eyes.

The evaluation of anterior segment parameters is an important part of ophthalmic examination particularly for the assessment of endothelial function because of complications following cataract surgery and the risk of glaucoma in patients with PXS.

Therefore, the aim of the present study was to evaluate anterior segment parameters in patients with PXS by a comparison with those in healthy subjects.

Submitted for publication: May 12, 2015
Accepted for publication: March 6, 2016

[1] Department of Ophthalmology, Süleyman Demirel University Faculty of Medicine, Isparta, Turkey.

Funding: No specific financial support was available for this study.

Disclosure of potential conflicts of interest: None of the authors have any potential conflict of interest to disclose.

Corresponding author: Alime Gunes. Department of Ophthalmology. Süleyman Demirel University Faculty of Medicine - Isparta 32260 - Turkey - E-mail: dralimesefer@hotmail.com

Approved by the following research ethics committee: Süleyman Demirel University (# 72867572-050).

METHODS

This cross-sectional study consecutively included 43 patients with PXS (27 men and 16 women) with a mean age of 70.0 ± 7.56 years (range, 56-85 years) and 43 healthy control subjects (27 men and 16 women) with a mean age of 67.3 ± 10.0 years (range, 52-85 years) from January 2014 to May 2015. The study was approved by the Institutional Ethics Committee and was conducted in accordance with the Declaration of Helsinki. Written informed consent was obtained from all patients and controls.

After pupil dilation with 1% tropicamide, a diagnosis of PXS was made based on the presence of typical gray-white material on the anterior lens capsule (homogeneous central disc, intermediate clear zone, and peripheral granular zone), on the corneal endothelium, and at the pupil margin. Subjects with glaucoma [high intraocular pressure (IOP) (over 21 mmHg), glaucomatous optic nerve head changes, and glaucomatous visual field defects on computerized visual field examination], corneal disease, retinal disease, active ocular infection or inflammation, previous ocular surgery, ocular trauma, use of contact lenses, and refractive errors more than ± 3 diopters (D) were excluded from the study.

Control subjects were the patients admitted to the ophthalmology clinic for a routine examination without any complaints. However, subjects with a history of ocular disease and pathologic ocular findings were excluded from the study.

All of the participants underwent a complete ophthalmic examination, including refraction, best corrected visual acuity, IOP with Goldmann applanation tonometry, slit-lamp examination, fundus examination, and axial length measurement (PacScan 300AP+ biometric pachymeter; Sonomed, Lake Success, NY).

Evaluation of anterior segment parameters

Anterior segment parameters were assessed using the Pentacam high-resolution rotating Scheimpflug imaging system (HR Pentacam; Oculus, Wetzlar, Germany). Measurements were performed with undilated pupils under scotopic conditions by the same ophthalmologist (A.G.). The automatic release mode was used, and unreasonable measurements were not evaluated and were marked in yellow and red on the monitor. The following parameters were extracted from the obtained topographic and pachymetric maps for statistical analysis: corneal power of the flat axis (K1), corneal power of the steep axis (K2), mean corneal power (Km), anterior chamber angle (ACA), anterior chamber depth (ACD), corneal volume (CV), anterior chamber volume (ACV), and corneal thickness at the apex point (regarded as CCT), the center of the pupil, and the thinnest point. Average values of three successful measurements were used for analysis.

Statistical analysis

Statistical analysis was performed using SPSS for Windows version 15.0 (SPSS Inc., Chicago, IL, USA). Only one eye of each participant was selected for statistical analysis. For patients with unilateral PXS, just the clinically involved eye was selected. In PXS patients affected bilaterally and control subjects, one of the eyes was randomly chosen. All data are reported as mean ± standard deviation. Normality for continuous variables was determined by the Kolmogorov-Smirnov test. An independent-samples t-test was used for continuous variables with a normal distribution and the Mann-Whitney *U* test was used for continuous variables without a normal distribution to compare the means of two groups. Pearson and Spearman tests were used to detect the strength of the relationship between the variables. A *p*-value of <0.05 was considered statistically significant.

RESULTS

The demographic and clinical features of the patient and control groups are shown in table 1. There was no statistically significant difference between the mean age of the PXS patients and that of the control subjects. The visual acuity was significantly lower and axial length was significantly longer in PXS eyes than in control eyes.

The mean values of K1, K2, Km, ACA, ACD, CV, ACV, and corneal thickness at the center of the pupil, the apex point (CCT), and the thinnest point are given in table 2. The mean corneal thicknesses at the center of the pupil (534 ± 31 versus 558 ± 33 µm, *p*=0.001), the apex point (536 ± 31 versus 560 ± 31 µm, *p*=0.001), and the thinnest point (528 ± 30 versus 546 ± 27 µm, *p*=0.005) were significantly thinner in the PXS patients than in the controls. There were no statistically significant differences between the patient and control group in K values or ACA, ACD, CV, or ACV values.

DISCUSSION

PXS is an elastotic, age-related disorder characterized by the accumulation of abnormal extracellular matrix material in intraocular and extraocular tissues. In PXS patients, small, fluffy, white pseudoexfoliative materials are usually observed on the corneal endothelium, along with pigment deposition on the central corneal endothelium. This material can damage the corneal endothelium of PXS eyes and may lead to endothelial decompensation. It is known that a distinct form of corneal endotheliopathy occurs in patients with PXS. This special endotheliopathy can cause early corneal endothelial decompensation and may have been previously misdiagnosed as an atypical non-guttata Fuchs' endothelial dystrophy[8,18,19]. In addition, *in vivo* confocal microscopy studies have shown significant morphologic alterations in the corneas of PXS patients[5,20-22].

Table 1. Comparison of demographic and clinical data of PXS patients and controls

	PXS patients (n=43)	Controls (n=43)	*p*
Age (years)	70.00 ± 7.56	67.30 ± 10.00	0.160
Sex (male)	27.00 (62.7%)	27 (62.7%)	1.000
BCVA (Snellen)	0.52 ± 0.37	0.88 ± 0.23	<0.001
IOP (mmHg)	16.00 ± 5.88	16.10 ± 3.20	0.900
AL (mm)	23.90 ± 0.70	23.20 ± 0.90	0.001

PXS= pseudoexfoliation syndrome; BCVA= best corrected visual acuity; IOP= intraocular pressure; AL= axial length.

Table 2. Comparison of the anterior segment parameters of PXS patients and controls

	PXS patients (n=43)	Controls (n=43)	*p*
Corneal power (front)			
K_1	43.80 ± 1.57	43.2 ± 1.81	0.130
K_2	44.50 ± 1.43	43.9 ± 1.72	0.070
K_m	44.10 ± 1.48	43.5 ± 1.66	0.080
Pachymetric measurements (µm)			
Central	534 ± 31	558 ± 33	0.001
Apex	536 ± 31	560 ± 31	0.001
Thinnest	528 ± 30	546 ± 27	0.005
Corneal volume (mm^3)	58.70 ± 4.21	59.70 ± 3.12	0.210
ACA (°)	30.30 ± 9.89	33.50 ± 9.66	0.110
ACD (mm)	2.71 ± 0.46	2.82 ± 0.77	0.790
ACV (mm^3)	123.00 ± 23.40	132.00 ± 41.30	0.250

Data are indicated as mean ± standard deviation.
PXS= pseudoexfoliation syndrome; K1= corneal power of the flat axis; K2= corneal power of the steep axis; Km= mean corneal power; ACA= anterior chamber angle; ACD= anterior chamber depth; ACV= anterior chamber volume.

Corneal thickness is an important indicator of corneal health. Evaluation of corneal parameters is essential in the diagnosis and monitoring of glaucoma and when refractive surgery is scheduled. Currently, the Pentacam with Scheimpflug technology is used to assess corneal parameters in detail. This method provides evaluation of corneal pachymetry, anterior and posterior corneal topography, lens thickness, and anterior chamber depth, angle, and volume[23].

Results reported in the literature have varied with respect to the CCT in pseudoexfoliative eyes. Arnarsson et al.[9] found that PXS was not associated with CCT. Rüfer et al.[24] determined that CCT was not significantly different among primary open-angle glaucoma, pseudoexfoliative glaucoma, and control groups, but patients with low-tension glaucoma had significantly lower CCT than that in the controls. Detorakis et al.[11] reported that differences in CCT between PXS eyes and age- and sex-matched controls were not statistically significant. Ventura et al.[12] and Yagci et al.[13] reported that there were no significant differences in CCT among normal-tension glaucoma, primary open-angle glaucoma, pseudoexfoliative glaucoma, and healthy control groups. However, Gorezis et al.[14] found that the CCT was significantly thinner in patients with pseudoexfoliative glaucoma. Similarly, Aghaian et al.[25] and Bechmann et al.[26] reported that the CCT was significantly lower in patients with pseudoexfoliative glaucoma, low-tension glaucoma, and primary open-angle glaucoma than in healthy individuals. Inoue et al.[15] examined the CCT and the endothelial morphology of the cornea in 26 eyes of 21 PXS patients (seven eyes with glaucoma and 19 eyes without glaucoma). The researchers represented that the corneal endothelial cell density and CCT were significantly lower in the PXS eyes than in the control eyes, but there were no significant differences in these factors between the PXS eyes in patients with and without glaucoma. Ozcura et al.[27] reported that CCT was significantly thinner in eyes with PXS than in control eyes, but was not thinner in the eyes of those with pseudoexfoliative glaucoma.

In the present study, the mean corneal thicknesses at the center of the pupil, the apex point, and the thinnest point were significantly thinner in the PXS patients than in the controls. We believe that the alterations of the corneal subepithelial nerve plexus, decreased corneal sensation, and dry eye with disturbances of the precorneal tear film may lead to corneal thinning as reported by Martone et al.[5] and Kozobolis et al.[7] The different results regarding corneal thickness in the literature might be because of racial differences, different methods, different sample sizes, and different age distributions in the sampled populations. Additionally, the PSX eyes had lower visual acuity and longer axial length than the healthy controls did in our study. These results are in agreement with a previous study reported by Jonas et al.[28].

Doganay et al.[29] reported that there were no significant differences in ACV, ACA, CCT, and corneal volume values among patients with PXS, those with pseudoexfoliative glaucoma, and healthy controls. Similarly, there were no statistically significant differences between the patient and control groups in K values or ACA, ACD, CV, or ACV values in our study.

There are some limitations to this study in that it was a single-center study with a relatively small sample size. The anterior segment parameters need to be investigated in further large studies with different devices to understand these changes more clearly.

In conclusion, PXS patients had thinner corneas, lower visual acuity, and longer axial length than healthy controls did.

REFERENCES

1. Naumann GO, Schlötzer-Schrehardt U, Küchle M. Pseudoexfoliation syndrome for the comprehensive ophthalmologist. Intraocular and systemic manifestations. Ophthalmology. 1998;105(6):951-68.
2. Schlötzer-Schrehardt U, von der Mark K, Sakai LY, Naumann GO. Increased extracellular deposition of fibrillin-containing fibrils in pseudoexfoliation syndrome. Invest Ophthalmol Vis Sci. 1997;38(5):970-84.
3. Ritch R, Schlötzer-Schrehardt U. Exfoliation syndrome. Surv Ophthalmol. 2001;45(4): 265-315.
4. Schlötzer-Schrehardt U, Naumann GO. Ocular and systemic exfoliation syndrome. Am J Ophthalmol. 2006;141(5):921-37.
5. Martone G, Casprini F, Traversi C, Lepri F, Pichierri P, Caporossi A. Pseudoexfoliation syndrome: in vivo confocal microscopy analysis. Clin Experiment Ophthalmol. 2007; 35(6):582-5.
6. Wang L, Yamasita R, Hommura S. Corneal endothelial changes and aqueous flare intensity in pseudoexfolation syndrome. Ophthalmologica. 1999;213(6):387-91.
7. Kozobolis VP, Detorakis ET, Tsopakis GM, Pallikaris IG. Evaluation of tear secretion and tear film stability in pseudoexfoliation syndrome. Acta Ophthalmol Scand. 1999;77(4): 406-9.
8. Naumann GOH, Schlötzer-Schrehardt U. Keratopathy in pseudoexfoliation syndrome as a cause of corneal endothelial decompensation. A clinicopathologic study. Ophthalmology. 2000;107(6):1111-24.
9. Arnarsson A, Damji KF, Sverrisson T, Sasaki H, Jonasson F. Pseudoexfoliation in the Reykjavik Eye Study: prevalence and related ophthalmological variables. Acta Ophthalmol Scand. 2007;85(8):822-7.
10. Hepsen IF, Yagci R, Keskin U. Corneal curvature and central corneal thickness in eyes with pseudoexfoliation syndrome. Can J Ophthalmol. 2007;42(5):677-80.
11. Detorakis ET, Koukoula S, Chrisohoou F, Konstas AG, Kozobolis VP. Central corneal mechanical sensitivity in pseudoexfoliation syndrome. Cornea. 2005;24(6):688-91.
12. Ventura AC, Böhnke M, Mojon DS. Central corneal thickness measurements in patients with normal tension glaucoma, primary open angle glaucoma, pseudoexfoliation glaucoma, or ocular hypertension. Br J Ophthalmol. 2001;85(7):792-5.
13. Yagci R, Eksioglu U, Midillioglu I, Yalvac I, Altiparmak E, Duman S. Central corneal thickness in primary open angle glaucoma, pseudoexfoliative glaucoma, ocular hypertension, and normal population. Eur J Ophthalmol. 2005;15(3):324-8.
14. Gorezis S, Christos G, Stefaniotou M, Moustaklis K, Skyrlas A, Kitsos G. Comparative results of central corneal thickness measurements in primary open-angle glaucoma, pseudoexfoliation glaucoma, and ocular hypertension. Ophthalmic Surg Lasers Imaging. 2008;39(1):17-21.
15. Inoue K, Okugawa K, Oshika T, Amano S. Morphological study of corneal endothelium and corneal thickness in pseudoexfoliation syndrome. Jpn J Ophthalmol. 2003;47(3): 235-9.
16. Puska P, Vasara K, Harju M, Setälä K. Corneal thickness and corneal endothelium in normotensive subjects with unilateral exfoliation syndrome. Graefes Arch Clin Exp Ophthalmol. 2000;238(8):659-63.
17. Stefaniotou M, Kalogeropoulos C, Razis N, Psilas K. The cornea in exfoliation syndrome. Doc Ophthalmol. 1992;80(4):329-33.
18. Miyake K, Matsuda M, Inaba M. Corneal endothelial changes in pseudoexfoliation syndrome. Am J Ophthalmol. 1989;108(1):49-52.
19. Schlötzer-Schrehardt UM, Dörfler S, Naumann GO. Corneal endothelial involvement in pseudoexfoliation syndrome. Arch Ophthalmol. 1993;111(5):666-74.
20. Sbeity Z, Palmiero PM, Tello C, Liebmann JM, Ritch R. Non-contact in vivo confocal scanning laser microscopy in exfoliation syndrome, exfoliation syndrome suspect and normal eyes. Acta Ophthalmol. 2011;89(3):241-7.
21. Zheng X, Shiraishi A, Okuma S, Mizoue S, Goto T, Kawasaki S, et al. In vivo confocal microscopic evidence of keratopathy in patients with pseudoexfoliation syndrome. Invest Ophthalmol Vis Sci. 2011;52(3):1755-61.
22. Zheng X, Inoue Y, Shiraishi A, Hara Y, Goto T, Ohashi Y. In vivo confocal microscopic and histological findings of unknown bullous keratopathy probably associated with pseudoexfoliation syndrome. BMC Ophthalmol. 2012;12:17.
23. Ambrosio Jr R, Alonso RS, Luz A, Coca Velarde LG. Corneal-thickness spatial profile and corneal-volume distribution: tomographic indices to detect keratoconus. J Cataract Refract Surg. 2006;32(11):1851-9.
24. Rüfer F, Westphal S, Erb C. Comparison of central and peripheral corneal thicknesses between normal subjects and patients with primary open angle glaucoma, normal tension glaucoma and pseudoexfoliation glaucoma. Klin Monatsbl Augenheilkd. 2007; 224(8):636-40.
25. Aghaian E, Choe JE, Lin S, Stamper RL. Central corneal thickness of Caucasians, Chinese, Hispanics, Filipinos, African Americans, and Japanese in a glaucoma clinic. Ophthalmology. 2004;111(12):2211-9.
26. Bechmann M, Thiel MJ, Roesen B, Ullrich S, Ulbig MW, Ludwig K. Central corneal thickness determined with optical coherence tomography in various types of glaucoma. Br J Ophthalmol. 2000;84(11):1233-7.
27. Ozcura F, Aydin S, Dayanir V. Central corneal thickness and corneal curvature in pseudoexfoliation syndrome with and without glaucoma. J Glaucoma. 2011;20(7):410-3.
28. Jonas JB, Nangia V, Matin A, Bhojwani K, Sinha A, Khare A, et al. Pseudoexfoliation: normative data and associations. The Central India Eye and Medical Study. PLoS One. 2013;8(10):e76770.
29. Doganay S, Tasar A, Cankaya C, Firat PG, Yologlu S. Evaluation of Pentacam-Scheimpflug imaging of anterior segment parameters in patients with pseudoexfoliation syndrome and pseudoexfoliative glaucoma. Clin Exp Optom. 2012;95(2):218-22.

The effects of riboflavin and ultraviolet light on keratocytes cultured *in vitro*

Avaliação do efeito da riboflavina e luz ultravioleta sobre os ceratócitos in vitro

Joyce L. Covre[1], Priscila C. Cristovam[1], Renata R. Loureiro[1], Rossen M. Hazarbassanov[1,2], Mauro Campos[1,3], Élcio H. Sato[1,2], José Álvaro P. Gomes[1,2]

ABSTRACT

Purpose: To culture quiescent human keratocytes and evaluate the effects of ultraviolet light and riboflavin on human corneal keratocytes *in vitro*.

Methods: Keratocytes were obtained from remaining corneoscleral ring donor corneas previously used in corneal transplant surgeries and cultured in DMEM/F12 with 2% FBS until confluence. Characterization of cultured cells was performed by immunofluorescence analysis for anti-cytokeratin-3, anti-Thy-1, anti-α-smooth muscle actin, and anti-lumican. Immunofluorescence was performed before and after treatment of cultured cells with either ultraviolet light or riboflavin. Corneal stromal cells were covered with collagen (200 µL or 500 µL) and 0.1% riboflavin, and then exposed to ultraviolet light at 370 nm for 30 minutes. After 24 hours, cytotoxicity was determined using MTT colorimetric assays, whereas cell viability was assessed using Hoechst 33342 and propidium iodide.

Results: Cell cultures achieved confluence in approximately 20 days. Expression of the lumican was high, whereas no expression of CK3, Thy-1, and α-SMA was observed. After crosslinking, MTT colorimetric assays demonstrated a low toxicity rate, whereas Hoechst 33342/propidium iodide staining demonstrated a low rate of apoptosis and necrosis, respectively, in all collagen-treatment groups.

Conclusion: Keratocytes can be successfully cultured *in vitro* and characterized by immunofluorescence using lumican. MTT colorimetric assays, and Hoechst 33342, and propidium iodide staining demonstrated a higher rate of cell death in cells cultured without collagen, indicating collagen protects keratocytes from the cytotoxic effects of ultraviolet light.

Keywords: Ultraviolet rays; Riboflavin; Cornea; Corneal stroma; Corneal keratocytes; Apoptosis

RESUMO

Objetivo: *Avaliar o efeito da aplicação da luz ultravioleta e riboflavina sobre ceratócitos da córnea humana* in vitro.

Métodos: *Os ceratócitos foram obtidos a partir das rimas corneoesclerais remanescentes da trepanação de córneas previamente utilizadas em cirurgias de transplante de córnea e cultivadas em meio DMEM/F12 com 2% de FBS até atingir confluência. As culturas de células foram caracterizadas por imunofluorescência com os anticorpos K3 (marcador de células epiteliais), Thy-1 (marcador de fibroblasto) SMA (marcador de miofibroblasto) e Lumican (marcador de ceratócitos). Imunofluorescência também foi feita após o tratamento. As células do estroma da córnea foram cobertas com colágeno (200 µL e 500 µL) e 0,1% de riboflavina e exposta a luz UVA a 370 nm por 30 minutos. Após 24 horas, citotoxicidade foi determinada por ensaio de MTT e a viabilidade celular foi feita por Hoechst 33342/Iodeto de propideo.*

Resultados: *As culturas de células atingiram confluência em aproximadamente 20 dias. Imunofluorescência apontou alta expressão para o marcador de ceratócitos (Lumican) e expressão negativa par os marcadores de células epiteliais (K3), fibroblasto (Thy-1) e miofibroblasto (α-SMA). Após o* cross linking *a análise de MTT mostrou baixa taxa de toxicidade e com a coloração de Hoechst 33342/Iodeto de propideo baixa taxa de apoptose e necrose respectivamente em todos os grupos que continham colágeno.*

Conclusão: *As culturas de ceratócitos foram obtidas e caracterizadas por imunofluorescência através do marcador Lumican com sucesso. O ensaio de MTT e a coloração por Hoechst 33342 e iodeto de propídio, apresentaram maior índice de morte celular nos grupos que não continham colágeno, provando que protege as células contra os efeitos da luz UVA.*

Descritores: *Raios ultravioleta; Riboflavina; Córnea; Substância própria; Ceratócitos da córnea; Apoptose*

INTRODUCTION

The cornea is the primary refractive element of the visual system. It is principally composed of stroma, which accounts for approximately 90% of its thickness[1]. The corneal stroma is covered anteriorly by four to six layers of stratified, nonkeratinized epithelium; posteriorly, it is covered by a single endothelial layer, which is in direct contact with the aqueous humor[1-3]. The corneal stroma consists of collagen fibers, extracellular matrix (ECM), and keratocytes, which exhibit dendritic morphology and function in the synthesis of collagen fibrils. The uniform arrangement of these collagen fibers allows corneal transparency[4,5].

A number of diseases have been shown to affect the arrangement and resistance of corneal collagen fibers. Keratoconus is defined as a noninflammatory disease, generally involving bilateral corneal ectasia, characterized by stromal thinning and loss of rigidity, leading to irregular asymmetric astigmatism and poor vision. In the majority of cases, the refractive error induced by keratoconus can be corrected with the use of rigid contact lenses. Nevertheless, a proportion of cases in which progression of the corneal irregularity results in significant visual deterioration require more invasive therapeutic options, such as intracorneal implants or corneal transplantation[6].

Recently, Seiler *et al.* proposed the use of crosslinking (CXL) for the treatment of keratoconus. This treatment is based on the chemical induction of interfibrillar and intrafibrillar covalent bonds in the corneal stroma, thus strengthening the cornea. CXL relies on photosensitive oxidation induced by the combination of riboflavin (vitamin B2) and ultraviolet A (UVA) light, thereby increasing the biomechanical resistance and stability of the cornea[7,8]. Other indications for crosslinking

Submitted for publication: November 4, 2015
Accepted for publication: February 17, 2016

[1] Ocular Surface Advanced Center (CASO), Department of Ophthalmology and Visual Sciences, Escola Paulista de Medicina (EPM), Universidade Federal de São Paulo (UNIFESP), São Paulo, SP, Brazil.
[2] Cornea and External Diseases Service, Department of Ophthalmology and Visual Sciences, Escola Paulista de Medicina (EPM), Universidade Federal de São Paulo (UNIFESP), São Paulo, SP, Brazil.
[3] Refractive Surgery Service, Department of Ophthalmology and Visual Sciences, Escola Paulista de Medicina (EPM), Universidade Federal de São Paulo (UNIFESP), São Paulo, SP, Brazil.

Funding: This study was supported in part by FAPESP and CAPES.

Disclosure of potential conflicts of interest: None of the authors have any potential conflict of interest to disclose.

Corresponding author: José Álvaro Pereira Gomes. R. Sabará, 566/43 - São Paulo, SP - 01239-010 Brazil - E-mail: japgomes@uol.com.br

Approved by the following research ethics committee: Universidade Federal de São Paulo, SP, Brazil (# 0419/10)

http://dx.doi.org/10.5935/0004-2749.20160052

have been reported, including the treatment of post-refractive surgery ectasia, bullous keratopathy, ocular infections, and corneal necrosis, among others[8].

The objective of the present study was to culture quiescent human keratocytes and evaluate the effect of UVA light and riboflavin on human corneal keratocytes *in vitro*.

METHODS

Study design

In all the groups assigned to receive 0.1% riboflavin (10 mg riboflavin-5-phosphate dissolved in 10 mL of 20% dextran T-500 [400 mOsm/mL]; Ophtalmos®, São Paulo, SP Brazil), a layer of riboflavin was applied to the surface of the plate, covering all cells for 30 minutes. This procedure was performed before continuous exposure to UVA light (IROC®, Germany) at 370 nm with a surface irradiance of 3 mW/cm^2, with a total radiant exposure of 5.375 J/cm^2 in cases in which riboflavin and UVA light were combined. The riboflavin concentration and UV wavelength used in the present study were identical to those used clinically. The twelve experimental groups are described below:

Keratocyte culture in the absence of collagen

1. Cells were exposed to 0.1% riboflavin for 30 minutes;
2. Cells were exposed to UVA light at 370 nm for 30 minutes;
3. Cells were simultaneously exposed to riboflavin and UVA light for 30 minutes.

Keratocyte culture in the presence of 200 µL of collagen at 0.1 g/mL

4. Cells were exposed to 0.1% riboflavin for 30 minutes;
5. Cells were exposed to UVA light at 370 nm for 30 minutes;
6. Cells were simultaneously exposed to riboflavin and UVA light for 30 minutes;
7. Cells were exposed to collagen alone.

Keratocyte culture in the presence of 500 µL of collagen at 0.1 g/mL

8. Cells were exposed to 0.1% riboflavin for 30 minutes;
9. Cells were exposed to UVA light at 370 nm for 30 minutes;
10. Cells were simultaneously exposed to riboflavin and to UVA light for 30 minutes;
1. Cells were exposed to collagen alone;
2. Control group: keratocytes were not submitted to any of the abovementioned experimental conditions.

Keratocyte culture

Keratocytes were isolated from remaining corneoscleral ring donor corneas previously used in corneal transplant surgeries at the Department of Ophthalmology and Visual Sciences, Escola Paulista de Medicina (EPM), Universidade Federal de São Paulo (UNIFESP). Explants of corneal stroma were prepared in a laminar flow hood under sterile conditions. Explants were cultured in Dulbecco's modified eagle medium and Ham's nutrient mixture F12 (DMEM/F12-1:1) supplemented with 2% fetal bovine serum (FBS; Invitrogen, Gibco, Portland, OR, USA) in 24-well plates. Cells were cultured in a humidified incubator at 37°C in 5% CO_2. Culture medium was changed three times a week for 3 weeks.

Cytotoxicity (MTT)

Twenty-four hours after treatment, RPMI medium (Invitrogen, Gibco, Portland, OR, USA) with 10% MTT solution was added and cells were incubated for 3 hours at 37°C. To solubilize formazan crystals, 100 µL of dimethyl sulfoxide (DMSO; Sigma Aldrich, St. Louis, MO, USA) was added to each well. Results were read using a spectrophotometer at a wavelength of 340 nm in an ELISA EXL800 plate reader (Universal Microplate Reader, Bio-Tek Instruments, Inc.). The cytotoxicity of each treatment was expressed by comparing absorption values with control values.

Apoptosis and necrosis (Hoechst 33342 and propidium iodide)

Cytomorphological assays to detect apoptotic and necrotic cells using Hoechst 33342 (Sigma Aldrich, St. Louis, MO, USA) and propidium iodide staining were performed following treatment in all groups. Cells were collected and centrifuged for 5 minutes at 1800 rpm. Next, a mixture of 3.5 µL of suspended cells, 1.5 µL of Hoescht 33342 (10 mg/mL), and 1.0 µL of propidium iodide was placed between a slide and coverslip. The reaction mixture was incubated and cells were observed using a fluorescence microscope with absorption spectra of 360 and 538 nm.

Immunofluorescence

Cells were cultured in 24-well culture plates (TPP, Zurich, Switzerland) on coverslips. After reaching 70% confluence, cells were divided into two groups: untreated, with immunofluorescence used only for cell characterization; treated, with immunofluorescence applied before and after CXL treatment to observe changes in protein expression.

Cells were incubated overnight with the following primary antibodies: lumican (keratocyte marker), Thy-1 (fibroblast marker), α-SMA (myofibroblast marker), and CK3 (epithelium marker, cell-characterization step only). Cells were then incubated with secondary anti-mouse antibody conjugated with fluorescein isothiocyanate (FITC). Slides were analyzed using a fluorescence microscope.

Statistical analysis

The software program used for the statistical analysis and for producing the graphs was GraphPad Prism, version 5.0 for Windows. The continuous, semi-continuous, and semi-categorical data were initially analyzed using the Kolmogorov-Smirnov test to determine how closely these data fitted to a normal (Gaussian) curve. The parametric data were represented as means and standard deviations of the means, and compared using Student's t-test, with or without Welch's correction, depending on the result of Levene's test used to determine the equality of variances.

For the parametric variables in independent samples, one-way analysis of variance (ANOVA) was used, followed by Dunnett's post-hoc test. The nonparametric data were represented as medians of quartiles and, when more than two samples were compared, the Kruskal-Wallis test was used followed by the Müller-Dunn post-test. Spearman's correlation coefficient was used to measure nonparametric correlations and Pearson's correlation was applied for parametric measurements.

An alpha (probability of making a type I error) ≤5% and a beta (probability of making a type II error) ≤20% were defined for the entire study. Probabilities <5% were considered statistically significant. For repeated measures, the Bonferroni method was used to correct cumulative type I errors.

RESULTS

Keratocyte culture

Corneal stromal cells were observed to have dendritic morphology after approximately 3 weeks' culture in DMEM/F12 medium containing 2% FBS, indicating cells remained quiescent during culture (Figure 1).

Cytotoxicity (MTT)

Cytotoxicity evaluations using MTT colorimetric assays 24 hours after treatment demonstrated a significantly lower number of meta-

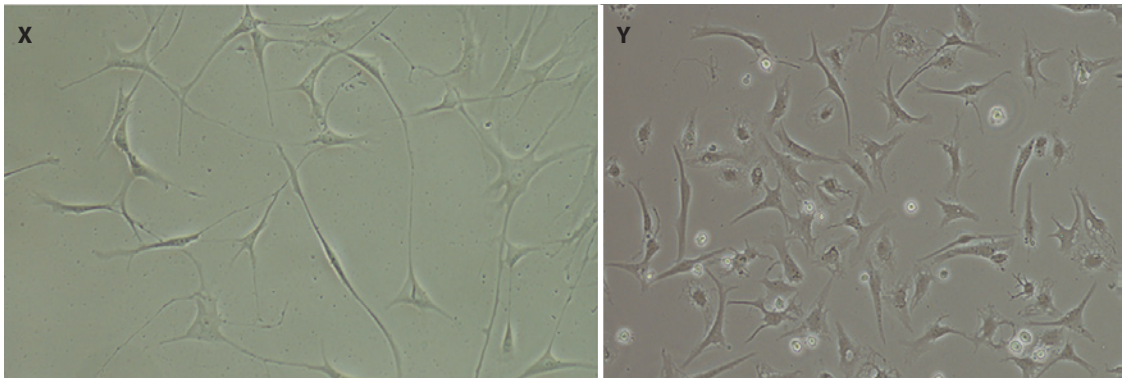

Figure 1. Morphological analysis of keratocytes. X) After 10 days in culture. Y) After 20 days in culture. Inverted microscope; 20×.

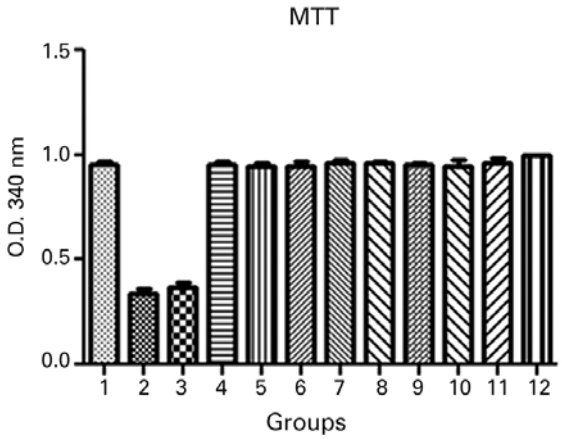

ANOVA= P<0.0001, Groups 2 and 3 *versus* Group 12 (control). Dunnett's post-hoc test= P<0.001, Groups 2 and 3 *versus* Group 12 (control).

Figure 2. Cytotoxicity evaluations using MTT colorimetric assays 24 hours after treatment: 1, keratocyte culture + riboflavin; 2, keratocyte culture + UVA light; 3, keratocyte culture + riboflavin + UVA light; 4, keratocyte culture + 200 µL of collagen + riboflavin; 5, keratocyte culture + 200 µL of collagen + UVA light; 6, keratocyte culture + 200 µL of collagen + riboflavin + UVA light; 7, keratocyte culture + 200 µL of collagen; 8, keratocyte culture + 500 µL of collagen + riboflavin; 9, keratocyte culture + 500 µL of collagen + UVA light; 10, keratocyte culture + 500 µL of collagen + riboflavin + UVA light; 11, keratocyte culture + 500 µL of collagen; 12, control group. All groups were treated for 30 minutes.

bolically active cells in cell cultures without collagen during exposure to UVA light, indicating poorer cell viability. No statistically significant differences were observed in the other treated groups compared to the control group (Figure 2).

Apoptosis versus necrosis (Hoechst 33342 and propidium iodide)

To confirm the results of the MTT assay, cell viability of all treatment groups was evaluated using Hoechst 33342 and propidium iodide staining, which permitted the identification and quantification of viable cells, apoptotic cells (bright blue-stained cells), and necrotic cells (red-stained cells; Figure 3). Differential staining demonstrated a significantly greater number of necrotic and apoptotic cells in the groups without collagen during exposure to UVA light compared to the other treatment and control groups (Figures 4, 5, and 6).

Immunofluorescence

All cultures tested negative for the epithelial cell marker CK3, which was used to characterize cells (Figure 7). In all groups, cells were

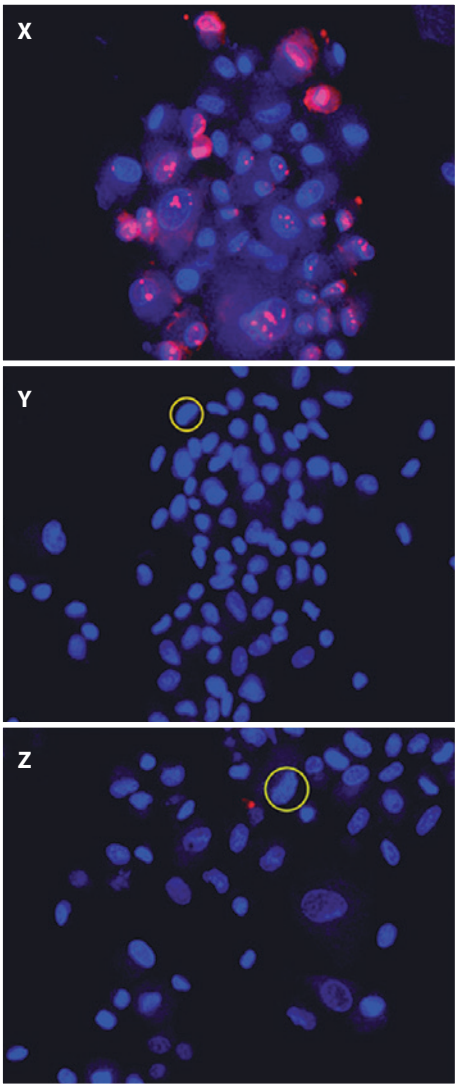

Figure 3. Cell viability in treatment groups evaluated using Hoechst 33342 and propidium iodide staining. X) Keratocyte culture + riboflavin + UVA light, without collagen; cells in necrosis are stained red. Y) Keratocyte culture + riboflavin + UVA light + 200 µL of collagen. Z) Keratocyte culture + riboflavin + UVA light + 500 µL of collagen. In Y and Z, chromatin was observed as highly compacted. Cells undergoing apoptosis are stained bright blue.

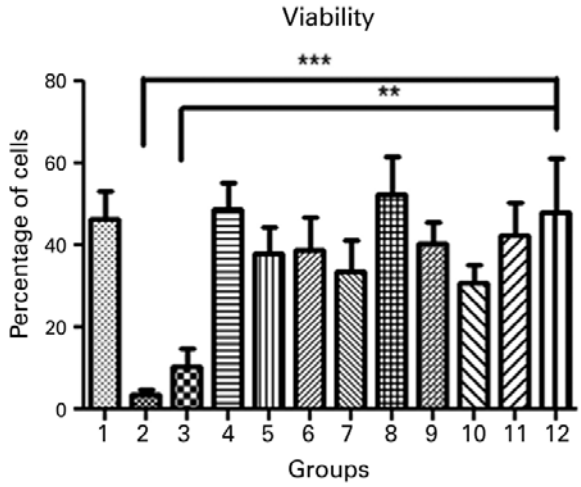

ANOVA= p=0.0002; Group 2 *versus* Group 12 (control). Dunnett's post-hoc test= p<0.001; Group 3 *versus* Group 12 (control); Dunnett's post-hoc test; p<0.01.

Figure 4. Cell viability in the different treatment groups: 1, keratocyte culture + riboflavin; 2, keratocyte culture + UVA light; 3, keratocyte culture + riboflavin + UVA light; 4, keratocyte culture + 200 µL of collagen + riboflavin; 5, keratocyte culture + 200 µL of collagen + UVA light; 6, keratocyte culture + 200 µL of collagen + riboflavin + UVA light; 7, keratocyte culture + 200 µL of collagen; 8, keratocyte culture + 500 µL of collagen + riboflavin; 9, keratocyte culture + 500 µL of collagen + UVA light; 10, keratocyte culture + 500 µL of collagen + riboflavin + UVA light; 11, keratocyte culture + 500 µL of collagen; 12, control group. All groups were treated for 30 minutes.

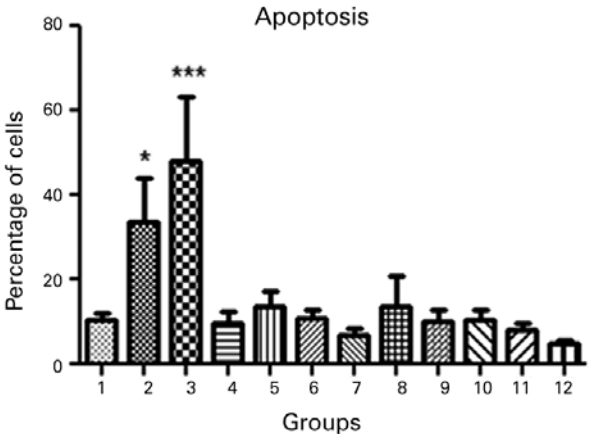

ANOVA= P<0.0001, Group 2 *versus* Group 12 (control). Dunnett's post-hoc test= P<0.05, Group 3 *versus* Group 12 (control); Dunnett's post-hoc test, P<0.001.

Figure 5. Apoptosis in the different treatment groups: 1, keratocyte culture + riboflavin; 2, keratocyte culture + UVA light; 3, keratocyte culture + riboflavin + UVA light; 4, keratocyte culture + 200 µL of collagen + riboflavin; 5, keratocyte culture + 200 µL of collagen + UVA light; 6, keratocyte culture + 200 µL of collagen + riboflavin + UVA light; 7, keratocyte culture + 200 µL of collagen; 8, keratocyte culture + 500 µL of collagen + riboflavin; 9, keratocyte culture + 500 µL of collagen + UVA light; 10, keratocyte culture + 500 µL of collagen + riboflavin + UVA light; 11, keratocyte culture + 500 µL of collagen; 12, control group. All groups were treated for 30 minutes.

negative for fibroblast (Thy-1) and myofibroblast (α-sma) markers, and positive only for the keratocyte marker, (lumican), both before and following crosslinking (Figure 8). This staining pattern demonstrates the success of keratocyte culture, with staining remaining unaltered in all groups compared to the control group up to 24 hours after treatment.

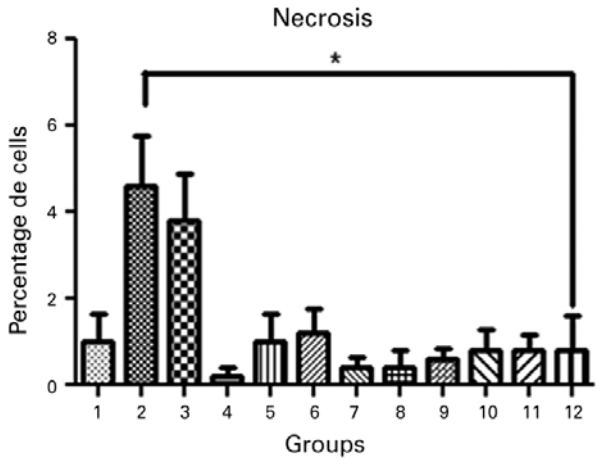

Kruskal-Wallis test= P=0.007, Group 2 *versus* Group 12 (control); Dunn's post-hoc test= P<0.05.

Figure 6. Necrosis in the different treatment groups: 1, keratocyte culture + riboflavin; 2, keratocyte culture + UVA light; 3, keratocyte culture + riboflavin + UVA light; 4, keratocyte culture + 200 µL of collagen + riboflavin; 5, keratocyte culture + 200 µL of collagen + UVA light; 6, keratocyte culture + 200 µL of collagen + riboflavin + UVA light; 7, keratocyte culture + 200 µL of collagen; 8, keratocyte culture + 500 µL of collagen + riboflavin; 9, keratocyte culture + 500 µL of collagen + UVA light; 10, keratocyte culture + 500 µL of collagen + riboflavin + UVA light; 11, keratocyte culture + 500 µL of collagen; 12, control group. All groups were treated for 30 minutes.

DISCUSSION

The results from the present study indicate crosslinking does not cause severe damage to the human cornea because extensive cell death was observed only in keratocytes exposed to UVA light without the presence of collagen. In corroboration with previous reports, the present study also demonstrates that riboflavin has no cytotoxic effect. This finding was expected as riboflavin is a crucial component of all living cells and a precursor of flavin mononucleotide and flavin-adenine dinucleotide, two coenzymes essential for carbohydrate, fat, and protein metabolism present in the retina, liver, and heart[9-11].

To standardize keratocyte cultures, various experiments were required because the maintenance of cultured cells in the quiescent state was technically challenging because of high concentrations (10%-20%) of fetal bovine serum (FBS) promoting cell differentiation. FBS contains factors such as lysophosphatidic acid (LPA) and sphingosine-1-phosphate (S1P), which stimulate cell contractility and play a fundamental role in the transformation of quiescent keratocytes with dendritic morphology into cells with an activated fibroblast phenotype[12,13]. On the other hand, the absence of FBS in culture medium hampers tissue adhesion to culture plates because culture medium is more fluid and facilitates cell detachment, thereby rendering cell growth impossible.

The findings of the present study may be clinically applicable as, to the best of our knowledge, no previous comparable studies using human keratocytes have been reported up to the present time.

The present study was performed using two-dimensional cultures to evaluate the effect of crosslinking by the addition of 200 or 500 µL of collagen to cell cultures, equivalent to the collagen thickness of the central and peripheral cornea, respectively. This research model partially reproduces the corneal stroma. 3 D culture models are generally considered to have greater model validity and to better mimic *in vivo* cell behavior[14,15] because keratocytes reside within a three-dimensional extracellular matrix. Therefore, 3 D models may allow more accurate observation of cell morphology, organization, and mechanical behavior[12]. Furthermore, such culture systems may

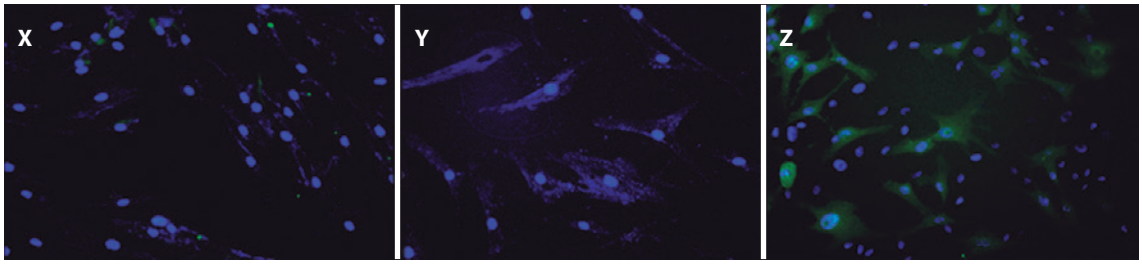

Figure 7. Immunofluorescence assay demonstrated negative expression of the differentiated corneal epithelial cell marker CK3 in cultured keratocytes. X) Immunofluorescence using CK3 antibody. Y) Negative control. Z) Positive control in cultured corneal epithelium.

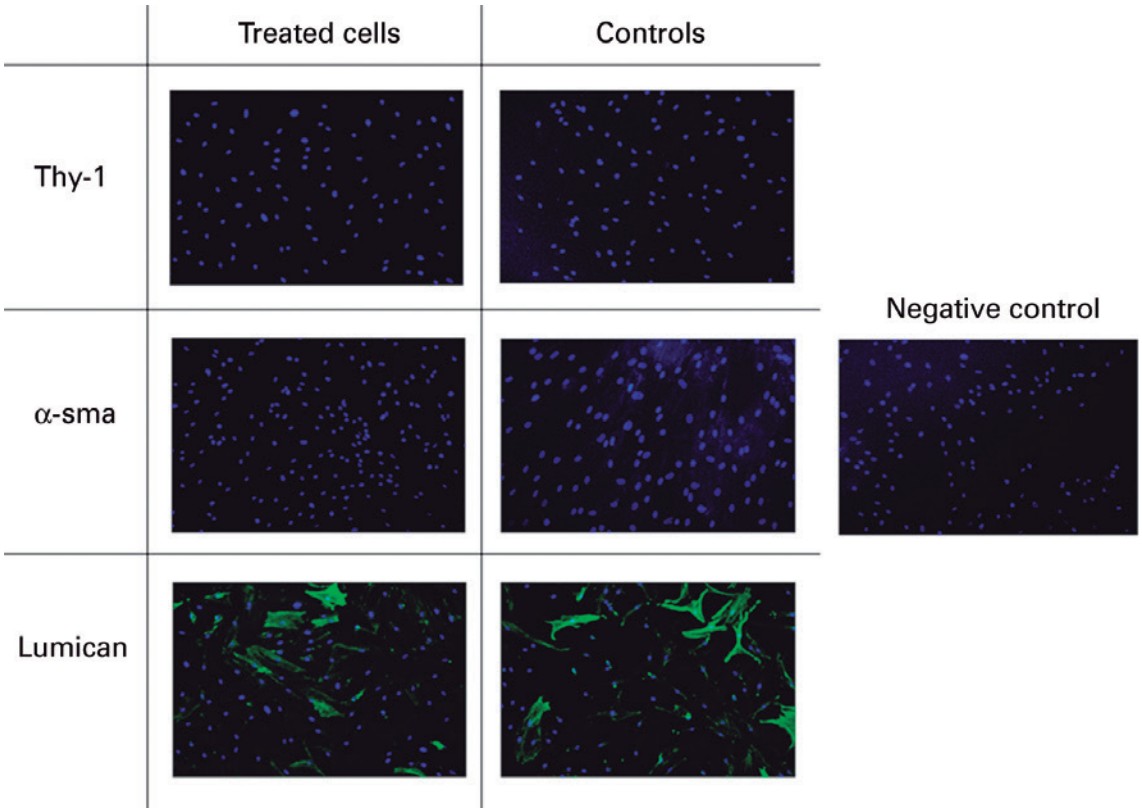

Figure 8. Immunofluorescence of cultured keratocytes submitted to crosslinking versus control cells not submitted to crosslinking (fluorescence microscope, 40×).

permit cell degradation and extracellular matrix remodeling to be investigated.

When culture medium with only 2% of FBS was used, optical analysis demonstrated that growing cells had a dendritic morphology similar to that of quiescent keratocytes. Cells were characterized by immunofluorescence analysis using the following markers: lumican, Thy-1, α-sma, and CK3. Lumican is one of the most abundant proteins in the corneal stroma and is expressed in the presence of quiescent keratocytes[16]. Thy-1 has been shown to contribute to the transformation of corneal keratocytes into fibroblasts, with its expression posited to indicate the involvement of fibroblasts in the healing process[17]. Alpha-smooth muscle actin (α-sma) is expressed during wound healing by fibroblasts undergoing transformation into myofibroblasts[18] with contractile activity that helps decrease the injured area[19,20]. Finally, CK3 is expressed by differentiated corneal epithelium. Immunofluorescence of cultured cells in the present study demonstrated positivity for the lumican protein only, confirming that cultured cells were keratocytes in a quiescent state.

Immunofluorescence assays were performed after the cells were submitted to different treatments to assess for morphological modifications after exposure to different variables. Once again, cells cultured in these conditions expressed lumican only. In this step, the CK3 antibody, a differentiated corneal epithelium marker, was not used because its negative expression during cell characterization had already been demonstrated.

To confirm the results of the MTT colorimetric assays, the viability of keratocytes was evaluated using Hoechst 33342 and propidium iodide staining, allowing living cells and those in apoptosis and necrosis to be identified and quantified. Apoptosis is a highly regulated physiological process of programmed cell death and plays an

important role in the homeostasis of different tissues in response to numerous stimuli. This process is characterized by various morphological and biochemical alterations that are of crucial importance for embryo development, for maturation of the immune system, and as a defense mechanism against external insults[21]. During apoptosis, alterations occur in the cytoskeleton that induce the contraction and loss of cell volume, chromatin condensation, nuclear fragmentation, and the formation of cytoplasmic vesicles that give rise to structures termed apoptotic bodies[22]. Necrosis is defined as a violent form of cell death initiated by environmental stimuli that results in rapid deregulation of homeostasis.

To validate the results of the present study, further studies using three-dimensional keratocyte culture with variations in the duration and intensity of UVA *in vitro* and in experimental animal models are required.

The present study evaluated the effects of riboflavin and UVA light, individually and in combination, on human corneal keratocytes *in vitro*. Cultures of keratocytes were successfully obtained and remained quiescent with dendritic morphology, as demonstrated by lumican immunofluorescence analysis. Immunofluorescence analysis of cells after exposure to riboflavin and UVA light demonstrated similar marker expression to untreated cells. MTT assays demonstrated lower cytotoxicity in groups containing collagen when exposed to UVA light. Staining with Hoechst 33342 and propidium iodide confirmed the results of MTT assays, with higher rates of apoptosis and necrosis observed in groups in which collagen was not added.

ACKNOWLEDGMENTS

Drs. Yara M. Michelacci Universidade Federal de São Paulo, department of Biochemistry, contributed to the conduct this research.

REFERENCES

1. Jester JV, Ho-Chang J. Modulation of cultured corneal keratocyte phenotype by growth factors/cytokines control in vitro contractility and extracellular matrix contraction. Exp Eye Res. 2003;77(5):581-92.
2. Kawakita T, Espana EM, He H, Smiddy R, Parel JM, Liu CY, Tseng SC. Preservation and expansion of the primate keratocyte phenotype by downregulating TGF-beta signaling in a low-calcium, serum-free medium. Invest Ophthalmol Vis Sci. 2006;47(5):1918-27. Erratum in: Invest Ophthalmol Vis Sci. 2006; 47(6):2279.
3. Michelacci YM. Collagens and proteoglycans of the corneal extracellular matrix. Braz J Med Biol Res. 2003;36(8):1037-46.
4. Jester JV, Barry-Lane PA, Cavanagh HD, Petroll WM. Induction of alpha-smooth muscle actin expression and myofibroblast transformation in cultured corneal keratocytes. Cornea. 1996;15(5):505-16.
5. Musselmann K, Alexandrou B, Kane B, Hassell JR. Maintenance of the keratocyte phenotype during cell proliferation stimulated by insulin. J Biol Chem. 2005;280(38): 32634-9.
6. Beales MP, Funderburgh JL, Jester JV, Hassell JR. Proteoglycan synthesis by bovine keratocytes and corneal fibroblasts: maintenance of the keratocyte phenotype in culture. Invest Ophthalmol Vis Sci. 1999;40(8):1658-63.
7. Agrawal VB. Corneal collagen cross-linking with riboflavin and ultraviolet a light for keratoconus: results in Indian eyes. Indian J Ophthalmol. 2009;57(2):111-4.
8. Jankov MR 2nd, Hafezi F, Beko M, Ignjatovic Z, Djurovic B, et al. [Corneal Cross-linking for the treatment of keratoconus: preliminary results]. Arq Bras Oftalmol. 2008;71(6):813-8 (in Portuguese).
9. Wollensak G, Spoerl E, Reber F, Seiler T. Keratocyte cytotoxicity of riboflavin/UVA-treatment in vitro. Eye (Lond). 2004;18(7):718-22.
10. Cho KS, Lee EH, Choi JS, Joo CK. Reactive oxygen species-induced apoptosis and necrosis in bovine corneal endothelial cells. Invest Ophthalmol Vis Sci. 1999;40(5):911-9.
11. Wilson SE, He YG, Weng J, Li Q, McDowall AW, Vital M, et al. Epithelial injury induces keratocyte apoptosis: hypothesized role for the interleukin-1 system in the modulation of corneal tissue organization and wound healing. Exp Eye Res. 1996;62(4):325-7.
12. Lakshman N, Kim A, Petroll WM. Characterization of corneal keratocyte morphology and mechanical activity within 3-D collagen matrices. Exp Eye Res. 2010;90(2):350-9.
13. Petroll WM, Ma L, Kim A, Ly L, Vishwanath M. Dynamic assessment of fibroblast mechanical activity during Rac-induced cell spreading in 3-D culture. J Cell Physiol. 2008; 217(1):162-71.
14. Bard JB, Hay ED. The behavior of fibroblasts from the developing avian cornea. Morphology and movement in situ and in vitro. J Cell Biol. 1975; 67(2PT.1):400-18.
15. Doyle AD, Wang FW, Matsumoto K, Yamada KM. One-dimensional topography underlies three-dimensional fibrillar cell migration. J Cell Biol. 2009; 184:481-90.
16. Kao WW, Liu CY. Roles of lumican and keratocan on corneal transparency. Glycoconj J. 2002;19(4-5):275-85.
17. Koumas L, King AE, Critchley HO, Kelly RW, Phipps RP. Fibroblast heterogeneity: existence of functionally distinct Thy 1(+) and Thy 1(-) human female reproductive tract fibroblasts. Am J Pathol. 2001;159(3):925-35.
18. Jester JV, Petroll WM, Cavanagh HD. Corneal stromal wound healing in refractive surgery: the role of myofibroblasts. Prog Retin Eye Res. 1999;18(3):311-56.
19. Jester JV, Petroll WM, Barry PA, Cavanagh HD. Expression of alpha-smooth muscle (alpha-SM) actin during corneal stromal wound healing. Invest Ophthalmol Vis Sci. 1995; 36(5):809-19.
20. Pei Y, Sherry DM, McDermott AM. Thy-1 distinguishes human corneal fibroblasts and myofibroblasts from keratocytes. Exp Eye Res. 2004;79(5):705-12.
21. Nicotera P, Leist M, Ferrando-May E. Apoptosis and necrosis: different execution of the same death. Biochem Soc Symp. 1999;66:69-73.
22. Maciorowski Z, Delic J, Padoy E, Klijanienko J, Dubray B, Cosset JM, et al. Comparative analysis of apoptosis measured by Hoechst 33342 and flow cytometry in non-Hodgkin's lymphomas. Cytometry. 1998;32(1):44-50.

Rothmund-Thomson syndrome and ocular surface findings: case reports and review of the literature

Síndrome de Rothmund-Thomson e achados da superfície ocular: casos clínicos e revisão da literatura

Ana Filipa Miranda[1], Maria Daniela Rivera-Monge[1], Charles Costa Farias[1,2]

ABSTRACT

Rothmund-Thomson syndrome (RTS) is a rare dermatosis with about 300 cases reported to date. The authors describe two siblings with RTS and inflammatory conjunctival disease featuring fornix shortening and symblepharon as well as palpebral disease with sparse eyelashes. These cases demonstrate RTS ocular surface findings different to those usually described.

Keywords: Rothmund-Thomson syndrome; Eye disease; Keratitis; Ectodermal dysplasia; Skin disease

RESUMO

A síndrome de Rothmund-Thomson (SRT) é uma dermatose rara com cerca de 300 casos reportados. Os autores descrevem dois irmãos com síndrome de Rothmund-Thomson e doença inflamatória conjuntival com encurtamento do fundo de saco e simbléfaro, assim como doença palpebral com escassez de cilíos. Ambos os casos demonstram achados da superfície ocular diferentes dos habitualmente descritos.

Descritores: *Síndrome de Rothmund-Thomson; Oftalmopatias hereditárias; Ceratite; Displasia ectodérmica; Dermatopatias*

INTRODUCTION

Rothmund-Thomson syndrome (RTS) is a rare dermatosis or a condition affecting the skin. Although its exact prevalence is unknown, about 300 cases have been reported to date[1]. Although its etiology is yet to be fully clarified, some patients show an autosomal recessive inheritance featuring a DNA damage repair defect and *RECQL4* gene mutations[2]. The diagnosis of RTS is established by clinical findings and the inability to identify a RECQL4 mutation does not rule out the diagnosis[2]. The first signs of RTS are dermatological in origin. The predominant signal is poikilodermatosis, which is a patch-like pigmentation usually developing between the age of 3 and 6 months as an erythema with swelling and blistering of the face[1]. Other clinical features may be present and may include congenital bone defects, short stature, sparse scalp hair, sparse or absent eyelashes and/or eyebrows, and dental abnormalities[1,3,4]. Ocular findings include not only cataracts but also microphthalmia, keratoconus, corneal scleralization, and pigment deposits on the cornea and conjunctiva[1,4,5]. Cataracts are reportedly bilateral, rapid in onset (usually at 2 to 3 months), and subcapsular[5,6]. Several types of malignancies have been described in RTS patients, of which osteosarcoma (OS) is the most common, followed in prevalence by squamous cell carcinoma and atypical meningioma[3]. Although some clinical signs suggest precocious aging, life expectancy is not impaired in RTS patients provided they do not develop cancer[7].

Case report 1

A 26-year-old man was diagnosed with RTS, with early-onset poikilodermatosis, sparse scalp hair, and dental abnormalities. He was the fifth child born to consanguineous parents after normal gestation and had an older sister and brother, both of whom were also diagnosed with RTS (Figure 1). The patient was presented to the Ophthalmology Department complaining of bilateral ocular hyperemia, photophobia, and itching for the last 12 years.

On ophthalmological examination, the patient had bilateral visual acuity of 20/20 and an intraocular pressure (IOP) of 13 and 15 mmHg, respectively. Slit-lamp examination showed bilateral bulbar and palpebral hyperemia, thickening and telangiectasia of the lid margins, inspissated orifices, secretion of the meibomian glands, and sparse inferior eyelashes, as shown in figure 2. A detailed examination of the conjunctiva revealed superior and inferior fornix foreshortening with superior and inferior symblepharon and upper lid entropion (Figure 2). Fluorescein staining showed inferior superficial keratitis. Tear break-up time (BUT) was reduced to 5 s, and reduced inferior conjunctival sac space precluded Schirmer's test. The remaining ophthalmological examination was unremarkable on both eyes.

Case report 2

The second case involved a 28-year-old woman who was also clinically diagnosed with RTS, with early-onset poikilodermatosis and sparse scalp hair (Figure 3). Five years prior to examination by the Ophthalmology Department, the patient underwent marginal rotation and lash electrolysis on her right eye; however, the symptoms persisted. She was referred for ocular hyperemia and a burning and foreign body sensation lasting for a total of 15 years.

On ophthalmological examination, the patient presented visual acuity of 20/20, and IOP was 15 mmHg on both eyes. Slit-lamp examination revealed bilateral sparse inferior eyelashes and trichiasis (Figure 4). A detailed examination of the conjunctiva led to the

Submitted for publication: July 15, 2015
Accepted for publication: October 1, 2015

[1] Cornea and External Disease Unit, Hospital de São Paulo, São Paulo, SP, Brazil.
[2] Ocular Surface Advanced Center (CASO), Department of Ophthalmology and Visual Sciences, Universidade Federal de São Paulo (UNIFESP), São Paulo, SP, Brazil.

Funding: No specific financial support was available for this study.

Disclosure of potential conflicts of interest: None of the authors have any potential conflict of interest to disclose.

Corresponding author: Charles Costa de Farias. Rua Botucatu, 820 - São Paulo, SP - 04023-062 - Brazil - E-mail: ccfarias7@gmail.com

http://dx.doi.org/10.5935/0004-2749.20160053

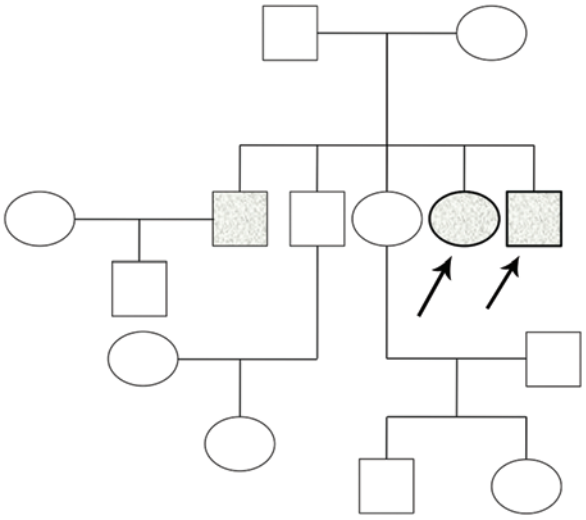

Figure 1. Family heredogram. Filled symbols represent affected individuals and unfilled symbols represent unaffected individuals; squares represent men, and circles represent women. Arrows represent the two cases.

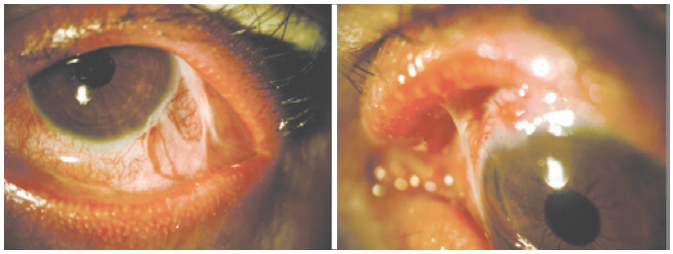

Figure 2. Case 1. Left eye showing bulbar and palpebral hyperemia, secretion in the meibomian glands, sparse inferior eyelashes, superior *(right)* and inferior (*left*) fornix foreshortening, and symblepharon.

Figure 3. Case 2. Photographs showing poikiloderma and sparse scalp hair.

demonstration of inferior symblepharon on the left eye (Figure 4). Inferior superficial keratitis was evident when fluorescein staining was performed. Tear BUT and Schirmer's tests were within the normal limits. The remaining ophthalmological examination was unremarkable on both eyes.

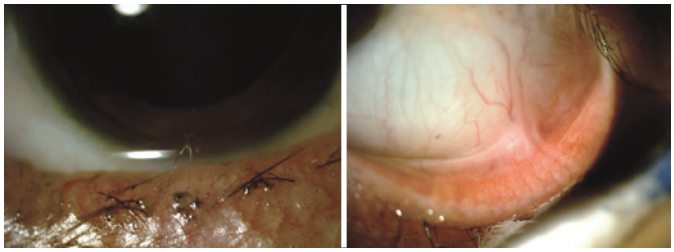

Figure 4. Case 2. Photographs showing sparse inferior eyelashes and inferior trichiasis *(left)* and inferior symblepharon *(right)*.

DISCUSSION

Previous reports have established bilateral cataracts, developing early in life, as the most common ocular lesion seen in RTS patients[3], the prevalence of which varies between 5% and 73%, depending on the study[5]. Absence or sparseness of eyelashes and eyebrows are also common in this syndrome[5]. Other, less common, ocular manifestations appear to include microphthalmia, lacrimal obliteration, keratoconus, corneal scleralization, pigment deposits on cornea and conjunctiva, coloboma atrophy in the iris and retina, chorioretinal atrophy, congenital glaucoma, and tilted optic discs[1,4,5,8].

This report presents two cases presenting with ocular surface findings uncharacteristic of RTS, including palpebral disease and conjunctival fibrotic process. The first case presented with meibomitis, shortening of both the superior and inferior fornix as well as superior and inferior symblepharon. The signs were evident on both eyes. In the second case, bilateral trichiasis as well as inferior symblepharon in the left eye were observed. In both patients, the ocular manifestations also included previously described sparseness of eyelashes.

The first patient was referred for long-term ocular symptoms probably associated with prolonged conjunctivitis, which could explain the fornix shortening, symblepharon, and upper eyelid fibrosis with entropion. Meibomian gland dysfunction may explain the inferior keratitis, which was supported by the reduced BUT. Schirmer's test would have been important for the evaluation of tear secretion but could not be performed in case 1.

The second patient was referred for symptoms that could be explained by trichiasis, resulting in keratitis. Prolonged conjunctivitis could have resulted in inferior symblepharon. Other ocular manifestations typically described in RTS patients, including cataracts, were absent in both patients.

For both patients, the cause of inflammation remains unknown. Cicatricial pemphigoid is a possibility because some patients with ocular disease do not develop oropharyngeal, other mucous membrane, or cutaneous disease. Referring to the patients' history, we were able to exclude Stevens-Johnson syndrome and chemical injury. Considering the heterogeneity of possible clinical findings in RTS and because the two patients described here are siblings, similar and unusual ocular manifestations may also be determined by genetic factors. Histologic evaluation could have been useful but was not performed because the surgery was postponed in both patients.

In conclusion, this case report shows different clinical aspects revealed through ocular examination in RTS patients. External surface disease, particularly inflammatory and fibrotic disease of the conjunctiva, should be taken into consideration in such patients to avoid potentially severe consequences.

REFERENCES

1. Canger EM, Celenk P, Devrim I, Avsar A. Oral findings of rothmund-thomson syndrome. Case Rep Dent. 2013;2013:935716.

2. Guerrero-González GA, Martínez-Cabriales SA, Hernández-Juárez AA, de Jesús Lugo-Trampe J, Espinoza-González NA, Gómez-Flores M, et al. Rothmund-thomson syndrome: a 13-year follow-up. Case Rep Dermatol. 2014;6(2):176-9.
3. Pencovich N, Margalit N, Constantini S. Atypical meningioma as a solitary malignancy in a patient with Rothmund-Thompson syndrome. Surg Neurol Int. 2012;3:148.
4. Manavi S, Mahajan VK. Rothmund-Thomson syndrome. Indian Dermatol Online J. 2014; 5(4):518-9.
5. Dollfus H, Porto F, Caussade P, Speeg-Schatz C, Sahel J, Grosshans E, et al. Ocular manifestations in the inherited DNA repair disorders. Surv Ophthalmol. 2003;48(1):107-22.
6. Cohen SY, Gaudric A, Lemerle S, Cadot M, Coscas G. [Rothmund's síndrome]. J Fr Ophtalmol. 1989;12(8-9):583-5. French.
7. Larizza L, Roversi G, Volpi L. Rothmund-Thomson syndrome. Orphanet J Rare Dis. 2010;5:2.
8. Mak RK, Griffiths WA, Mellerio JE. An unusual patient with Rothmund-Thomson syndrome, porokeratosis and bilateral iris dysgenesis. Clin Exp Dermatol. 2006;31(3):401-3.

Combined branch retinal vein and artery occlusion in toxoplasmosis

Oclusão combinada de ramo arterial e venoso retinianos em toxoplasmose

Fabio Bom Aggio[1], Fernando José de Novelli[1], Evandro Luis Rosa[1], Mário Junqueira Nobrega[1]

ABSTRACT

A 22-year-old man complained of low visual acuity and pain in his left eye for five days. His ophthalmological examination revealed 2+ anterior chamber reaction and a white, poorly defined retinal lesion at the proximal portion of the inferotemporal vascular arcade. There were retinal hemorrhages in the inferotemporal region extending to the retinal periphery. In addition, venous dilation, increased tortuosity, and ischemic retinal whitening along the inferotemporal vascular arcade were also observed. A proper systemic work-up was performed, and the patient was diagnosed with ocular toxoplasmosis. He was treated with an anti-toxoplasma medication, and his condition slowly improved. Inferior macular inner and middle retinal atrophy could be observed on optical coherence tomography as a sequela of ischemic injury. To our knowledge, this is the first report of combined retinal branch vein and artery occlusion in toxoplasmosis resulting in a striking and unusual macular appearance.

Keywords: Ocular toxoplasmosis; Uveitis; Retinal artery occlusion; Retinal vessels; Visual acuity; Optical coherence tomography; Vision disorders

RESUMO

Um paciente do sexo masculino, com 22 anos de idade, queixou-se de redução da acuidade visual no olho esquerdo por 5 dias. O exame oftalmológico mostrou reação de câmara anterior 2+ e uma lesão retiniana esbranquiçada, pouco definida, na porção proximal da arcada vascular temporal inferior. Foram observadas hemorragias retinianas na região temporal inferior estendendo-se à periferia, assim como ingurgitamento venoso, aumento da tortuosidade e palidez isquêmica da retina no mesmo quadrante. Exames laboratoriais corroboraram o diagnóstico de toxoplasmose ocular. O paciente melhorou lentamente após tratamento apropriado. Foi evidenciada atrofia da retina macular inferior interna e média à tomografia de coerência óptica, como sequela da isquemia retiniana. Para nosso conhecimento, este é o primeiro relato de oclusão retiniana combinada de ramo arterial e venoso em toxoplasmose ocular, levando a um aspecto fundoscópico atípico e peculiar.

Descritores: *Toxoplasmose ocular; Uveítes; Oclusão da artéria retiniana; Vasos retinianos; Acuidade Visual; Tomografia de coerência óptica; Transtornos da visão*

INTRODUCTION

Toxoplasmosis is the leading cause of infectious posterior uveitis worldwide, accounting for 80% of the cases in some regions[1]. Although toxoplasmic retinochoroiditis usually has a self-limiting course, it can lead to an irreversible visual loss, particularly when the macula and optic nerve head are involved. Vascular involvement typically consists of diffuse or segmental sheathing produced by antigen-antibody complex deposition in the vessel wall, as well as by localized mononuclear cell infiltrates[1]. Retinal vein occlusion may occur, but artery obstruction is rare[2-4]. We herein report an atypical presentation of toxoplasmic retinochoroiditis characterized by the occurrence of combined branch retinal vein and artery occlusion.

CASE REPORT

A 22-year-old healthy man complained of low visual acuity and pain in his left eye [oculus sinister (OS)] for five days. His past ocular and family history were unremarkable. Best-corrected visual acuity (BCVA) was 20/20 in the right eye [oculus dexter (OD)] and 20/400 in the left eye (OS). His anterior segment examination was normal OD and revealed 2+ anterior chamber reaction OS. Intraocular pressure by applanation tonometry was 10 mmHg in both eyes at 08:00. Funduscopy showed a normal OD and a white, poorly demarcated, and slightly elevated retinal lesion at the proximal portion of the inferotemporal vascular arcade OS. There were retinal hemorrhages in the inferotemporal region extending to the periphery with venous dilation and increased tortuosity, as well as ischemic retinal whitening along the inferotemporal vascular arcade, 2+ vitreous cells, and diffuse periphlebitis. The striking macular appearance was reminiscent of viral retinitis, given its necrotic and hemorrhagic features (Figure 1).

Blood tests revealed normal leukocyte and erythrocyte counts and erythrocyte sedimentation rates. Serological tests for human immunodeficiency virus (HIV) and syphilis (venereal disease research laboratory and fluorescent treponemal antibody absorption tests) were negative. Chest X-ray films were normal. Toxoplasma immunoglobulin (Ig) G antibodies were positive in an enzyme-linked immunosorbent assay (132 IU/mL), whereas anti-toxoplasma IgM antibodies were negative.

Two days after initial presentation, the patient was started on pyrimethamine at 50 mg daily, sulfadiazine at 2 g daily, folinic acid at 15 mg three times a week, prednisone at 60 mg daily, in a tapering schedule, as well as topical prednisolone acetate 1% and tropicamide 1%. Five days later, BCVA was maintained, and the ophthalmologic examination did not reveal any changes. Three weeks later, BCVA was 20/150 OS. His anterior segment examination was unchanged OD and showed 1+ anterior chamber reaction OS. Intraocular pressure was 16 mmHg OD and 14 mmHg OS. Funduscopy was unchanged OD and showed a well-demarcated, whitish inferotemporal retinochoroidal lesion. There was sheathing of the inferotemporal retinal artery, mild juxtafoveal inferior retinal whitening, a macular star, and 1+ vitreous cells (Figure 2, left). Six weeks after the beginning of treatment, BCVA was 20/30 OS. There was no anterior chamber or vitreous cells. The inferotemporal retinochoroidal lesion showed signs of scarring (Figure 2, middle). Oral medication was discontinued, and the prednisolone acetate 1% drops were tapered.

Three months after the initial presentation, BCVA was 20/30 OS. His anterior segment examination revealed no changes. The intraocular pressure was 16 mmHg OD and 15 mmHg OS. Funduscopy showed an inferotemporal retinochoroidal scar and partial resolution

Submitted for publication: April 1, 2015
Accepted for publication: June 18, 2015

[1] Hospital de Olhos Sadalla Amin Ghanem, Joinville, SC, Brazil.

Funding: No specific financial support was available for this study.

Disclosure of potential conflicts of interest: None of the authors have any potential conflict of interest to disclose.

Corresponding author: Fabio Bom Aggio. Rua Camboriú, 35 - Joinville - SC - 89216-222 - Brazil - E-mail: fabioaggio@me.com

of the macular star (Figure 2, right). Fluorescein angiography revealed focal hypofluorescence with surrounding early hyperfluorescence corresponding to the inferotemporal scar and blocked hypofluorescence corresponding to the retinal hemorrhages. No areas of non-perfusion were detected (Figure 3). Optical coherence tomography showed signs of partial posterior hyaloid detachment, inferior macular inner and middle retinal atrophy, hyperreflective intraretinal dots superior to the fovea corresponding to the hard exudates, as well as a mild foveal discontinuity of the outer retina and pigment epithelium layer (Figure 4).

DISCUSSION

The diagnosis of ocular toxoplasmosis is usually straightforward; however, challenging cases may occur. In the case presented here, vascular occlusion of the inferotemporal retinal artery and vein led to unusual fundus findings characterized by ischemic retinal whitening and numerous scattered retinal hemorrhages obscuring the boundaries of the focal inflammatory lesion. The appearance of the fundus resembled viral retinitis. Considering the high prevalence of toxoplasmosis in Brazil[5], the health status of the patient, and absence of peripheral retinitis, toxoplasmosis was strongly suspected. An anti-toxoplasma medication was introduced, and the patient was closely followed.

Ocular toxoplasmosis begins in the superficial retina. As retinitis progresses, the involvement of full-thickness retina, adjacent choroid, vitreous, and even sclera may occur. The initial lesion with ill-defined margins due to retinal edema tends to become more defined with treatment. After a variable time period, pigmentation mainly occurs in the lesion margins[1]. These findings were observed in our case.

Vascular changes in toxoplasmosis typically involve veins, but arteries may also be affected, particularly in the form of Kyrieleis arteritis[1], characterized by nodular periarterial plaques that were observed in our case (Figure 2). Although classically described in toxoplasmosis, Kyrieleis arteritis may occur in syphilis, rickettsial retinal vasculitis, acute retinal necrosis, and other diseases. Its presence should raise suspicion of an infectious cause of retinal vasculitis[1].

Branch artery occlusion may result from direct artery compression by retinochoroiditis or by arteriolar contraction associated with increased viscosity of blood and inhibition of coagulation due to heparin release from mast cells as a response to acute inflammatory stimuli. It may also be a consequence of perivasculitis, which may cause thickening of the vessel wall, disruption of blood flow, and thrombosis[6]. Yu et al.[7] identified the following three patterns of retinal capillary ischemia using optical coherence tomography in arterial occlusive disease in the acute phase: (1) thickening and hyperreflectivity of the inner retinal layers owing to ischemia of the superficial capillary plexus, (2) hyperreflective band at the level of the inner nuclear layer represen-

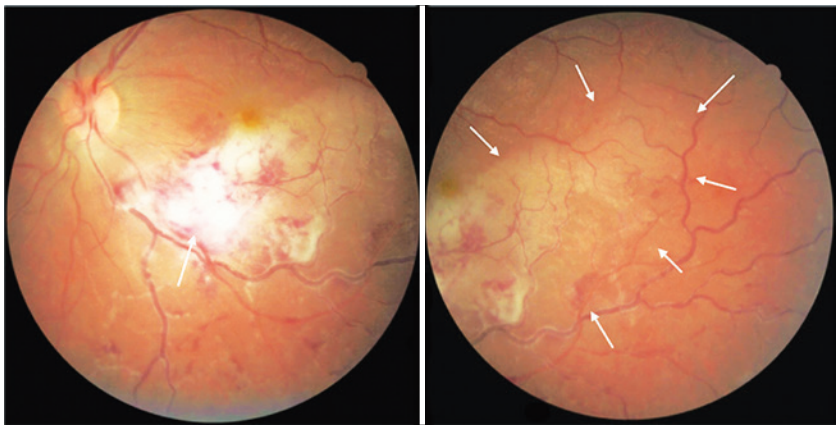

Figure 1. Initial presentation: Fundus photography of the left eye showing a white, poorly demarcated, and slightly elevated retinal lesion at the proximal portion of the inferotemporal vascular arcade (arrow, left). There were retinal hemorrhages in the inferotemporal region extending to the periphery with venous dilation and increased tortuosity, as well as ischemic retinal whitening along the inferotemporal vascular arcade (arrows, right), 2+ vitreous cells, and diffuse periphlebitis.

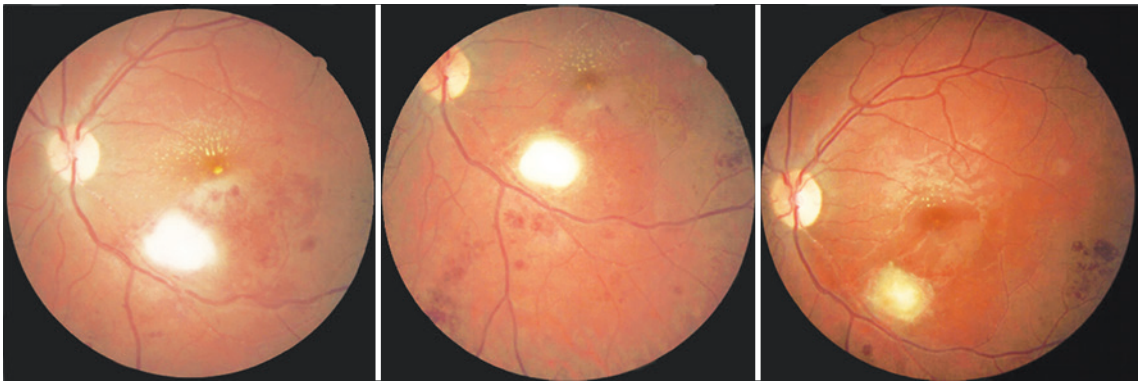

Figure 2. Fundus photography of the left eye at three weeks (left), six weeks (middle), and three months (right) after the beginning of treatment showing progressive improvement of the inferotemporal retinochoroidal lesion with complete scarring at the time of the last visit. A macular star is observed, as well as sheathing of the inferotemporal artery and numerous scattered hemorrhages. Periarterial plaques known as Kyrieleis arteritis can also be noted alongside the inferotemporal artery.

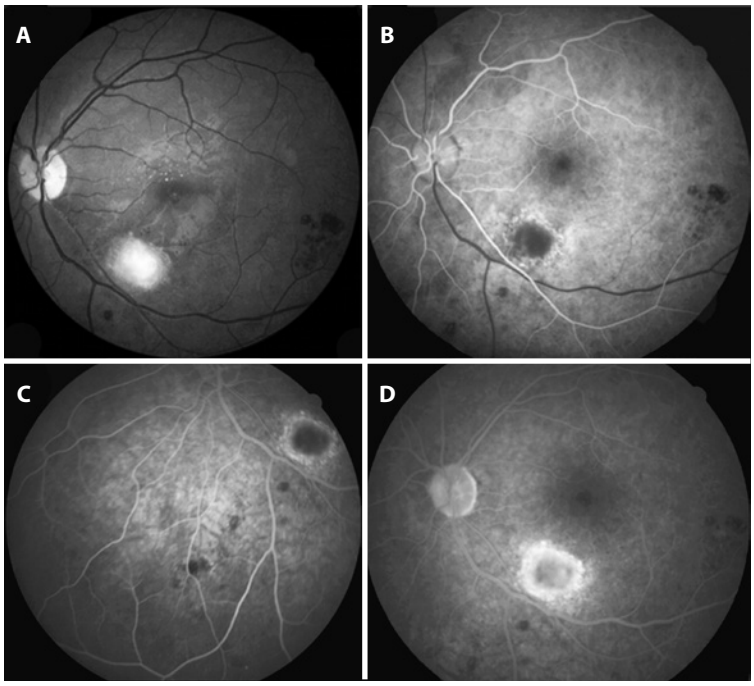

Figure 3. Fluorescein angiography (FA) frames of the left eye three months after the beginning of treatment. (A) Red-free fundus photography. (B) Early FA frame disclosing hypofluorescence corresponding to the inferotemporal lesion surrounded by early hyperfluorescence. (C) Intermediate FA frame of the inferior region. No areas of non-perfusion are observed. (D) Late FA frame showing no leakage at the macular region. Blocked hypofluorescence is seen corresponding to the scattered retinal hemorrhages.

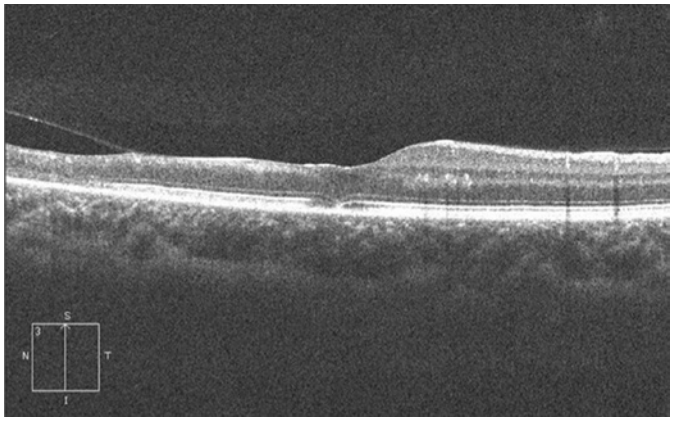

Figure 4. Vertical cross-sectional optical coherence tomography image of the left eye showing signs of partial posterior hyaloid detachment, inferior macular inner and middle retinal atrophy, hyperreflective intraretinal dots superior to the fovea, as well as mild foveal discontinuity of the outer retina and pigment epithelium layer.

ting ischemia of the intermediate and deep capillary plexuses, and (3) diffuse thickening and hyperreflectivity of the inner and middle retinal layers representing both superficial and deep capillary ischemia. In the chronic phase, thinning and atrophy of the affected retinal layers were seen. In our case, optical coherence tomography in the chronic phase revealed inner and middle inferior retinal macular atrophy, consistent with both superficial and deep capillary ischemia.

Atypical forms of ocular toxoplasmosis include punctate outer retinal toxoplasmosis, neuroretinitis, neuritis, pseudomultifocal retinochoroiditis, multifocal retinochoroiditis, peripheral lesions, and anterior uveitis[1]. Atypical presentations have been reported in patients with HIV infection, iatrogenic immunosuppression, or advanced age[8]. Moshfeghi et al. reported findings on 25 eyes with widespread retinochoroiditis mimicking acute retinal necrosis[8]. In their cases, lesions were atypical, large, multifocal, bilateral, or associated with diffuse retinal involvement or panophthalmitis. The diagnosis of toxoplasmosis was confirmed by the response to anti-toxoplasmosis medications, intraocular diagnostic studies such as polymerase chain reaction, intraocular antibody analysis, ocular fluid culture, or histopathological examination identifying *Toxoplasma gondii* in necrotic retinal tissue.

In conclusion, we report an uncommon presentation of toxoplasmosis, characterized by combined branch artery and vein occlusion, resulting in ischemic retinal whitening and numerous scattered retinal hemorrhages in the inferotemporal region along with a poorly defined proximal whitish retinal lesion. The possibility of toxoplasmosis in cases presenting with these features must be considered because prompt treatment may prevent a poor visual outcome.

REFERENCES

1. Oréfice F, Vasconcelos-Santos DV, Cordeiro CA, Oréfice JL, Costa RA. Toxoplasmosis. In: Foster CS, Vitale AT. Diagnosis and treatment of uveitis. New Delhi, India: Jaypee - Highlights; 2013. p.543-68.
2. Williamson TH, Meyer PA. Branch retinal artery occlusion in toxoplasma retinochoroiditis. Br J Ophthalmol. 1991;75(4):253.
3. Chiang E, Goldstein DA, Shapiro MJ, Mets MB. Branch retinal artery occlusion caused by toxoplasmosis in an adolescent. Case Rep Ophthalmol. 2012;3(3):333-8.
4. Arai H, Sakai T, Okano K, Aoyagi R, Imai A, Takase H, et al. Presumed toxoplasmic central retinal artery occlusion and multifocal retinitis with perivascular sheathing. Clin Ophthalmol. 2014;8:789-92.
5. Dubey JP, Lago EG, Gennari SM, Jones JL. Toxoplasmosis in humans and animals in Brazil: high prevalence, high burden of the disease, and epidemiology. Parasitology. 2012;139(11):1375-424.
6. Kahloun R, Mbarek S, Khairallah-Ksiaa I, Jelliti B, Yahia SB, Khairallah M. Branch retinal artery occlusion associated with posterior uveitis. J Ophthalmic Inflamm Infect. 2013;3(1):16.
7. Yu S, Pang CE, Gong Y, Freund KB, Yannuzzi LA, Rahimy E, et al. The spectrum of superficial and deep capillary ischemia in retinal artery occlusion. Am J Ophthalmol. 2015; 159(1):53-63.
8. Moshfeghi DM, Dodds EM, Couto CA, Santos CI, Nicholson DH, Lowder CY, et al. Diagnostic approaches to severe, atypical toxoplasmosis mimicking acute retinal necrosis. Ophthalmology. 2004;111(4):716-25.

DRESS syndrome in ophthalmic patients

Síndrome DRESS em pacientes oftalmológicos

Jacqueline Martins de Sousa[1], Heloisa Nascimento[1], Rubens Belfort Junior[1]

ABSTRACT

Drug reaction with eosinophilia and systemic symptoms (DRESS) syndrome is a rare and potentially fatal adverse drug reaction associated with skin rash, fever, eosinophilia, and multiple organ injury. A number of pharmacological agents are known to cause DRESS syndrome such as allopurinol, anticonvulsants, vancomycin, trimethoprime-sulfamethoxazole, and pyrimethamine-sulfadiazine. Here, we describe two patients who developed DRESS syndrome during ocular treatment. The first case was being treated for late postoperative endophthalmitis with topical antibiotics, intravenous cephalothin, meropenem, and intravitreal injection of vancomycin and ceftazidime before symptoms developed. We were unable to identify the causal drug owing to the large number of medications concurrently administered. The second case presented with DRESS syndrome symptoms during ocular toxoplasmosis treatment. In this case, a clearer association with pyrimethamine-sulfadiazine was observed. As a result of the regular prescription of pharmacological agents associated with DRESS syndrome, ophthalmologists should be aware of the potentially serious complications of DRESS syndrome.

Keywords: Eosinophilia/chemically induced; Drug eruptions; Syndrome; Drug-related side effects and adverse reactions/complications; Drug hypersensitivity

RESUMO

*Síndrome DRESS (*drug reaction with eosinophilia and systemic symptoms*) é uma reação adversa a medicamentos rara e potencialmente fatal, associada à* rash *cutâneo, febre, eosinofilia e lesão de múltiplos órgãos. Algumas drogas podem desencadeá-la, como: alopurinol, anticonvulsivantes, vancomicina, sulfametoxazol-trimetoprim, sulfadiazina-pirimetamina, entre outras. Descrevemos dois casos que desenvolverem DRESS síndrome durante tratamento ocular. O primeiro caso apresentou os sintomas durante tratamento para endoftalmite pós-operatória tardia com antibióticos tópicos, cefalotina e meropenem intravenosos e injeção intravítrea de vancomicina e ceftazidima; não podemos identificar a droga causadora, pois múltiplas medicações foram utilizadas. O segundo caso desenvolveu os sintomas durante tratamento clássico para toxoplasmose ocular, então a associação com sulfadiazina-pirimetamina foi mais clara. Como muitos oftalmologistas prescrevem regularmente drogas que podem desencadear a síndrome DRESS, esse diagnóstico deve ser lembrado já que pode levar a sérias complicações.*

Descritores: *Eosinofilia/quimicamente inducida; Erupção por droga; Síndrome; Efeitos colaterais e reações adversas relacionados a medicamentos; Hipersensibilidade a drogas*

INTRODUCTION

Drug reaction with eosinophilic and systemic symptoms (DRESS) syndrome is an adverse drug reaction characterized by generalized skin rash, enlarged lymph nodes, and fever. Laboratory testing typically demonstrates eosinophilia, atypical lymphocytes, and multiple organ injury[1-5]. The incidence of DRESS syndrome is reportedly 1 in 1,000-10,000 prescriptions of each causal drug, and symptoms may appear within 8 weeks after the first use[2-6]. Herein, we report two cases of DRESS syndrome in patients who developed during ocular treatment.

Case 1

A 65-year-old man presented with pain, redness, tearing, and decreased vision in his left eye (OS) for 10 days and fever for 1 day. His medical history included hypertension, diabetes, and dyslipidemia. The patient had undergone phacoemulsification with intraocular lens implantation complicated with posterior capsule rupture in OS 2 months prior to this evaluation. His best corrected visual acuity (VA) was 20/25 in the right eye (OD) and light perception in OS. Anterior biomicroscopy was normal in OD. Conjunctival hyperemia 3+/4, a corneal ulcer with stromal infiltrate, hypopyon, and vitritis 4+/4 were observed in OS. Fundoscopy was normal in OD and impossible in OS. The patient was hospitalized, and empirical intravenous (IV) cephalothin, topical moxifloxacin 0.5%, and atropine 1% in OS were initiated. Further, intravitreal injection of vancomycin and ceftazidime was performed in OS. Corneal scrap cultures were positive for *Enterobacter aerogenes* sensitive to carbapenems. IV meropenem was added to the antibiotic regimen, and the patient improved after 4 days of treatment.

During hospitalization, he developed severe systemic hypertension and eosinophilia (1,417 eosinophils per microliter of blood; 15.5% leukocytes) and a macular rash involving the neck, chest, abdomen, and arms (Figure 1). Skin biopsy demonstrated urticarial dermatitis. Despite treatment, the skin lesions worsened, and the patient developed fever, tachypnea, tachycardia, hypotension, generalized tremors, and disorientation. Laboratory testing demonstrated leukopenia, elevated hepatic enzymes, and hyponatremia. He was first diagnosed as having bacterial sepsis. Treatment was expanded with IV polymyxin B and vancomycin. However, fever and hypotension persisted with worsening of skin lesions, reduced urinary output, increased serum creatinine levels, and eosinophilia. Blood and urine

Submitted for publication: April 27, 2015
Accepted publication: October 1, 2015

[1] Department of Ophthalmology and Visual Sciences, Universidade Federal de São Paulo (UNIFESP), São Paulo, SP, Brazil.

Funding: No specific financial support was available for this study.

Disclosure of potential conflicts of interest: None of the authors have any potential conflicts of interest to disclose.

Corresponding author: Jacqueline M. Sousa. Rua Botucatu, 821 - São Paulo, SP - 04023-062 - Brazil E-mail: jacmsousa@gmail.com

http://dx.doi.org/10.5935/0004-2749.20160055

cultures were negative. DRESS syndrome was diagnosed, and the patient i.v. prednisone 1 mg/kg/day was initiated. After 4 days in the intensive care unit (ICU), the patient was hemodynamically stabilized with clinical improvement. VA in OS remained light perception due to the complications of serious endophthalmitis.

Case 2

A 54-year-old woman complained of low VA in OS for 2 days associated with sudden onset of ocular pain and a paracentral dark spot affecting the visual field in OD. The patient had myalgia, fever, and lymphadenopathy. Medical, family, and ocular histories were unremarkable. VA was 20/20 in OD and 20/400 in OS. Anterior biomicroscopy and intraocular pressures were normal in both eyes. Fundoscopy of OD was normal and OS demonstrated vitritis 2+/4+ and a yellowish exudative plaque at the posterior pole affecting the fovea. Serology test was positive for toxoplasmosis IgM only. Treatment was initiated with topical prednisolone acetate 1%, topical tropicamide 1%, systemic pyrimethamine 50 mg/day, sulfadiazine 4 mg/day, folinic acid 5 mg/day, and oral prednisone 1 mg/kg/day. Symptoms and ocular signs improved with treatment.

After 1 month, the patient developed a macular morbilliform rash affecting the chest, abdomen, and back (Figure 2). She also developed eosinophilia and persistent lymphadenopathy. DRESS syndrome was diagnosed, and the patient was admitted to ICU and treated with oral pyrimethamine, folinic acid, azithromycin, and i.v. prednisolone 1 mg/kg/day. The patient was discharged after improvement in systemic symptoms with a VA of 20/50 in OS due to a chorioretinitis scar adjacent to the fovea.

DISCUSSION

DRESS syndrome is a severe drug reaction that typically develops between 2 and 8 weeks after drug exposure with symptoms persisting for longer than 2 weeks[2-4]. Diagnostic criteria include widespread rash, fever, and laboratory abnormalities (eosinophilia >1,500/mm^3 or atypical lymphocytes)[1-7]. Systemic involvement affecting the liver (50%), kidneys (10%), lungs (10%), heart, pancreas, and others may also be observed with laboratory testing revealing specific organ damage[2-4]. Histological examinations of skin biopsy are nonspecific, for DRESS syndrome but may be important in ruling out other etiologies[4]. Differential diagnoses of DRESS syndrome include infections, Stevens Johnson syndrome, connective tissue diseases, and hematological diseases[2,6,8].

Several drugs have been reported to cause DRESS syndrome, including allopurinol, anticonvulsants (phenobarbital, carbamazepine, phenytoin, lamotrigine, and sodium valproate), vancomycin, minocycline, trimethoprime-sulfamethoxazole, pyrimethamine-sulfadia-

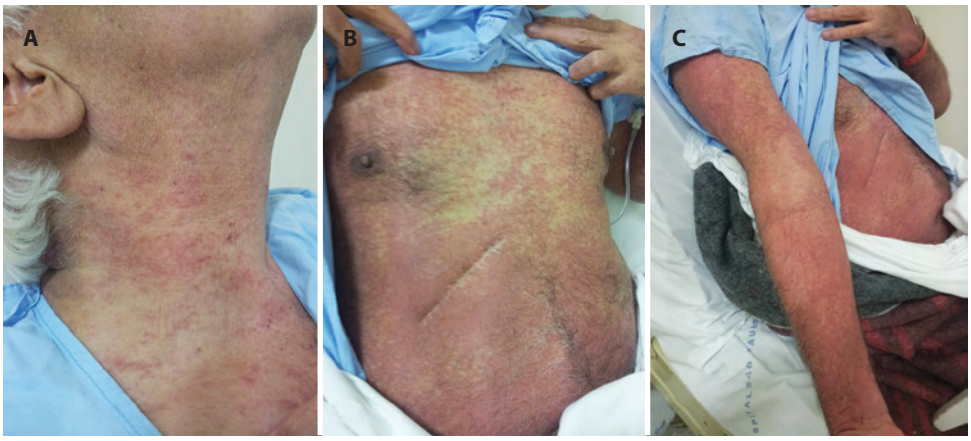

Figure 1. Macular morbilliform rash involving the neck (A), chest, abdomen (B), and arms (C).

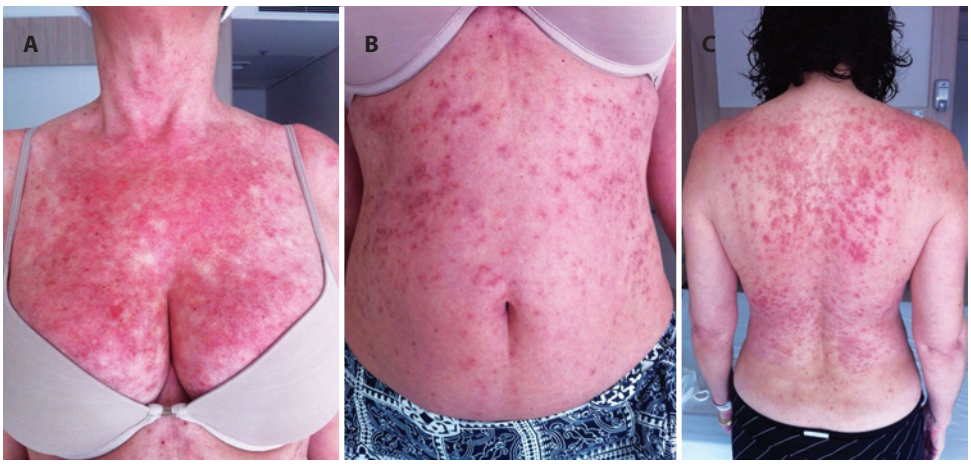

Figure 2. Patient with macular morbilliform rash involving the chest (A), abdomen (B), and back (C).

zine, proton pump inhibitors, azathioprine, and hydroxychloroquine, among others[2-5]. Amoxicillin has been variously described either as a cause or as an aggravating factor of DRESS syndrome[2]. In our first case, DRESS syndrome may have been triggered by i.v. cephatotin, i.v. meropenem, or intravitreal injection of vancomicin or ceftazidime. As vancomycin is one of the medications most commonly associated with DRESS syndrome, it is possible that DRESS syndrome was triggered by intravitreal injection of this drug. To our knowledge, there are no previously reported cases of DRESS syndrome associated with intravitreous injection of antibiotics. In our second case, the association between DRESS syndrome and sulfadiazine was more evident and easier to identify. The pathogenesis of DRESS syndrome has yet to be elucidated; however, a number of authors have reported associations with specific HLA groups and herpes virus reactivation[2-5,8].

As prospective randomized trials for DRESS syndrome treatment have yet to be reported, data regarding the management of DRESS syndrome have exclusively been provided by case and series reports. Ideally, patients with DRESS syndrome are treated in ICU, causal drugs must be discontinued, and systemic involvement should be treated specifically[2,9]. The majority of authors recommend systemic glucocorticoid administration (1 mg/kg/d) until the disease is controlled before slowly tapering the dose[2,9]. Cutaneous rash may persist for weeks and return if corticosteroids are quickly discontinued or if there is new exposure to the causative drug. The prognosis of DRESS syndrome is associated with early recognition and discontinuation of the offending drug. Due to the severity and multiplicity of systemic involvement, DRESS syndrome has a high morbidity and mortality reaching 10%-40%[2,3,9]. The patient must be informed of the lifetime contraindication to the use of the causal drug and increased risk of developing autoimmune diseases (thyroiditis, adrenal insufficiency, diabetes insipidus, connective tissue disease, or a reaction resembling graft-versus-host disease)[2,10].

DRESS syndrome is a rare but potentially fatal complication related to an adverse reaction to one of several potentially causative medications. Many of these pharmacological agents are routinely used in ophthalmic practice, such as trimethoprim-sulfamethoxazole and vancomycin. Herein, we report two cases of DRESS syndrome associated with ocular treatment. Thus, ophthalmologists should be aware of DRESS syndrome and be able to recognize the initial signs of this condition. Treatment of DRESS syndrome requires hospitalization and intensive care follow-up.

REFERENCES

1. Shiohara T, Iijima M, Ikezawa Z, Hashimoto K. The diagnosis of a DRESS syndrome has been sufficiently established on the basis of typical clinical features and viral reactivations. Br J Dermatol. 2007;156(5):1083-4. Comment in: Br J Dermatol. 2006;155(2): 422-8.
2. Descamps V, Ranfer-Rogez S. DRESS syndrome. Joint Bone Spine. 2014;81(1):15-21.
3. Cacoub P, Musette P, Descamps V, Meyer O, Speirs C, Finzi L, et al. The DRESS syndrome: a literature review. Am J Med. 2011;124(7):588-97. Comment in: Am J Med. 2012; 125(7):e9-10.
4. Husain Z, Reddy BY, Schwartz RA. DRESS syndrome: Part I. Clinical perspectives. J Am Acad Dermatol. 2013;68(5): 693.e1-14. Comment in: J Am Acad Dermatol. 2013; 69(6):1057. J Am Acad Dermatol. 2013;69(6):1056-7. J Am Acad Dermatol. 2013;69(6): 1057-8.
5. Walss SA, Creamer D. Drug reaction with eosinophilia and systemic symptoms (DRESS): a clinical uptade and review of current thinking. Clin Exp Dermatol. 2011;36(1):6-11.
6. Jeung YJ, Lee JY, Oh MJ, Choi DC, Lee BJ. Comparison of the causes and clinical features of drug rach with eosinophilia and systemic symptoms and Stevens-Johnson syndrome. Allergy Asthma Immunol Res. 2010;2(2):123-6.
7. Eshki M, Allanore L, Musette P, Milpied B, Grange A, Guillaume JC, et al. Twelve-year analysis of severe cases of drug reaction with eosinophilia and systemic symptoms: a cause of unpredictable multiorgan failure. Arch Dermatol. 2009;145(1):67-72.
8. Camous X, Calbo S, Picard D, Musette P. Drug reaction with eosinophilia and systemic symptoms: an update on pathogenesis. Curr Opin Immunol. 2012;24(6):730-5.
9. Husain Z, Reddy BY, Schwartz RA. DRESS syndrome: Part II. Management and therapeutics. J Am Acad Dermatol. 2013;68(5):709.e1-9.
10. Ushigome Y, Kano Y, Ishida T, et al. Short- and long-term outcomes of 34 patients with drug-induced hypersensitivity syndrome in a single institution. J Am Acad Dermatol. 2012.

Keratoacanthoma of the conjunctiva in a young patient

Ceratoacantoma da conjuntiva em um paciente jovem

Gokhan Ozge[1], Yusuf Uysal[1], Osman Melih Ceylan[2], Onder Onguru[3], Fatih Mehmet Mutlu[1]

ABSTRACT

Keratoacanthomas rarely occur in the conjunctiva. We report a case of a 24-year-old man with a rapidly growing conjunctival mass. The tumor was excised with a safety margin to exclude squamous cell carcinoma and was histopathologically diagnosed as a keratoacanthoma. There has been no recurrence over 2 years of follow-up. To the best of our knowledge, he is the youngest patient to be diagnosed with conjunctival keratoacanthoma who had no known risk factors such as skin disorders, trauma, surgery, or infection. In similar cases, we recommend complete early surgical excision and careful follow-up to exclude malignancy.

Keywords: Keratoacanthoma/diagnosis; Keratoacanthoma/surgery; Carcinoma squamous cell; Diagnosis, differential; Case reports

RESUMO

Ceratoacantoma raramente ocorre na conjuntiva. Nós relatamos o caso de um homem de 24 anos de idade, com uma massa conjuntival de rápido crescimento. O tumor foi retirado com uma margem de segurança para excluir carcinoma de células escamosas. Ele foi diagnosticado histopatologicamente como sendo ceratoacantoma. Não houve recidiva em dois anos de seguimento. Ele é o paciente mais jovem com ceratoacantoma conjuntival que não tinham fatores de risco conhecidos como doenças de pele a ser descrito. Em casos semelhantes, recomendamos excisão cirúrgica precoce completo e um acompanhamento cuidadoso para excluir malignidade.

Descritores: *Ceratoacantoma/diagnóstico; Ceratoacantoma/cirurgia; Carcinoma de células escamosas; Diagnóstico diferencial; Relatos de casos*

INTRODUCTİON

Keratoacanthomas (KAs) are common low-grade tumors that originate in the pilosebaceous glands of hair follicles[1] and are considered to be a form of squamous cell carcinoma (SCC)[1]. Pathologists often label KAs as "well-differentiated squamous cell carcinoma, keratoacanthoma variant," because approximately 6% of KAs manifest as SCC when left untreated[2]. KAs are characterized by rapid growth over a few weeks, followed by spontaneous regression over 4-6 months.

KAs are commonly found on sun-exposed areas, such as the face, neck, and dorsum of the upper extremities[3]; however, KA of the conjunctiva is rare. We report here a case of conjunctival KA that was surgically treated in a young patient.

CASE REPORT

A 23-year-old man presented with a 3-month history of redness, foreign body sensation, and conjunctival mass that grew rapidly in his left eye. His visual acuity was 20/20 and fundoscopic exam was normal in both eyes. In the left eye, a white, nodular mass was noted on the nasal conjunctiva adjacent to the limbus. The conjunctival mass was 4 × 5 mm in size, had a hyperkeratotic surface, and was surrounded by dilated vessels (Figure 1). No palpable lymphadenopathy was observed. The patient had no history of injury, previous ophthalmic surgery, or human papilloma virus infection, and was human ımmunodeficiency virus (HIV) negative.

The lesion was totally excised under local anesthesia, and cryotherapy was applied to the surgical margins. Subsequent histopathologic examination under low-power microscopy showed that the tumoral lesion had overhanging edges and a hemispheric-like shape without a keratin plug. The lesion was composed of deeply elongated, enlarged, and merged solid islands of large, pale squamous cells with little keratinization (Figure 2 A). The squamous cells showed moderate to marked atypia, and mitotic figures were easily found (Figure 2 B). Additionally, mild inflammatory cell infiltration was observed. From these findings, conjunctival KA was diagnosed. The resected site on the conjunctiva healed well without complications. No recurrence was detected over 2 years of follow-up.

DİSCUSSİON

KAs are commonly found on sun-exposed areas of the skin. The first case of conjunctival KA was described by Freeman et al.[4], and only a few cases have been described to date[5-7]. Most of the documented cases have been found on the temporal bulbar conjunctiva within the palpebral aperture and adjacent to the limbus. However, in our patient, the KA formed on the nasal conjunctiva, which was similar to cases reported by Perdigao et al.[6] and Chowdhury et al.[8]. A male predominance was observed in previously reported cases, and our patient was also male.

Cutaneous KAs are characterized by an initial period of rapid growth followed by spontaneous regression, usually within 6 months. However, the natural history of conjunctival KA is unclear because of timely resection. In addition, our patient's symptoms, including foreign body sensation, redness, and the rapidly growing mass had been ongoing for 3 months, and early surgery was performed in order differential diagnose with SCC.

Submitted for publication: February 19, 2015
Accepted for publication: July 21, 2015

[1] Department of Ophthalmology, Gulhane Military Medical Academy and Faculty of Medicine, Ankara, Turkey.
[2] Department of Ophthalmology, Medicalpark Hospital, Ankara, Turkey.
[3] Department of pathology, Gulhane Military Medical Academy and Faculty of Medicine, Ankara, Turkey.

Funding: No specific financial support was available for this study.

Disclosure of potential conflicts of interest: None of the authors have any potential conflict of interest to disclose.

Corresponding author: Gokhan Ozge. Department of Ophthalmology - Gulhane Military Medical School - Ankara, Turkey, 06010 - E-mail: dr_gozge@yahoo.com

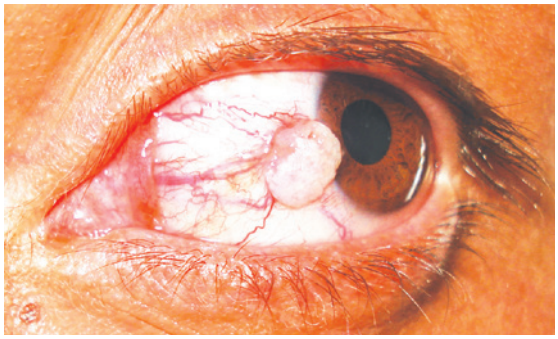

Figure 1. White, nodular mass on the nasal conjunctiva adjacent to the limbus. The mass was 4 × 5 mm in size and surrounded by dilated vessels.

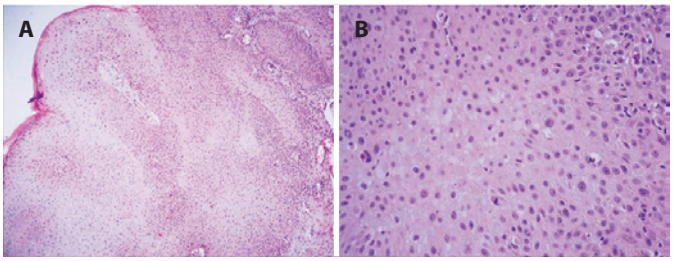

Figure 2. (A) The lesion was composed of deeply elongated, enlarged, and merged solid islands of large, pale squamous cells (hematoxylin-eosin ×100). (B) The squamous cells showed moderate to marked atypia and frequent mitosis (hematoxylin-eosin ×200).

Conjunctival SCC is more common in elderly patients, but may occur earlier in patients with xeroderma pigmentosum or acquired immune deficiency syndrome (AIDS)[9]. Differentiation between SCC and KA can be challenging. KAs can easily be mistaken for SCC as their clinical presentation and histopathologic findings are very similar. Some authors regard KAs as a variant of SCC. Grossniklaus et al. reported cases of conjunctival KA with invasive features[10], describing a case with a rapidly growing limbal lesion that was excised after 3 weeks with histological evidence of invasion. Subsequent rapid recurrence was observed in their patient, with intraocular invasion requiring enucleation, and surgical removal was justified to prevent possible eventual malignancy, as well as the difficulty of clinically differentiating this lesion from SCC. In our patient, we excised the lesion surgically with cryotherapy application to the limbus and conjunctival margins. As mentioned earlier, it may be difficult to histopathologically differentiate KA from SCC, particularly when lesions are incompletely excised. KAs are hemispheric-like, symmetric lesions with both exophytic and endophytic growth. They usually present with a keratin-filled central crater with overhanging epidermal edges and are composed of keratinocyte proliferations with large glassy, eosinophilic cytoplasm. The keratinocytes in KA show mild-to-moderate nuclear atypia. Mild-to-moderate inflammatory infiltrate at the base of the lesion may be present. SCC shows invasion of the dermis or subepithelial tissue, with irregular islands of squamous cells. Although keratinized and squamous pearls are abundant in well-differentiated SCC, they are absent in poorly differentiated tumors. Dermal/subepithelial inflammatory infiltrate may be observed. Histopathologic examination showing overhanging edges and a hemispheric-like lesion with marked atypical squamous cells suggest KA. The rapid growth of the lesion in our young patient also supports this diagnosis. Normal conjunctival epithelium was observed at the resected edges.

In literature, KA is typically reported in middle-aged and elderly patients, except for a 17-year-old patient with xeroderma pigmentosum, which was probably responsible for the younger age of onset[8]. However, we report a 23-year-old patient who had no history of trauma, surgery, infection, or skin disorders. To the best of our knowledge, he is the youngest patient to be reported with KA who had no risk factors for the disease.

In conclusion, both KA and SCC are possible in young patients, and we recommend early excision of suspected conjunctival KA for differential diagnosis with SCC. Careful follow-up is important for all patients with conjunctival KA after complete excision.

REFERENCES

1. Manstein CH, Frauenhoffer CJ, Besden JE. Keratoacanthoma: is it a real entity? Ann Plast Surg. 1998;40(5):469-72.
2. Weedon DD, Malo J, Brooks D, Williason R. Squamous cell carcinoma arising in keratoacanthoma: a neglected phenomenon in the elderly. Am J Dermatopathol. 2010;32(5):423-6.
3. Kossard S, Tan KB, Choy C. Keratoacanthoma and infundibulocystic squamous cell carcinoma. Am J Dermatopathol. 2008;30(2):127-34.
4. Freeman RG, Cloud TM, Knox JM. Keratoacanthoma of the conjunctiva. A case report. Arch Ophthalmol. 1961;65:817-9.
5. Hughes EH, Intzedy L, Dick AD, Tole DM. Keratoacanthoma of the conjunctiva. Eye (Lond). 2003;17(6):781-2.
6. Perdigao FB, Pierre-Filho PT, Natalino RJ, Caldato R, Torigoe M, Cintra ML. Conjunctival keratoacanthoma. Rev Hosp Clin Fac Med Sao Paulo. 2004;59(3):135-7.
7. Oellers P, Karp CL, Shah RR, Winnick M, Matthews J, Dubovy S. Conjunctival keratoacanthoma. Br J Ophthalmol. 2014;98(2):275-6, 285.
8. Chowdhury RK, Padhi T, Das GS. Keratoacanthoma of the conjunctiva complicating xeroderma pigmentosum. Indian J Dermatol Venereol Leprol. 2005;71(6):430-1.
9. Muccioli C, Belfort R Jr, Burnier M, Rao N. Squamous cell carcinoma of the conjunctiva in a patient with the acquired immunodeficiency syndrome. Am J Ophthalmol. 1996;121(1):94-6.
10. Grossniklaus HE, Martin DF, Solomon AR. Invasive conjunctival tumor with keratoacanthoma features. Am J Ophthalmol. 1990;109(6):736-8.

Enhanced depth imaging optical coherence tomography of choroidal osteoma with secondary neovascular membranes: report of two cases

Tomografia de coerência óptica com imagem profunda aprimorada de osteoma de coroide com membrana neovascular secundária: relato de 2 casos

Patrícia Correa de Mello[1], Patricia Berensztejn[2], Oswaldo Ferreira Moura Brasil[2]

ABSTRACT

We report enhanced depth imaging optical coherence tomography (EDI-OCT) features based on clinical and imaging data from two newly diagnosed cases of choroidal osteoma presenting with recent visual loss secondary to choroidal neovascular membranes. The features described in the two cases, compression of the choriocapillaris and disorganization of the medium and large vessel layers, are consistent with those of previous reports. We noticed a sponge-like pattern previously reported, but it was subtle. Both lesions had multiple intralesional layers and a typical intrinsic transparency with visibility of the sclerochoroidal junction.

Keywords: Osteoma; Tomography, optical coherence; Choroidal neovascularization; Choroid neoplasms

RESUMO

Relatamos as características na tomografia computadorizada óptica (EDI-OCT) de 2 pacientes recém diagnosticados com osteoma de coroide apresentando perda visual secundária à membranas neovasculares coroideanas. As características descritas em nossos 2 casos foram consistentes com trabalhos anteriores, exibindo a compressão da coriocapilar e desorganização das camadas médias e de grandes vasos. Notamos também o padrão em esponja anteriormente descrito, porém de forma discreta. Ambas as lesões tinham várias camadas intralesionais e uma transparência intrínseca típica com visibilidade da junção da esclero-coroideana.

Descritores: *Osteoma; Tomografia de coerência óptica; Neovascularização de coroide; Neoplasias da coroide*

INTRODUCTION

Optical coherence tomography (OCT) plays an instrumental role in the diagnosis and follow-up of several retinal and choroidal diseases such as macular degeneration, vascular occlusion, and inflammation. Recently, OCT studies of intraocular tumors evaluated the intrinsic optical characteristics of choroidal tumors imaged using enhanced depth imaging OCT (EDI-OCT)[1].

Among body structures, the choroid has one of the highest metabolic rates and supplies oxygen to the photoreceptor layer of the retina, which is also a highly metabolic structure[2]. However, the choroid is one of the most difficult structures to image in vivo because pigments in the retinal pigment epithelium (RPE) and choroid impede image capturing.

EDI-OCT provides a more detailed view than spectral-domain OCT (SD-OCT) of deep anatomic structures[3]. The current axial resolution with EDI-OCT is approximately 3.9 micra[4]. Recently, several papers have been published describing the aspects of choroidal tumors revealed with this new technology[4-6]. With this technology, various choroidal tumors can be imaged and measured. Using EDI-OCT, choroidal nevi and melanomas show a smooth, dome-shaped surface, whereas choroidal metastases display a "lumpy-bumpy," irregular surface topography and choroidal hemangiomas present a smooth, acutely dome-shaped surface; choroidal lymphomas show a "placid," rippled, or "seasick" surface[4].

Choroidal osteomas are rare, benign, and usually unilateral intraocular tumors composed of mature bone affecting the choroid. These tumors can be asymptomatic or can produce visual loss because of choroidal neovascularization (CNV) or tumor decalcification, presence of subretinal fluid, and photoreceptor atrophy[7].

CNV is an important cause of vision loss in patients with choroidal osteoma and is reported to occur in 31% of affected eyes by 10 years after the diagnosis[8].

In this study, we evaluated the EDI-OCT features of two cases of choroidal osteoma with neovascular membranes.

CASE REPORTS

Case 1

A 24-year-old Caucasian male experienced a sudden vision loss in his left eye. His best corrected visual acuity was 20/20 in the right eye and 20/40 in the left eye. His anterior segment examination was normal. The fundus examination revealed a choroidal osteoma involving the macular area and upper temporal vascular arcade with subretinal hemorrhage and subretinal fluid in the fovea (Figure 1).

Case 2

A 26-year-old Caucasian female experienced a sudden vision loss in her left eye. Her best corrected visual acuity was 20/20 in the right eye and 20/40 in the left eye. Her anterior segment examination was unremarkable. The fundus examination revealed a choroidal osteoma involving the entire macular area with subretinal hemorrhage and subretinal fluid in the fovea (Figure 2).

Submitted for publication: January 14, 2015
Accepted for publication: June 23, 2015

[1] Setor de Retina e Tumores do Instituto Brasileiro de Oftalmologia (IBOL) e Serviço de Oftalmologia. Hospital Federal dos Servidores do Estado do Rio de Janeiro, Rio de Janeiro, RJ, Brazil.
[2] Setor de Retina e Vítreo do Instituto Brasileiro de Oftalmologia (IBOL), Rio de Janeiro, RJ, Brazil.

Funding: No specific financial support was available for this study.

Disclosure of potential conflicts of interest: None of the authors have any potential conflict of interest to disclose.

Corresponding author: Patrícia C. de Mello. Praia de Botafogo, 206 - Rio de Janeiro - RJ - Brazil
E-mail: paticma@gmail.com

Both patients were evaluated with SD-OCT including EDI-OCT using Cirrus Carl Zeiss OCT, fluorescein angiography, and ultrasonography.

DISCUSSION

In both cases, the lesion had a yellow-white coloration with finger-like projections and pigmentary changes in the overlying RPE. The lesions were minimally elevated (<1.2 mm) and hyperreflective on ultrasonography, and both cases showed small areas of decalcification. Fluorescein angiography showed early patchy hyperfluorescence and late staining, and the choroidal neovascular membranes were found in the decalcified areas in both cases. We observed an angiographic leakage in the area of the membrane. On SD-OCT, the neovascular membrane was superior to the fovea and nasal to the fovea in cases 1 and 2, respectively; both cases had the presence of subretinal fluid.

On analyzing the EDI-OCT images (Figures 3 and 4), both cases had normal inner retinal features, and the outer retina showed inte-

Figure 1. Color photograph of a choroidal osteoma with associated choroidal neovascularization. The neovascularization lies in the center of the lesion, and a subretinal hemorrhage is nasally and inferiorly noted.

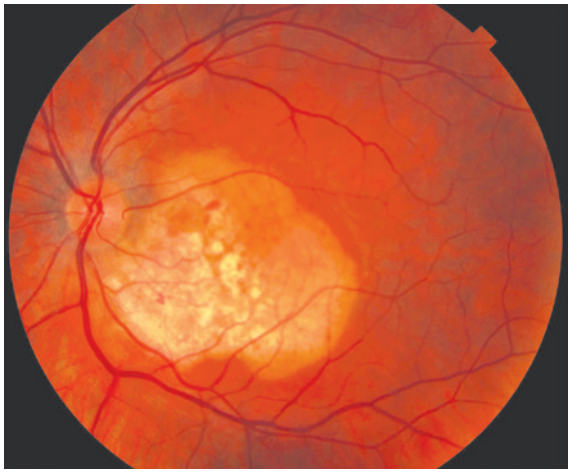

Figure 2. Color photograph of a choroidal osteoma with associated choroidal neovascularization. The neovascularization is located on the papillomacular bundle, and small spots of subretinal hemorrhage are noticed around it.

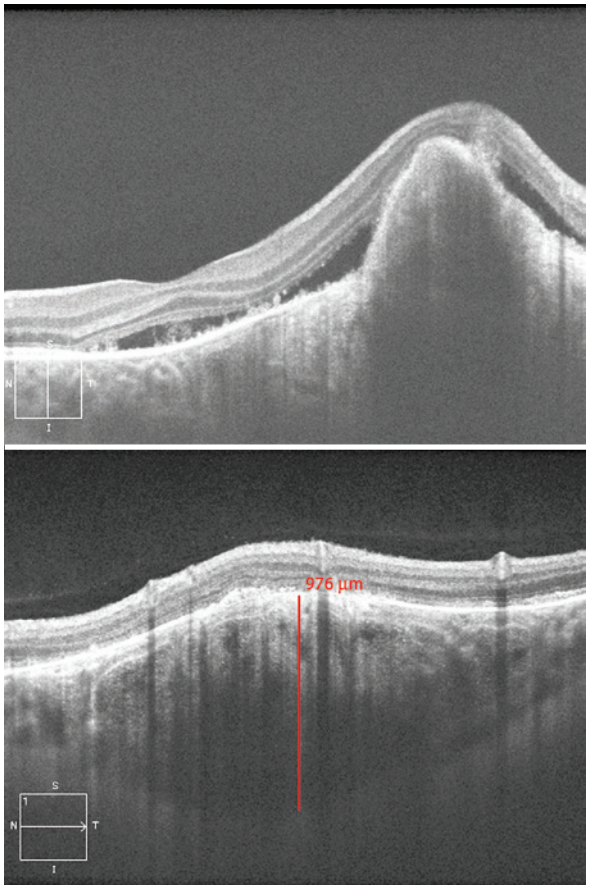

Figure 3. Enhanced depth imaging optical coherence tomography (EDI-OCT) images from case 1 affected by a choroidal osteoma with neovascular membrane. A multilayer configuration with a discrete sponge-like pattern was observed. The sclerochoroidal junction was detected, but we could not see it in all parts under the tumor because CNV had a fibrotic component that obscured the posterior part of the membrane. The choroidal thickness was 976 micra at the parafoveal area.

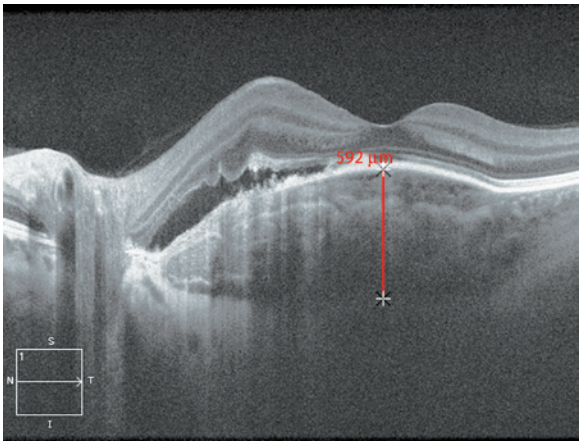

Figure 4. EDI-OCT images from case 2 affected by a choroidal osteoma with neovascular membrane. A multilayer configuration with a discrete sponge-like pattern was observed. The sclerochoroidal junction was detected in all parts of the tumor revealing a typical intrinsic transparency. The choroidal thickness was 592 micra at the foveal area.

grity of the photoreceptor layer in calcified areas and disruption in decalcified areas, similar to what was previously reported in 2007[9]. The choriocapillaris was thinned in both cases. Medium-caliber vessels (Sattler's layer) showed thinning and no visibility in both cases, whereas large-caliber vessels (Haller's layer) appeared as thinned rims of vessels between the tumor and sclerochoroidal junction, as was recently reported[6]. This finding is supported by histopathologic evidence from previous reports[10].

EDI-OCT of the osteoma revealed a typical reflectivity pattern in both cases with the presence of hyperreflective horizontal lamellar lines, which were described in other reports[5,6]. These characteristics could represent varying degrees of calcification within the tumor because of the different phases of bone tissue formation. We noticed multiple hyperreflective dots scattered in the hyporeflective matrix creating a sponge-like appearance as previously reported[6], but they were very subtle, especially under the CNV area. The sclerochoroidal junction was detected in both cases; however, in case 1, we were unable to detect it in all parts under the tumor because CNV had a fibrotic component that produced shadowing posterior to the membrane. The choroidal thickness was 976 micra in case 1 and 592 micra in case 2.

The features described in the two cases mentioned above, compression of the choriocapillaris and disorganization of the medium and large vessel layers, are consistent with those of previous reports[4-6]. We noticed the sponge-like pattern previously reported[4-6], but it was subtle. Both lesions had multiple intralesional layers and a typical intrinsic transparency with visibility of the sclerochoroidal junction, except in the area where CNV had a fibrotic component.

In agreement with the findings of other authors[4], we showed that EDI-OCT is a new and important tool in the differential diagnoses of amelanotic lesions. Our findings highlight how EDI-OCT may be helpful in studying CNVs secondary to choroidal osteomas.

REFERENCES

1. Torres VL, Brugnoni N, Kaiser PK, Singh AD. Optical coherence tomography enhanced depth imaging of choroidal tumors. Am J Ophthalmol. 2011;151(4):586-93 e.2.
2. Linsenmeier RA, Padnick-Silver L. Metabolic dependence of photoreceptors on the choroid in the normal and retina. Invest Opthalmol Vis Sci. 2000;41(10):3117-23.
3. Spaide RF, Koizumi H, Pozonni MC. Enhanced depth imaging spectral-domain optical coherence tomography. Am J Ophthalmol. 2008;146(4):496-500.
4. .Shields CL, Pellegrini M, Ferenczy SR, Shields JA. Enhanced depth imaging optical coherence tomography of intraocular tumors. from placid to seasick to rock and rolling topography- the 2013 Francesco Orzalesi Lecture. Retina. 2014;34(8):1495-512.
5. Shields CL, Arepalli S, Atalayl HT, Ferenczy SR, Fulco E, Shields JA. Choroidal osteoma shows bone lamella and vascular channels on enhanced depth imaging optical coherence tomography in 15 eyes. Retina. 2015;35(4):750-7.
6. Pellegrini M, Invernizzi A, Giani A, Staurenghi G. Enhanced depth imaging optical coherence tomography features of choroidal osteoma. Retina. 2014;34(5):958-63.
7. Aylward GW, Chang TS, Pautler SE, Gass JD. A long term follow-up of choroidal osteoma. Arch Opthalmol. 1998;116(10):1337-41.
8. Shields CL, Sun H, Demerci H, Shields JA. Factors predictive of tumor growth, tumor decalcification, choroidal neovascularization, and visual outcome in 74 eyes with choroidal osteoma. Arch Ophthalmol. 2005;123(12):1658-66.
9. Shields CL, Perez B, Materin MA, Mehta S, Shields JA. Optical coherence tomography of choroidal osteoma in 22 cases: evidence for photoreceptor atrophy over the decalcified portion of the tumor. Ophthalmology. 2007;114(12):e53-8.
10. Foster BS, Fernandez-Suntay JP, Dryja TP, Jakobiec FA, D' Amico DJ. Clinicopathologic reports, case reports, and small case series: surgical removal and histopathologic findings of a subfoveal neovascular membrane associated with choroidal osteoma. Arch Ophthalmol. 2003:121(2):273-6.

Silent polypoidal choroidal vasculopathy in a patient with angioid streaks

Vasculopatia polipoidal de coróide quiescente em um paciente com estrias angióides

Zafer Cebeci[1], Serife Bayraktar[1], Merih Oray[1], Nur Kir[1]

ABSTRACT

We present a case of silent polypoidal choroidal vasculopathy (PCV) in a patient with angioid streaks. PCV was detected during a routine ophthalmic examination and confirmed by fluorescein angiography, indocyanine green angiography, and optical coherence tomography. After 2 years of follow-up, the PCV remained silent without any complications. We report this rare coexistence and review literature on this topic.

Keywords: Polyps; Choroid; Choroidal neovascularization; Fluorescein angiography; Indocyanine green; Retinal pigment epithelium; Tomography, optical coherence; Vascular endothelial growth factor A; Angioid streaks

RESUMO

Nós apresentamos um relato de vasculopatia polipoidal de coroide (PCV) em paciente com estrias angióides. Vasculopatia polipoidal de coroide detectada em exame oftalmológico de rotina e confirmado por angiofluoresceinografia, angiografia com indocianina verde e tomografia de coerência óptica. Após 2 anos de seguimento a vasculopatia polipoidal de coroide permaneceu quiescente, sem qualquer complicação. Nós relatamos esta coexistência rara e apresentamos revisão da literatura.

Descritores: *Pólipos; Coroide; Neovascularização de coroide; Angiofluoresceinografia; Verde de indocianina; Epitélio pigmentado da retina; Tomografia de coerência óptica; Fator A de crescimento do endotélio vascular; Estrias angióides*

INTRODUCTION

Polypoidal choroidal vasculopathy (PCV) is a disorder that is characterized by dilatation of the choroidal vessels. This disorder was initially reported as idiopathic PCV in 1990[1]. Angioid streaks (AS) are breaks in the Bruch's membrane that result in irregular radial or concentric lines around the optic disc; these are mostly associated with pseudoxanthoma elasticum (PXE)[2]. In literature, PCV and AS are rarely described in the same patient[3-5], and visual impairment usually occurs because of complications, such as choroidal neovascularization (CNV) during the natural course of both diseases[2,5]. Visual acuity can remain unaffected if hemorrhage, subretinal or intraretinal exudation, or pigment epithelial detachments do not develop. Herein we present a case of silent PCV in a patient with AS.

CASE REPORT

A 26-year-old woman was admitted to our clinic for routine ophthalmic examination. Her past ocular and medical histories were unremarkable. At presentation, visual acuities were 20/20 for both eyes, and anterior segment findings for both eyes were normal. Fundoscopy disclosed AS radiating from the optic disc and bilateral changes in the retinal pigment epithelium (RPE) that were evident on the nasal side of the fovea of the right eye (Figure 1 A, B). Optical coherence tomography (OCT) showed a steep, dome-shaped RPE elevation with moderate hyperreflectivity beneath the RPE (Figure 1 C). Due to the suspicion of PCV, we performed fluorescein angiography (FA) and indocyanine green angiography (ICGA). FA demonstrated irregular hyperfluorescence around the optic disc associated with AS in both eyes and increasing hyperfluorescent foci in the nasal side of the fovea of the right eye (Figure 1 D). ICGA showed a focal area of hyperfluorescence surrounded by a hypofluorescent halo in the right macula (Figure 1 E). Neovascularization was excluded by the imaging modalities, and no associated systemic conditions related to AS were found on consultation.

With these findings, we diagnosed the patient with AS in both eyes and PCV in the right eye. Because she had no symptoms and no intraretinal or subretinal fluid was seen on imaging (Figure 1 F), our initial plan was to monitor the patient. The PCV remained silent with no leakage, and no decrease in vision was seen during the 2 years of follow-up.

DISCUSSION

PCV is a localized enlargement of the choroidal vasculature that forms polyps and originates from the inner choroid[1]. Hyalinization of vessels as well as plasma and/or fibrin exudation are the histopathological features of PCV[6]. Serous or hemorrhagic pigment epithelial detachments, subretinal hemorrhages, and exudation are the common signs of PCV, and these secondary complications cause visual disturbances[6]. If the patient has no symptoms and there are no ophthalmoscopic signs, imaging modalities, especially ICGA, can assist physicians in diagnosing the lesion.

PCV has been shown to be associated with pathologies such as tilted disc, high myopia, retinitis pigmentosa, central serous chorioretinopathy, and AS[7-9].

Few cases with coexistence of AS and PCV have been reported in literature[3-5]. PCV has been detected at initial examination in some of the cases in literature, and some have developed PCV as observed during the follow-up of CNV due to AS[3-5]. The first reported case was initially treated for CNV as a complication of AS in both eyes, and the

Submitted for publication: August 3, 2015
Accepted for publication: September 23, 2015

[1] Department of Ophthalmology, Istanbul Faculty of Medicine, Istanbul University, Istanbul, Turkey.

Funding: No specific financial support was available for this study.

Disclosure of potential conflicts of interest: None of the authors have any potential conflict of interest to disclose.

Corresponding author: Zafer Cebeci. Istanbul Tip Fakultesi, Goz Hastaliklari A.D. Capa, Istanbul 34390 - Turkey - E-mail: zafceb@gmail.com

http://dx.doi.org/10.5935/0004-2749.20160058

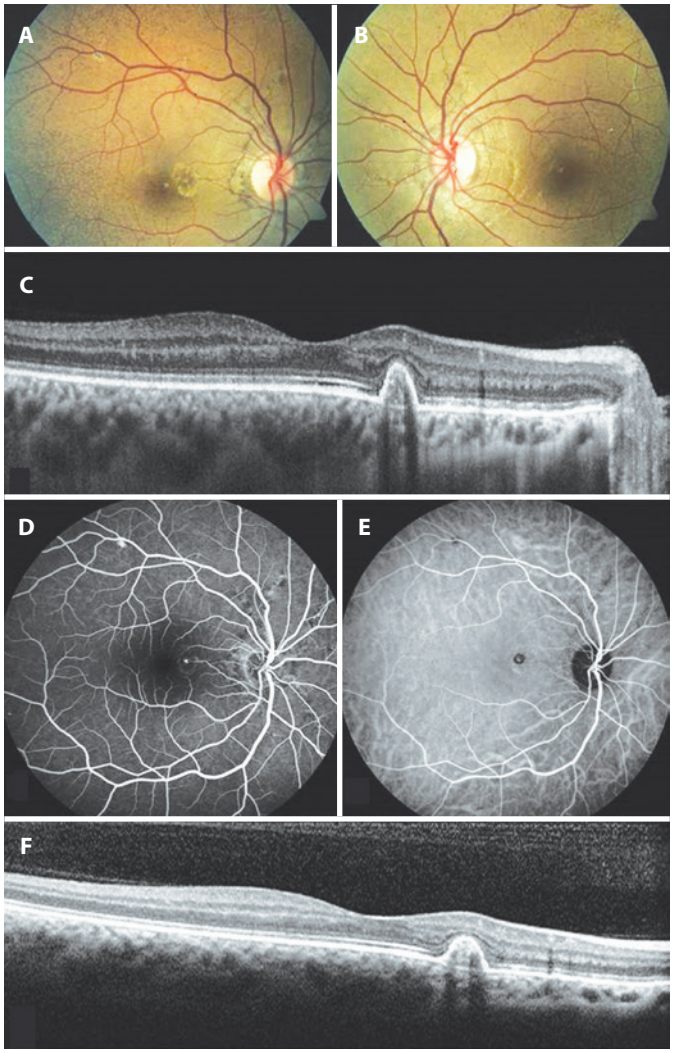

Figure 1. A) Color fundus photography of the right eye demonstrated radial and circumferential angioid streaks (AS) around the optic disc as well as pigment epithelial changes at the nasal side of the fovea. B) Color fundus photography of the left eye showed AS around the optic disc. C) Optical cohorence tomography (OCT) scan through the retinal pigment epithelium (RPE) changes in the right macula at the initial visit demonstrated sharply elevated RPE with moderate hyperreflectivity under it. D) Fluorescein angiography showed dye leakage nasal to the macula in the right fundus. E) Indocyanine green angiography showed a foci of hyperfluorescence surrounded by a hypofluorescent halo in the right macula. F) OCT scan of the same area after 2 years of follow-up showed a polypoidal lesion.

patient developed PCV temporally to the macula and in the nasal side of the fovea of the right eye during the follow-up period[3].

In a series of 44 cases with AS, PCV was found in six eyes of five patients[4]. PCV was identified in two eyes at initial examination, and polypoidal lesions were detected on follow-up visits in four eyes. A patient who was initially diagnosed with PCV developed CNV during the follow-up and was treated with intravitreal SF_6 injection, photodynamic therapy, and intravitreal anti-VEGF injection. PCV was identified at the edge of type 2 CNV in two eyes during the follow-up visits. As the lesions were far away from the fovea, they did not require any treatment, which suggests that vascular anomalies causing PCV can be initially detected in patients with AS. Further, some patients may have a predisposition for developing polypoidal lesions.

A 59-year-old male patient with a history of PXE and CNV due to AS developed PCV 1 year after the diagnosis of neovascularization; the patient had already undergone nine intravitreal anti-VEGF injections for CNV[5].

AS is usually related to a systemic condition, with PXE being the most common. Smooth muscle cells play a role in the systemic pathological changes of PXE[10]. Abnormalities in the smooth muscle cells of the choroidal vascular structure lead to dilatations that form PCV, and these two entities can show similarities in their pathogenesis[3]. Moreover, alterations of Bruch's membrane, which simplify the development of CNV in patients with AS, may also facilitate complications due to polyps. It is also important to keep in mind that there were no associated systemic diseases in the present case, but the patient is still young and there is a possibility that she may develop systemic findings in future. The reported PCV cases in patients with AS have been diagnosed at older ages[3-5]. In addition to the pathology of Bruch's membrane in AS, which usually progresses over many years, aging may contribute to the impairment of Bruch's membrane; therefore, complications may easily occur.

PCV lesions can stay silent and do not affect visual acuity if there are no signs of leakage or hemorrhage from the polypoidal lesions[6]. Our patient did not report visual loss, and her PCV was diagnosed incidentally. Ophthalmoscopic examination and imaging modalities confirmed the diagnosis of PCV, and she did not develop any complications during the 2 years of follow-up.

In conclusion, patients with AS should be followed-up not only for the development of CNV but should also be followed-up routinely for polypoidal lesions. Vision-threatening complications can occur during the natural course of PCV, and imaging techniques such as ICGA and OCT are the most important tools for the diagnosis of this rare association.

REFERENCES

1. Yannuzzi LA, Sorenson J, Spaide RF, Lipson B. Idiopathic polypoidal choroidal vasculopathy (IPCV). Retina. 1990;10(1):1-8.
2. Gliem M, Finger RP, Fimmers R, Brinkmann CK, Holz FG, Charbel Issa P. Treatment of choroidal neovascularization due to angioid streaks: a comprehensive review. Retina. 2013;33(37):1300-14.
3. Baillif-Gostoli S, Quaranta-El Maftouhi M, Mauget-Faÿsse M. Polypoidal choroidal vasculopathy in a patient with angioid streaks secondary to pseudoxanthoma elasticum. Graefes Arch Clin Exp Ophthalmol. 2010;248(12):1845-8.
4. Nakagawa S, Yamashiro K, Tsujikawa A, Otani A, Tamura H, Ooto S, et al. The time course changes of choroidal neovascularization in angioid streaks. Retina. 2013;33(4): 825-33.
5. Khan S, Engelbert M, Imamura Y, Freund KB. Polypoidal choroidal vasculopathy: simultaneous indocyanine green angiography and eye-tracked spectral domain optical coherence tomography findings. Retina. 2012(6);32:1057-68.
6. Nowak-Sliwinska P, van den Bergh H, Sickenberg M, Koh AH. Photodynamic therapy for polypoidal choroidal vasculopathy. Prog Retin Eye Res. 2013;37:182-99.
7. Nakanishi H, Tsujikawa A, Gotoh N, Hayashi H, Iwama D, Tamura H, et al. Macular complications on the border of an inferior staphyloma associated with tilted disc syndrome. Retina. 2008;28(10):1493-501.
8. Ishida T, Moriyama M, Morohoshi K, Furuse Y, Fukuda T, Ohno-Matsui K, et al. Polypoidal choroidal vasculopathy in a case with retinitis pigmentosa. Int Ophthalmol. 2013; 33(3):305-8.
9. Toyama T, Ohtomo K, Noda Y, Ueta T. Polypoidal choroidal vasculopathy and history of central serous chorioretinopathy. Eye (Lond). 2014;28(8):992-7.
10. Gheduzzi D, Sammarco R, Quaglino D, Bercovitch L, Terry S, Taylor W, et al. Extracutaneous ultrastructural alterations in pseudoxanthoma elasticum. Ultrastruct Pathol. 2003;27(6):375-84.

Update and review of Urrets-Zavalia syndrome

Atualizando e revisando a síndrome de Urrets-Zavalia

Otavio A. Magalhães[1], Claudia L. Kronbauer[1], Eduardo G. Müller[2], Carina T. Sanvicente[2]

ABSTRACT

For more than half a century, Urrets-Zavalia syndrome (fixed dilated pupil) has been described as a postoperative complication of ophthalmic surgery. Since first reported as a complication of penetrating keratoplasty for keratoconus in patients receiving atropine, the characteristic features of Urrets-Zavalia syndrome have been expanded. In previous literature, a total of 110 cases resulted in a fixed and dilated pupil. Increased intraocular pressure (IOP) in the immediate postoperative period, phakia, and air or gas in the anterior chamber appear to be the most important risk factors for Urrets-Zavalia syndrome following ophthalmic procedures. Mannitol, IOP control, the removal of air or gas in the anterior chamber, and iridectomy have all demonstrated utility in managing Urrets-Zavalia syndrome.

Keywords: Pupil anatomy and physiology; Pupil disorder prevention and control; Intraocular pressure; Risk factors

RESUMO

Por mais de meio século, a síndrome de Urrets-Zavalia (pupila fixa e dilatada) foi descrita como uma complicação pós-operatória em oftalmologia. Desde o primeiro relato após ceratoplastia penetrante em pacientes portadores de ceratocone em uso de atropina, seu conceito foi ampliado. Na literatura, um total de 110 casos resultaram em pupila fixa e dilatada. Aumento da pressão intraocular (PIO) no pós-operatório imediato, facia, ar ou gás na câmara anterior parecem ser fatores de risco importantes para o aparecimento da síndrome. Sua prevenção pode ser alcançada com o uso de manitol, controle adequado da PIO e quantidade de ar ou gás na camâra anterior e iridectomia.

Descritores: *Pupila/anatomia & fisiologia; Distúrbios pupilares/prevenção & controle; Pressão intraocular; Fatores de risco*

INTRODUCTION

Urrets-Zavalia syndrome (UZS; fixed dilated pupil) was first recognized by Castroviejo and published in 1963 by *Alberto Urrets-Zavalia Jr.*, who described six cases of atrophic and mydriatic pupil associated with secondary glaucoma following penetrating keratoplasty (PK) in patients with keratoconus[1,2]. Other findings of UZS were subsequently reported, including peripheral synechiae, posterior subcapsular opacity, iris ectropion, pigmentary dispersion, and glaukomflecken[3-11].

Other procedures shown to be associated with UZS include trabeculectomy (TREC)[5], deep anterior lamellar keratoplasty (DALK)[12-15], Descemet-stripping automated endothelial keratoplasty (DSAEK)[16-18], cataract surgery[11,19], goniotomy[20], phakic intraocular lens implant (IOL)[21-23], argon laser peripheral iridoplasty (ALPI)[7], and octafluoropropane injection (C3F8)[24].

Although the reported incidence of UZS is low, the associated visual symptoms can cause limitations in activities of daily life requiring preventative measures by ophthalmic surgeons[7,14]. The purpose of the present review is to identify all reported cases of UZS published prior to December, 2014 in Medline and EMBASE databases, highlight the most prevalent risk factors, and describe measures for the prevention of Urrets-Zavalia syndrome.

Risk factors and pathogenesis

There are numerous and conflicting risk factors of the development of UZS. Neurogenic changes, inflammatory response, genetic predisposition, and direct iris trauma have all been posited to contribute to the pathophysiology of UZS[7,8,10,25]. Early reports indicated the use of atropine in PK as associated with such complications[1]. Keratoconus was also suggested to be involved in the pathogenesis of UZS as a result of decreased corneal rigidity and enhanced response to mydriatics[3,26]. Intraocular pressure (IOP) elevation, with or without pupillary block, has been implicated as the trigger mechanism of UZS[4,27]. Use of viscoelastic substances during surgery have been suspected as toxic to the iris sphincter and a cause of acute rises in IOP[10,11]. The use of miotics before and during surgery has been considered prophylactic by some authors and a risk factor of pupillary atrophy by others[4,10,18,25,28].

Urrets-Zavalia posited that iris compression against the peripheral cornea under the effect of intense mydriasis without compromising the ciliary body and pars plana was the most important factor related to the development of UZS[1,17]. Severe iris ischemia was later reported in several angiography studies[4-6,21]. The UZS spectrum comprises anterior segment changes ranging from focal pupillary atrophy with posterior pigment layer injury and no stromal involvement to diffuse or sector atrophy, including the iris stroma[28,29]. Ischemic events are not thought to contribute to focal cases and pupillary dilation is considered less intense (6 mm or less). Focal cases of UZS typically respond partially or totally to miotics, which may allow regression of mydriasis. A study on combination therapy with guanethidine and pilocarpine has demonstrated its efficacy and associated miosis in patients with this type of atrophy[28]. Conversely, stromal ischemic injury has been reported to be irreversible, promote intense mydriasis (more than 6 mm), and not respond to miotics (Figure 1)[14].

Submitted for publication: October 14, 2015
Accepted for publication: January 12, 2016

[1] Cornea and External Disease Department, Hospital Banco de Olhos de Porto Alegre, Porto Alegre, RS, Brazil.
[2] Hospital Banco de Olhos de Porto Alegre, Porto Alegre, RS, Brazil.

Funding: No financial support was available for this study.

Disclosure of potential conflicts of interest: None of the authors have any potential conflict of interest to disclose.

Corresponding author: Otavio Magalhães. Rua Mostardeiro, 333/503 - Porto Alegre, RS - 90430-001 Brazil - E-mail: otaviomaga@yahoo.com.br

http://dx.doi.org/10.5935/0004-2749.20160059

Literature review

More than 30 studies have been published since the first description of UZS, comprising a total of 110 reported cases[1,4-25,29-42]. The mean age of the patients in reported cases was 46.1 years (range: 13-90). Reported surgical interventions include PK (51.8%), DALK (18.1%), DSAEK (8.2%), cataract surgery (8.2%), ALPI (8.2%), phakic IOL implantation (2.7%), TREC (1.9%), goniotomy (0.9%), and anterior chamber injection of C3F8 for the treatment of acute hydrops (0.9%). Diagnoses associated with these interventions include keratoconus (45.2%), stromal dystrophies (23.7%), Fuchs' dystrophy (9.4%), plateau iris syndrome (8.5%), senile cataract (8.5%), primary open-angle glaucoma (1.9%), high myopia (1.9%), and congenital glaucoma (0.9%). Individuals affected by bilateral UZS had the same type of ophthalmic procedure on different occasions, corresponding to 8.2% of all patients. The use of mydriatic drops during or after surgical intervention has been reported in only 26% of cases, including the first description of UZS. Viscoelastic was injected to completely maintain the anterior chamber in 44.5% of all surgical procedures. Increased IOP was observed in 59.1% of patients during the first postoperative day and approximately half of these patients (26.7%) had maintained elevated IOP measures during the following days. Only 13.1% of patients with UZS were pseudophakic. Injection of air or C3F8 was performed in 27.3% of cases, particularly in cases of lamellar keratoplasty (89.6% of DALK and DSAEK). The use of miotics (pilocarpine or acetylcholine) was described in 40.9% of patients during the preoperative or intraoperative periods, with 27.3% of patients not receiving any type miotic therapy. There was no reference to the use or not of miotics in 31.8% of the patients.

DISCUSSION

Many retrospective studies and case and series reports of UZS have been published over the past few decades. UZS reportedly has no predilection for age and has been observed as a postoperative response in both young and elderly patients. We believe that the majority of cases of UZS are related to PK, as this has been the predominant technique during the last century[33]. In the 1970s, lamellar keratoplasty was used in less than 5% of all transplants[43]. With the increasing recognition of lamellar techniques and the use of artificial anterior chambers, reports of UZS increased in subsequent decades. The majority of UZS cases were reported in patients with keratoconus, following the same prevalence pattern as other conditions when considering all uneventful corneal transplantations[29]. In a retrospective study that analyzed more than 2,000 patients with PK, the incidence of UZS was higher in patients with macular dystrophy than in patients with keratoconus[7]. We believe that patients with keratoconus are not at increased risk of UZS, as stated in previous studies[26]. Increased IOP during and immediately after presentation of UZS has been verified in the majority of reported cases; however, the maintenance of ocular hypertension was not clearly demonstrated in these cases[34]. This pattern has previously been suggested by some authors[2,5]. However, the causal relationship between increased IOP and iris ischemia remains unclear. Progression to secondary glaucoma is reportedly observed in approximately one quarter of cases and should not be considered a definitive characteristic of UZS[2]. A retrospective study demonstrated a statistically significant increase in IOP within the first 24 h after surgery in patients undergoing PK for keratoconus[35]. Mydriatic instillation during and after the procedure was reportedly performed in a quarter of patients, including the cases originally described by Urrets-Zavalia. Our observations, in corroboration with those of other authors, indicate atropine does not increase the risk of UZS development[32,44-45]. In fact, it is questionable whether the use of these measures prevents iris injury[13].

The mechanisms underlying pupillary block remain controversial. It was believed that acute angle closure was required to initiate the pupil atrophy process[5,12,39]. Recently, several cases have been described with the absence of pupillary block[10,40]. We observed that angle closure was not present in the majority of patients with UZS. The proposed mechanism for iris ischemia in lamellar transplantation is compression against the lens as a result of the injection of large amounts of air or gas into the anterior chamber (Figure 2).

The vast majority of UZS cases are observed in phakic patients. This may explain the limited number of reported cases of UZS in patients undergoing cataract extraction. Protective measures against UZS have also been described, such as iridectomy and intravenous hyperosmotics[8,27]. The use of 20% mannitol has been reported to decrease the incidence of UZS from 4% to 1.5%[46]. Hyperosmotic agents have demonstrated efficacy in decreasing vitreous volume and subsequently attenuating iris compression due to the lens. Ensuring anterior chamber formation as soon as possible during surgery may also prevent iris strangulation[8]. Prophylactic iridectomy or YAG laser iridotomy a few days prior to surgical intervention appear to have efficacy in decreasing risk of pupillary block[2,9,46]. However, this practice remains controversial, and some authors have reported

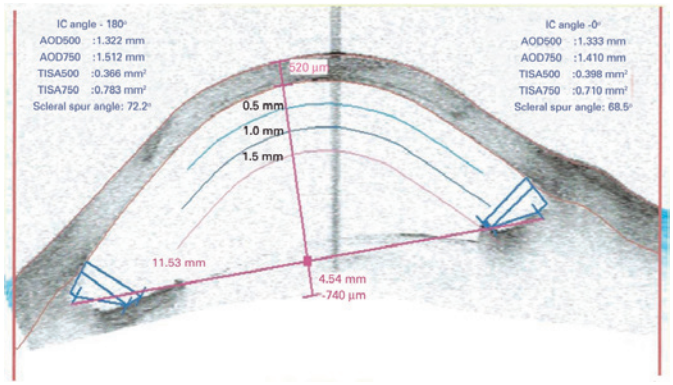

Figure 1. Anterior segment optical coherence tomography (Visante®; Carl Zeiss Meditec, Dublin, CA) demonstrating diffuse fixed dilated pupil after DALK with air bubble. A wide open-angle is observed.

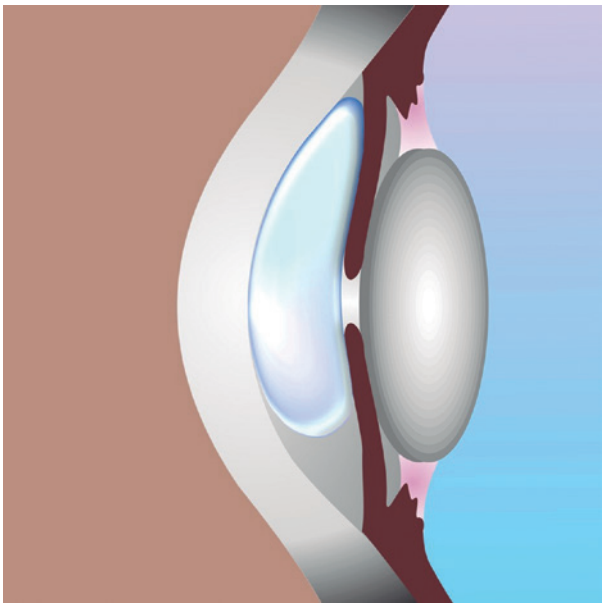

Figure 2. Voluminous air bubble in the anterior chamber compressing the iris against the lens.

that these therapies provide no benefit[11]. Careful management of surgical equipment, such as trephines and scissors, may also prevent iris damage[8]. There are currently no specific treatments for diffuse pupillary atrophy. Corneal tattooing, specialty contact lenses, and artificial iris implants are options for glare reduction and appearance improvement. In focal atrophy, miotics such as guanethidine and pilocarpine have demonstrated efficacy in treating UZS and attenuating mydriasis[28].

Direct neuronal injury may also be involved in the development of pupillary atrophy. Patients undergoing ALPI may be at risk of damage to the radial parasympathetic fibers of the pupillary constrictor muscle, explaining the observed cases of UZS[7]. Likewise, the observation of UZS in both eyes of some patients may indicate a genetic predisposition of the iris sphincter to ischemia in selected corneal pathologies[8]. Some authors have attributed the persistence of viscoelastics in the anterior chamber to IOP elevation and UZS. Intraoperative use of viscoelastics was performed in less than half of patients in previous reports. However, the use of viscoelastics is unlikely to be associated with UZS because their use is extremely widespread in cataract extraction surgery and significant pupillary atrophy is not observed following these procedures[47]. Despite a lack of data in almost a third of previously reported cases, the use of preoperative and intraoperative miotics was observed in the majority of cases, indicating that these drugs may not prevent irreversible pupil dilation[20,48]. Last year, a major review did not address the importance of phakia and the use of miotics in UZS[32].

CONCLUSION

Patient undergoing keratoplasty for the treatment of any corneal pathology, mainly phakic, with increased IOP in the immediate postoperative period and with air or gas left in the anterior chamber are at increased risk of UZS. We believe that the use of viscoelastic or mydriatic substances during or after surgery is not associated with risk of UZS. Pilocarpine and acetylcholine have not demonstrated efficacy in preventing UZS. However, intravenous use of mannitol, IOP control in the immediate postoperative period, and avoidance of massive air or gas injection into the anterior chamber may decrease the incidence of UZS. Iridectomy may be indicated in selected cases, such as patients with increased vitreous pressure, shallow anterior chambers, or the presence of voluminous air or gas in the anterior segment.

REFERENCES

1. Urrets Zavalia A Jr. Fixed, dilated pupil, iris atrophy and secondary glaucoma. Am J Ophthalmol. 1963;56:257-65.
2. Grzybowski A, Urrets-Zavalía JA, Ascaso FJ. Alberto Urrets-Zavalía Jr, MD, PhD (1920-2010). Am J Ophthalmol. 2013;155(5):957-8.
3. Davies PD, Ruben M. The paretic pupil: its incidence and aetiology after keratoplasty for keratoconus. Br J Ophthalmol. 1975;59(4):223-8.
4. Silva LRE, Gonçalves MM, Kappel GM, Gomes JAP. Iris ischemia following penetrating keratoplasty for keratoconus (Urrets-Zavalia syndrome). Cornea. 1995;14(6):618-22.
5. Jain R, Assi A, Murdoch IE. Urrets-Zavalia syndrome following trabeculectomy. Br J Ophthalmol. 2000;84:338-9.
6. Tuft SJ, Buckley RJ. Iris ischaemia following penetrating keratoplasty for keratoconus (Urrets-Zavalia syndrome). Cornea. 1995;14:618-22.
7. Espana EM, Ioannidis A, Tello C, et al. Urrets-Zavalia syndrome as a complication of argon laser peripheral iridoplasty. Br J Ophthalmol. 2007;91:427-9.
8. Jastaneiah S, Al-Towerki AE, Al-Assiri A. Fixed dilated pupil after penetrating keratoplasty for macular corneal dystrophy and keratoconus. Am J Ophthalmol. 2005;140: 484-9.
9. Niknam S, Rajabi MT. Fixed dilated pupil (urrets-zavalia syndrome) after deep anterior lamellar keratoplasty. Cornea. 2009;28:1187-90.
10. Uribe LE. Fixed pupil following keratoplasty evaluation of six cases. Am J Ophthalmol. 1967;63:1682-6.
11. Tan AK, Humphry RC. The fixed dilated pupil after cataract surgery: is it related to intraocular use of hypromellose? Br J Ophthalmol. 1993;77:639-41.
12. Maurino V, Allan BD, Stevens JD, et al. Fixed dilated pupil (Urrets-Zavalia syndrome) after air/gas injection after deep lamellar keratoplasty for keratoconus. Am J Ophthalmol. 2002;133:266-8.
13. Minasian M, Ayliffe W. Fixed dilated pupil following deep lamellar keratoplasty (Urrets-Zavalia syndrome). Br J Ophthalmol. 2002;86:115-6.
14. Maurino V, Allan BDS, Stevens JD, Tuft SJ. Fixed dilated pupil (Urrets-Zavalia Syndrome) after air/gas injection after deep lamellar keratoplasty for keratoconus. Am J Ophthalmol. 2002;133:266-8.
15. Bozkurt KT, Acar BE, Acar S. Fixed dilated pupilla as a common complication of deep anterior lamellar keratoplasty complicated with Descemet membrane perforation. Eur J Ophthalmol. 2013;23:164-70.
16. Anwar DS, Chu CY, Prasher P, et al. Features of Urrets-Zavalia syndrome after Descemet stripping automated endothelial keratoplasty. Cornea. 2012;31:1330-4.
17. Fournié P, Ponchel C, Malecaze F, et al. Fixed dilated pupil (Urrets-Zavalia syndrome) and anterior subcapsular cataract formation after Descemet stripping endothelial keratoplasty. Cornea. 2009;28:1184-6.
18. Russell HC, Srinivasan S. Urrets-Zavalia syndrome following Descemet's stripping endothelial keratoplasty triple procedure. Clin Experiment Ophthalmol. 2011;39:85-7.
19. Pinho SA, Cronemberg S, Calixto N. Sindrome de Urrets-Zavalia na pseudofacia. Rev Bras Oftalmol. 1994;53(4):61-5.
20. Chelnis JG, Sieminski SF, Reynolds JD. Urrets-Zavalia syndrome following goniotomy in a child. J AAPOS. 2012;16:312-3.
21. Yuzbasioglu E, Helvacioglu F, Sencan S. Fixed, dilated pupil after phakic intraocular lens implantation. J Cataract Refract Surg. 2006;32:174-6.
22. Park SH, Kim SY, Kim HI, et al. Urrets-Zavalia syndrome following iris-claw phakic intraocular lens implantation. J Refract Surg. 2008;24:959-61.
23. Pérez-Cambrodí RJ, Piñero-Llorens DP, Ruiz-Fortes JP, Blanes-Mompó FJ, Cerviño-Expósito. Fixed mydriatic pupil associated with an intraocular pressure rise as a complication of the implant of a Phakic Refractive Lens (PRL). A. Semin Ophthalmol. 2014;29(4):205-9.
24. Aralikatti AK, Tomlins PJ, Shah S. Urrets-Zavalia syndrome following intracameral C3F8 injection for acute corneal hydrops. Clin Experiment Ophthalmol. 2008;36:198-9.
25. Nizamani NB, Bhutto IA, Talpur KI. Cluster of Urrets-Zavalia syndrome: a sequel of toxic anterior segment syndrome. Br J Ophthalmol. 2013;97(8):976-9.
26. Kirkness CM, Ficker LA, Steele AD, Rice NS. The success of penetrating keratoplasty for keratoconus. Eye. 1990;4:673-88.
27. Bowden B. Keratoconus, keratoplasty and iris atrophy. Trans Ophthalmol Soc Aust. 1966;25:20-22.
28. Lagoutte F, Thienpont P, Comte P. Proposition de traitment du syndrome dUrrets-Zavalia. A propos d'un cas reversible. J Fr Ophthalmol. 1983;6:291-4.
29. Gasset AR. Fixed dilated pupil following penetrating keratoplasty in keratoconus (Castroviejo syndrome). Ann Ophthalmol. 1977;9:623-8.
30. Price FW Jr. Fixed dilated pupil (Urrets-Zavalia syndrome) in corneal dystrophies. Cornea. 2005;24(3):363; author reply
31. Flament J, Schraub M, Guimaraes R, Bronner A. Urrets-Zavalia syndrome and glaucomatous cataract. Etiopathogenic and nosologic discussion. Ophthalmologica. 1984; 189(4):186-94.
32. Spierer O, Lazar M. Urrets-Zavalia syndrome (fixed and dilated pupil following penetrating keratoplasty for keratoconus) and its variants. Surv Ophthalmol. 2014;59(3): 304-10.
33. Walton DS. Urrets-Zavalia syndrome following goniotomy in a child. J AAPOS. 2013; 17(1):114-5.
34. Figueiredo GS, Kolli SS, Ahmad S, et al. Urrets-Zavalia syndrome following penetrating keratoplasty for keratoconus. Graefes Arch Clin Exp Ophthalmol. 2013;251:809-15.
35. Srinivasan M, Patnaik L. Fixed dilated pupil (Urrets-Zavalia syndrome) in corneal dystrophies. Cornea. 2004;23(1):81-3.
36. Spadea L, Viola M, Viola G. Regression of urrets-zavalia syndrome after deep lamellar keratoplasty for keratoconus: a case study. Open Ophthalmol J. 2008;8:130-1.
37. Mocan MC, Bozkurt B, Irkec M, et al. Urrets-Zavalia syndrome following iatrogenic pupil dilation in eyes with pigment dispersion. Can J Ophthalmol. 2009;44:216-7.
38. Bourcier T, Laplace O, Touzeau O, et al. Urrets-Zavalia syndrome. J Fr Ophtalmol. 2001; 24:303-8.
39. Batista, JLA, Grisolia, ABD, Pazos HB, et al. Fixed dilated pupil (Urrets-Zavalia syndrome) after deep lamellar keratoplasty. Rev Bras Oftalmol. 2011;70(4):248-51.
40. Naumann GO. Iris ischaemia following penetrating keratoplasty for keratoconus (Urrets-Zavalia syndrome). Cornea.1997;16:120.
41. Gonzalez F, Suarez-Peñaranda JM, Diez-Feijoo E, Pazos B, Sanchez-Salorio M. Histopathological and ultrasound biomicroscopy findings in a case of irreversible mydriasis after keratoplasty in keratoconus. Acta Ophthalmol Scand. 1997;75(4):474-6.
42. Flament J, Schraub M, Guimaraes R, Bronner A. Urrets-Zavalia syndrome and glaucomatous cataract. Etiopathogenic and nosologic discussion. Ophthalmologica. 1984;189(4):186-94.
43. Terry MA. The evolution of lamellar grafting techniques over twenty-five years. Cornea. 2000;19(5):611-6.
44. Tzelikis PF, Santos JD, Garcez RC, Akaishi L. Deep anterior lamellar keratoplasty by big-bubble technique. Arq Bras Oftalmol. 2011;74(6):435-40.
45. Geyer O, Rothkoff L, Lazar M. Atropine in keratoplasty for keratoconus. Cornea. 1991; 10:372-3.
46. Sharif KW, Casey TA. Penetrating keratoplasty for keratoconus: complications and long-term success. Br J Ophthalmol. 1991;75:142-6.
47. Terry MA, Shamie N, Chen ES, Hoar KL, Friend DJ. Endothelial keratoplasty a simplified technique to minimize graft dislocation, iatrogenic graft failure, and pupillary block. Ophthalmology. 2008;115(7):1179-86.
48. Gutman C. Atonic pupil a rare cosmetic problem in cataract patients. Euro Times. 2003; 8:16.

INSTRUCTIONS TO AUTHORS

- Scope and policy
- Methods
- Types of Manuscripts
- Editorial Process
- Manuscript Preparation

ABO-ARQUIVOS BRASILEIROS DE OFTALMOLOGIA (ABO, ISSN 0004-2749 - printed version and ISSN 1678-2925 - online version) is the official bimonthly publication of the Brazilian Council of Ophthalmology (Conselho Brasileiro de Oftalmologia - CBO). The purpose of the journal is to publish scientific studies in Ophthalmology, Visual Sciences, and Public Health, encouraging research, as well as qualification and updating of the professionals involved in this field.

METHODS

Original manuscripts are accepted only in English. Manuscripts are grouped into one of the following categories, based on the methodology used:

Clinical Studies

Descriptive or analytical studies involving humans or evaluating the literature relevant to humans.

Epidemiological Studies

Analytical studies involving results from human populations.

Laboratory Experimental Studies

Descriptive or analytical studies involving animal models or other biological, physical or chemical techniques.

Theoretical Studies

Descriptive studies involving description and theoretical analysis of new hypotheses based on the knowledge available in the literature. Theoretical results must add new information to literature.

TYPES OF MANUSCRIPTS

Manuscripts submitted to ABO should fit into one of the following categories according to their format. The maximum number of words, figures, tables and, references for each type of manuscript are in parentheses at the end of the description for each category. The word count of the manuscript includes the text from the beginning of the introduction up to the end of the discussion; therefore, the following items are not included: title page, abstract, references, acknowledgments, tables and figures, including legends.

Editorials

Editorials are contributed by invitation and should be related to topics of current interest, preferentially related to articles published in the same issue of ABO (title, maximum of 1,000 words, 2 figures or tables, and 10 references).

Original Articles

Original articles present complete experiments with results that have never been published before (title, structured abstract, maximum of 3,000 words, 7 figures or tables, and 30 references). The evaluation of the manuscripts will be based on the following priorities:

1. *New and relevant information based on a study that uses appropriate methodology.*
2. *Repetition of information available in the literature, not previously confirmed locally, based on a study that uses appropriate methodology.*
3. *Repetition of information available in the literature and previously confirmed locally, based on a study that uses appropriate methodology.*

* *Manuscripts containing speculative conclusions, unsubstantiated by the results or based on a study with inappropriate methodology will not be accepted.*

Case Reports and Case Series

Case reports or case series will be considered for publication when describing rare and original findings that have not been internationally confirmed, or when presenting clinical or surgical responses that can contribute to elucidate the pathophysiology of a disease (title, unstructured abstract, maximum of 1,000 words, 4 figures or tables, and 10 references).

Letters to the Editor

Letters to the editor are considered for publication if they contain comments related to manuscripts previously published in ABO or, exceptionally, the results of original studies with insufficient content to be submitted as Original Article. These letters should present new information or new interpretation of existing information. When the content of the letter refers to an article previously published in ABO, such article should be mentioned in the first paragraph of the letter and included in its reference list. In these cases, the letters will be linked to the article, and the authors of the article will have their right of reply guaranteed in the same issue. Congratulation letters will not be published (title, maximum of 700 words, 2 figures or tables, and 5 references).

Review Articles

Review articles follow the editorial line and are accepted only by invitation from the editor. Suggestions of topics for review articles should be sent directly to the editor, but manuscripts cannot be sent without an invitation (title, unstructured abstract, maximum of 4,000 words, 8 figures or tables, and 100 references).

EDITORIAL PROCESS

Manuscripts will only be considered for publication if they meet all the journal's requirements. The editorial office will inform the authors if their manuscript fails to meet such requirements. Upon notification, the corresponding author will have 30 days to make the necessary changes in the manuscript. If the deadline is not met, the manuscript will be excluded from the editorial process.

The manuscripts submitted to ABO are initially evaluated by the editors to check for content compliance with the editorial line of the journal. After this assessment, all manuscripts are sent for peer review. The anonymity of reviewers is preserved throughout the whole process. However, the authors of manuscripts do not remain anonymous.

After the initial editorial evaluation, the reviewers' comments can be sent to the authors to guide the changes to be implemented in the text. After implementing the changes suggested by the reviewers, the revised manuscript should be resubmitted along with a letter (which is sent as a supplementary document) with specific indications of all changes made to the manuscript or the reasons why the suggested changes were not made. Manuscripts that are resubmitted without a letter will be withheld until the editorial office receives the letter. The deadline to submit the new version of the ma-

nuscript is 30 days after the authors are informed of the need to make changes in their manuscript. Manuscripts will be excluded from the process if authors fail to meet this deadline. The ultimate publication will be based on the final approval of the editors.

Manuscripts submitted to ABO should not be simultaneously considered for publication by other journals. In addition, total or partial publication or translation for publication in another language of the manuscripts submitted to ABO should not be considered without the permission of the editors of ABO.

AUTHORSHIP

The criteria for authorship of manuscripts in medical journals are well established. Individuals who have contributed in a concrete way during the following three phases of manuscript preparation should be considered authors:

I. Conception and design, acquisition of data, or analysis and interpretation of data.
II. Draft or critical revision of the article for important intellectual content.
III. Final approval of the version to be published.

The authors of manuscripts submitted to ABO should make sure that all authors meet the criteria mentioned above and that all persons who meet these criteria are listed. Individuals who hold headship positions cannot be considered authors of manuscripts based only on their positions. ABO does not accept the participation of honorary authors.

The corresponding author should complete and submit the Author Contribution Statement as a supplementary document.

GUIDELINES FOR EXCELLENT RESEARCH

It is recommended that authors follow the appropriate guideline bellow before submitting your work:

- CONSORT (Controlled and randomized clinical trials)
- STARD (Diagnostic instruments or techniques)
- PRISMA (Systematic reviews and meta-analyses)
- STROBE (Observational studies)

MANUSCRIPT PREPARATION

Manuscripts should only be submitted online using the appropriate interface of ABO. The following guidelines were based on the format suggested by the International Committee of Medical Journal Editors (ICMJE) and published in the document: Uniform Requirements for Manuscripts Submitted to Biomedical Journals.

Only the manuscripts complying with these guidelines will be considered for analysis.

The text should be sent as a digital file. Only the following formats are accepted: .doc or .rtf. The text should be typed double-spaced, in 12 point font. The pages should be numbered in Arabic numerals, starting each section on a new page.

The sections should be presented according to the following sequence: Title page (as a separate document); Abstract and Keywords; Introduction; Methods; Results; Discussion; Acknowledgements (if any); References; Tables (optional) and Figures (optional) including legends.

1. Title Page. It should contain: a) title (no more than 135 characters with spaces); b) running title to be used as a page heading (no more than 60 characters with spaces); c) authors' names as they should appear in print; d) each author's affiliation* (city, state, country and, if applicable, department, school, university); e) corresponding author's, name, address, phone number, and email; f) sources of financial support (if any); g) project number and institution responsible for the approval of the Research Ethics Committee; h) statement of conflicts of interests of all authors; i) clinical trial registration number on a public trials registry.

* Professional or academic degrees, as well as job position will not be published.

Approval of the Institutional Review Board (IRB). All retrospective, cross-sectional, or prospective studies involving primary data collection or clinical and surgical reports should include the project number and name of the institution that provided the approval of the IRB on the title page. Studies involving humans should be compliant with the Declaration of Helsinki, whereas studies involving animals should be in accordance with the principles suggested by the Association for Research in Vision and Ophthalmology (ARVO).

As a supplementary document, the corresponding author should send the IRB approval or its report stating that the evaluation of the project by the Committee is not necessary. The author cannot decide on the need for evaluation by the Research Ethics Committee.

Statement of Conflicts of Interest. The title page should contain the statement of conflicts of interest of all authors (even if there is no conflict of interest). For more information about potential conflicts of interest, refer to: World Association of Medical Editors: Conflict of interest in peer-reviewed medical journals.

All authors should send the Form for Disclosure of Potential Conflicts of Interest as supplementary documents.

Clinical Trials. All Clinical Trials shall include on the title page the registration number in an international registry that allows free access to trial information (examples: U.S. National Institutes of Health, Australian and New Zealand Clinical Trials Registry, International Standard Randomised Controlled Trial Number - ISRCTN, University Hospital Medical Information Network Clinical Trials Registry - UMIN CTR, Nederlands Trial Register, Registros Brasileiros de Ensaios Clínicos).

2. Abstract and Keywords. Structured abstract (Objective, Methods, Results, Conclusions) with no more than 300 words. Unstructured abstract with no more than 150 words. Five keywords in English listed by the National Library of Medicine (MeSH - Medical Subject Headings).

3. Abstract and Keywords in Portuguese. Structured abstract (Objective, Methods, Results, Conclusions) with no more than 300 words. Unstructured abstract with no more than 150 words. Five keywords in Portuguese listed by BIREME (DeCS - Descritores em Ciências da Saúde). Portuguese translation may be provided by ABO at publication.

4. Introduction, Methods, Results, and Discussion. Citations in the text should be numbered sequentially in superscript Arabic numerals and in parentheses. The names of the authors should not be cited in the text.

5. Acknowledgements. This section should include the collaboration of people, groups or institutions that deserve to be acknowledged but do not meet the criteria for authorship. Statisticians and medical editors may meet the criteria for authorship and, in this case, should be acknowledged as authors. When they do not meet the criteria for authorship, they should be mentioned in this section. Writers who are not identified in the manuscript cannot be accepted as authors; therefore, professional writers should be acknowledged in this section.

6. References. Citations (references) of authors in the text should be numbered sequentially in the same order as they are cited and identified using superscript Arabic numerals. References should be in accordance with the format suggested by the International

Committee of Medical Journal Editors (ICMJE), based on the examples below.

The titles of the journals should be abbreviated according to the style provided by the List of Journal Indexed in Index Medicus of the National Library of Medicine.

The names of all authors should be cited for references with up to six authors. For studies with seven or more authors, cite only the first six authors followed by *et al*.

Examples of references:

Journal Articles

Costa VP, Vasconcellos JP, Comegno PEC, José NK. O uso da mitomicina C em cirurgia combinada. Arq Bras Oftalmol. 1999;62(5):577-80.

Books

Bicas HEA. Oftalmologia: fundamentos. São Paulo: Contexto; 1991.

Book Chapters

Gómez de Liaño F, Gómez de Liaño P, Gómez de Liaño R. Exploración del niño estrábico. In: Horta-Barbosa P, editor. Estrabismo. Rio de Janeiro: Cultura Médica; 1997. p. 47-72.

Annals

Höfling-Lima AL, Belfort R Jr. Infecção herpética do recém-nascido. In: IV Congresso Brasileiro de Prevenção da Cegueira; 1980 Jul 28-30, Belo Horizonte, Brasil. Anais. Belo Horizonte; 1980. v.2. p. 205-12.

Dissertations

Schor P. Idealização, desenho, construção e teste de um ceratômetro cirúrgico quantitativo [dissertation]. São Paulo: Universidade Federal de São Paulo; 1997.

Electronic Documents

Monteiro MLR, Scapolan HB. Constrição campimétrica causada por vigabatrin. Arq Bras Oftalmol. [online journal]. 2000 [cited 2005 Jan 31]; 63(5): [about 4 p.]. Available at:http://www.scielo.br/scielo.php?script=sci_arttext&pid=S0004-27492000000500012&lng=pt&nrm=iso

7. Tables. Tables should be numbered sequentially using Arabic numerals in the order they are mentioned in the text. All tables should have a title and a heading for all columns. Their format should be simple, with no vertical lines or color in the background. All abbreviations (even if previously defined in the text) and statistical tests should be explained below the table. The bibliographical source of the table should also be informed when the table is extracted from another study.
Do not include tables in the main document of the manuscript, they should be uploaded as supplementary documents

8. Figures (graphs, photos, illustrations, charts). Figures should be numbered sequentially using Arabic numerals in the order they are mentioned in the text. ABO will publish the figures in black and white at no cost to the authors. Manuscripts with color figures will be published only after the authors pay a publication fee of R$ 500.00 per manuscript.

Graphs should preferably be in shades of gray, on a white background and without three-dimensional or depth effects. Instead of using pie charts, the data should be included in tables or described in the text. Photos and illustrations should have a minimum resolution of 300 DPI for the size of the publication (about 2,500 x 3,300 pixels for a full page). The quality of the images is considered in the evaluation of the manuscript.

The main document should contain all figure legends, typed double-spaced and numbered using Arabic numerals.

Do not include figures in the main document of the manuscript; they should be uploaded as supplementary documents.

Supplemental files can have the following extensions: JPG, BMP, TIF, GIF, EPS, PSD, WMF, EMF or PDF.

9. Abbreviations and Acronyms. Abbreviations and acronyms should be preceded by the spelled-out abbreviation on first mention and in the legends of tables and figures (even if they have been previously mentioned in the text). Titles and abstracts should not contain abbreviations and acronyms.

10. Units of Measurement: Values of physical quantities should be used in accordance with the standards of the International System of Units.

11. Language. Texts should be clear to be considered appropriate for publication in a scientific journal. Use short sentences, written in a direct and active voice. Foreign words should be in italics. Therapeutic agents should be mentioned by their generic names with the following information in parentheses: trade name, manufacturer's name, city, state and country of origin. All instruments or apparatus should be mentioned including their trade name, manufacturer's name, city, state and country of origin. The superscript symbol of trademark ® or™ should be used in all names of instruments or trade names of drugs. Whenever there are doubts about style, terminology, units of measurement and related issues, refer to the AMA Manual of Style 10th edition.

12. Original Documents. Corresponding authors should keep the original documents and the letter of approval from the Research Ethics Committee for studies involving humans or animals, the consent form signed by all patients involved, the statement of agreement with the full content of the study signed by all authors and the statement of conflict of interest of all authors, as well as the records of the data collected for the study results.

13. Corrections and Retractions. Errors may be noted in published manuscripts that require the publication of a correction. However, some errors pointed out by any reader may invalidate the results or the authorship of a manuscript. If substantial doubt arises about the honesty or integrity of a submitted manuscript, it is the editor's responsibility to exclude the possibility of fraud. In these situations, the editor will inform the institutions involved and the funding agencies about the suspicion and wait for their final decision. If there is confirmation of a fraudulent publication in ABO, the editor will act in compliance with the protocols suggested by the International Committee of Medical Journal Editors (ICMJE) and by the Committee on Publication Ethics (COPE).

CHECKLIST

Before submitting their manuscript, authors should make sure that all the following items are available:

- ☐ Manuscript prepared in accordance with the instructions to authors.
- ☐ Maximum number of words, tables, figures, and references according to the type of manuscript.
- ☐ Title page including the clinical trial registration number is not included in the main document
- ☐ No figures and tables are included in the main document of the manuscript.
- ☐ All figures and tables were uploaded separately as supplementary documents.
- ☐ Author Contribution Statement completed and saved as a digital file to be sent as a supplementary document.
- ☐ Form for Disclosure of Potential Conflicts of Interest of all authors completed and saved as digital files to be sent as supplementary documents.
- ☐ Digital version of the report provided by the Institutional Review Board containing the approval of the project to be sent as a supplementary document.

LIST OF WEBSITES

Authorship Principles according to the ICMJE
http://www.icmje.org/recommendations/browse/roles-and-responsibilities/defining-the-role-of-authors-and-contributors.html

Authors' Participation Form
http://www.cbo.com.br/site/files/Formulario Contribuicao dos Autores.pdf

CONSORT (Consolidated Standards of Reporting Trials)
http://www.consort-statement.org/consort-statement/

STARD (Standards for the Reporting of Diagnostic accuracy studies)
http://www.stard-statement.org/

PRISMA (Preferred Reporting Items for Systematic Reviews and Meta-Analyses)
http://www.prisma-statement.org/index.htm

STROBE (Strengthening the Reporting of Observational studies in Epidemiology)
http://www.strobe-statement.org/

Online interface for submission of manuscripts to ABO
http://www.scielo.br/ABO

International Committee of Medical Journal Editors (ICMJE)
http://www.icmje.org/

Uniform requirements for manuscripts submitted to biomedical journals
http://www.nlm.nih.gov/bsd/uniform_requirements.html

Declaration of Helsinki
http://www.wma.net/en/30publications/10policies/b3/index.html

Principles of the Association for Research in Vision and Ophthalmology (ARVO)
http://www.arvo.org/About_ARVO/Policies/Statement_for_the_Use_of_Animals_in_Ophthalmic_and_Visual_Research/

World Association of Medical Editors: Conflict of interest in peer-reviewed medical journals
http://www.wame.org/about/wame-editorial-on-coi

Form for Disclosure of Potential Conflicts of Interest
http://www.icmje.org/coi_disclosure.pdf

U.S. National Institutes of Health
http://www.clinicaltrials.gov

Australian and New Zealand Clinical Trials Registry
http://www.anzctr.org.au

International Standard Randomised Controlled Trial Number - ISRCTN
http://isrctn.org/

University Hospital Medical Information Network Clinical Trials Registry - UMIN CTR
http://www.umin.ac.jp/ctr/index.htm

Nederlands Trial Register
http://www.trialregister.nl/trialreg/index.asp

Registros Brasileiros de Ensaios Clínicos
http://www.ensaiosclinicos.gov.br/

MeSH - Medical Subject Headings
http://www.ncbi.nlm.nih.gov/sites/entrez?db=mesh&term=

DeCS - Health Sciences Keywords in Portuguese
http://decs.bvs.br/

Format suggested by the International Committee of Medical Journal Editors (ICMJE)
http://www.nlm.nih.gov/bsd/uniform_requirements.html

List of Journal Indexed in Index Medicus
http://www.ncbi.nlm.nih.gov/journals

AMA Manual of Style 10th edition
http://www.amamanualofstyle.com/

Protocols of the International Committee of Medical Journal Editors (ICMJE)
http://www.icmje.org/recommendations/browse/publishing-and-editorial-issues/scientific-misconduct-expressions-of-concern-and-retraction.html

Protocols of the Committee on Publication Ethics (COPE)
http://publicationethics.org/resources/flowcharts

ipsis gráfica e editora

Edited by
IPSIS GRÁFICA E EDITORA S.A.
Rua Vereador José Nanci, 151 - Parque Jaçatuba
09290-415 - Santo André - SP - Brazil
Phone: (5511) 2172-0511 - Fax (5511) 2273-1557

Chief Executive Officer: Fernando Steven Ullmann;
Commercial Director: Helen Suzana Perlmann; **Art Director:** Elza Rudolf;
Publishing, Printing and CTP: Ipsis Gráfica e Editora S.A.
Frequency of publication: Bimonthly; **Circulation:** 7.500 copies

Advertising
CONSELHO BRASILEIRO DE OFTALMOLOGIA
R. Casa do Ator, 1.117 - 2nd Floor -
São Paulo - SP - Brazil - 04546-004
Contact: Fabrício Lacerda
Phone: (5511) 3266-4000 - **Fax:** (5511) 3171-0953
E-mail: assessoria@cbo.com.br